THE UNIVERSITY
of EDINBURGH

Metocean Risk Analysis in Offshore Wind Installation

Jack Paterson

August 2018

This thesis is submitted in partial fulfilment of the requirements for the award of an Engineering Doctorate, jointly awarded by the University of Edinburgh, the University of Exeter, and the University of Strathclyde. The work presented has been conducted under the industrial supervision of EDF Energy Research and Development (EDF R&D) as a project within the Industrial Doctoral Centre for Offshore Renewable Energy (IDCORE).

THE UNIVERSITY of EDINBURGH

UNIVERSITY OF EXETER

Declaration

I declare that this thesis has been composed solely by myself and that it has not been submitted, either in whole or in part, in any previous application for a degree. Except where otherwise acknowledged, the work presented is entirely my own.

Jack Paterson

May 2019

Lay Summary

Marine operations play a pivotal role throughout all phases of a wind farm's life cycle. In particular uncertainties associated with offshore installation can extend construction schedules and increase the capital expenditure (CAPEX) required for a given project, which typically account for approximately 30% of the overall project cost. The increasing remoteness of and variable weather conditions likely to be experienced by the UK's future offshore wind farms, add to the complexity of the marine operations and the importance of making the correct decisions prior to development. Metocean studies aim to quantify the effects of weather or sea conditions on a variety of offshore applications and can be used to provide reliable statistics or construct long term data sets to help anticipate potential risks before project execution or during offshore activities. Therefore an understanding of the potential risks to these operations using metocean simulation methods, can support planning decisions and reduce the costs of future projects. It is the purpose of this research to demonstrate the application and development of methodologies to support offshore planning decisions with respect to metocean criteria within EDF Group.

Abstract

Marine operations play a pivotal role throughout all phases of an offshore wind farm's life cycle. In particular, uncertainties associated with offshore installation can extend construction schedules and increase the capital expenditure (CAPEX) required for a given project. Installation costs typically account for approximately 30% of the overall CAPEX. Therefore an understanding of the potential risks to these operations using simulation methods, can support planning decisions and reduce the costs of future projects.

This research reviews the risks deriving from marine operations with an appreciation of the current standards in metocean risk management. It is intended that the analysis and benchmarking of existing tools, simulation methods and software to review metocean risks, will support and inform technical decisions prior to the construction of offshore wind projects in EDF Energy. By applying and testing the current state of the art in metocean risk analysis, this supports the estimation of risk profiles for marine operations.

Several time series simulation techniques are adopted, expanded and tested to provide reliable metocean risk estimates. This has included the development of a comparative vessel risk methodology by adopting EDF's existing probabilistic simulation tool 'ECUME I'. The results provide a quantification of installation vessel performance and the structured method can be used to identify and

benchmark offshore wind installation risk for developers or contractors. A commercially available simulation package 'Mermaid' was used to assess a range of marine operations for two planned offshore wind projects from EDF Energy's portfolio: 1) Blyth Offshore Demonstrator and 2) Fecamp. The documentation of both analyses presents two different modelling approaches and supportive metrics such as percentage increase against baseline schedules, highlight the project phases with the greatest risk and where EDF Energy should prepare suitable mitigations or contingencies. A metocean weather modelling methodology has been investigated by applying and extending an existing Markov Switching Autoregressive (MS-AR) toolbox to produce stochastic wind speed and significant wave height time series. This model is analysed for inclusion in a next generation marine risk planning software tool and it is identified that the overall methodology produces similar weather window and workability outcomes compared to observed time series. Furthermore, an analysis of different marine operations, each with different metocean limits, revealed that the methodology can enhance the resolution of the risk profile, leading to improved estimates at intermediate percentiles.

Each of the presented modelling approaches and simulation methods have limitations and a discussion of their impact is presented, offering recommendations for future analyses. It is intended that the methods analysed in this work will provide a useful reference for future metocean risk assessments in the offshore wind industry. These approaches have supported both academic and commercial practices, where project specific metocean risk assessments were used directly in project planning and the investigation of a MS-AR metocean modelling method has demonstrated the suitability of this approach for inclusion in a holistic simulation environment.

Acknowledgements

I am most grateful to everyone who has supported my academic studies and contributed to the development of this thesis. Firstly, I would like to thank my supervisors for their mentoring and guidance; Dr. Philipp Thies, Dr. Federico D'Amico, Prof. Gareth Harrison and Dr. Rafet Kurt.

A big thank you to the industrial partner for this project; EDF Energy R&D UK Centre and my colleagues for their inspirational support throughout. I'd like to extend this appreciation to members of EDF R&D in France, EDF ER and EDF EN. My exposure and access to in-house expertise and project information has been an invaluable resource during my project and I look forward to joining the R&D team as a full-time member in 2018.

A special thank you to my fiancée, Marianne and various family members who have all offered as usual, their unconditional support during my academic pursuits. A particular mention to my Mum, as well as to my good friend Erif for their unstinting proofreading endeavours.

Finally, I'd like to thank my peers at the Industrial Doctorate for Offshore Renewable Energy (IDCORE) for their enthusiasm and friendship over the past four years. I am sure we will meet again, as friends and colleagues alike.

Contents

Lay Summary **v**

Abstract **vii**

Contents **xi**

List of Tables **xv**

List of Figures **xvii**

List of Acronyms **xxi**

List of Notations **xxiii**

1 Introduction **1**
1.1 Thesis Context 1
1.2 Research Aims and Objectives 5
1.3 Thesis Contributions 7
1.4 Thesis Outline 8

2 Literature Review **13**
2.1 Offshore Wind Installation 13
2.2 Standards in Offshore Risk Management & Decision Making . . . 15
2.3 Metocean Risk and Marine Operations 25
2.4 Metocean Risk Modelling for Marine Operations 36
2.5 Stochastic Weather Models for Metocean Risk Modelling 43
2.6 Literature Summary 51

3 Methods to Improve Metocean Risk Management in Offshore Wind Installation **55**
3.1 Comparative Vessel Assessment with ECUME I 57
3.2 Commercial Metocean Risk Modelling Case Studies 79
3.3 Stochastic Metocean Modelling Methodology 98
3.4 Summary 118

4 Results - Comparative Vessel Assessment with ECUME I 121
4.1 Results Assessing Vessel Technology 121
4.2 Results Overview 123
4.3 Results by Round 125
4.4 Summary 128

5 Commercial Metocean Risk Assessments 131
5.1 Blyth Offshore Demonstrator - Installation Metocean Risk Analysis 132
5.2 Fecamp - Installation Metocean Risk Analysis 140
5.3 Summary 147

6 Results from Stochastic Metocean Model 149
6.1 Simulation Results 150
6.2 Weather Window Assessment 154
6.3 Weather Window Persistence and Lengths - i) Paired-by-means . 156
6.4 Weather Window Persistence and Lengths - ii) Correlated Pairing 168
6.5 Example of MS-AR Metocean Model applied within EDF R&D's new Metocean Risk Simulation Software Prototype 179
6.6 Summary 184

7 Discussion 187
7.1 Comparative Vessel Assessment with ECUME I 187
7.2 Commercial Metocean Risk Analyses 200
7.3 Discussion on the Stochastic Metocean Modelling Method 206
7.4 Summary 229

8 Conclusions, Industrial Impact, Limitations and Future Work 231
8.1 Conclusions 232
8.2 Limitations 237
8.3 Industrial Impact 246
8.4 Future Work 248

References 253

Appendices 263

A Assumed vessel characteristics 263

B Inputs used in Mermaid modelling 265
B.1 Inputs Used in MERMAID modelling 266

C BOD weathered Gantt charts - Scenario 1 - No learning 267

D BOD P90 weathered Gantt chart - Scenario 2 - GBF & WTG learning 269

E BOD P90 weathered Gantt chart - Scenario 3 - GBF & WTG learning - 1 Month delay **271**

F BOD P90 weathered Gantt chart - Scenario 4 - 1 x WTG only **273**

G Percentage increase in duration by percentile tables - BOD & Fecamp metocean risk analyses **275**
G.1 276
G.2 277
G.3 278

H Average values & percentage difference, average and absolute average error for wind speed U and wave height H_s - observed and simulated **279**

I Distribution of monthly weather windows and percentage workability: ≥30 hours, ≤ 13.6 m/s & ≤ 1.5 m - Paired-by-means **281**

J Distribution of monthly weather windows and percentage workability: ≥30 hours, ≤ 13.6 m/s & ≤ 1.5 m - Correlated Pairing **283**

K Publications **285**
K.1 Published 285
K.2 Submitted 286
K.3 Conference Presentations 286
K.4 Conference Posters 287
K.5 Attached Publications 288

List of Tables

3.1 Round 1 OWF characteristics 67
3.2 Round 2 OWF characteristics 67
3.3 Round 3 OWF characteristics 67
3.4 Vessel types and spread by round 69
3.5 Task durations and operational limits 77
3.6 Observed time series 101

5.1 Percentile Results: BOD - No Learning 133
5.2 Percentile Results: BOD - GBF & WTG Learning 135
5.3 Percentile Results: BOD - GBF & WTG Learning - 1 Month Delay 136
5.4 Percentile Results: Scenario 4 - 1 x WTG Only 139
5.5 Fecamp - Installation Campaign 1 141
5.6 Fecamp - Installation Campaign 2 142

6.1 Percentage difference, average percentage difference and absolute average percentage difference for wind speed U and wave height H_s - observed vs. simulated 150
6.2 Weather Window requirements 154
6.3 Average Number of Weather Windows $U \leq 13.6$ m/s, $H_s \leq 1.5$ m for ≥ 30 hours 162
6.4 Average Number of Weather Windows $U \leq 13.6$ m/s, $H_s \leq 1.5$ m for ≥ 30 hours 174
6.5 Dredge & FPPV Vessel Limits 180
6.6 Dredging Operations 181
6.7 Filter Layer Operations 181

7.1 Comparison of pairing techniques against observed 216
7.2 Percentage difference of simulated data to number of years of observed data used to train the model 219
7.3 Marine operations, environmental limits and weather window requirements 220

A.1 Assumed vessel characteristics 264

H.1 Average magnitudes, percentage difference, average and absolute average for wind speed U and wave height H_s - observed and simulated 280

List of Figures

1.1 Annual offshore wind installations by country and cumulative capacity (MW) . . . 2
1.2 Thesis Outline . . . 11

2.1 Flowchart for formal safety assessment . . . 16
2.2 Operation Periods . . . 27
2.3 Restricted or Unrestricted Operation . . . 29
2.4 Weather Forecast Levels . . . 34

3.1 ECUME I simulation tool schematic . . . 58
3.2 Schematic representation of the Markov chain: wind speed (U_t), wave height (H_{s_t}), current speed (C_t). . . . 59
3.3 Schematic of the principal method . . . 61
3.4 Flowchart of ECUME I logistical process . . . 64
3.5 TSHD Dredger . . . 69
3.6 Svanen heavy lift vessel installing a monopile . . . 70
3.7 MPI Discovery WTIV transiting with monopiles and transition pieces 71
3.8 Brave Tern WTIV Installing a turbine blade on a jacket foundation 72
3.9 Brave Tern WTIV Installing a 'bunny ear' rotor assembly . . . 73
3.10 Flexible FPV installing scour protection . . . 75
3.11 Zwerver III multicat . . . 75
3.12 Cable Lay Vessel . . . 76
3.13 Mermaid map example - Pentland Firth . . . 82
3.14 Generalised commercial weather risk analysis methodology . . . 85
3.15 Blyth Offshore Demonstrator - GBF Design . . . 88
3.16 Mermaid - BOD site, Transit Routes, Meteorological Reference Points 89
3.17 GBF towing configuration . . . 90
3.18 Mermaid - Transit routes and meteorological reference points (Turbines: Esbjerg; Cable: Rotterdam; Filter Layer & Scour Protection Rock: Kvantum) . . . 91
3.19 BOD: Modelled GBF and WTG learning rates . . . 92
3.20 Fecamp - Met points, Transit Routes and Offshore Site . . . 96
3.21 MS-AR modelling & verification methodology . . . 100

3.22 Resulting Viterbi algorithm from homogeneous MS-AR Gaussian model; Wind speed at three hour Time-steps; 34 years of observations; December; UK North East, $p = 6, M = 3$ 107
3.23 Sample autocorrelation (ACF) and partial autocorrelation (PACF) correlograms; U (m/s); UK North East; March 108
3.24 Two numerical solutions 110
3.25 Two numerical solutions 111
3.26 English Channel - January - Realisation 500 Pearson r:-0.078 . . . 113
3.27 English Channel - January - All Realisations Pearson r:0.06 115
3.28 English Channel - January - All Realisations Pearson r:0.47 116
3.29 English Channel - January - Realisation 500 Pearson r:0.5 117
3.30 Concentration of simulated wind speed and H_s vs. scatter of observed data (white transparent plots) - English Channel 118

4.1 Average installation rate in days/WTG (or WTG location) 123
4.2 Average Weather Downtime in days/WTG (or WTG Location) . . 124
4.3 Installation Rates (IR) and Weather Downtime (WDT) by round 126

5.1 Fecamp Unweathered Gantt Chart - Campaigns One and Two . . 143
5.2 Fecamp P50 Gantt Chart - Campaigns One and Two 144
5.3 Fecamp P60 Gantt Chart - Campaigns One and Two 145
5.4 Fecamp P70 Gantt Chart - Campaigns One and Two 146
5.5 Fecamp P90 Gantt Chart - Campaigns One and Two 146

6.1 CDFs of annual wind speed - Observed vs. simulated - UK North East 151
6.2 CDFs of annual wave height - Observed vs. simulated - UK North East 152
6.3 QQ plot: observed and simulated wind speed - UK North East . . 153
6.4 QQ plot: observed and simulated wave height - UK North East . 153
6.5 Typical Crew Transfer Task - Turbine Transfers Ltd. 155
6.6 Weather window persistence histogram and average window length $\leq$ 13.6 m/s & $\leq$ 1.5 m 157
6.7 Mean percentage workability for time $\geq$ 30 h at $\leq$ 13.6 m/s & $\leq$ 1.5 m - **UK North East** 159
6.8 Mean percentage workability for time $\geq$ 30 h at $\leq$ 13.6 m/s & $\leq$ 1.5 m - **French West** 160
6.9 Mean percentage workability for time $\geq$ 30 h at $\leq$ 13.6 m/s & $\leq$ 1.5 m - **English Channel** 161
6.10 CDFs and percentiles of monthly weather windows: $\geq$30 hours, $\leq$ 13.6 m/s & $\leq$ 1.5 m - **Paired-by-means** 166
6.11 CDFs and percentiles of monthly percentage workability: $\geq$30 hours, $\leq$ 13.6 m/s & $\leq$ 1.5 m - **Paired-by-means** 167
6.12 Weather window persistence histogram and average window length $\leq$ 13.6 m/s & $\leq$ 1.5 m 169

6.13 Mean percentage workability for time ≥ 30 h at ≤ 13.6 m/s & ≤ 1.5 m - **UK North East** 170
6.14 Mean percentage workability for time ≥ 30 h at ≤ 13.6 m/s & ≤ 1.5 m - **French West** 171
6.15 Mean percentage workability for time ≥ 30 h at ≤ 13.6 m/s & ≤ 1.5 m - **English Channel** 173
6.16 CDFs and Percentiles of monthly weather windows: ≥30 hours, ≤ 13.6 m/s & ≤ 1.5 m - **Correlated Pairing** 177
6.17 CDFs and Percentiles of monthly percentage workability: ≥30 hours, ≤ 13.6 m/s & ≤ 1.5 m - **Correlated Pairing** 178
6.18 Dredging: CDF of Simulated, observed and overlaid percentiles from Mermaid simulation 182
6.19 Filter layer: CDF of Simulated, observed and overlaid percentiles from Mermaid simulation 183

7.1 Phase IQR Quantification: Rounds 1, 2 & 3 188
7.2 Average Prediction vs. Recorded Installation Rates - Round 1 . . 197
7.3 Average prediction vs average recorded installation rates - Round 1 [± 1 S.D.] 198
7.4 Workability Percentage Distributions - **UK North East**: Paired-by-means (L); Correlated Pairing (R). Black Lines: Observed Percentiles. Red Lines: Simulated Percentiles (P10, P50 and P90) 223
7.5 Workability Percentage Distributions - **France West**: Paired-by-means (L); Correlated Pairing (R). Black Lines: Observed Percentiles. Red Lines: Simulated Percentiles (P10, P50 and P90) 225
7.6 Workability Percentage Distributions - **English Channel**: Paired-by-means (L); Correlated Pairing (R). Black Lines: Observed Percentiles. Red Lines: Simulated Percentiles (P10, P50 and P90) 227

C.1 BOD P90 Weathered Gantt Chart - No Learning 268

D.1 BOD P90 Weathered Gantt Chart - GBF & WTG Learning . . . 270

E.1 BOD P90 Weathered Gantt Chart - GBF & WTG Learning - 1 Month Delay 272

F.1 BOD P90 Weathered Gantt Chart - 1 x WTG Only 274

I.1 Distribution of monthly weather windows and percentage workability: ≥30 hours, ≤ 13.6 m/s & ≤ 1.5 m - **Paired-by-means** . . 282

J.1 Distribution of monthly weather windows and percentage workability: ≥30 hours, ≤ 13.6 m/s & ≤ 1.5 m - **Correlated Pairing** . 284

List of Acronyms

AHT	anchor handling tugs
AIC	Akaike information criterion
ALARP	as low as is reasonably practicable
AR	autoregressive model
ARIMA	autoregressive integrated moving average model
ARMA	autoregressive moving average model
BBN	Bayesian belief network
BIC	Bayesian information criterion
BOD	Blyth Offshore Demonstrator Project
CDF	cumulative distribution functions
CLV	cable lay vessel
CTV	crew transfer vessel
DNV GL	Det Norske Veritas and Germanischer Lloyd
DP	dynamic positioning
EDF EN	EDF Énergies Nouvelles (EDF Renewables France)
EDF ER	EDF Energy Renewables UK
EM	expectation maximisation algorithm
FMECA	failure mode, effects and criticality analysis
FPV	fall pipe vessels
GBF	gravity base foundations
GBS	gravity base foundations

HAZID hazard identification

HAZOP hazard and operability

HMM hidden Markov model

HSE Health and Safety Executive

IAG inter-array grid/cabling

IR installation rate

LCOE levelised cost of energy

metocean meteorology and physical oceanography

MPSV multipurpose service vessel

MS-AR Markov-switching autoregressive model

MWS marine warranty surveyor

O&M operations and maintenance

OWF Offshore wind farm

PLGR Pre-lay Grapnel Run

PLL potential loss of life

SETAR self-exciting threshold autoregressive model

STAR self-exciting threshold autoregressive model

TGP translated Gaussian process

TSHD trailing suction hopper dredger

WDT weather downtime

WTG wind turbine

WTIV wind turbine installation vessels

List of Notations

U	Wind speed (m/s)
H_s	Significant wave height (m)
C	Tidal current speed (m)
T_p	Peak wave period (s)
Φ	Wind direction (deg)
Θ	Wave direction (deg)
λ	Failure rate
α	Alpha factor
t	time
$\mathrm{T_R}$	Reference Period
$\mathrm{T_{POP}}$	Operation Period
$\mathrm{T_C}$	Contingency time
$\mathrm{T_{Safe}}$	Safe condition
$\mathrm{T_{WF}}$	Time between weather forecasts
$\mathrm{OP_{LIM}}$	Limiting operational environmental criteria
°N	Latitude North
°E	Longitude East
P_{xx}	Percentile of interest (e.g. 50, 75 or 90)
Q_{xx}	Location of P_{xx} in the recorded durations, ranked in ascending order
n_w	Number of years of weather data
WDT_{Pxx}	Weather downtime for the selected percentile 'P_{xx}'

P_{xx_d}	Estimated duration for the selected percentile 'P_{xx}'
P_0	Base time to complete the operation without the impact of weather

ECUME I

i	state i
j	state j
k	month k
A	Transition matrix
π	Vector of initial probabilities
$\tilde{A}(i)$	Non zero values
$P(i)$	Associated indices
$X_{i.k}$	Meteorological vector at state i and month k
h	Meteorological parameter (U, H_s, C)
μ	Mean
σ	Standard deviation

MS-AR model & analytical parameters

A	Monthly realisations of wind speed
B	Monthly realisations of significant wave height
N	Number of observations
μ_A	Mean of monthly realisations of wind speed (U)
σ_A	Standard deviation of monthly realisations of wind speed (U)
μ_B	Mean of monthly realisations of significant wave height (H_s)
σ_B	Standard deviation of monthly realisations of significant wave height(H_s)
S_t	Hidden state or 'weather type' at time t
M	Number of hidden states or 'weather type'
Y_t	Magnitude of meteorological parameter at time t (U or H_s)

p	Order of the autoregressive process
P	Condition distribution
E	Conditional mean
var	Variance
BIC	Bayesian Information Criteria
L	likelihood of the data
k	number of parameters
$\overline{W}_{\%_i}$	Average workability percentage for month i
h_{T_i}	Total number of hours in month i
$h_{i,j}$	Combined duration of weather windows $\geq$ 30 hours for month i in realisation j
n	Number of monthly meteorological realisations for month i

Chapter 1

Introduction

This chapter provides an overview of the thesis for the reader. It begins with a general overview of the current state of the offshore wind industry, predominantly from a UK perspective. More specifically, the role of marine operations in the development of offshore wind projects is summarised, highlighting the importance of meteorology and physical oceanography (metocean) studies and modelling techniques used to evaluate the risk profile of installation campaigns. Section 1.2 presents the main research objectives, which are accompanied by the contributions of the thesis in Section 1.3; the overall outline of the thesis is presented in Section 1.4.

1.1 Thesis Context

Offshore wind farm (OWF) development has increased steadily throughout the UK over the last decade and is predicted to maintain this momentum until at

least 2020 [1, 2]. The UK has more offshore wind turbines than the whole of the rest of Europe. However, cumulative trends demonstrate that the total European installed capacity has risen form under 0.5GW in 2008 to 18.5GW in 2018 as shown in Figure 1.1 and a further 4GW of additional capacity is confirmed for development [3]. As turbine sizes and distances from shore increase, weather becomes more severe and water depths span beyond 30m, the logistical issues become more challenging for prospective developers.

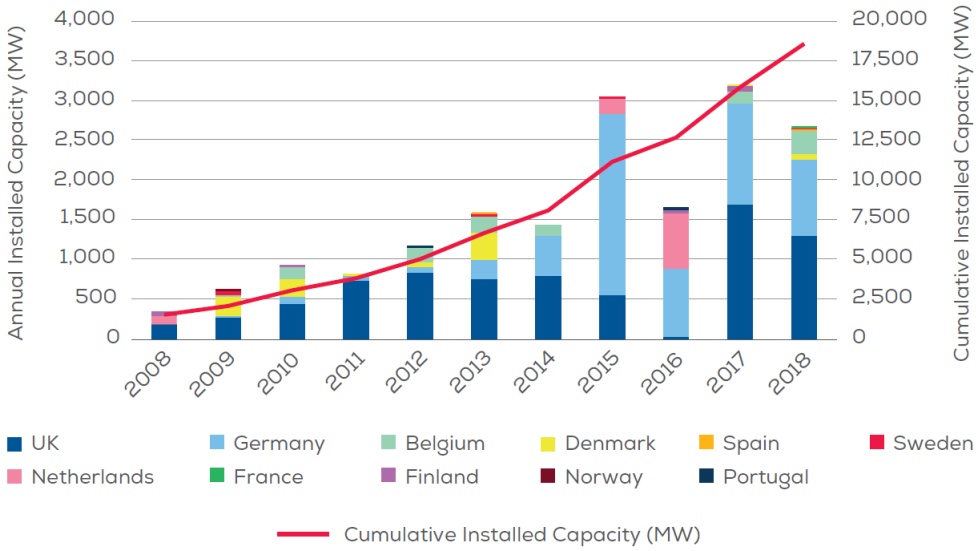

Figure 1.1: Annual offshore wind installations by country and cumulative capacity (MW) [3]

Marine operations play a pivotal role throughout all phases of a wind farm's life cycle, yet uncertainties associated with offshore installation can extend construction schedules and increase the capital expenditure (CAPEX) required for a given project. Installation costs can account for approximately 30% of the overall CAPEX and it is anticipated that informed engineering decisions in this area have the potential to contribute to valuable cost savings [4],[5]. The increasing remoteness of and variable weather conditions likely to be experienced by the UK's future OWFs, adds to the complexity of the marine operations and importance of making the correct decisions prior to development.

At the beginning of the OWF development in the UK in 2001, the vessels used for construction resulted in bottlenecks and delays in construction. This was caused by a lack in availability of specialised vessels, which were predominantly on charter in the oil and gas sector. In some cases the vessels used for installation were oversized or not ideally suited to the operations and were often sourced at overinflated charter rates due to the competition in the market. As OWF development progressed, the industry began to manufacture more purpose built offshore wind installation vessels that would offer increased deck space, lifting capabilities, cope with more severe weather and reduce overall installation durations [6].

This thesis considers the modelling and desktop-based risk management methods relating to metocean impacts for the installation of offshore wind projects, including scheduling, operational delays, equipment and vessel selection. Metocean is described by IMarEST's ORSIG group as "a technical engineering discipline that addresses meteorological and physical oceanographic matters"[7]. Metocean studies and analyses originated in the oil and gas industry and now due to the continuous growth in the European and the emerging global offshore wind markets, this discipline can be directly applied to offshore construction activities.

Operating within metocean limits brings significant challenges in understanding the impact of variable weather characteristics on installation downtimes or health and safety risks. As metocean conditions are site specific, a bespoke assessment for each project is required and thus adaptable assessment tools are necessary to simulate the characteristics of each site. International standards and guidance is available to support these activities by defining structured methods to assess safety, hazards and failure modes [8, 9, 10, 11, 12, 13]. Specific guidance to define metocean limits, modelling and the execution of marine operations is also

provided by international standards and certification bodies such as DNV GL and API [9, 13, 14, 15, 16, 17, 18].

Metocean studies aim to quantify the effects of weather or sea conditions on a variety of offshore applications. Studies can primarily provide reliable statistics or construct long term data sets to help anticipate potential risks before project execution or during offshore activities. Metocean models are commonly used to produce data sets for planning, modelling and review of offshore wind installations and ongoing operations and maintenance (O&M) tasks. These models are often employed when there is insufficient recorded data for a specific offshore location.

Increasing efforts have been made in the offshore wind industry to better predict the uncertainties during the progression of weather sensitive installation tasks. Offshore wind installation costs can account for up to one third of the overall project cost and a better understanding of the potential delays during marine operations will support developers in reducing the levelised cost of energy (LCOE). Future projects are planned for increasingly remote locations with challenging weather conditions such as high winds and wave heights that can cause significant disruption to a planned installation schedule, thus increasing the overall risk profile for installation or O&M campaigns. It is therefore important that marine operations can be scrutinised in advance to ensure correct planning, resourcing and equipment decisions are made before construction activities begin [19],[20],[21].

The generation of stochastic metocean time series has been widely researched for use in a variety of offshore applications. By generating a significant number of stochastic weather series that resemble the variability in key metocean parameters, probabilistic outcomes can be obtained to predict the weather windows, delays and subsequent installation durations for specific tasks or multiple installation phases. In recent years, dedicated probabilistic simulation tools have been developed to

predict the progression of marine operations and the suitability of resourcing strategies against synthetically produced metocean data. Embedding a stochastic metocean model within these simulation tools allows user to first input observed weather data for a finite number of years and generate many synthetic realisations of the weather to assess the progression of marine operations. Using a stochastic weather model is beneficial as it confers more certainty on predicted outcomes, yet still encloses the random variability which exists within the observed weather data [22], [23], [24].

1.2 Research Aims and Objectives

1.2.1 Aim

The key aim of this research is the application and development of methodologies to better understand and mitigate the metocean risks for offshore wind installation. In early offshore wind projects, unanticipated delays and subsequent cost overruns had a significant impact on project profitability and this thesis looks to assess the existing EDF R&D practices, commercial tools and contribute to new software solutions that can mitigate potential negative impacts during the development of a commercial offshore wind farm project.

1.2.2 Objectives

1. **Knowledge and understanding of the phenomena and issues**
    - Review of risks deriving from marine operations and associated ex-ante and ex-post measures in the oil & gas industry.

- Review of key lessons learned from previous in-house studies, practices and recommend methods which could be applied to the offshore wind industry.
- Review, identification and analysis of risks, ex-ante and ex-post measures and impacts on existing offshore wind farms.
- Analysis of current standards in offshore risk management, project management and marine operations in the offshore industry

2. **Development of tools/models to help the developer**

- Review of the state of the art risk management methodologies.
- Analysis and benchmarking of existing tools and software solutions to manage metocean risks and enable more informed technical and business decisions.
- Examine and develop methods to estimate the risk profile for offshore wind farm installations including recommendations on how to quantify them.
- Make proposals for innovative metocean risk management systems which could mitigate potential cost overruns and project delays are also proposed.

3. **Experimental case**

- Adopted tools and developed methodologies are applied to an experimental case where possible, such as offshore wind developments directed by EDF Énergies Nouvelles (EDF Renewables France) (EDF EN) and EDF Energy Renewables UK (EDF ER). It is intended that one of these projects could provide an invaluable opportunity to analyse, propose or implement innovative metocean risk management methods.

1.3 Thesis Contributions

This thesis makes the following contribution to metocean risk management in the field of offshore wind installation and associated marine operations.

- A generalised methodology to assess offshore wind installation vessels and associated risk using the first version of the ECUME I simulation tool.
- An assessment of vessel technology to provide a structured method to identify and benchmark offshore wind installation risks
- Round 2 vessels were found to have greater weather downtimes compared to Round 1. Round 1 vessels exhibit greater installation risk. Round 3 vessels were predicted to have the lowest weather downtimes and installation risk, despite a limited range of results for this round.
- The vessel performance predictions are verified by comparing against field data from a range of Round 1 sites.
- Application and comparison of two metocean risk modelling approaches are made using a commercial simulation tool for two in house projects, detailing the results, pros and cons of each method.
- Results from one metocean risk assessment directly supported planning and contingency allocations at EDF ER's Blyth Offshore Demonstrator Project.
- A stochastic weather modelling methodology was applied using an embedded MS-AR model to produce sufficiently long U and H_s time series, assessed for inclusion in a next generation marine operations simulation environment.
- Adaptation and extension of an Markov-switching autoregressive model (MS-AR) model, originally intended to simulate monthly wind speed simulations and applied to significant wave height.

- Implementation of a Bayesian information criterion (BIC) scoring approach for MS-AR model type section, improving adaptability to variable offshore conditions and metocean regimes.
- Implementation of a pragmatic correlated pairing technique to maintain wind wave relationships after univariate MS-AR simulations.
- Presentation of methods to summarise weather window and workability characteristics, comparing the differences between observed and simulated data for a personnel transfer operation, supported by summarised workability distributions for other offshore operations.
- Establishing that the stochastic weather modelling methodology is not suitable for locations with Pearson R correlations between wind speed and significant wave height greater than 0.8.
- Showing that the weather modelling methodology is not directly sensitive to the number of years of observed data used to inform the model, but rather the dataset should enclose the variability of the conditions at each site.

1.4 Thesis Outline

The thesis is structured around three core studies to reduce the metocean risks associated with marine operations. The content of each chapter is summarised below and supported by a flowchart in Figure 1.2.

Chapter two reviews the available literature relating to offshore wind installation, standards, metocean risk assessments and stochastic weather modelling methods. The review includes literature relevant to all three core metocean risk assessment studies. It begins with an overview of recent perspectives in offshore wind

construction, coverage on marine risk assessments, planning around the specific meteorological impacts and metocean risk modelling.

Chapter three describes the main methodological processes for the three core studies. Firstly, the modelling tool and procedure for a comparative vessel review is introduced, describing the embedded model calculations, data and vessel types under assessment. Next a commercial modelling tool, Mermaid, is presented, which was utilised to complete commercial metocean weather risk assessments for EDF ER's Blyth Offshore Demonstrator and EDF EN's Fecamp offshore wind farms. A high level perspective on the modelling constraints and operational phases is provided for each project. The last section of this chapter covers an extended metocean weather modelling methodology built around a Markov-switching autoregressive model, which was researched and built to support the next generation internal marine operations modelling software for EDF Group.

Chapter four describes the results for the comparative vessel assessment in EC-UME I. This covers average installation rate (IR) and weather downtime (WDT) predicted for the vessels employed for eight operational phases, throughout the three offshore wind rounds.

Chapter five presents the results from the metocean risk assessments for both the Blyth Offshore Demonstrator and Fecamp offshore wind projects.

Chapter six presents the outcomes from the stochastic weather modelling process. The two key sections review the impact of two pairing approaches to account for the correlation between the wind and the waves at three different sites.

Chapter seven discusses the results of the three metocean risk studies, highlighting any limitations, sensitivities and extensions to the analyses completed.

Chapter eight concludes the work, summarising the findings of the various studies and their industrial impact. Limitations and further work possibilities are also discussed.

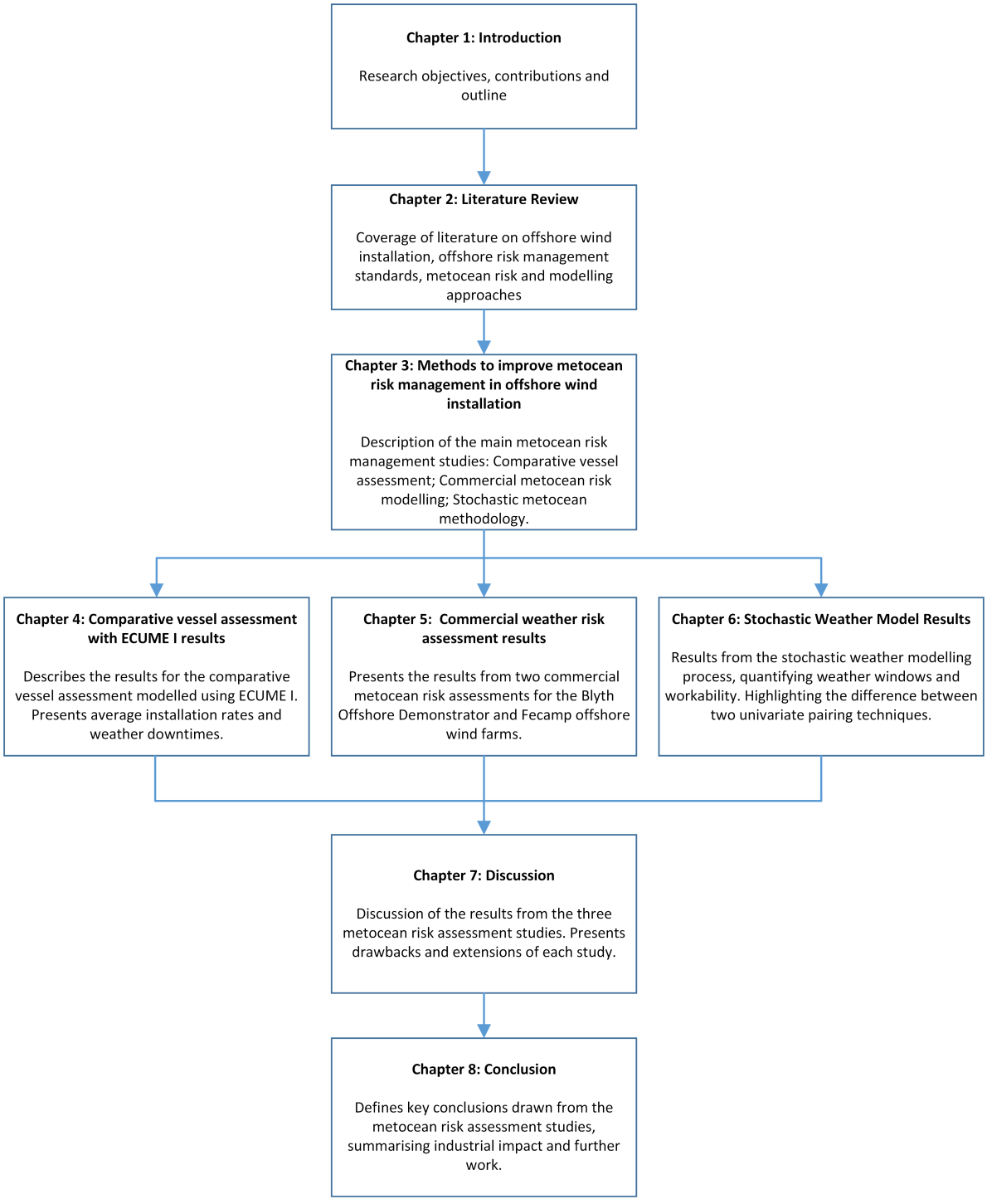

Figure 1.2: Thesis Outline

Chapter 2

Literature Review

2.1 Offshore Wind Installation

There are several published texts focused on offshore wind farm installation [25, 26, 27, 28] and in specified areas such as submarine cabling and metocean conditions [29, 30]. These provide an invaluable resource for background knowledge of the topic area, describing key planning objectives through to detailed installation sequences. Uncertainties relating to unknown seabed conditions, offshore erection, vessel availability and submarine cable laying operations are some of the most pertinent risks within the offshore wind industry [31, 32, 33].

Studies have indicated that 70-80% of European offshore wind farm insurance claims were submarine cabling related, with a number originating during the construction phase due to inadequate route planning, cable kinking or anchoring damages caused by installation vessels [29, 33, 34]. Natural hazards such as sand waves unsettled by ocean currents or submarine landslides can pose additional

risks to submarine cabling although less than 10% of all cable faults are related to natural hazards [35, 36]. This demonstrates a fundamental need for adequate surveys, as well as burial and protection measures which can be planned for prior to installation, to avoid negative impacts during the construction phase and the prevention of highly problematic failures during the operational phase.

As technical problems often arise due to inadequate management of the installation strategy, tools and methods should be identified and applied in conjunction with rigorous planning [34]. The Carbon Trust has delivered it's 'Cable Burial Risk Assessment Methodology', which provides thorough detail of the threats to submarine cable integrity and a probabilistic risk assessment is completed from a post construction perspective [33]. Lack of knowledge and skills with cabling installation can pose a considerable threat to the quality of these operations; highlighting the impact that human factors can have if adequate training and project management is not in place. Additionally, it is clear that cost overruns and installation delays should be tackled with quantitative analysis, with emphasis on the quality of the installation process overall [34].

As the offshore wind industry has grown, turnaround installation times have varied from site to site, even when using the same vessel [26]. The variability of offshore installation tasks are a result of the uncertainties associated with differing seabed environments and metocean conditions, often requiring adaptable or specialised installation vessels to be employed at short notice. The availability of vessels to react to unforeseen restrictions within a given installation operation has been limited in the past [32] and a thorough explanation of vessel types and a description of the associated offshore installation operations is included in Section 3.1.2.3.

2.2 Standards in Offshore Risk Management & Decision Making

A summary of the key offshore risk management standards is presented in this section, highlighting the key risk management processes applicable to offshore wind farm development. An introduction of offshore risk management and decision making processes is completed and a more specified overview on weather restricted operations is also presented.

Risk assessment generally assesses both severity (consequence) and frequency (likelihood) of hazardous events. The UK Health and Safety Executive (HSE) provides a succinct description: "The main purpose of risk assessment is to identify and rank the risks so that they can be adequately managed", essentially providing an input to the decision making processes [8]. Health and Safety Executive (HSE), with the help of Det Norske Veritas and Germanischer Lloyd (DNV GL), a globally recognised marine classification, quality assurance and risk management organisation, has promoted greater use of risk assessments for marine operations over the last two decades. They provide guidance on regulatory systems for safety, approaches to risk assessment and how to make the most of results from these activities [9]. To generalise, the risk management process begins with the identification of hazards, then estimation and ranking of the risks, followed by implementing risk mitigations to align with regulations and the process is completed with a final review.

A number of key hazard identification methods such as hazard identification (HAZID), hazard and operability (HAZOP) and failure mode, effects and criticality analysis (FMECA), are commonly used, all of which should be comprehensively executed at this stage of the risk management process. In terms of

estimating and ranking the risks, the complexity of the operation or task(s) to be reviewed will highlight the level of assessment and risk mitigations strategies to be implemented. Qualitative and semi-quantitative analyses are best used for review of hazards that have been either previously covered by standards or have low complexity. Quantitative risk assessments such as bespoke numerical modelling exercises, fault tree analyses or potential loss of life (PLL) are often used for highly complex operations not currently supported by standards. The HSE indicates that a systematic review of these analyses should be completed, moving to the more quantitative approaches, if it is found the qualitative methods do not adequately assess or distinguish between the risks [8].

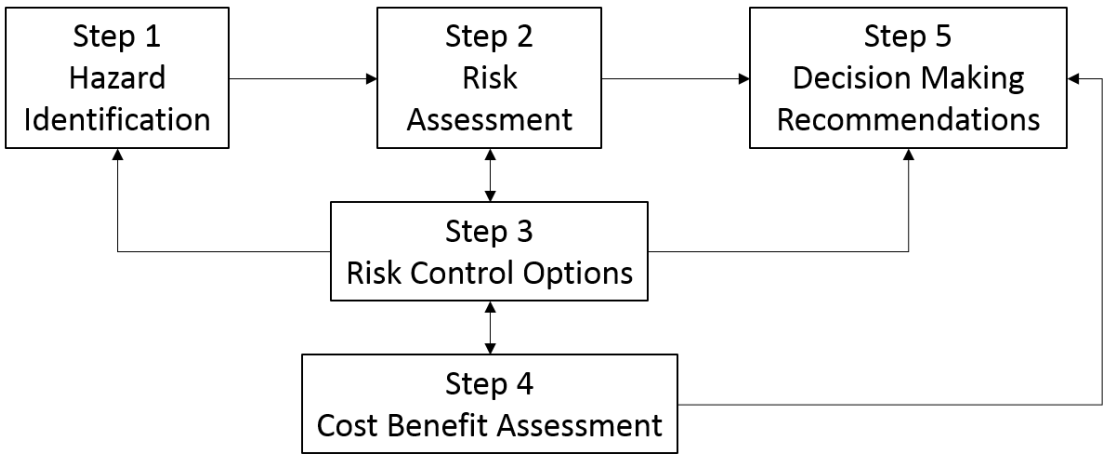

Figure 2.1: Flowchart for formal safety assessment [9]

The British Standards Institution provide guidance on a range of risk assessment techniques and tools that can be applied in the design of offshore production installations [10].

The objective of the hazard identification method (HAZID) is described in [10] as the use of "structured review techniques to identify all hazards associated with a particular concept, design, operation or activity, including the likely initiating causes and possible consequences or safeguards". HAZID studies can draw on several different inputs such as process flow diagrams, method statements,

technical drawings, the conditions where the activity will be executed and experiences from previous operations in similar or related disciplines. HAZID studies are usually completed in teams and rely on an mix of expertise and stakeholder backgrounds, which ensures studies are well informed with reference to different perspectives.

It is noted in [10] that appropriate techniques that reflect the scale and nature of major accident hazards should be adopted such as structured brainstorming, check-lists and "what if" analysis. A structured HAZID approach is essential to ensure no potential hazards are overlooked and subordinates at all levels in the operation under review should be included to identify all potential risks and improve the transparency of the review process. Furthermore, HAZID reviews must be fully documented following template worksheets that explicitly define the hazardous events, safeguards and actions based on the following list of recommended questions [10]:

a) Is the guideword hazard-relevant, or is there something similar that should be identified?

b) Is the type of hazard well understood in this context, or new/uncertain?

c) What are the likely causes that could lead to realization of hazard consequences (major accident)?

d) What are the credible and worst-case potential consequences?

e) What are the ISD measures and barriers already specified (or expected)?

f) Are there any additional ISD measures or barriers that could be proposed?

g) Are there human barriers or expectations regarding reliable human performance and are they reasonable?

h) Is further analysis required to understand the consequences of the hazard?

i) What recommendations should be made (actions for follow up)?

The actions that result from a HAZID process should be managed during implementation and should be applied for the entire life cycle of an installation where relevant. The outcome of a HAZID can instruct modifications to plants or processes and provide a key input to global project risk assessments. Major accident management strategies and performance standards can also draw on the outcomes of the HAZID to optimise efficiencies and safety.

The objectives of a HAZOP is described in [10] as "the application of a structured and systematic review technique to a defined system, carried out by a team, to identify hazards and operability problems, including causes, consequences, safeguards and remedial actions". A HAZOP study looks to reveal any hazards or operability issues that deviate from the intended process, highlighting their potential cause and consequences. The study relies on inputs such as process flow diagrams, instrumentation diagrams, cause and effect reviews and control procedures.

HAZOPs are best applied during the early design stage of a new facility or modification to an existing plant as changes instructed by the review are easily addressed. An experienced team is essential in a HAZOP review and should be led by a highly trained, recognised practitioner who relies on a scribe to record the identified hazards or operational limitations. The study must consider each of the subsystems or nodes in the process under review, evaluating the effects of deviations in the intended operations. Specific guide works are necessary to structure the examinations, which follow a series of repeated steps [10]:

a) identify a section of plant;

b) establish the design intent and normal operating conditions of this section;

c) identify a deviation from design intent or operating conditions by applying a set of guide-words;

d) identify possible causes for, and consequences of, the deviation;

e) identify existing safeguards and decide what action, if any, is necessary;

f) record the discussion and action.

HAZOP reports must be issued at the end of each session and after remedial actions have been completed to ensure the de-risking steps can be tracked. HAZOP studies are regarded as systematic and comprehensive yet are highly dependent on the experience of the leader, the team and thorough documentation provisions [10].

Failure mode, effects and criticality analysis (FMECA) are employed to "identify all possible single failure modes within systems or equipment, the likely effects of these failures and any potential consequences in terms of severity and criticality". FMECA attempts to "predict the probability that an identified failure mode will result in failure of design measures (barriers) and the increased level of risk" [10]. These studies relies on inputs such as defined boundaries of the analysis accompanied with a clear definition of the system and historical failure rates of the components. These inputs can be reviewed using a number of different techniques such as fault tree analyses that highlight critical failure paths. A fault tree is described in [11] as "an organized graphical representation of the conditions or other factors causing or contributing to the occurrence of a defined outcome, referred to as the 'top event'. When the outcome is a success, then the fault tree becomes a success tree, where the input events are those that contribute to the top success event. The representation of a fault tree is in a form that can be clearly

understood, analysed and, as necessary, rearranged to facilitate the identification of:

- factors affecting the investigated top event as it is carried out in most of the traditional fault tree analyses;
- factors affecting the reliability and performance characteristics of the system, when the FTA technique is used for reliability analysis, for example design deficiencies, environmental or operational stresses, component failure modes, operator mistakes, software faults;
- events affecting more than one functional component, which could cancel the benefits of specific redundancies or affect two or more parts of a product that may otherwise seem operationally unrelated or independent (common cause events)."

FMECA techniques are commonly used in offshore industries to a review engineered systems such as wind turbines or asset subsystems to identify the likely failure modes of a system, where best to apply reliability design measures or criticality analysis that define the significance of each failure mode. FMECA analyses should be employed at the most appropriate stage of a project with respect to the maturity of the design and detail required in the outputs. The results of an FMECA are usually presented in using a spreadsheet. The results can be used to assess if the system can a adequately manage the potential hazards and if any remedial design measures should be implemented to improve the overall reliability of the system. These are usually supported by criticality matrices that provide a graphical reference of the failure distributions [10].

Markov techniques can also be used in the offshore context, by adopting the state transition diagram to represent reliability, availability, maintainability and safety

characteristics of systems, to arrive at an measure of overall performance [12]. Fundamentally, these techniques can model the behaviour of a system over time with respect to two states: up or down. Intermediate states can also be defined, which are reliant on the combined effect of functioning or failed element. This implies that as each element in the system either fails or is restored the combined system moves between these states, which can be referred to as "a discrete-state, continuous time model" [12].

Markov techniques can be used to model redundant systems such as vessel dynamic positioning systems and the maintenance strategy applied to appreciate how a system will perform over time. It is essential that a user ensures that the model is a fair representation of how the system operates with respect to the memory-less characteristic of Markov models. Modelling reliability an failure using Markov models also implies that the failure and restoration rates of elements are constant with respect to time, but this should be justified against the known characteristics of the components and overall system under review. In [12] a set of assumptions for each element within a system are described as:

- "the failure rate, λ, and the restoration rate, μ, are constant (time-independent);
- the transition probability from a state i to a state j within the small time interval $(t, t + t)$ given that the system is in state i at time t is q_{ij} , where q_{ij} is a sum of failure and restoration rates of involved elements."

Once risks have been assessed, modelled and recorded it is essential that risk mitigations are prepared. This process should primarily consider the physical steps that lead to a hazard scenario as these could reveal some immediate options. It is also advised that a ranked list is developed and multidisciplinary

teams should brainstorm a range of risk reduction measures, taking each risk in turn [8]. It is important that operatives with extensive experience of the installation steps be involved in more detailed brainstorming activities, adopting supportive engineering methods, standards and best practices. HSE advises that a hierarchical approach to risk reduction should be applied, by first designing out the hazards in the installation process. Next, prevention should be addressed to reduce the likelihood of a risk event, followed by detection to improve awareness if a risk event were to occur. Thereafter, the control of a hazard (i.e. limiting exposure or scale) needs to be considered and finally, the protection against the potential consequences should be applied [8].

Accurate and strategic decision making is a critical part of the risk management process. In terms of safety and execution, decisions are needed to determine if operations should be started in the current conditions and what risk evasion strategies might be employed. This should be considered with the expenditure of the available strategies, to assess how much investment is required to maintain acceptable levels of safety and asset integrity. It must be decided if the installation operation is 'safe enough', where further safety measures are not needed as the risk levels are low. HSE states the importance of risks beyond immediate safety and topics such as economic, social and environmental factors should be incorporated within the decision making process [9].

The as low as is reasonably practicable (ALARP) framework is used to determine if it is economically appropriate to implement risk mitigations against the actual improvement to safety. This principle originates from UK legislation that "requires every employer to ensure, so far as is reasonably practicable, the health, safety and welfare of all his employees". This ensures that employers (in this context the offshore developer or subcontractor) adopt safety measures, unless the cost is disproportionate to the risk reduction that can be achieved [9]. Furthermore, the

tolerable and acceptable risk levels can be defined with reference to criteria in the text, which essentially recommends cost benefit analysis (CBA) to check if the benefits outweigh the costs and thus if it is appropriate to implement further steps. The ALARP guidance provides steps to identify if a qualitative or quantitative risk assessment (QRA) should be employed. It reiterates that a QRA should not be used to demonstrate why risk measures were not employed, but rather include a thorough CBA for all the employed or potential risk measures in order to demonstrate if the pay-offs are practicable.

Uncertainty exists in all risk assessments and in some instances the choice of the decision making criteria can be equally unclear. If the uncertainties are not addressed, decision makers may wrongly take a risk assessment to be fully reliable, which could lead to unforeseen issues in the execution of operations. DNV GL and HSE recommend two ways to approach uncertainty in risk assessments. Firstly, the classical approach considers best estimates of the risk and criteria to generate a basic evaluation of the risk. The uncertainties in both the risk and criteria are then considered in terms of how confident the assessors are about the solution. The assessors decide if the uncertainties make the risk assessment unreliable; if so, external or expert judgement should be sought to clarify any unknowns. Bayesian approaches include uncertainty 'as an intrinsic component of risk' and allocates quantities that reflect the assessors' belief in the final conclusions [9]. These steps are therefore vital to ensure that a reliable evaluation of the risk assessment has been completed.

Work has been completed in the modelling of risk assessments and decision making in various sub categories of the offshore wind sector such as turbine reliability, project value and construction and maintenance planning (e.g [37, 38, 39, 40]). Kougioumtzoglou and Lazakis consider both installation and O&M issues [41] and present a methodology to consider the likelihood of failure within the

main components of a turbine with the adoption of Failure Modes, Effects and Criticality Analysis (FMECA). To address the potential hazards from transportation, installation and O&M, a HAZID analysis is conducted. This considers the direct issues that relate to handling of the wind turbine and indirect issues that stem from the overall installation activity or the vessel employed for the given operation. A Bayesian belief network (BBN) is employed within the proposed methodology, but mainly considers the cost benefit analysis for the outcomes of the FMEA. The authors indicate that the BBN could have been extended to analyse the HAZID analysis. They state that this would allow the costs associated with most critical operations to be calculated, which would further improve the decisions made at the transportation and installation stages of a project. Furthermore, an integrated optimisation problem is discussed by the authors, indicating that extension of the methodology could be used to identify the most cost effective and risk averse solution, should a variety of overarching strategies exist for a given project.

Several academic investigations using Bayesian approaches in offshore wind are focused on resource assessment, operations and maintenance and reliability testing. The paper introduced by Borunda et al. discusses these studies alongside other renewable sources [42]. In all, the use of Bayesian approaches at the decision making stage improves confidence in the final conclusion and it seems that there is scope for utilising this method for modelling decision making in risk management of offshore wind development.

2.3 Metocean Risk and Marine Operations

2.3.1 Weather restricted operations

Weather restricted operations are commonplace in offshore projects and ways to categorise, quantify operational risks and predict potential delays for the installation of key assets, were first introduced in the oil and gas sector (e.g. [43, 44, 45, 46, 47]).

Over time, experience and practices from private companies, certification bodies and independent foundations has led to the provision of rigorous standards to ensure that "marine operations are performed within defined and recognised safety levels" [17], [15]. These standards are applicable to all marine operations, following similar detail included in the ISO 19901-6:2009 [13] and therefore should be followed during the planning and execution of offshore wind construction activities. DNV GL describes a marine operation as a "non-routine operation of a limited defined duration related to handling of object(s) and/or vessel(s) in the marine environment during temporary phases. In this context the marine environment is defined as construction sites, quay areas, inshore/offshore waters or sub-sea" [17]. A specific standard for port and marine operations for offshore wind industry [16] is currently under preparation and the reader is specifically directed to ISO 19901-1:2015 [14] for a full scope of metocean guidance and requirements.

Part one of the international standard ISO 19901-1:2015 [14] provides guidance and a description of the requirements to determine metocean limits for the design and operation of offshore structures. These requirements are split into two broad types: i) requirements to determine environmental conditions and the metocean parameters to describe them and ii) requirements to characterise

metocean parameters for the design, construction and operation of offshore structures. This standard provides description of extreme or abnormal values related to return periods, long term distributions, statistical format of metocean parameters and the normal environmental conditions that are expected for the majority of the time structures are in operation. Of specific interest for this research, it is mentioned that metocean parameters are applicable to determine environmental limits, weather windows and actions for offshore fabrication, transport, installation and decommissioning. This standard provides a crucial reference for the offshore industry and supports other specified operational standards such as those developed by DNV GL and API [9, 17, 18].

DNV GL regards reference periods (T_R) that are less than 96 hours and operation times (T_{POP}) of less than 72 hours as weather restricted. If available weather forecasts are believed to be inaccurate or there is a lack of consistent data the reference period can be extended to account for this uncertainty. A reference period can be defined as the combination of operational time and an estimated contingency time for the operation (T_C). A shorter reference period may be considered if there is a lack of weather data and/or forecasting uncertainty[17].

The start point for a weather restricted operation can be identified based on the provision of the most recent weather forecast. This process is presented in the standard using Figure 2.2:

Environmental design conditions imposed by contractors or vessel owners are often included in this approach but overly strict limitations should be avoided to allow progression of the tasks. Furthermore, it is widely accepted that an operation can only be complete once the object being handled has been taken from one safe condition to another. This can be simply exemplified for the installation of wind turbine components:

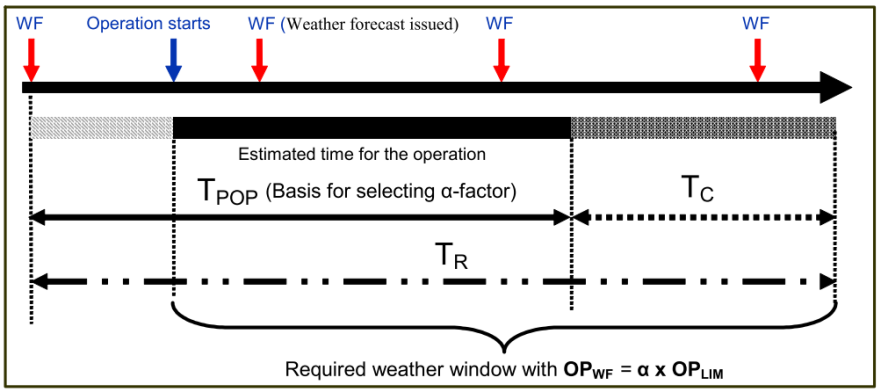

Figure 2.2: Operation Periods [17]

- Turbine components ready at quayside with vessel alongside **(1st safe condition)**
- Loading of the main components at the quay
- Transit to site
- Installation of the components
- Turbine is fully installed on the support structure **(2nd Safe condition)**

ISO 19901-1:2015 [14] provides guidance to determine relevant metocean parameters. This standard indicates that the owner or operator of an offshore installation is responsible for selection of environmental conditions for specific design situations. This calls on the various types of metocean information ranging from extreme environmental conditions, long term distributions, time series and short term data. All of these metocean sources should be considered depending on the application of the structure under review and can be used to estimate downtime or workability, conditions for checking fatigue limit states, serviceability limit states, operational safety and the general planning of marine activities. For very low probability events such as long return periods, it is recommended that experts

in meteorology and oceanography are employed to obtain reliable operational parameters. A return period can be described as the "average period between occurrences of an event or of a particular value being exceeded" [14]. In the offshore industry return periods are usually measured in years and can be used to define the annual probability of exceededance of an environmental event. Experts are required to primarily analyse data and interpret the outcomes into limiting design criteria, fundamentally guiding the design of structures or operations.

ISO 19901-1:2015 also covers design actions that are used in the assessment of marine structures highlighting that several fundamental parameters must be considered such as the structural form, the geographic location, the exposure of the structures or related operations and the limit state under review. Offshore transportation and installation and maintenance are generally categorised under short to medium term activities in the standard. Specific operations such as the installation of fixed offshore structures, operation of floating installations, seabed placement and loading of specialised vessels such as jack-ups are highlighted for their weather sensitivity and it is emphasised that the definition of weather windows is essential to ensure operations can be safely completed. Weather windows are defined by limiting environmental criteria for a fixed period of time and is indicated that the probability of sufficiently calm conditions varies across the seasons[14].

DNV GL states that the weather restricted operations are conditional to the availability of the most recent weather forecast. In some instances, the operations can extend beyond the provisional 96 and 72 hour classifications. To adequately consider these operations as weather restricted, continuous reference to the forecasted weather is required. The time to safely stop the operation bringing the object to a safe condition T_{Safe}, account for contingency T_C; the time between the weather forecasts T_{WF} is required to determine if these tasks can

be considered under the weather restricted window. If the combination of these tasks still exceed the provisional durations, they should be handled as unrestricted operations and require more in depth analyses using statistical data against the environmental limits for both the operations and vessel. The fundamental process is demonstrated in the standard as a flow chart as shown in Figure 2.3

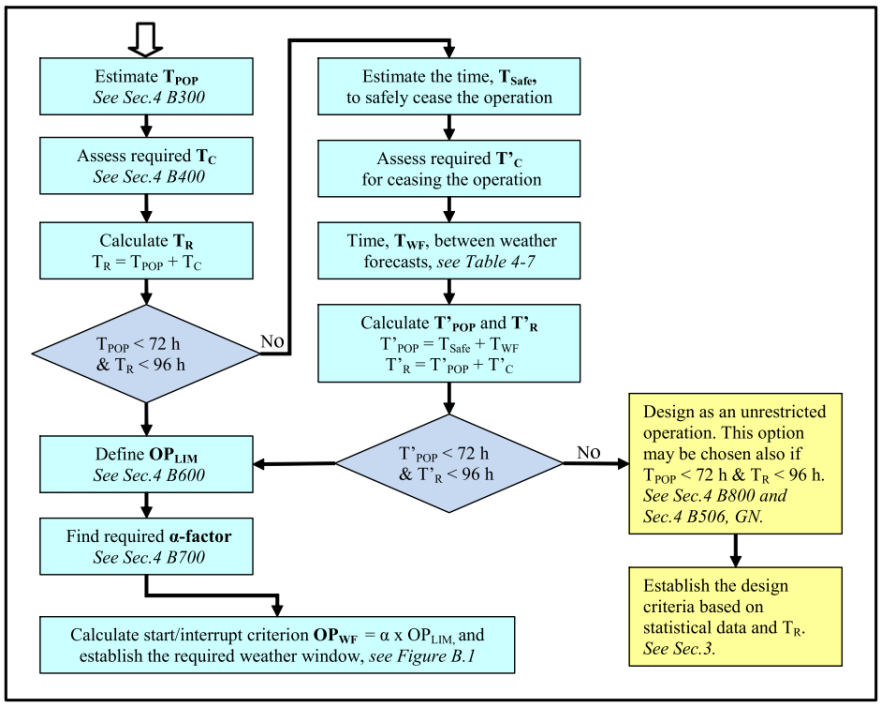

Figure 2.3: Restricted or Unrestricted Operation [17]

2.3.1.1 Operational Limiting Criteria

The limiting operational environmental criteria, denoted OP_{LIM}, must be defined and included in the main operations manual or method statements. DNV GL provides a set of boundaries for this assessment and states that the OP_{LIM} should not be greater than the environmental design criteria, maximum wind and wave heights for safe working, equipment restrictions for safe working, environmental limits for diving systems (if used), limits of positioning systems, limits imposed as

outcomes from hazard identification stages and the weather restrictions associated with the execution of contingency practices.

2.3.1.2 Alpha Factor

The standard accepts that uncertainty may exist in the monitoring and forecasting of the weather [17]. DNV GL recommends that forecasted operational criteria (OP_{WF}) be identified as follows: $OP_{WF} = \alpha$ x OP_{LIM}. In this assessment, the operational time from the issue of the latest weather forecast T_{POP} is used as the minimum time input for the selection of the α factor. If an operation can be halted, the time between weather forecasts and time to halt the operation safely can be accepted as a suitable value for α. As a guideline, DNV GL indicates that continuous monitoring of the weather conditions can allow for removal of the time between each forecast, but the time required to react to alterations in the weather should still be included in this assessment. It advises that the uncertainties associated with the weather be identified from statistical analysis and that the final selection of alpha factor should be such that the probability of exceeding the operational limits (OP_{LIM}) by more than 50%, is less than 10^{-4} [17].

DNV GL also provides comprehensive table sets for the selection of the α factor for waves in the North and Norwegian seas as established as part of a Joint Industry Project completed in 2005-2007. Each table can be selected based on the proposed forecasting support and active monitoring in place on the vessel. The first table considers a base case compiled of one forecast or when the resulting mean from two or more forecasts is used. As the level of forecasting competency or sources used for the operation increase, the next or most relevant table can be used. The final table in the set concerns the most comprehensive monitoring practices

where the monitoring and forecasts have been calibrated, supported by an on site meteorologist.

It is evident that as the overall accuracy of the forecasts are improved (i.e. less uncertainty) the alpha factors increase in the tables. This reflects the higher certainty regarding these conditions being realised, while the earlier tables show lower values to reflect the uncertainty in the weather predictions. It is noted that some variance will exist in the α factor. For operations of over 12 hours, the corresponding α factor should first be referenced on the relevant table, starting from the largest value in the column. For each 12 hour step in the operation, the next α factor in the column can be selected until the operation is complete within the maximum 72 hour window. It is recommended that the uncertainty associated with the wave periods should not go unnoticed and if operations are particularly susceptible to these conditions, the α factor may be altered accordingly.

If data is not made available for the waves, DNV GL provides guidance for the use of wind forecasts to identify an acceptable α factor. It is likely that this approach adopts greater uncertainty and more conservative values are recommended to reflect this. It is important to note that a number of the operations adopted during offshore wind farm construction are wave and wind sensitive, particularly the lifting of the turbine components. This undoubtedly has an impact in the planned operational durations and the selection of α factors for these types of operations. A Marine warranty surveyor marine warranty surveyor (MWS) is often employed to confirm the correct risk mitigations and contingencies are in place to satisfy insurers. The MWS, applying their experience and expertise in addition to the available standards, can have a significant influence on the α factor selected for a range of marine operations. Modelling of these imposed alpha factors may be applied and the predicted durations compared to the original base plan, revealing possible extensions to an installation campaign.

2.3.1.3 Unrestricted Operations

DNV GL describes the handling of unrestricted operations ($T_{POP} \leq 72h$, $T_R \leq 96h$) and indicates that any analysis should be completed considering extreme value statistics. It states that if extreme value statistics are used to determine the limiting criteria of operations, these values may be used as a typical reflection of the environmental conditions, although it is recommended that operations should not begin when extreme weather has been predicted and that they should be subject to a specified start criterion.

2.3.1.4 Weather Forecast

DNV indicates that arrangements should be made to obtain weather forecasts regularly from recognised bodies, before and during the completion of marine operations. The forecasts should be specific to the area and/or transit routes used and the position of the vessel considered on the delivery of updated forecasts. This will allow alternative routes to be identified if the conditions are likely to hinder the operations on the existing vessel heading. DNV GL states that the forecasting procedure should always consider the type and duration of the marine operations, addressing any sensitivities and should be accompanied by a written overview including the confidence level for the forecast. A list of the main criteria (as relevant) for each forecast is provided in the standard and these are included below:

- Wind speed and direction
- Waves and swell, significant and maximum height, mean or peak period and direction

- Rain, snow, lightning, ice etc.
- Tide variations and/or storm surge
- Visibility
- Temperature
- Barometric pressure

It is fair to assume that most of these criteria are relevant throughout offshore wind construction and provide a useful check to ensure the chosen forecaster can meet these requirements. The format of the forecast should be agreed between the client and meteorologist in advance of the operations. A forecast should be provided every 12 hours for the minimum reference period and should normally include a 24 hour look-ahead. A clear definition of the parameters should be provided in each forecast, such as the mean zero up-crossing period/peak period of waves.

2.3.1.5 Weather Forecast Levels

DNV GL provides these explanations to accompany the weather forecast levels discussed in the previous section; these are key throughout the selection of α factors. Once a clear understanding of the sensitivities for the planned operations is established and the related reference period T_R is identified, the categorisation of the planned operation(s) into forecast levels should be made [17] and are summarised below:

Level A

This category of forecast is to be applied to major marine operations that are

sensitive to environmental conditions and considers tasks such as offshore float-overs, gravity base structure (GBS) tow out operations and offshore installation operations. To some extent, this approach can be considered for the handling of valuable assets such as turbine components and where the operation to be completed is subject to strict environmental limits.

Level B

This level of forecast can be considered for operations that are sensitive to the environment and have fair to significant importance in terms of potential consequences and value of the operation as a whole. This type of forecast can be considered for operations that involve float-outs, lifts and less sensitive installation tasks.

Level C

This forecast is best suited to operations that are regularly executed and where the impact of environmental conditions is less significant. Typical applications are for nearshore lifts, quay load-outs and operations or tows in sheltered areas.

As a guide, DNV GL provides a table set of requirements for each forecasting level, as included in Figure 2.4 below:

Weather Forecast Level	*Meteorologist required on site?*	*Independent WF sources*	*Maximum WF interval*
A	Yes[1)]	2[2)]	12 hours[3)]
B	No[4)]	2[5)]	12 hours
C	No	1	12 hours

1) There should be a dedicated meteorologist, but it may be acceptable that he/she is not physically present at site. The meteorologist opinion regarding his preferable location should be duly considered. It is anyhow mandatory that the dedicated meteorologist has continuous access to weather information from the site and that he/she is familiar with any local phenomena that may influence the weather conditions. Note also that the meteorologist shall be on site in order to use alpha factors from Table 4-3 and Table 4-5.

2) It is assumed that the dedicated meteorologist (and other involved key personnel) will consider weather information/forecasts from several (all available) sources.

3) Based on sensitivity with regards to weather conditions smaller intervals may be required. However, see 305.

4) Meteorologist shall be conferred if the weather situation is unstable and/or close to the defined limit.

5) The most severe weather forecast to be used.

Figure 2.4: Weather Forecast Levels [17]

2.3.1.6 Acceptance Criteria

It is vital that the relevant limitations and required weather window for the operations be included as part of the acceptance criteria listed in the marine operation manual. DNV GL also indicates that if two sources of forecast are inconsistent for the same given area, the most severe forecast should be used, but if the difference between the forecasts is too wide, the uncertainty should be discussed to ensure operations are conducted safely. The worst case weather situation should be identified from all available forecasts, particularly when there is inherent low confidence in the quality of the reports. In an intermediate update between specified forecast intervals, DNV indicates that the data used for these updates must have sufficient accuracy [17].

2.3.1.7 Monitoring

DNV GL states that "Monitoring of design parameters (assumptions) should be used to as great an extent as practicable during marine operations." [17]. It is important that the monitoring methods align with the required accuracy and that target values (including acceptable deviations) be specified prior to monitoring stages. The environmental conditions offshore can be monitored directly or through the responses on board the vessel. For weather sensitive operations, it is important that monitoring prior to cast off and during operations be completed for criteria such as swell, wave heights and currents. Ongoing analysis of the remaining time for the marine operation in hand and environmental conditions should be practised.

It is proposed in DNV GL standard that the use of monitoring systems can be applied as a means to increase the α factor of waves, should these systems operate

with an acceptable level of accuracy and reliability. Generally accuracies of ±5% are acceptable and this data should be continuously analysed using statistical approaches to improve confidence in the outcome and thus change the α factor. It is also advised that a secondary system be adopted to detect any errors that may exist in the primary readings. For areas that have large tidal variations, it is recommended that a localised tide variation curve be developed or consulted, ensuring that the information aligns with the same lunar phase in which the operation(s) will be completed. All of these processes should be included as part of the monitoring procedure documentation.

2.4 Metocean Risk Modelling for Marine Operations

DNV GL states it is essential that availability analysis is used at the planning and design phase, including the weather criteria or limits for starting or interrupting operations. This assessment is referred to as the 'availability analysis' and uses historical weather data collected over a five to ten year period. In addition to weather conditions, the duration of each task is critical to this assessment, while the subsequent period that is expected to exceed the specified limits should be known. The application of time domain simulations can be used within specially created software packages to assess operational performance and historical weather data or models are used as an input to these analyses. It is states that "the marine operation performance simulation programs should include specification of durations, weather limits and a sequence of activities" [15].

In an attempt to reduce uncertainty associated with accessing and completing work at offshore locations, work on the modelling of logistical requirements and

installation of OWFs has been ongoing . This type of modelling and analysis allows practitioners to review the installation of an OWF in advance to ensure developers can prepare for certain outcomes in terms of cost or delay.

Irawan et al. [48] focused on the modelling of the construction operations and subsequent weather risk analyses to address the scheduling issues surrounding offshore wind construction by means of an integer linear programming. Their study develops a method to identify the optimal installation strategy that produces the lowest costs and shortest schedules, with respect to weather data and vessel availability. Their investigation in the use of metaheuristic approaches such as Variable Neighbourhood Search (VNS) and Simulated Annealing (SA) offers reasonable results with low computation time. When compared against a linear programming optimiser known as CPLEX, their approach is found to identify the optimum solution but takes longer to reveal the answer.

Barlow et al. [19] considered specific modelling of the logistics surrounding the installation steps, reviewing which vessels and operations are most susceptible to weather constraints in offshore wind installation. Their study aims to assess the impact of operational and vessel improvements over recent times and indicates that a non-linear relationship exists between vessel limits and the duration of the installation. They conclude that load out operations appear most susceptible during adverse weather conditions.

Logistics are again the topic in the paper presented by Vis et al. [49] and their modelling approach reveals that the key activities impacting performance are the vessel loads, distance to shore and the pre-assembly strategy adopted for the main wind turbine components. They recommend that a pre-assembly strategy should be employed which presents the optimum choice between the lowest number of lifts possible and the maximum number of turbines that can fit on a vessel. This reflects that the optimum will differ in each offshore wind project and careful

consideration of these two parameters should help reveal the best solution for a given project.

Scholz-Reiter et al. [50] point out that bad weather conditions are the main cause for delays in the logistics and installation of an offshore wind farm. They apply their mixed integer linear programming (MILP) model to identify the optimal installation schedule for different weather conditions and loading operations. Their study considers the installation of 12 turbines across three synthetically produced weather scenarios, each representing either good, medium or bad weather and the tool is used to identify optimal installation schedules for the vessels. They acknowledge the stochastic nature of weather conditions and express an interest in developing their tool and assess the impact of weather uncertainty beyond these initial three categories.

Ait-Alla et al. [51] developed a MILP model to minimise the installation costs by considering vessel utilisation and fixed costs that span the length of the installation period. Their approach considers the weather in a deterministic manner and reviews the outcome of two installation scenarios.

Muhabie et al. [52] consider the use of discrete event simulation by considering weather restrictions, distances, vessel capabilities and assembly scenarios. They consider the use of both historical weather data and synthetically generated data sets, adopting a probabilistic approach. The results demonstrate a good level of agreement between these two approaches when considering the average mean lead-time and reference future work required to optimise the fleet sizes, capacities and overall installation strategies.

Monte Carlo simulations have been employed for metocean planning and risk analysis as they facilitate parametric simulations, providing a means to assess uncertain variables such as the duration of offshore installation tasks, human

factors or equipment failure. Tyapin et al. [28] argue that a combination of Markov theory, analytically derived probability distributions for installation task durations and a PNET algorithm may reduce overall simulation times when compared to Monte Carlo Methods. Their comparison of both methods, reveals that there is little difference in predicted installation durations when a weather window is not required, yet differ when a predefined duration of specific weather conditions are specified. They state that the Monte Carlo method tends to be more conservative than the Markov-PNET approach, which was also found to be approximately two times faster than 1,000 Monte Carlo runs.

Ahn et al. [53] reviewed various vessel options for the installation of offshore wind turbines at the Korean West-South offshore wind farm. Their study considered a range of vessel types such as wind turbine installation vessels wind turbine installation vessels (WTIV), jack-up barges, towed cranes, barges and tug configurations. Their study follows the assembly and installation options provided by Kaiser and Thomsen [26, 39], which specifies four vessel and two primary installation methods. The one by one method which involves no onshore pre-assembly and a star pre-assembled rotor option are considered in terms of the maximum and minimum durations. A set of standard day rates are assumed for each vessel configuration. Two linear equations are used to assess the associated costs and installation times of the various installation methods along with each vessel spread. They conclude that the WTIV and jack-up vessels will lead to higher costs when compared to barge and tug configurations but will ultimately take less time to complete the installations. They conclude that the cost of the WTIV and jack-ups can significantly increase installation costs if there is any uncertainty in the installation schedule or delays in the delivery of turbine components

Lacal-Arantegui et al. [27] investigated the evidence behind costs reductions in

the installation of foundations and turbines at offshore wind farms. They collected data from 87 offshore wind farms to generate a picture of the installation time of each project. They state that the installation costs are directly influenced by the day rates associated with the vessels used and identify a reduction in foundation plus turbine installation times from 7.6 days in the early 2000s to 5.9 days at more modern installations, despite many of these sites being located further from shore. They indicate that these reductions had an improved effect when the project used higher rated turbines and monopole foundations, at 4 days/MW reducing to 1.06 days/MW for earlier and more modern projects respectively. This is equivalent to approximately a 70% reduction and it is noted that improvements with foundation installation (87%) were the predominant factor. It is concluded that economies of scale for the size of each project have not had a significant impact on the installation times and that incremental improvements were observed specifically for turbine installation.

Barlow et al. [54] use a mixed method framework to utilise discrete-event simulation and robust optimisation decision support methods. Through simulation, the study describes a means to predict and therefore optimise the planning of the installation operations by considering the available asset selection options. Their study considers the installation period of wind turbines but could be expanded to other installation phases. It provides a perspective on the anticipated cost, and duration and generates an optimal installation schedule that accounts for delays due to weather uncertainties. It is noted that the overall framework was validated by experts to provide reliable scheduling, accounting for seasonal uncertainty and optimal activity planning.

Morandeau et al. [55] state that future marine energy deployments will require cost effective marine operations, executed in an efficient and timely manner. Key to success is accessibility at each site and the importance of support from

appropriate vessels. Their study investigates two solutions to assess this issue; employing a time domain simulation package, Mermaid (Marine Economic Risk Management Aid), and an optimal 'fit for purpose' vessel design for efficient installation of marine energy technology. Mermaid is described as a transparent simulation package which is capable of presenting the anticipated downtime for marine installation operations by sequencing defined tasks against historical weather series. Additionally, Mermaid facilitates comparison between different vessels, ports and scheduling. By comparing the costs of traditional vessels from the oil and gas sector against the new vessel design within a Mermaid case study, it demonstrates that the improved capabilities and reduced day rate of the fit for purpose vessel can be easily quantified. Furthermore, the study emphasises the importance of completing weather risk assessments for marine energy based installations.

Walker et al. present a method to consider the availability of weather windows by employing a Weibull model [56]. This model uses cumulative distributions for the mean durations of persistence of exceedance. The Weibull approach accounts for the length of window at a specified threshold. This method is fairly simple and can provide a view on access and waiting periods in a timely manner. The approach is dependent on available and accurate observations and therefore a proven hindcast model was employed to provide input data. The method can identify potential delays or bottle necks for multiple project phases such as mobilisation, installation and decomissioning, which can aid budgetary assessments and inform planning of marine operations.

Chang et al. analyse weather windows employing nine years of wave data from two sites in Taiwan [57]. Their study considers two key factors: wave height limit and the length of available weather windows and they present various figures such as histograms, exceedance charts and probability of occurrence to convey

the weather conditions at the two locations. Furthermore they use occurrence percentage matrices and minimum, mean and maximum window lengths for a range of different wave height thresholds to identify the window availabilities of each site. It is acknowledged this study is limited to H_s assessments and that the methodology employed does not account for other conditions such as wind speed, wave period and ocean currents.

A weather window assessment completed by O'Connor et al. [58] across three sites aimed to quantify weather windows for operation and maintenance activities. The study developed work from previous assessments to complete a multivariate analysis of wave height, peak wave period (T_p), mean wind speed and tidal current speed. Percentage persistence tables and percentage access graphs for different window lengths and wave height thresholds are shown for H_s. It is stated that the H_s is still believed to be the predominant factor for accessibility in the majority of O&M applications but the other weather parameters may influence these outcomes, particularly if longer weather window durations are specified. The authors recommend that a minimum of five to ten years of historical data be used for weather window analysis.

Kikuchi and Ishihara investigate the assessment of weather downtimes for the construction of an offshore windfarm using wind and wave simulations [59]. They utilise both the Weather Research and Forecasting (WRF) model [60] and Wave Watch III (WW3) [61] for wind speed and wave simulations respectively. Their study considered three main construction operations: bottom preparation, substructure and wind turbine installation, as well as associated limits at two offshore wind farms in Japan. The authors define operational limits of each task, relevant to each operation and present the results in terms of percentage workability, i.e. the amount of time above the threshold available to complete the operations. It is noted that bias corrections were necessary when low wave

height and short wave periods were analysed, thus improving the accuracy of the predictions. It was also found that that the modelled data resulted in very similar workability percentages in comparison to observed weather data.

2.5 Stochastic Weather Models for Metocean Risk Modelling

O'Carroll, Bowers and Mould [43, 44] were among the first practitioners to apply metocean weather models for weather risk assessments in offshore construction. O'Carroll presents methods developed in British Petroleum (BP) to model offshore weather series that capture the same statistical parameters as included within three hourly observations of wave height and period. Firstly, the approach transforms the data, removing seasonal components and Box and Jenkins methods are used to model directly a synthetic bivariate series. This approach produces good agreement when compared to the observed dataset while it is noted that inaccuracies produced in a previous study by Jardine and Latham [62] were a result of inappropriate transformations. It concludes that linear time series models approximate the true wave conditions, although when a suitable transformation technique is used, the generated series is normally suitable for practical application.

Bowers and Mould [44] investigate the inclusion of a Markov weather model that incorporates a separate residence time to convey the distribution of different weather states. The Markov model is capable of categorising the weather and sea into a number of states based on operational limits. Their model is built to account for five different states and this division helps focus the modelling process on the areas of interest rather than reproducing data that precisely matches all

conditions at site. A simple Markov weather model and an adapted version that incorporates gamma parameters to improve the residence times at each state are compared to the observed data. It is found that the model with gamma features is close to the observed data, yet the gamma model still demonstrated some significant differences. The authors state that despite these discrepancies, this approach can help quantify the impact of varying start dates, the employment of different equipment options and inform managerial decision making.

There has been ongoing research on the development and application of environmental models to produce offshore weather series and notably the authors of the METIS toolbox, Monbet et al. [23], present a review of stochastic models to generate wind and sea state characteristics. Their study begins with Gaussian processes such as the Box and Jenkins [63] approach and the translated Gaussian process (TGP) [64]. The Box and Jenkins method is widely regarded as the most classical method, where the data is first made stationary by blocking it into monthly or seasonal sets and then applying a Box Cox transformation [65], which is used to transform non-normal variables into a normal distribution, thus facilitating a range of statistical tests [66]. A time series with a Gaussian-like marginal distribution is produced and finally an autoregressive integrated moving average model (ARIMA) model is fitted to generate the synthetic time series [63]. An ARIMA model uses the process of differencing many times, to reduce the forecast to an autoregressive moving average model (ARMA) [63]. An ARMA model relies on a set number of previous values in a given time series and memory function, denoted by the 'MA' or moving average, to produce forecasts. A moving average is a common technique to appreciate trends in data and is particularly useful for long term forecasts. It calculates an average on windowed subsets of data series, where the size of each subset is defined by the order of the MA model. TGP can be described in three steps. For a univariate process it starts by transforming the observed data into a Gaussian variable, then generating a second order random

time series with the same spectral properties. This second order time series can then be re-transformed back into a full univariate time series and it is noted that auto and partial correlation functions may reveal significant differences between the original and synthetically produced data.

Whilst these methods are less sensitive to noisy data, they are reliant on large data sets to generate estimates and have difficulty reproducing an accurate distribution of stormy and calm conditions within the generated time series. Non-parametric methods are investigated, including block resampling and resampling Markov chains [67, 68]. Block resampling is described as a method to implement bootstrapping techniques, where each 'block' is representative of a time step in the observed data set and random sampling of the blocks is used to reconstruct a sequence of values. This process demonstrates sensitivity to the size of block, as short blocks can struggle to replicate the existence of storms and larger blocks commonly reproduce the observed time series, negating any benefit from employing such models.

Resampling Markov chains such as 'nearest-neighbour' are also presented, which begin with a few starting values and search the data for the nearest lying neighbours to particular points. One of these neighbours is then randomly selected and allocated to the given time step in the series. Monbet et al. [23] also discuss the inclusion of selection weighting of closer points by introducing higher probabilities to these values. Further sophistications such as the Local Grid Bootstrap method have demonstrated good reproduction of the weather characteristics. Parametric approaches such as Artificial Neural Networks (ANN) [69], MS-AR [70] and GARCH [71] models are promoted for their ability in describing particular weather regimes. ANN models are described for application in short term forecasts and correcting meteorological models, although these models are inherently difficult to interpret. Alternatively, MS-AR models and

GARCH models are identified as easily interpretable and capable of restoring the weather regimes similar to those in observed data sets. These models can be reviewed and broken down to understand the embedded computations whereas ANN examples are less accessible for interpretation. It is remarked that choosing the correct model types can be time consuming, particularly when applying steps such as maximum likliehood and least squares. Assessments can be made using the statistical properties from each computation by applying Akaike information criterion (AIC) and Bayesian information criterion (BIC), which provide quantifiable values to identify the best model for the meteorological data.

Alliot et al. [70] investigate the specific application of homogeneous and non-homogeneous MS-AR models to produce wind time series. These models are composed of a blend of autoregressive model (AR) to describe the evolution of wind speeds over different intervals and the switching between each AR model is handled by a hidden Markov chain. An autoregressive model is a process that is able to forecast based on past values in a sequence or time series and is a form of linear regression. These past values are regarded as 'lags' and the order of an autoregressive model is defined by the number of lags used to generate the forecast. Furthermore, an assumed stochastic error term is included, which is fundamentally white noise with unit variance and mean of zero. Alliot et al. highlight that MS-AR models with Gaussian innovations are preferable to those with Gamma innovations owing to computational benefits and numerical problems associated with the Gamma case. The study demonstrates the operability of a homogeneous MS-AR model, which by applying a non-homogeneous MSAR model is expanded to account for diurnal and seasonal fluctuations. The impact of inter-annual variations observed in historical data, associated with climate change, are also considered with the recommendation for the potential inclusion of trend models to improve long term predictions.

Markov chains have been in many studies generate stochastic multivariate meteorological scenarios, which are then used to estimate the progression of planned installation operations, with respect to the metocean limits of each task [20, 22, 72, 73]. De Masi et al.[72] investigate the application of a first order multivariate Markov chain model to produce 20 years of synthetic time series for significant wave height (H_s), peak wave period (T_p) and wave direction. They demonstrate that the statistical properties such as mean values, correlations and probability distributions are reproduced in the simulated time series. The authors apply threshold (H_s) values to compare persistence and waiting times between operable weather windows and show similar distributions are produced by the model. This method provides a useful means for comparison of results and concludes that the outcomes from the Markov chain model are suitable to conduct operability analysis. The authors also suggest that the model could be extended to consider other meteorological parameters and highlight that varied temporal scales could also be applied to support the analysis of different marine operations.

Hagen et al. [22] present a multivariate Markov chain model to produce time series for wind speed (U), wave height (H_s), wave period (T), wind direction (Φ) and wave direction (Θ). Two methods of handling seasonal variations in an observed data set are presented, where the transition probabilities for the Markov chain and subsequent weather states are identified. In the first method, the transition probabilities are produced separately for each month and the transition to the next state is applied at monthly interfaces. The second approach applies a transformation, taking the empirical mean and standard deviation, implementing seasonal transitions without monthly restrictions. To assess the application of these models for offshore operation and maintenance tasks (O&M), they are reviewed in terms of persistence and waiting times for a specified weather window of $H_s \leq 2$m, $U \leq 10$m/s and $T \leq 5.5$s at three hour time steps. This assessment demonstrates that both model types can reproduce the persistence statistics in

the observed data with very slight variations. It is concluded that both Markov chain models are suitable to assess the weather availability for marine operations, but are dependent on suitably long observed data sets in the region of 20 years or more to prevent replications in the simulated outcomes.

Leontaris et al. [74] indicate that large observed data sets of approximately 20 years are required in order to produce useful meteorological estimates from a copula model. The scarcity of long observed environmental time series is a key driver for their study, where they use copulas to reproduce multiple years of wind speed (U) and significant wave height (H_s). Copulas are defined as functions that are capable of joining multivariate distributions, which can be broken into univariate marginal distributions with a copula to describe the dependence between random variables. The authors review the dependence of U and H_s by considering three copula families, Gaussian, Clayton and Gumbel. They identify that the Gumbel copula describes the dependence between both parameters for all months with the exception of November and December, where the Gaussian copula was selected. To compare the 1000 years of simulated U and H_s time series against 10 years of observations, the mean monthly workability and persistence of weather windows were reviewed for six hour time steps. Primarily, one operation of $H_s \leq 1.5$m and $U \leq 12$m/s is defined to assess the persistence and mean workability characteristics. It is shown that the mean workability and persistence cumulative distribution functions (CDF) are very similar to the observed data and confirms that this method can reproduce realistic time series and also highlights the importance of the correlation between U and H_s. To assess the progression of sub-tasks below six hours within an infield cable installation scenario, linear interpolation of the generated time series to hourly time steps is discussed. This improves the resolution of the simulated data and it shows that scaling up the time series in this way leads to similar results, as observed with six hour intervals. Finally, the impact of dependently and independently produced environmental

parameters is discussed with the caveat that if the dependence between variables is ignored in similar models, this will reproduce inaccurate time series.

Brokish et al. investigate the pitfalls of using Markov chains to produce synthetic wind data [73]. They found that, Markov chains are inappropriate for time steps shorter than 15-40 minutes, subject to the order of the Markov chain used. They state that despite Markov chains ability to reproduce the probability density function of wind data, they are limited in scope for time dependent analyses such as energy storage requirements. They recommend that new methods be developed to generate the required probability density function for short time steps, whilst replicating autocorrelation in the observed time series.

Stefanakos et al. develop and validate a composite stochastic model for significant wave height (H_s). Their model builds on previous work and is capable of resolving seasonal and inter-annual variations by using a state-by-state process [75, 76]. The approach can use different sources of wave height measurement to estimate the parameters of the model. Buoy measurements were used for the state-to-state correlation structure and satellite measurements are used to assess seasonal patterns and variabilities. This process effectively uses the satellite measurements to 'de-seasonalise' the buoy data. The analysis of the de-seasonalised measurements is therefore assumed to be a stationary stochastic process, which allows the autocorrelation to be calculated and the correlation structure from state-to-state. They indicate key advantages such as no gaps in the data when using such a model in comparison to measured H_s time series.

Guanche et al. present a methodology to simulate trivariate sea states [77]. The three parameters of interest are H_s, mean period (T_m) and mean direction (θ_m). The methodology combined univariate ARIMA models and cross correlation with an autoregressive logistic regression model. This approach allowed the generation of varied atmospheric scenarios relating to daily sea level pressure (DSLP) and is

adaptable to multiple locations of interest. The model produces good agreement for the trivariate series and can account for climate change effects using future DSLP projections, but further analysis is required to validate this feature. It is noted that the model may be limited in its ability to describe extreme conditions and that by fitting a Pareto distribution, the adaptability of the model may be improved.

Pérez-landa et al. compare the results from a one year simulation of H_s and T_m using four different models for the Liverpool Bay area [78]. The models assessed are wind forcing using global and mesoscale sources, shallow water models and varied spatial resolutions. A comparison against a wave rider buoy in the same location showed that the wind forcing using mesoscale approach outperformed the global case. Furthermore, improved resolution and shallow water paramerisations using SWAN [79] produced good results. They advise that a high resolution approach should be used where possible to accurately assess the progression of marine operations, whereas lower resolutions may lead to inaccurate predictions.

Kerkhove and Vanhoucke investigated an approach to improve the accuracy of offshore construction simulations using an integrated weather model to account for the uncertainties of activities [30]. Furthermore, metaheuristic optimisation and dedicated heuristics are used to optimise project planning in combination with a weather model. Their weather model uses a combination of transition probability matrices and Weibull distributions to reproduce realistic wind speed and H_s conditions, introducing conditional probabilities to account for the correlation between both parameters. A first order Markov chain is used to simulate the wind speed and two methods for H_s: a second order Markov chain and a correlated approach employing a Weibull method considers the available wave states given the distribution of wind. The second order Markov chain allows for the simulation of the wave height given the current wind state, thus accurately replicating the

correlation between both parameters. It is noted that there may be insufficient data to accurately inform the first model to recreate wave data and the Weibull approach is capable of addressing this issue.

Pinson et al. reviewed regime switching modelling for the simulation offshore wind conditions [80]. They investigated two approaches: self-exciting threshold autoregressive model (SETAR) and self-exciting threshold autoregressive model (STAR) models in comparison to MSAR models. They state that SETAR and STAR models use explicit rules to determine the current weather regime in contrast to the hidden Markov process employed within MSAR models and compare the models using observations at one, five and ten minute intervals. They identify that the MSAR models managed to capture the influence of more complex weather patterns and therefore outperformed the SETAR and STAR approaches at these temporal scales and also state that the SETAR and STAR models offer no real advantage when compared to more simplistic models such as ARMA.

2.6 Literature Summary

The literature review has covered a range of topics relating to offshore wind installation, marine risk management practices and modelling in the metocean context. The topics have relevance to the intended focus of this thesis and this short summary aims to direct the reader to the most pertinent issues that were carried through into fully developed studies, driven by the needs of EDF Energy R&D.

In terms of the risk management standards, the detail included for weather restricted operations in Section 2.3.1 had considerable relevance for offshore wind

installation downtime assessments under investigation in EDF Energy. International standards such as ISO 19901-6:2009 [13] and ISO 19901-1:2015 [14] present core considerations to determine the limiting metocean conditions for several operations, structures and operational states. Furthermore, standards such as those provided by DNV GL [17], [15], build on the international standards, providing clear definitions of operational durations and when subsequent metocean restrictions or weather monitoring should be applied during the planning of marine operations, as summarised by 2.3. Indeed, it is emphasised that metocean operational limits are necessary to ensure the operations are conducted safely and within the operational design criteria of the structure, installation vessels and equipment in hand. The application of the alpha factor is prescribed when there is uncertainty in weather forecasts during offshore activities, which are informed by different levels or qualities of forecast. This guidance has highlighted that these factors should be well understood to ensure that the limits to operational tasks are adequately captured during modelling and simulation of marine operations, thus generating relevant downtime estimates.

As a number of offshore wind developments were underway within EDF Energy, there was an immediate need to model the marine operations related to each project against anticipated weather conditions. A review of various different metocean modelling techniques was completed in Section 2.4. A range of publications were reviewed that demonstrated the application of logistical scenarios to appreciate the sensitivity of installation strategies, vessel types and pre-installation strategies. These studies highlighted the relevance of modelling marine operations with different techniques such as MILP, VNS, Markov, Monte Carlo and time domain simulations, including the application deterministic and stochastic metocean data. The review highlights the benefits of recursive analyses offered by Monte Carlo approaches and estimates produced from multiple stochastic weather

series, as they can generate informed estimates of residual metocean risks for marine operations. Additionally, different metrics such as the cost of the operations, percentage increase, days/MW and overall days of downtime are used to compare the sensitivity of the operations, vessel or equipment under review. An off-the-shelf metocean modelling environment, Mermaid, was identified as a readymade time domain simulation tool, which incorporated a number of standard practices reviewed in Section 2.3.1, such as alpha factors and learning rates.

An investigation of stochastic weather models was completed to support the selection of a suitable modelling methodology in a next generation metocean risk simulation tool within EDF Energy. Section 2.5 investigated a range of different metocean models and from direction from EDF R&D in France, there was interest to incorporate a hybrid metocean model within the next generation prototype. A thorough review of different time series modelling methods is presented such as Markov chains, copulas, ANN and AR models including variations such as ARIMA and ARMA. It was evident that many of the techniques incorporate Markov chains, which are useful as they can define the transition to different weather patterns present in historical data and can therefore support the generation of realistic metocean conditions. A flexible and interpretable MS-AR method from [70] was reviewed, which facilitates the transition of weather types during autoregressive simulation of metocean data. The literature also highlights that metocean simulations should respect correlations that exist between two or more weather parameters, whilst significant wave height (H_s) is widely regarded as the most sensitive metocean parameter for marine operations. This review highlighted the availability of the METIS Matlab toolbox [81] and the embedded MS-AR model was selected for investigation and adaptation in Section 3.3.

Chapter 3

Methods to Improve Metocean Risk Management in Offshore Wind Installation

In this section, the methods that were devised and implemented throughout metocean risk management research are presented. The EDF R&D computer model 'ECUME I' is first introduced; this was originally developed to assess and predict delays that could be experienced during the installation of an offshore wind farm, through the execution of a variety of marine operations. To demonstrate suitability of ECUME I for predicting installation risk across a range of project phases, a case study is applied that considers the assessment of vessel technology trends framed across the three offshore wind rounds in the UK. The limitations of using this tool, particularly for more complex and intermediate operations are also discussed.

The application of a commercial software metocean risk software Mermaid and

the methods applied in the assessment of two offshore wind projects are also presented, highlighting the improved flexibility of this tool in comparison to the ECUME I solution. Two approaches are proposed, each of which are implemented depending on the size of project to be modelled and analysed. The benefits and limitations of each modelling approach are discussed in more detail in Sections 5 and 7.

Based on the experience using the ECUME I and Mermaid, this inspired the specification of a next generation marine operations simulation tool within the EDF R&D teams in the UK and France. A process of workshops, prescribed improvements and concurrent development was completed as a part of a collaborative activity between UK and French teams throughout the course of this doctorate project. The most significant research contribution in this activity was the development of a stochastic weather model, which was required to produce a large number of annual wind speed and wave height time series. By producing a large number of metocean time series that fairly represent the conditions at an offshore site with similar characteristics, this supports the quantification of the residual risks when predicting the progression of marine operations. The development of the metocean model and overarching methodology, which utilises a Markov Switching autoregressive model, is described in Section 3.3.

3.1 Comparative Vessel Assessment with ECUME I

3.1.1 ECUME I overview

This study assesses the installation modelling for UK offshore Wind Rounds 1, 2 and 3. The analysis is based on time-domain predictions for the completion of key installation operations under user specified exceedance probabilities, commonly used by investors to determine a project's viability and used by developers to assess their risk preferences. By varying key wind farm characteristics, an assessment on the performance of typical installation vessels adopted for each of the UK development rounds is investigated with the use of EDF's existing installation decision support software tool.

EDF Group have developed a tool to assess the installation of an offshore wind farm in advance, prior to construction known as 'ECUME I' which is shown diagrammatically in 3.1.This tool currently provides results detailing schedules, vessels, and installation costs, aiding the decision process by providing an unlimited range of exceedance probabilities such as P50 and P90 values. A comparative analysis of the predicted durations between each of the three offshore wind rounds is completed. It is intended this analysis will help inform planning operatives when considering vessel selection in their next project and reveal if further innovation is needed to overcome delays when developing future OWFs.

ECUME I accounts for elementary tasks that form the basis of offshore subtasks in the software, which can then be combined in sequences to resemble an operation. The associated weather limits for both the operation and vessels can be defined by the user, based on known specifications or restrictions included in the planning

documentation. The tool uses historical meteorological data in .csv file format, drawing on inputs for wind speed, wave height, wave period and current speed. ECUME I then applies a Markov chain to produce stochastic weather patterns across specified dates using the historical data as a reference. The Markov chain simulation generates numerous weather scenarios with similar characteristics as the historical data series, which provides a basis to repetitively simulate the specified marine operations and quantify the weather risks associated with the installation vessels or operations. Within each simulation the given weather scenario determines if vessels or operations may progress or be delayed and cumulative outputs produce the resulting duration for a particular installation phase that are presented under user defined exceedance probabilities. The inputs and resulting prediction methods of ECUME I align sufficiently with DNV's recommended practice for modelling and analysis of marine operations in the time domain [82].

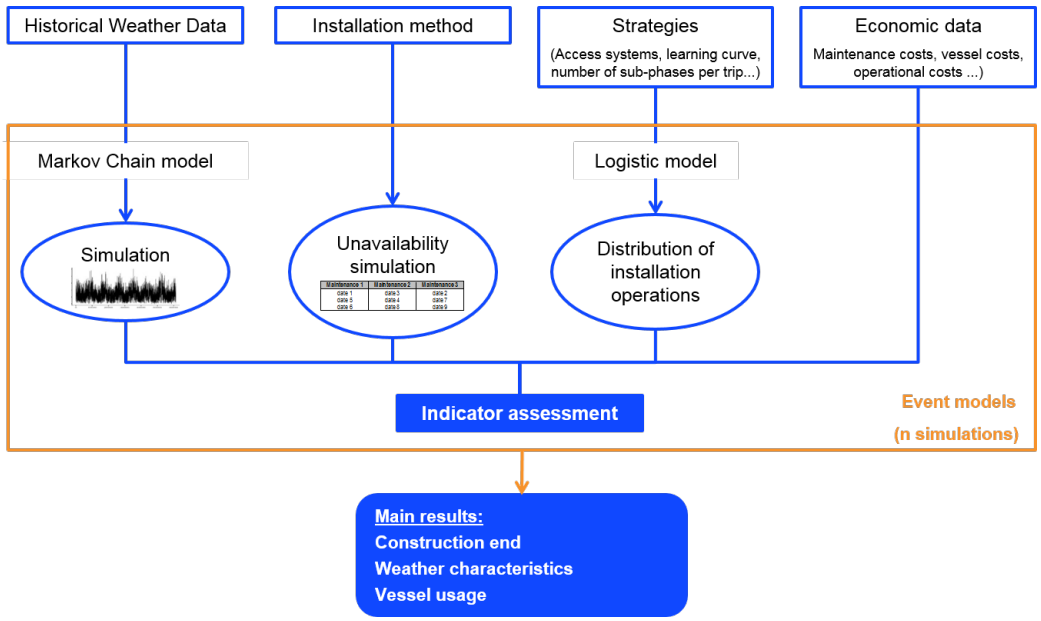

Figure 3.1: ECUME I simulation tool schematic

3.1.1.1 Meteorological Model

The software tool relies on Monte Carlo methods to simulate multiple independent scenarios of the defined installation strategy for an offshore wind farm. The tool considers risk as delays to the installation, imposed by adverse weather conditions. A hidden Markov model (HMM) model [83] has been used to generate each meteorological scenario, informed by historical weather data, which begins with the evaluation of a transition matrix A for the Markov chain. This matrix represents the evolution of the weather parameters: wind speed (U_t), wave height (H_{s_t}) and speed of the sea current (C_t). For the assessments completed in this project, the wind speed and wave height characteristics are the only weather conditions evaluated. Meteorological parameters are intrinsically stochastic but also exhibit some continuity over time. Therefore, at any one time, if the sea is in a certain state, it is more likely that the next time (one hour, for example), the sea will remain in the same state. The main characteristic of a Markov chain is that the next state depends only on the state at the current point in time, which is described by Figure 3.2. If the probability of moving from one state to another is known, then it is possible to generate meteorological parameters and thus to obtain a new weather scenario.

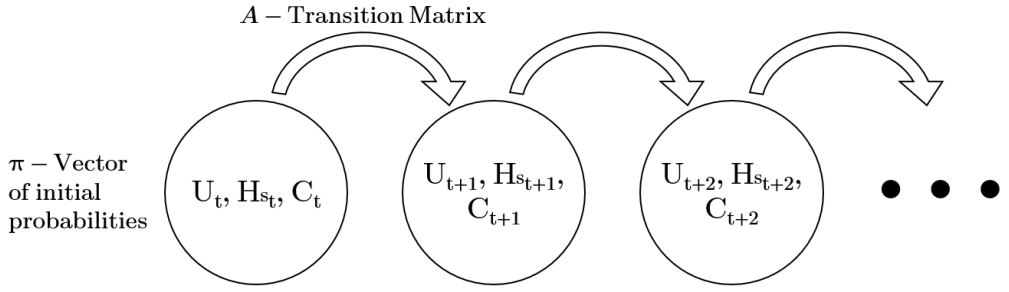

Figure 3.2: Schematic representation of the Markov chain: wind speed (U_t), wave height (H_{s_t}), current speed (C_t).

Each element of the transition matrix A, is the probability for the arrival of state

j, knowing the initial state i. A is a matrix of size $n * n$ with n the number of states of the Markov chain. The vector π of the initial probability array of the hidden states is also determined for chain size n. It is possible to obtain empirical estimates of this matrix and vector by:

$$A = (a_{i,j})_{1 \leq i,j \leq n} \quad \textbf{and} \quad \pi = (\pi_i)_{1 \leq i \leq n} \tag{3.1}$$

where:

$$a_{i,j} = \frac{number\,of\,transitions\,i \to j}{number\,of\,transitions\,from\,i} \quad \textbf{and} \quad \pi_i = \frac{number\,of\,observations\,in\,the\,state\,i}{total\,number\,of\,observations}$$

For a given initial state, the number of arrivals of possible states is relatively low, with a maximum of 30. Thus the matrix A, contains many zeros and forms what is called a matrix dig. For each initial state i, it is best to store only the non-zero values $\tilde{A}(i)$ and associated indices $P(i)$, which are defined as:

$$P(i) = j | a_{i,j} > 0 \quad \textbf{and} \quad \tilde{A}(i) = (a_{i,j})_{j \in P(i)} \tag{3.2}$$

Once the estimated transition matrix is established, the software will simulate a weather scenario over a period specified, which corresponds the maximum installation duration envisaged by the user. The software simulates the weather at the time $i + 1$, knowing the state of the weather at the time i according to transition matrix. The method relies on a monthly transformation in the data in order to 'normalise' the environmental data to a stationary form, which is inspired by [84]. The transformed data is assumed to be an embodiment of a Markov chain and the matrix A, and the vector π are estimated on these transformed

data. After the simulation of the Markov chain is applied, the monthly outcomes are reconstructed into one meteorological scenario. An overview of these steps is demonstrated by Figure 3.3.

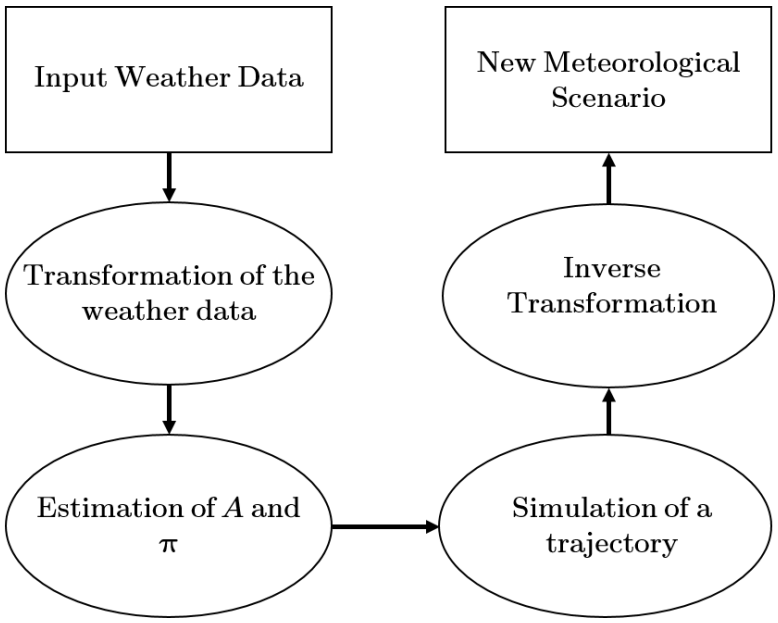

Figure 3.3: Schematic of the principal method

$X_{i.k} = (X_{i.k}^{(1)}, X_{i.k}^{(2)}, X_{i.k}^{(3)})$ is regarded as the vector of three meteorological parameters for the i-th observation, during month number k, $k \in \{1, 2, 12\}$. The monthly processing carried out in the method is as follows for each of the parameters $h\{1, 2, 3\}$:

$$y_{i.k}^{(h)} = \frac{X_{i.k}^{(h)} - \mu_{i.k}^{(h)}}{\sigma_{i.k}^{(h)}} \tag{3.3}$$

where:

$\mu_{i.k}^{(h)}$ and $\sigma_{i.k}^{(h)}$ are the mean and standard deviation of the parameter number h over the month number k. The meteorological parameters are supposed to take their values in a discrete space and have a finite number of states.

A given meteorological scenario is used directly within each Monte Carlo simulation to calculate a duration for each primary installation phase. In the analysis to follow, eight installation phases are considered within this study, which are: Dredging & Survey, Foundation, Transition Piece, wind turbine (WTG), Scour Protection, Pre-lay Grapnel Run (PLGR), Cable Installation and Cable Burial. These phases include sequences that are comprised of sub-tasks, elementary to the operations. The tool allows phases to be suspended once a sequence has been completed and uses their base duration to determine if an adequate weather window is available or if the vessel should hold station offshore. A weather window can be defined simply as weather conditions that are predicted to stay within the environmental limits of a sequence for a specified duration.

Once the software has computed the predicted durations, these can be processed to reveal the average Installation Rates (IRs) and WDT for each installation phase. The P90 exceedance quantile was selected as the referenced result category, providing 90% confidence that the predicted durations will not be exceeded. The numerical results allow the calculation of key performance indicators (KPIs). In this study, the duration for each phase is divided by the number of wind turbines associated with the given model to reveal an average IR in days per turbine (days/WTG). Similarly, the base unweathered duration for each installation phases is deducted from the predicted duration to reveal the average weather downtime (WDT) that can be expected for each turbine location under the individual phases. These IRs and WDT values can then be generally compared between the rounds to assess the impact of vessel technology. Additionally, the variation about the mean IR and WDT predictions can be used to estimate the installation risk that may be anticipated for each installation phase.

3.1.1.2 Model Calculations

The methodology applied within ECUME I for the execution of installation phases is summarised in Figure 3.4 and is extracted from original ECUME I documentation used to specify the development of the software tool [85]. The following text describes the functionality of this methodology in the ECUME I tool.

Firstly, the ship to be used for an installation phase is mobilised. The vessel goes offshore as soon as it's transit weather limits are satisfied. Next the logistics process, as outlined in Figure 3.4 is used to apply the installation phases considering the make-up sequences and tasks within each phase. This process initially recognises the steps that were not completed in the previous weather window and the process begins at the first of the remaining sequences, alternatively the tool identifies the maximum number of repeated phases to be handled by the vessel and if it is within these bounds, the process begins with the next phase in hand. It is determined if a weather window exists, where the environmental limits of the next sequence are satisfied for the corresponding duration. If the conditions are not satisfied, the software continues to search for a suitable weather window and if none are available, the vessel holds it position. This stands unless the weather conditions become worse than the waiting condition limits for the vessel, meaning the vessel returns to port and awaits the next opportunity to set sail to site.

The completion of each sequence marks the end of the weather window search and the tool assesses if the vessel can remain on site, either by the maximum number of phases or by the predicted weather conditions. Again, if poorer weather is predicted and the environmental limits allow, the vessel can hold it's position offshore. If the vessel is in the middle of a current phase or there are phases

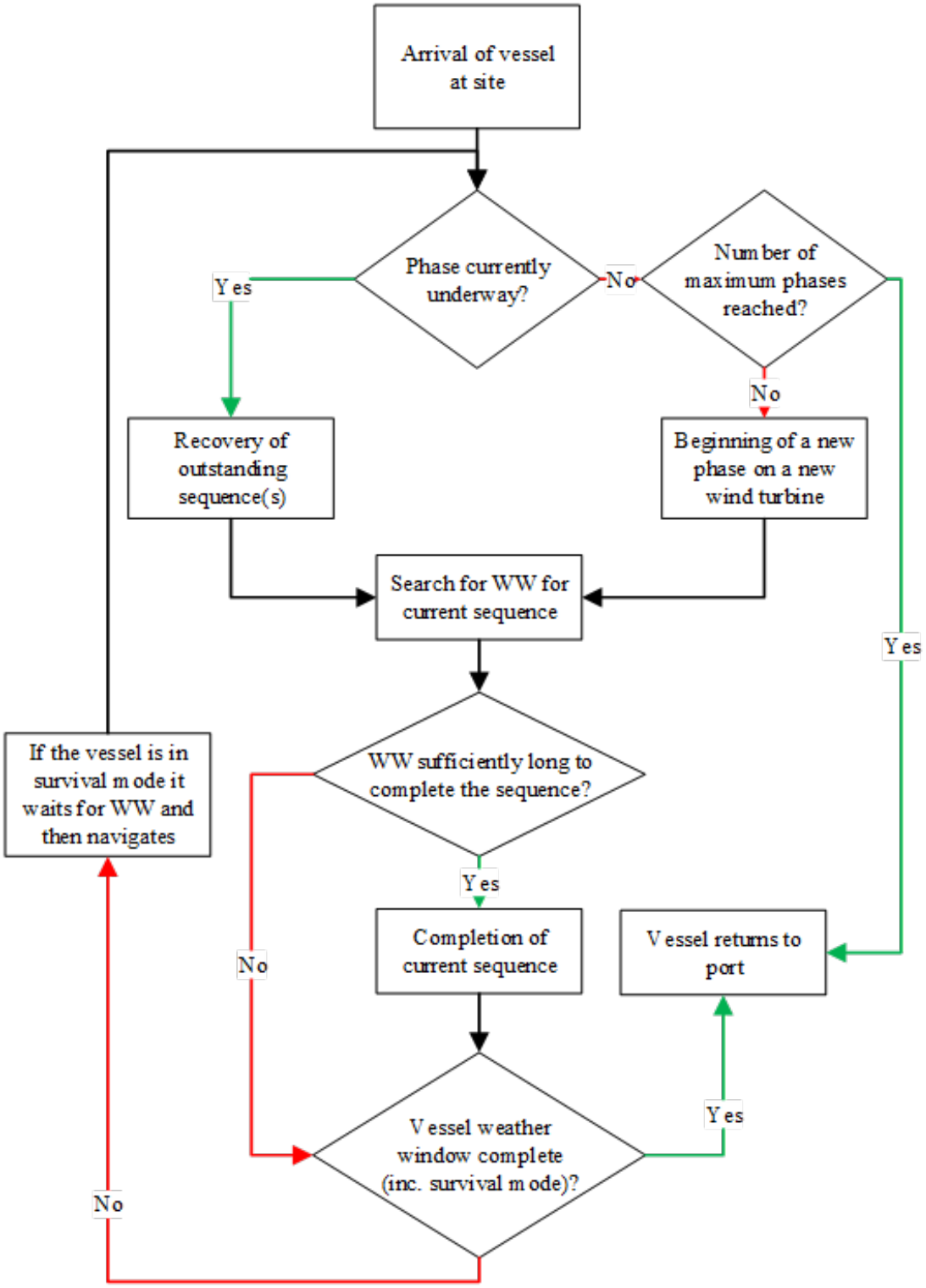

Figure 3.4: Flowchart of ECUME I logistical process [85]

to complete, the process starts over and searches for a window to complete the next sequence. This iterative process summarised by Figure 3.4 continues and is applied to all installation phases until they are complete for each wind turbine location, after which the vessel for the given phase is demobilised and the next vessel begins the subsequent phase in the defined schedule. Finally, the process is complete when the maximum number of Monte Carlo simulations has been reached. The predicted durations for each installation phase are presented with a start and an end date. These dates are recorded under user-specified exceedance quantiles such as P50, P70 and P90. It is these predicted durations that are used as the main source of results in this study, as presented in Section 4.1.

3.1.2 Offshore Wind Installation Vessel Downtime Analysis - Data and Inputs

This subsection outlines the methodology that was developed using ECUME I to complete an assessment on the predicted performance of offshore wind installation vessel technology, synonymous of typical vessel spreads used throughout the first three UK offshore wind rounds. The vessel types employed in each round are analysed to identify the variation in installation durations, weather downtime and draw industrial perspectives.

3.1.2.1 Meteorological Data

Meteorological data was obtained from separate hindcasts used for the three offshore wind rounds. In each simulation, a single metocean time series is used to inform the HMM, which generates 1000 stochastic weather scenarios. These scenarios provide a basis to assess the progression of the installation phases by

considering the environmental limits of the sub-tasks and vessels specified for each round. Data from Teesside, Greater Gabbard and Blyth Offshore Demonstrator wind farms was selected, representing Rounds 1, 2 and 3 respectively. The wind speeds in each data set are referenced at 10m. Teesside offshore wind farm is located off the north east coast of England and its near shore location is synonymous of a Round 1 project. The data set was developed by a private consultant, drawing on field and modelled data to construct a metocean time series. For Round 2, publicly available data for the Greater Gabbard offshore wind farm was sourced from The Crown Estate's Marine Data Exchange [86]. Greater Gabbard is located off the English Suffolk coast and is close to the average distance of all Round 2 sites. The Round 3 data was sourced from a privately commissioned metocean study for another upcoming EDF Energy development in the north east of the UK, which will be referred to as 'UK North East' herein.

3.1.2.2 Wind Farm Characteristics

The key OWF characteristics for each project within the thre offshore wind rounds have been reviewed based on the information included in [87]. This identified mean, maximum and minimum characteristic values across all of the OWFs in each round. The characteristics varied within the simulation tool and the values identified for each round are listed in Tables 3.1 and 3.2. For each OWF round, 11 cases were simulated, beginning with a mean case for all parameters and then varying one parameter at a time with either a maximum or minimum value. Two 'extreme' cases are included, comprising of maximum and minimum case for the number of turbines and distance to shore combined. To consider the impact of start date selection, three dates were selected to investigate the impact of seasonality across the two rounds. April was chosen to resemble construction beginning in the spring, August for summer and December for a winter start.

Table 3.1: Round 1 OWF characteristics

Parameter	Maximum	Mean	Minimum
No. of turbines	60	31	2
Expected start date	01/04/2017	01/08/2017	01/12/2017
Inter-turbine distance (km)	0.82	0.67	0.46
Distance to shore (km)	11	6	2

Table 3.2: Round 2 OWF characteristics

Parameter	Maximum	Mean	Minimum
No. of turbines	175	93	18
Expected start date	01/04/2017	01/08/2017	01/12/2017
Inter-turbine distance (km)	1.08	0.84	0.63
Distance to shore (km)	40	19	7

Table 3.3: Round 3 OWF characteristics

Parameter	Maximum	Mean	Minimum
No. of turbines	400	251	102
Expected start date	01/04/2017	01/08/2017	01/12/2017
Inter-turbine distance (km)	1.51	1.02	0.78
Distance to shore (km)	190	93	25

3.1.2.3 Vessel Technology and Spreads

From reference to the consenting rounds listed in [87], an assessment of the vessels used across all of the OWFs was completed to identify the typical vessel spread used within in each round. It is accepted that the categorisation by UK Offshore Wind rounds does not mean all construction activities were completed within

an allocated time frame, as some Round 2 sites were installed before Round 1 projects. However these general categories were used to gauge the impact of step changes in vessel technology.

To identify the main vessel types used to install or planned for installation of each OWF, reference to the vessel listings for each respective wind farm on 4C Offshore were used to populate a vessel database for each round [88]. Using the main installation phases as a guide, the vessel database for each round was then assessed to reveal the most common vessel type chartered for each phase. This produced a representative vessel spread for each round. It should be noted that the vessel spreads for each round, included in Table 3.4, are based on the transparency of information published on the 4C Offshore website. The references give more detail on the general vessel type and a full list of vessel characteristics used in the study are appended in Appendix A.

For each vessel type identified and listed in Table 3.4, the referenced vessel specifications were used to generate approximations for the loaded and unloaded transit speeds in conjunction with survival limits for wave height and wind speed. Where some environmental limits were not listed on the specification sheets, generic references or limits for similar vessels were used to approximate the relevant values [89] [90] [91] [92] [93]. Whilst this information is sufficiently detailed for modelling, analysts will have more specific information from the vessel operators to plan the marine operations. The commissioning phase of the wind farm, which predominantly uses crew transfer vessel crew transfer vessel (CTV) to transfer technical personnel to the turbines, has not been considered.

Eight offshore installation phases were considered for analysis and are summarised in Table 3.4, which specifies the installation phase and vessel used in the model set-up. It should be noted that all vessels are assumed to have the capacity to remain offshore to complete the work at all turbine locations, with the exception

Table 3.4: Vessel types and spread by round

	Round 1		Round 2		Round 3	
Phase	**Vessel Type**	**Ref.**	**Vessel Type**	**Ref.**	**Vessel Type**	**Ref.**
Dredging & Survey	Injection Dredger	[94]	TSHD	[95]	TSHD	[96]
Foundation	WTIV	[97]	Heavy Lift Vessel	[98]	WTIV	[99]
Transition Piece	WTIV	[97]	Floating Crane	[100]	WTIV	[99]
WTG	Jack-up Barge	[101]	WTIV	[97]	WTIV	[99]
Scour Protection	Rock Dump	[102]	FPV	[103]	FPV	[104]
PLGR	Multicat	[105]	Offshore Vessel	[106]	Multicat	[107]
Cable Inst.	Barge	[108]	CLV	[109]	CLV	[109]
Cable Burial	MPSV	[110]	MPSV	[111]	MPSV	[112]

of the vessels used for the foundation, transition piece and WTG installation phases, which are limited to a maximum of three turbine locations per voyage. This limitation is discussed further in Section 8.2.1.

Figure 3.5: TSHD Dredger [113]

Each phase and vessel choice for the different rounds is described in the following passage. The dredging and survey phase prepares or clears the seabed before the main OWF construction activities begin and ensures the work has been completed to a sufficient standard. Dredging is not required for all projects but has been included to acknowledge some form of seabed preparation common to many sites. It is assumed that the dredging phase follows on from and is

prescribed by, an extensive seabed survey. This is completed in advance of the main construction activities to inform project teams of any unexploded ordnances, potential obstacles, seabed integrity, the applicable foundation type(s) for the site and the extent of dredging operations required. A dredge vessel can be fairly simple, consisting of a barge equipped with a backhoe excavator to more advanced dynamic positioning (DP) vessels that include trailing suction hopper dredger (TSHD) technology as shown in Figure 3.5[114]. Less sophisticated dredgers were used in earlier UK projects, but as installations have moved further from shore, developers have discarded traditional monopile foundations for gravity based or jacket structures. This requires improved accuracy and demands better manoeuvrability of the dredge vessels, and is heavily reliant on the most advanced technology available to developers.

Figure 3.6: Svanen heavy lift vessel installing a monopile [115]

The second phase considered is the foundation installation phase. From review of the vessels used for foundation works across all 3 rounds, it is evident that different types of vessels have been employed to deal with the variation or trends in foundation type used between rounds [87]. The majority of Round 1 sites

adopted monopile foundations, as these could be installed quite easily in the nearshore locations synonymous with the majority of these sites. This type of installation can be handled on board jack-up barges and dedicated wind turbine installation vessels (WTIVs) and these types of vessel were identified as the most common vessels in Round 1. Round 2 sites are generally greater in size and located farther from shore, leading to more challenging conditions for installation. This shift presented further logistical challenges and often heavy lift vessels as shown in Figure 3.6 that could deliver and install foundations were employed to reduce materials handling at the offshore locations. More recently, the new breed of WTIVs, boasting increased deck space, lifting operability and survival capabilities are expected for use in Round 3 foundation installations. These vessels were built specifically for the demands of future European sites located in deeper water and farther from shore, similar to the UK's Round 3 sites. It is expected that these vessels will cope with variable foundation types such as tripods or jackets, which are likely to become more common throughout Round 3 whilst still reducing overall installation durations.

Figure 3.7: MPI Discovery WTIV transiting with monopiles and transition pieces[116]

The installation of the transition piece, which is the structural section that links the monopile and wind turbine, is the next installation phase. The transition piece provides a fendering area for crew transfer vessels to interface with the structure and a ladder for personnel to climb onto the platform before entering the turbine for either construction or maintenance tasks. In some projects the transition piece is installed onto a jacket or tripod foundations, but as a significant number of the Round 3 projects still incorporate monopile designs, this phase has been modelled and assumed to occur as part of the Round 3 sites. Similar to the foundation phase, heavy lift or dedicated WTIVs are hired for these construction activities as demonstrated in Figure 3.7. The transition piece must be hoisted into position and lowered onto the monopile foundation before grouting operations fix this intermediate structure in place.

Figure 3.8: Brave Tern WTIV Installing a turbine blade on a jacket foundation[117]

The wind turbine installation phase was found to adopt some form of dedicated WTIV across all three OWF rounds. These vessel types incorporate four to six legs that rest on the seabed and elevate the main body of the WTIV above the water. This protects the vessel from wave heights between 1.5 - 3 Hs, depending on vessel design and helps stabilise the lifting operations. The whole lifting process

remains sensitive to the conditions, particularly wind speed, and when individual blades or assembled rotor sections are hoisted, the environmental limits are often lowered. These vessels are also used to transport between three to eight turbines at a time, depending on the available cargo capacity and the installation strategy adopted. A number of different WTG installation strategies have been used in various projects as presented in [114]. These range from individual sub-section lifts for the towers and single blades through to fully assembled turbine lifts. It is assumed that the lifting strategy is identical for all three rounds to limit the amount of modelling permutations considered. The 'bunny-ear' configuration with a two stage tower lift was selected as the most applicable strategy as this presented a compromise between fully assembled and an individual component installation, which is exemplified in Figure 3.9.

Figure 3.9: Brave Tern WTIV Installing a 'bunny ear' rotor assembly[118]

In the bunny ear installation strategy the upper and lower tower sections are connected on land, as with the rotor, which is pre-assembled, consisting of a

nacelle and 2 blades attached. This results in a total of three lifts at the turbine location beginning with the tower, then rotor and finally the third blade [119]. It should be noted that the reference duration for the WTG installation in Table 3.5 represents the approximate time to install each turbine using the bunny-ear configuration and this figure would fluctuate for each of the WTG installation methods included in [39]. In Round 1, jack-up barges without their own means of propulsion were commonly used. These vessels often have modest elevation heights and are dependent on other vessels such as anchor handling tugs (AHT) to transit and manoeuvre the barge to each wind turbine location. Self-propelled jack-ups started to be used in Round 1 but were more commonly chartered for Round 2 projects and an example vessel during a bunny ear lift is shown in 3.9. This next stage in WTIV design presented improved manoeuvrability, elevation heights and deck space, offering improved cargo capacities and logistical options. As many of the Round 3 sites are not completely installed, it is assumed the most advanced WTIV types will be used as much as possible.

Scour protection is installed to prevent structural instability around the foundation of an offshore wind turbine induced by tidal flow or wave action. The specific solution depends on the foundation selected, the long-term meteorological conditions and the seabed material. Rock-dumping is often used to place variable grades of stone around foundations or protection may be placed over vulnerable cable lengths in the form of concrete mattresses. This phase can be completed with a hopper barge and towing tug or more commonly with a dedicated side stone dumping vessel or with more sophisticated fall pipe vessels (FPV) as shown in Figure 3.10. It is assumed in these analyses that the scour protection is installed around the base of the mono-pile foundations.

The pre-lay grapnel run (PLGR) is used to clear debris along the cable route before installation, ensuring that hazards do not interfere with cable laying and

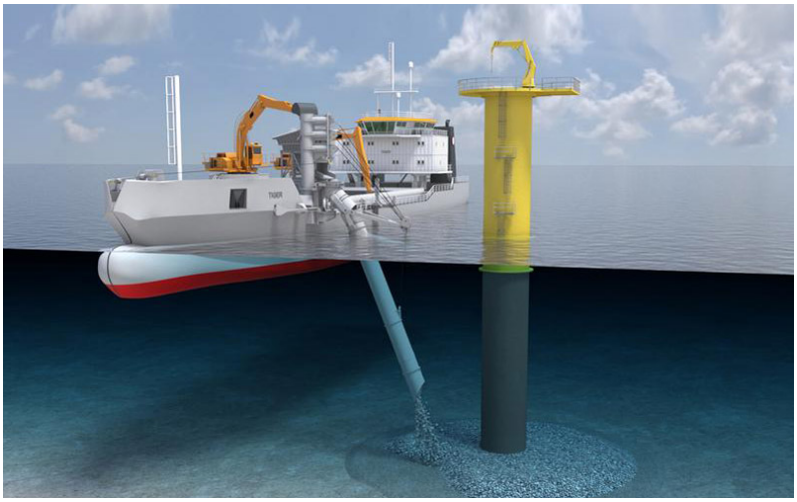

Figure 3.10: Flexible FPV installing scour protection [120]

burial phases or during future maintenance operations [121]. A hook-like anchor is pulled during this process and relies on the forward motion of the vessel to work the seabed, creating a narrow trench of approximately 1 m depth along the cable route. A multi-purpose workboat with a bollard pull of roughly 20 tons is normally used for this activity such as the multicat shown in Figure 3.11.

Figure 3.11: Zwerver III multicat [122]

Cable laying operations require a dedicated cable lay vessel (CLV) to lay the inter-array cables between the turbines and export cable to the onshore substation or from the offshore substation to the cable landfall point. Due to the near shore, sheltered conditions, earlier projects often employed adapted barges that feed out cable from a pre-installed cable carousel [123]. These rely on other vessels to tow and install anchoring arrangements to keep the barge on the designated cable path, as these vessels are not equipped with DP systems. It is assumed that this type of installation was used for the Round 1 project and is modelled with a transit speed that resembles the speed of an AHT, of between 6 - 8 knots. In some instances, an adapted supply vessel was used to take advantage of the DP capabilities, but for the majority of the round two and three projects, specifically designed CLVs were employed to cope with more extreme conditions and exposed cable routes, shown in Figure 3.12. Many of these vessels can handle simultaneous laying, trenching and burial operations, but often a secondary vessel is used to complete the trenching and burial phases [124].

Figure 3.12: Cable Lay Vessel [125]

In this study, the cable burial phase is assumed to enclose both the trenching process and final burial of the cable. This study also assumes that a post-lay burial operation is applied in both rounds utilising a secondary multipurpose

service vessel (MPSV) or large survey vessels. This 'lay and trench' technique deploys an remotely operated trencher from the parent multi-purpose vessel to trench around and bury the cable in one operation. The main logistical steps of this phase are assumed to relate to the parent multi-purpose vessel and the burial duration listed in Table 3.5 was selected on a per wind turbine basis.

3.1.2.4 Operations, Environmental Limits and Durations

To assess the vessel technology from the three rounds, a set installation scenario is used, presented in Table 3.5. Three main characteristics are used for each installation step within the models: 1. Reference Duration (average number of hours spent per WTG), 2. Maximum wind speed (m/s) and 3. Maximum significant wave height (m). Reference to available literature such as [90], [119] and in-house planning documentation was used to establish the base installation durations, wind speeds and wave heights for each phase listed in Table 3.5.

Table 3.5: Task durations and operational limits

Phase	Reference duration (h/WTG)	Max. wind speed (m/s)	Max. H_s (m)
Dredging & Survey	48	11	1.5
Foundation	48	12	2
Transition Piece	24	12	2
WTG	24.5	8	2
Scour Protection	14.4	15	2.5
PLGR	14.4	20	2
Cable Inst.	31.7	15	1.5
Cable Burial	36	12	3

To resemble a typical installation programme, a number of the phases were set to run simultaneously. The foundation phase was specified to begin once the dredging and survey phase had reached 60% completion, the transition piece installation began when 40% of the foundation phase was completed, turbine

installation began after 20% of the foundations were installed, scour protection follows at 80% of completion, 100% for the PLGR phase, cable installation at 60% of the PLGR phase and cable burial only begins after the cable installation had been completed to 100%.

Each of the main installation phases was allocated with environmental limits, independent of the associated vessel restrictions and resembles the maximum conditions that can be experienced when completing these offshore operations, separate from vessel capabilities. The same task parameters are assumed in both rounds, which are to the author's best knowledge and experience a fair representation of the expected values for these installation operations. It is reiterated that separate environmental limits exist for the different vessels in terms of transit and waiting modes. As soon as the weather conditions are below a vessel's transit limits, the vessel will set sail to the offshore site. The transit time is calculated simply by dividing the distance between the farm and the port by the vessel speed. If at any point the weather conditions exceed the transiting limits during an outward or inter-turbine voyage, the vessel returns to port. When the transit duration has been completed, the vessel is on site and the software calls on the limits and durations applied to the installation phases. This determines if a sufficient weather window exists to start an installation sequence or if the vessel should wait for the next available weather window, provided the waiting conditions of the vessel are satisfied.

3.2 Commercial Metocean Risk Modelling Case Studies

As part of the commercial contributions in this thesis, weather risk analyses were completed for the installation of two offshore wind projects in EDF's portfolio: Blyth Offshore Demonstrator (UK) and Fecamp (FR). A weather risk analysis can be described as a desk top study that compiles a sequence of logistical operations with attached meteorological constraints, vessel types and specified durations. This data is then simulated against sufficiently long hindcasts or modelled meteorological data.

These analyses are usually compiled using dedicated software simulation tools and the progression of the defined operations can be assessed using various statistical outcomes, which are usually described in terms of probability of exceedance for varying levels of confidence such as P50, P75 and P90. The simulations provide a perspective on the durations required to complete the operations in respect of delays caused by the weather conditions; the greater the exceedance probability used to express the outcomes, the larger the predicted duration. This predicted duration can be used to reveal the expected downtime that will be experienced when conducting the operations under different levels of confidence. The downtime associated with marine operations is under particular scrutiny for many offshore wind projects, as any delay during vessel charter are at the cost of the hiring organisation. Offshore construction vessels have significant daily charter and stand-by rates, often between tens to hundreds of thousands of pounds. An understanding of the expected downtime is therefore essential before executing a given project, ensuring the varying levels of confidence can be used commercially and are considered against the risk appetite of the respective party. The outcomes can be used as a platform to negotiate with

contractors, mould contracts, test alternative operational sequencing, prepare suitable financial contingencies and propose potential mitigation strategies.

From experience of working with ECUME I, it was decided that the lack of modelling flexibility was likely to be a barrier to accurately model both installations. ECUME I exhibited a number of significant limitations when completing the early testing and the vessel technology assessment, such as inflexibilities for modelling intermediate, one off operations and allocation of multiple vessels for specific tasks. As a result, a commercial weather risk software Mermaid was employed to build installation scenarios that matched the master installation schedule for both projects. A description of the Mermaid software is included in the following subsection and the different overarching methods employed when using the tool, driven by the commercial needs and urgency of each project, are also summarised. Owing to the commercial sensitivity of some of the planning information in each project, some details, such as the specific operational and vessel limits are not fully disclosed.

3.2.1 Commercial Metocean Risk Modelling Tool: Mermaid

This section summarises the main functionalities and characteristics of the Mermaid software, which is a marine operation risk management and planning tool. Mermaid combines a flexible logistical model including operational limits and vessel parameters in conjunction with multiple user-defined meteorological (met) data points to assess the weather delay that can be anticipated for each operation, at any location. Mermaid uses a graphical flow diagram interface to build up the operations, where multiple task cards are connected in line or parallel. These can be located in individual strands or within embedded groups

and the elements can be adjusted to define the operational conditions such as the duration, weather limits, allowances to suspension and the associated vessel(s) required to complete the operations. The automatically compiled Gantt chart serves as a useful reference to ensure the build model is an accurate or acceptable representation of the sequence and overall duration of the operations. Such 'sense checks' were not available in ECUME I, as users would have to trust that the build up of operations, sequences and phases had been accurately compiled within the software, to ensure the correct sequence of operations was simulated in each Monte Carlo iteration.

Mermaid has a significant difference to ECUME I as it does not generate multiple independent weather scenarios to apply against the defined installation strategy. Mermaid instead, relies on the number of years of historical weather data loaded into the software to facilitate independent installation simulations. In contrast, ECUME I uses a historical weather reference to inform a hidden Markov model (HMM), which predicts future weather patterns for the given location based on the maximum installation time specified by the user. The Monte Carlo simulations applied within ECUME I are usually executed across 1000 weather scenarios, whereas Mermaid is dependent on the number on the historical data to produce the final probabilistic outcomes. ECUME I benefits from a greater number of stochastic weather sets to draw probabilistic values that helps hone in on residual risks, yet the time required to complete the computations is considerably longer. A typical Mermaid simulation for a five WTG windfarm requires about an hour to complete the simulations, whereas ECUME I will normally take around six to eight hours to generate probabilistic results for multiple installation phases.

An advantage of Mermaid is the functionality to upload metocean data for an unlimited number of meteorological points located along transit routes at the wind farm installation site and ports. This arguably provides improved accuracy for

the typical weather regimes experienced during a ship's voyage, whilst ECUME I relies on multiple weather scenarios generated from the historical data for only one meteorological location, thus assuming the weather conditions are the same at all locations throughout the model. To ensure the data from multiple meteorological points are referenced throughout any simulation, Mermaid requires that the data across multiple met points share a number of common or overlapping reference years. Furthermore, to account for the variability in the offshore conditions, a minimum of 10 years has been sought for all analyses completed using this tool. The met points, ports, transit routes and offshore locations can be easily defined using the map functionality embedded in the software as shown in Figure 3.13. When combined, this set of modelling features in Mermaid leads to improved transparency and confidence in the executed simulations, whilst the dependence on a number of sufficiently long and overlapping data sets can restrict the scope of the analyses.

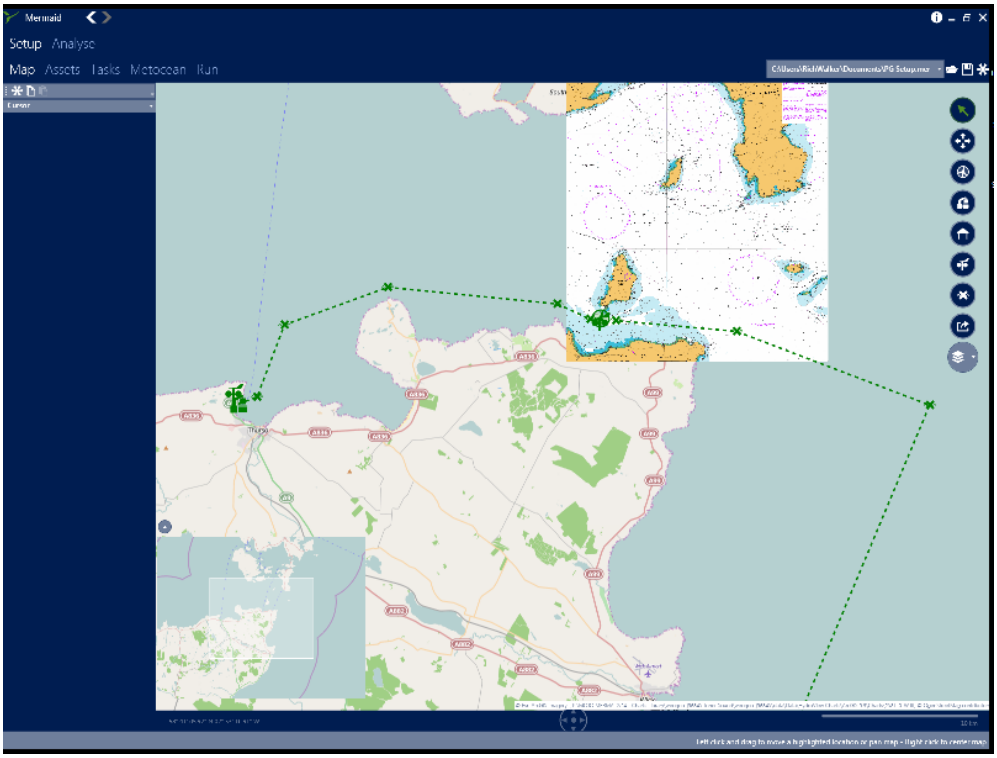

Figure 3.13: Mermaid map example - Pentland Firth [126]

To maintain an accurate and concise account of all modelling parameters, limits, constraints and vessels to be modelled, an excel record was produced to keep track of these variables for both case studies. A summary of this record is included in Appendix B.1. For the majority of the analyses using Mermaid, the predominant weather conditions considered for the operations were normally wind speed, wind speed at height, significant wave height, current and tidal elevation. However Mermaid can also handle other key meteorological values such as peak period (T_p), swell height, humidity and daylight.

Met points, ports, transit routes and offshore locations can all be defined using geo-positional coordinates (Lat°N) and (Long°E), which are automatically located on the map feature of the tool. For each task a range of constraints can be defined in addition to the core meteorological limitations such as the duration, number of times the tasks are repeated at each asset and the vessel used to complete the operations. Mermaid allows for different states of 'suspendability', which define if a task or a group of tasks can or cannot be interrupted once started. 'Non-suspendable', when applied to a task or group in the flow chart, means that the task will not begin until a sufficiently long weather window for the operations is available. 'Suspendable if vessel holds station' allows for suspension of a task or in between tasks of a group if the vessel remains in its position offshore, whilst 'fully suspendable' provides the greatest flexibility as operations can be aborted as necessary and the associated vessels can leave the site, seeking refuge in port before re-commencing the work.

The vessels defined in each model have two primary sets of limits, transit and station-keeping conditions. The transit limits are predominantly defined by a transit speed and significant wave height limit (H_s), whilst the station-keeping limits can be defined by the full range of meteorological conditions. The station-keeping constraints define the most extreme conditions each vessel can endure,

holding its position offshore, before returning to port. Start dates, which can be defined at the start or intermediately throughout the flow chart models, are also listed in the example included in Appendix B.1. There are a number of other features available in Mermaid, such as functional limits that define joint constraints between two weather parameters and departure or arrival limits that define specific conditions before a vessel leaves or accesses an offshore location or port.

3.2.2 Commercial Metocean Risk Analysis Summary

For the Blyth demonstrator, the smaller project and the significance of a potential delay to the commercial viability or profitability required that a combined model was built with interdependences between each installation phase to resemble the impact of knock-on delays during the entire installation campaign. As such, to separate the outcomes for each installation phase, a secondary analysis step was built in Matlab to extract the relevant data and produce duration predictions under chosen exceedance quantiles for delivery to the planning team.

Conversely, as the Fecamp analysis was significantly larger by approximately 75 more turbines, a different approach was adopted, where a dedicated model was built for each installation phase across the two staggered installation campaigns. This break up of models led to a much faster calculation of weather downtime for each respective installation phase, whilst the knock-on effect was not carried through subsequent installation phases owing to this segmented modelling approach. The weathered Gantt charts that were extracted from the Blyth study were useful to demonstrate the impact of knock on delays between phases, which could only be produced on a per phase basis for the Fecamp study. An attempt

was made to build 'post-processed' weathered Gantt charts for the Fecamp installation, using the durational predictions from each of the segmented models. As a shift in start dates for subsequent phases is not shown these charts serve rather as a sense check, highlighting unrealistic completion dates for phases that would be fully dependent on progression of previous phases.

Both approaches are valid for assessing weather downtime, each with pros and cons for particular predictive measures. The methodology adopted for the Blyth Offshore Demonstrator allowed for accurate interdependencies between project phases to be built, yet required significant post processing of the data to produce WDT for each phase. The Fecamp case made it much easier to produce the WDT per phase, but did not account for the interdependencies between phases. It was down to the requirements of planning personnel from each project as to which method was used. The general methodology that was used in both weather risk analyses is summarised in Figure 3.14.

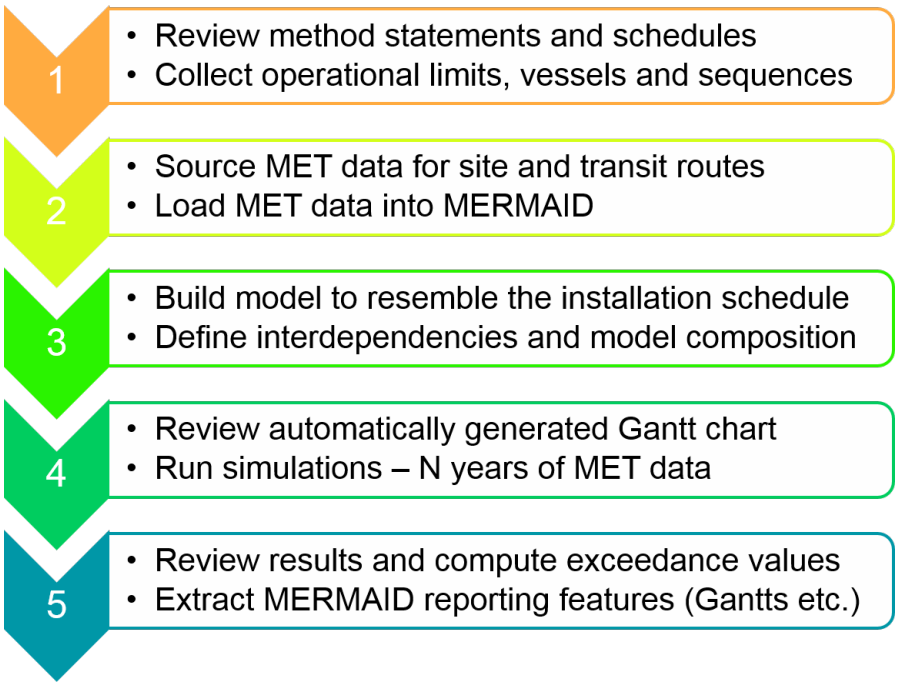

Figure 3.14: Generalised commercial weather risk analysis methodology

A significant limitation of ECUME I is the multiplication of the installation phases by the number of wind turbines defined within each model. This feature restricts flexibility of modelling the logistical scenarios, as intermediate or one-off operations cannot be easily implemented. As a result, a variety of workarounds such as manual and scripted handling of separate ECUME I files were applied, each representing a separate installation phase. This allowed intermediate tasks to be inserted within or between simulated ECUME I files and built a chain of installation phases that closely matched the corresponding installation schedule. The final computation took approximately eight days for manually executed simulations and around five days for the scripted method, which automatically launched successive ECUME I simulations, until all installation phases were complete. A comparison of the results revealed different outcomes for the manual and scripted methods. After correspondence with the members of EDF R&D in France, it was concluded that the computational engine of ECUME I was not operating correctly and has subsequently led to the development of a new software tool within EDF Energy, described in Section 3.3.

3.2.3 Blyth Offshore Demonstrator (BOD) - Metocean Risk Analysis Methodology

The Blyth Offshore Demonstrator Project (BOD) weather risk analysis was a key deliverable in year three and Mermaid was used to complete the modelling and simulations. EDF Energy Renewables' (EDF ER) Blyth Offshore Wind Demonstration Project is located 5.7 km off the cost of Blyth, Northumberland. The project consists of five 8.3 MW turbines at a total generation capacity of 41.5 MW. This installation used float and sink gravity base foundations (GBF) fabricated by BAM Nuttall at Shepherd Offshore Neptune Energy Park in North Tyneside. It was intended that the project would demonstrate the potential for

the self-installing GBFs to identify an economical solution for foundations in deep water locations. The foundations are approximately 30m in diameter, 60m high and are designed to be installed in water depths of approximately 40m. Figure 3.15 summarises the GBF design at Blyth.

To model the required scenarios, a variety of planning documentation such as vessel specifications, method statements and schedules were reviewed to formulate an accurate representation of the installation plan. An example of the structured modelling inputs assembled to model the installation phases are included in Appendix B.1. The installation tasks and parent phases are constructed using the Mermaid flow chart that compiles a work breakdown structure similar to MS project, which in turn generates a Gantt chart for the installation. The modelled installation phases and a short description of the operations are listed below.

- **Dredging and Survey** - Clearing and levelling of the seabed
- **Filter Layer** - Stone and rock placement to support the GBFs
- **GBF Installation** - GBFs towed to site, water and sand ballasted in position
- **Scour Protection** - Stone and rock placement to protect the GBFs
- **Pre-lay Grapnel Run** - Clearing of cable route from any obstructions
- **Export Cable Installation** - Laying of export cable from shore
- **Array Cable Installation** - Laying of inter-array cable
- **Post-Lay Burial** - Burial of inter-array cable
- **Wind Turbine Installation** - Installation of the turbines
- **Mechanical Completion of Wind Turbines** - Completion of turbine installation
- **Electrical Completion (hang-off, routing etc.)** - Electrical Completion
- **Commissioning** - Final commissioning of the turbines and infrastructure

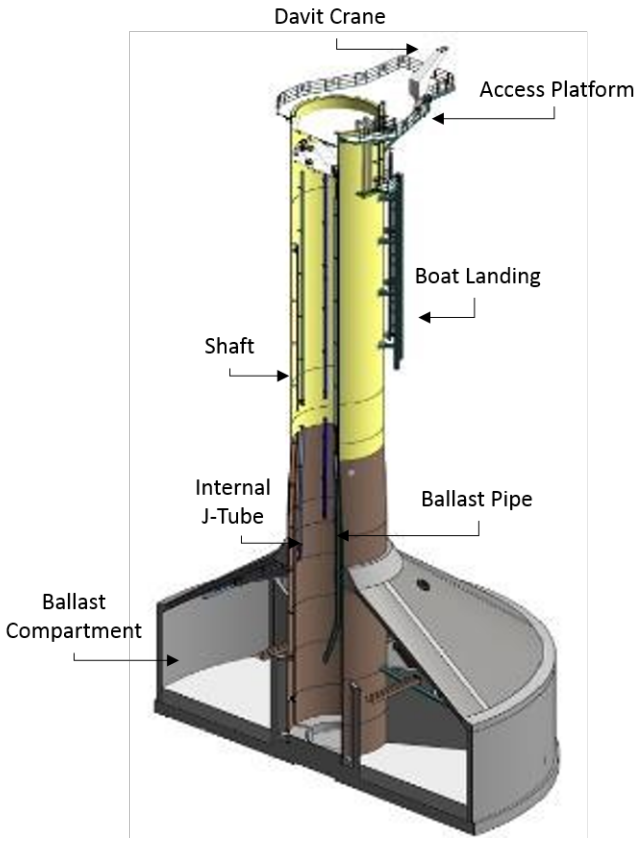

Figure 3.15: Blyth Offshore Demonstrator - GBF Design

3.2.3.1 Mermaid Modelling - BOD

An annotated Mermaid map view that includes the GBF transit routes, port locations, the met points and the five locations for the WTGs in the BOD project is shown in Figure 3.16. Four scenarios were constructed within individual Mermaid files and are listed below:

- Scenario 1 - No Learning
- Scenario 2 - GBF & WTG installation with Learning
- Scenario 3 - Month Delay with GBF & WTG installation with Learning
- Scenario 4 - 1 x WTG Only (assumed GBF has been towed out of dry dock and is ready at Port of Tyne)

Figure 3.16: Mermaid - BOD site, Transit Routes, Meteorological Reference Points

The scenarios were selected to understand the impact of learning curves on the installation durations and subsequent downtimes. Based on the instruction of the planning team at the BOD project, learning rates were considered for the anchoring and water ballasting tasks for the first two GBF installations at 1 and 0.5 days each respectively. These learning rates were defined by the BOD project planning team who assumed the majority of the learning would be completed in the first two GBF installations and are summarised in 3.19. The GBFs were constructed in a dry dock on the river Tyne and the towing out of the GBFs, once in a flooded state, was of particular concern to the project planners. Specific tidal limits were required to ensure the under-keel clearance was achieved when GBFs were towed out into the river Tyne. Hourly tidal elevation data at meters

from chart datum was obtained for the Port of Tyne and was used directly in the Mermaid simulations.

The GBFs were to be installed using three tugs in a similar configuration shown in Figure 3.17, where the tugs would eventually reach the intended location and a combination of water ballasting and slackening of the tugs moorings allowed the GBFs to gradually submerge and rest on the prepared seabed. Once ballasted, the water was replaced with a slurry of sand, which permanently secured each GBF in place.

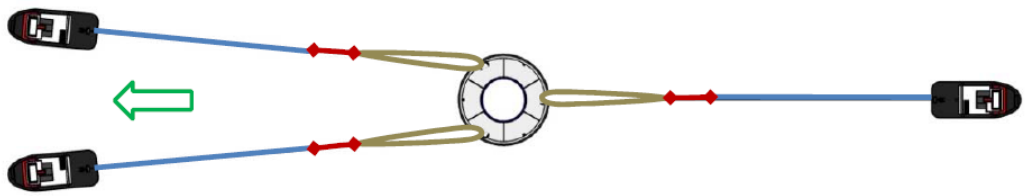

Figure 3.17: GBF towing configuration

A learning rate of 4.1% was defined by the BOD project team for the turbine installation tasks, with an assumption some learning would remain on the final task. Both these learning rates are summarised by the plots in Figure 3.19. The third scenario assessed the impact of one month's delay to the start of the installation operations in addition to these learning rates. Scenario four was modelled to simulate a contingency option, which considered the installation of only one foundation, WTG and related infrastructure. This analysis was completed to identify the latest possible start date for the installation operations, ensuring one turbine was operational and generating power before the cut-off date for eligibility in a UK renewable generation incentive.

A total of 24 meteorological locations were used within each of the modelled scenarios. Four main transit routes were considered within each analysis: Tugs

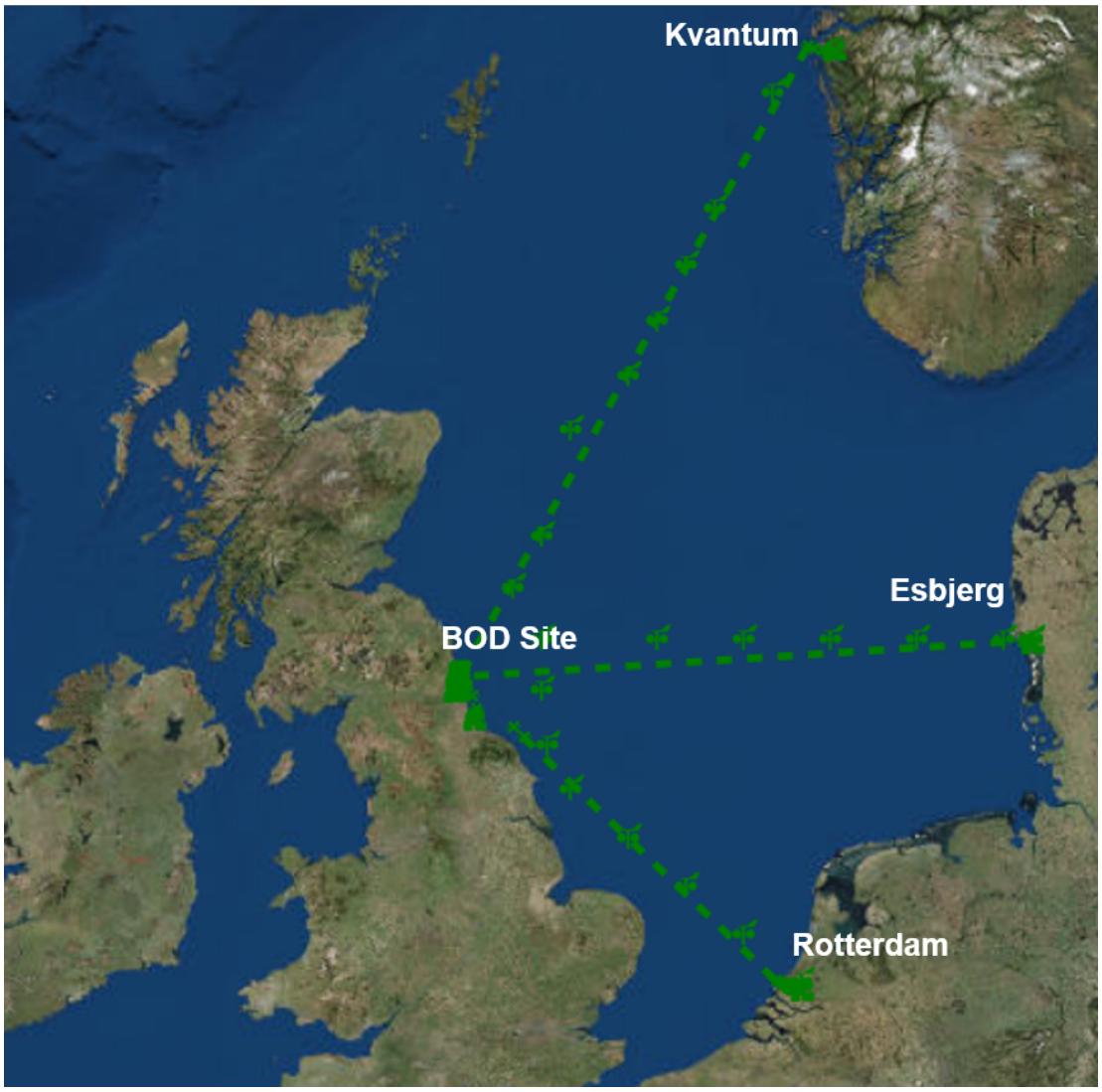

Figure 3.18: Mermaid - Transit routes and meteorological reference points (Turbines: Esbjerg; Cable: Rotterdam; Filter Layer & Scour Protection Rock: Kvantum)

towing GBFs down the River Tyne and from the Port of Tyne to the BOD site; WTIV transit between Esbjerg, Denmark and the BOD site; CLV transit between Rotterdam, The Netherlands and the BOD site; FFPV transit between Kvantum, Norway and the BOD site. DNV states that simulations of this kind should use 5-10 years weather data [82]. Mermaid automatically reviews the number of days and subsequent years of overlapping data to establish how many simulations can be run. Once the total number of years is known, Mermaid applies the first start

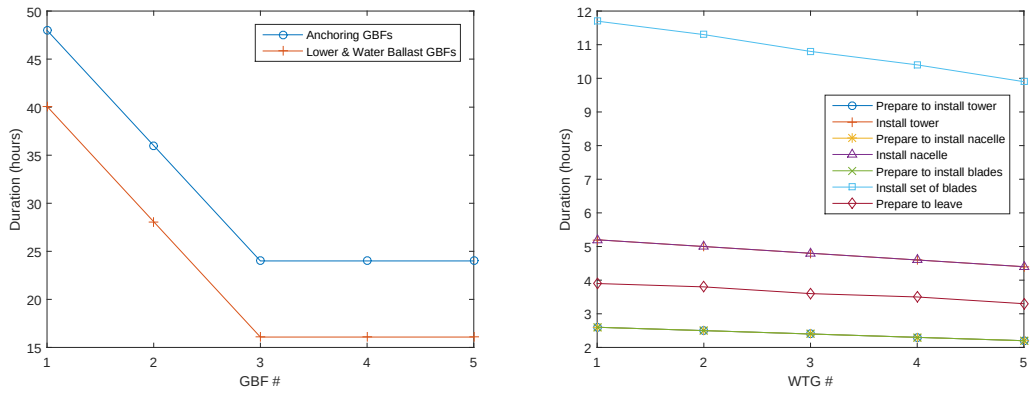

(a) GBF Learning Rates **(b)** WTG Learning Rates

Figure 3.19: BOD: Modelled GBF and WTG learning rates

date in the model for each year of data, which usually means the number of overlapping years will define the number of simulations that are completed. For the BOD analysis and across the 24 met locations, 30 years of overlapping data was available, satisfying DNV's recommendation. In the following sub-section, the post-processing and analysis used to produce the results is described.

3.2.3.2 Matlab Data Processing and Analysis

Mermaid provides an in-built 'analyse' section that provides statistical outputs of the final results. One of the most useful references is the weathered Gantt chart produced under user-defined exceedance percentiles, which help characterise the progression of operations or delays experienced for a typical installation campaign. These exceedance estimates are used in this context to provide a confidence level or probability that a calculated duration will not be exceeded. However, as all installation phases for the BOD project were included within the one Mermaid model and a number of phases were overlapping, the statistical outputs in Mermaid masked the total duration for some of the key installation phases in the project. This meant that the exceedance values provided within

the summary tables in Mermaid were not suitable for the purpose of obtaining final results for the installation. Fortunately, Mermaid produces external .csv files for each completed simulation, facilitating external analyses. Each file originates from one of the years of overlapping data and includes a print-out of the duration for each task, after the impact of weather.

Matlab script was produced to calculate the probability of exceedance under defined quantiles from the external .csv files and operates as follows. Firstly the duration for each installation phase was extracted from each resulting file, which were then sorted and ranked in ascending order. By selecting the relevant rows in each file, the script could be easily adapted to extract the relevant tasks for each installation phase and the summation of the embedded tasks would provide durations for each installation phase, which populated the ranked list. This negated the impact of overlapping installation phases, as the true duration for each task and subsequent phases after the impact of weather could be computed. This approach gathered the data from each simulation run, then the percentile durations for each installation phase were identified using the 'prctile' function in Matlab [127]. The fundamental steps of this process are summarised by Equations 3.4 and 3.5.

$$Q_{xx} = \frac{P_{xx}(n_w + 1)}{100} \tag{3.4}$$

where:

P_{xx} = Percentile of interest (e.g. 50, 75 or 90)
Q_{xx} = Location of P_{xx} in the recorded durations, ranked in ascending order
n_w = Number of years of weather data

The Q_{xx} outcome from Equation 3.4 is not normally an integer, meaning a specific

location within the ranked data is not defined for the chosen percentile. In this case, the Matlab 'prctile' function applies linear interpolation to identify a numeric value, as demonstrated using example values in Equation 3.5 below [127].

If the 100(1.5/n)th percentile is $y_{1.5/n}$ and the 100(2.5/n)th percentile is $y_{2.5/n}$, then linear interpolation finds the 100(2.3/n)th percentile, $y_{2.3/n}$ as:

$$y_{\frac{2.3}{n}} = y_{\frac{1.5}{n}} + \frac{\left(\frac{2.3}{n} - \frac{1.5}{n}\right)}{\left(\frac{2.5}{n} - \frac{1.5}{n}\right)} \left(y_{\frac{2.5}{n}} - y_{\frac{1.5}{n}}\right) \tag{3.5}$$

Finally, once a predicted duration was identified for each corresponding percentile, the base duration for each installation phase was deducted to reveal the amount of weather downtime (WDT) that could be anticipated for each set of operations as demonstrated by Equation 3.6.

$$WDT_{P_{xx}} = P_{xx_d} - P_0 \tag{3.6}$$

where:

$WDT_{P_{xx}}$ = Weather downtime for the selected percentile 'P_{xx}'
P_{xx_d} = Estimated duration for the selected percentile 'P_{xx}'
P_0 = Base time to complete the operation without the impact of weather

3.2.4 Fecamp Offshore Wind Farm - Weather Risk Analysis Methodology

EDF Énergies Nouvelles' Fecamp offshore wind farm is located approximately 15km north west of Fecamp coast in Normandy, France. The project will consist of

83, 6 MW General Electric Haliade turbines with gravity base foundations (GBS) in a similar configuration to the Blyth Offshore Demonstrator, resulting in a total generation capacity of 498 MW. This study was completed to model and review the progression of the various installation phases to be completed in the project. This section describes the main modelling approach used throughout the assessment of the logistical and installation steps. Because of the commercial sensitivity of the project specific values, constraints and start dates are not explicitly listed.

3.2.4.1 Mermaid Modelling - Fecamp

The main ports, transit routes, meteorological points and the location of the turbine array at Fecamp are summarised by Figure 3.20. The specific details for the Mermaid model were made available via excel files from the project team located at EDF Énergies Nouvelles' in France, reducing the time required to scrutinise and review the installation schedules, which could be easily transferred into a similar format, as included in the example in Appendix B.1.

This project was evidently much bigger in size in comparison to the BOD project and consisted of two primary installation campaigns. These two campaigns were planned to be completed across two separate years with a view to restricting operations during the winter months as much as possible. Two identical installation campaigns were modelled across the two years selected for installation as listed below, which were specified as 51 and 32 turbines in first and second years respectively. The WTG installation phase was scheduled to begin half way through campaign 2. It has been specified that the Fecamp project will use a similar GBF design to BOD and the tow-out operations were again under close scrutiny.

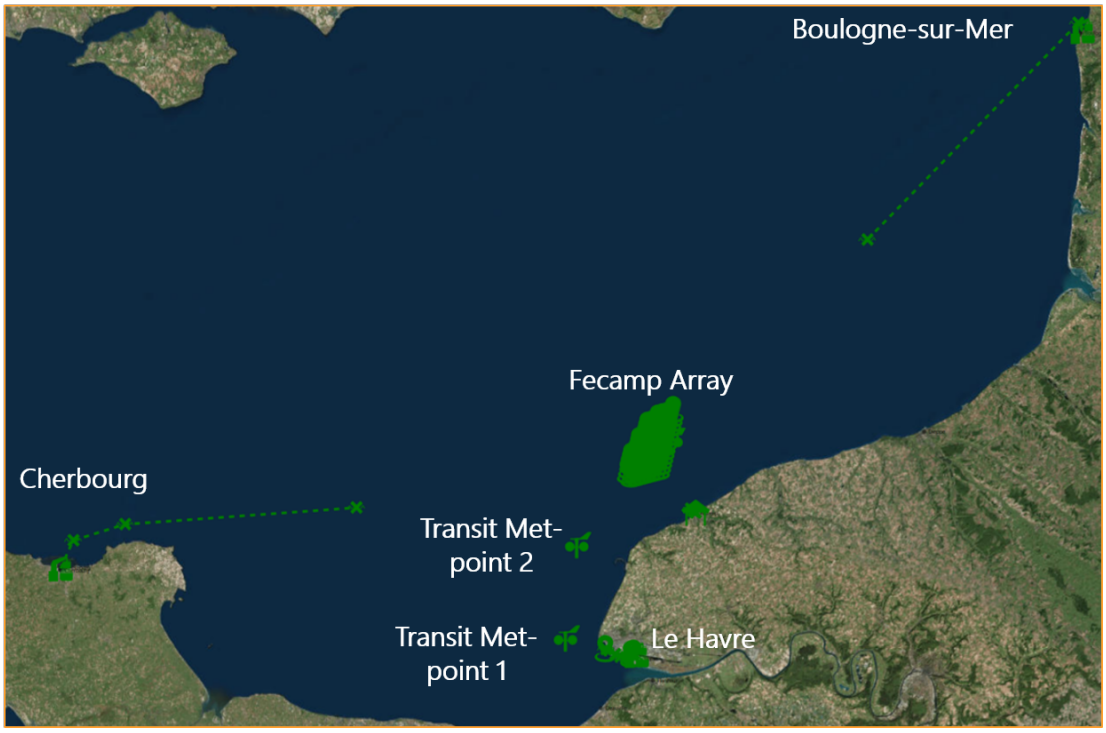

Figure 3.20: Fecamp - Met points, Transit Routes and Offshore Site

Installation Campaigns 1 and 2

- **GBF Bedding** - Stone and rock placement to support the GBFs
- **GBF Installation** - GBFs towed to site, water and sand ballasted in position
- **GBF Scour Protection and Ballast** - GBFs sand ballasted in position and rock placement to prevent scour
- **IAG Laying** - Laying of inter-array cable
- **IAG Burial** - Burial of inter-array cable
- **IAG Termination** - Completion of cable infrastructure inside turbines.

Dedicated WTG Installation Campaign

- **WTG Installation** - Installation of the turbines

3.2.4.2 Data Processing and Analysis

Dedicated models for each primary installation phase were built in Mermaid, which meant that the Matlab post-processing, as used in the BOD weather risk analysis, was not required. Each installation phase could be reviewed independently as no concurrent project phases were included in each model. The results for each installation phase under the P50 and P90 quantiles are taken directly from the summary tables produced by Mermaid. The recorded duration and weather downtime values are based on the Pxx durations in days, which is a summarising statistic produced from the 21 simulations completed for each installation phase. The P60 and P70 outcomes are derived from the dates included on weathered Gantt charts created in Mermaid. The completion dates on the corresponding Gantt charts were then used against the original start date to reveal the duration in each case and by simply following the same logic as Equation 3.6, this revealed the associated weather downtime. The Gantt chart referenced for each Pxx value is based on the closest lying simulation to the Pxx duration, meaning the completion dates may deviate slightly from the summarised P50 and P90 duration and WDT values

This breakup of models led to a much faster calculation of weather downtime for each respective installation phase, whilst the knock-on effect was not carried through subsequent installation phases due to this segmented modelling approach. The weathered Gantt charts extracted from the Blyth study were useful to demonstrate the impact of knock-on delays between phases, which could only be produced on a per phase basis for the Fecamp study. An attempt was made to build 'post-processed' weathered Gantt charts for the Fecamp installation, using the durational predictions from each of the segmented models, but a shift in start dates for subsequent phases is not conveyed, highlighting unrealistic completion dates for phases that would be fully dependent on the progress of previous phases.

Multiple runs of the installation campaigns are simulated by Mermaid based on the number of years of overlapping met data between the three met point locations. There was 21 years of overlapping data between the two met data points, meaning that a total of 21 repetitions of the installation campaign were simulated by Mermaid. This provides 21 different durational outcomes that can be assessed to reveal exceedance probabilities for the installation steps. Summarised results for the Fecamp weather risk analysis are included in Chapter 5, Section 5.2.

3.3 Stochastic Metocean Modelling Methodology

This section describes the methodology that was prescribed and developed for EDF's next generation marine operations simulation package, which utilises a Markov switching autoregressive model to produce annual time series data sets of wind speed and wave height. It was intended that the model will produce a large number of metocean time series that fairly represents the conditions and characteristics for any given offshore site. When composed as part of a larger logistical simulation package, this will support quantification of the residual risks and reduced uncertainty in order to accurately predict the progression of marine operations. For all studies completed within this work, wind speeds at 10m and significant wave height (H_s) were the primary input parameters used in the simulations.

To cope with the variation in the offshore weather conditions at each project, it is vital that a stochastic weather model is adaptable to account for seasonal or monthly variations to produce realistic weather time series. The Markov Switching Autoregressive (MS-AR) model included in the METIS Matlab toolbox, developed by Monbet & Ailliot [81], has been investigated in this study and

configured to produce monthly realisations of wind speed and wave height, which is conditioned into one full continuous time series. The fundamental aim of this study is the implementation of a modelling methodology to produce synthetic metocean data for the assessment of marine operations. The generated time series is cross examined against a typical offshore operation in Chapter 6, to validate the adopted methodology and MS-AR model configurations. By demonstrating that the model is capable of producing characteristics such as the average length of operational weather windows and monthly workability, this supports the case to implement the methodology and embedded MS-AR models, within offshore simulation tools.

3.3.1 Metocean Modelling Simulations

The stochastic weather modelling method applies the homogeneous MS-AR model with Gaussian innovations embedded within the METIS Matlab tool box, for an intended application in a marine operations simulation tool. This section describes the observed meteorological data sets, the MS-AR model tested, the model selection process and a summary of the steps to produce the final time series. The methodology can be used to generate annual time series of U and H_s and the steps used to assess the results. The main steps of the overall method are shown in Figure 3.21. A brief summary of these steps are as follows: Firstly the observed data that is re-sampled to three hourly intervals and compiled into monthly sets to obtain stationary, non seasonal collections. The METIS MS-AR model is first used to assess various model type configurations using the EM algorithm, which are individually evaluated using BIC to identify the most suitable model for each month. The simulation produces 1000 years of synthetic time series of U and H_s, which we then compare against the observed data using cumulative distributions and Q-Q plots. Assuming satisfactory plots are

obtained, the separate U and H_s simulations are paired. Two methods have been investigated: i) Simply taking the mean of each monthly realisation, which is used to rank these in ascending order and therefore define the corresponding months of U and H_s. It is appreciated that this approach may not account for the close correlation between wind speed of wave height. ii) The secondary pairing technique uses Pearson R coefficients to account for the relationship between the wind speed and wave height realisations, which takes considerably longer than the first pairing method. This is described in more detail in Section 3.3.5.

After either pairing technique is applied the simulated data is then interpolated from three hour to hourly intervals. A weather window assessment is included in Section 6 to demonstrate the validity of the overall methodology and pairing techniques, in the assessment of marine operations. In the following sections we detail the key stages of the modelling methodology.

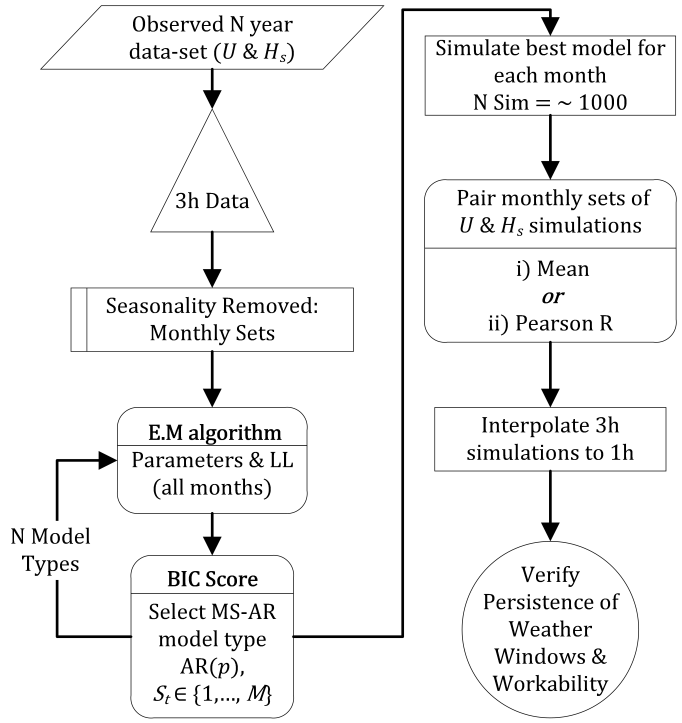

Figure 3.21: MS-AR modelling & verification methodology

3.3.2 Data

Three different environmental data sets have been sourced to review the consistency of the MS-AR model simulations at various sites with different energies. Wind speed (m/s) and significant wave height (m) are the two meteorological parameters under investigation. The wind speed is taken at a reference height of 10m and significant wave height represents the average of the highest third of individual waves over a specified period of time at each site [128]. A summary of each data set is included in Table 3.6, all of which have a three hour resolution.

Table 3.6: Observed time series

	UK North East	France West	English Channel
μU (m/s) $[10m]$	6.63	5.67	7.48
μHs (m)	1.15	1.38	0.85
First Observation Date	01/01/1981	01/01/1994	01/01/1994
Years of Data	34	21	21
Pearson R (U,H_s)	0.5	0.7	0.9
Record Frequency (h)	1	1	1
Sampling Frequency (h)	3	3	3
Number of Samples	99345	61361	61361

It should be noted that all three data sets were originally recorded at hourly intervals and were subsequently resampled to three hour observations by extracting the relevant time steps for each day, beginning at 00:00 then every three hours through to 21:00. Fundamentally, this step reduces the order of the AR model and hence the complexity of the MS-AR model overall. We have chosen the three hour time step as a compromise between six hour and one hour intervals. Our experience testing the model has found that the three hour time step provides a suitable balance between accuracy and simulation time. Experience modelling

marine operations in various software environment has highlighted that time steps of at least one hour should be used as an input weather data series, as this provides reasonable resolution for intermediate interpolation, facilitating the simulation of tasks with a time step of less than one hour. Therefore it was decided that three hour results from the MS-AR model would be linearly interpolated to one hour intervals and compared against the original data set of an hourly resolution. The validity of this approach was of interest as it follows on from the recommendations of [74], who indicate simulations should be completed at the same scale as the observed data set and then interpolated to the required resolution.

3.3.3 MS-AR Model

This section describes the homogeneous MS-AR model embedded within the weather modelling methodology that was implemented to generate wind speed (U) and wave height time series (H_s). The model is included with the METIS matlab toolbox and was obtained directly from the developers: Monbet and Ailliot [81]. The description of the model is based on the information included in the METIS toolbox documentation [81] and a description of the most standardised MS-AR model is included in Section 2 of [70]. The following description summarises the functionality of the MS-AR model and should provide sufficient detail to support the reader's understanding of the computational steps.

Wind and wave data and recorded time series commonly demonstrate non-stationary, which is characterised by daily factors, seasonal fluctuations and inter-annual variations. The issue of seasonality in a wind time series can be treated by dividing the data into months and fitting a separate model to each month, which assumes that the same month across each year is an individual representation of a common stochastic process [70]. Segmentation of monthly wind data sets

from the original three hour meteorological file was necessary to inform the MS-AR algorithm. Within the METIS toolbox, three different MS-AR models are provided: Gaussian MS-AR Model, Gamma or Lognormal MS-AR model and a Non-homogeneous gamma MS-AR model, the latter developed to handle bivariate processes for wind speed and direction. The Gaussian MS-AR model was selected as Monbet and Ailliot state that the formulae for the estimation step can be explicitly described, supporting overall interpretation of this modelling approach. As the majority of the available metocean data sets did not include comprehensive wind speed and directional observations, the bivariate case was not applicable. To fundamentally describe the MS-AR model, it is important to consider the different evolutions in the wind speed that can occur over a month. Because of this, the MS-AR model applies a dedicated autoregressive model to accurately resemble the evolution of the wind speed within each hidden state or 'weather type', defined as $S_t \in \{1, ..., M\}$. In this method the weather types are categorised by the average wind speed and variability, subject to the number of different hidden states predefined in the model set up. The embedded Markov chain controls the transition between the autoregressive models based on the most likely distribution of the weather types across the times steps in each month.

A MS-AR model involves a discrete time process with two components $\{S_t, Y_t\}$. In this context, $\{Y_t\}$ represents the wind speed or wave height in $(0, +\infty)$ and $\{S_t\}$ is a non-observable or 'hidden' process where $S_t \in \{1, ..., M\}$ represents the weather type at time t. $\{S_t\}$ is a Markov Chain within the finite space $S = \{1, ..., M\}$, with $M > 0$ the number of weather types. Monbet and Ailliot [70] state that the MS-AR process is characterised by two conditional independence assumptions, which are core to the operation of a Markov chain and an autoregressive process:

- "The conditional distribution of S_t given the values of $\{S_{t'}\}_{t'<t}$ and $\{Y_{t'}\}_{t'<t}$ only depends on the value of S_{t-1}. In other terms, we assume that the

weather type S_t is a first order Markov chain the evolution of which is independent of the past wind conditions

- The conditional distribution of Y_t given the values of $\{Y_{t'}\}_{t'<t}$ and $\{S_{t'}\}_{t'<t}$ only depends on the values of S_t and $Y_{t-1}, ..., Y_{t-p}$. For this particular application, it means that the wind speed process $\{Y_t\}$ is an autoregressive process of order $p \geq 0$ the coefficients of which evolve in time with the weather type sequence."

The standardised AR(p) model with Gaussian innovations, where (p) represents the order of the autoregressive model, or in other terms the number of immediately preceding values used to produce a forecast, is described by [70] as follows.

If $S_t = s_t$

$$Y_t = a_0^{(s_t)} + a_1^{(s_t)} Y_{t-1} + ... + a_p^{(s_t)} Y_{t-p} + \sigma^{(s_t)} \epsilon_t \tag{3.7}$$

$(a_0^{(s)}, a_1^{(s)}, ...a_p^{(s)}, \sigma^{(s)}) \in^{p+1} \mathrm{x}(0, +\infty)$ represents the unknown parameters of the $p \geq 0$ AR(p) model that operates within the regime $S_t \in \{1, ..., M\}$ to describe the evolution of the observed weather parameters. The ϵ_t denotes a white noise or error term, which in this case is a sequence of independent and identically distributed Gaussian variable with zero mean and and unit variance, independent of the Markov chain S_t. This can be described differently where the conditional distribution $P(Y_t | Y_{t-1} = y_{t-1}, ..., Y_{t-p} = y_{t-p}, S_t = s_t)$ is assumed to be a Gaussian distribution with conditional mean and variance:

$$\begin{aligned} &E(Y_t | Y_{t-1} = y_{t-1}, ..., Y_{t-p} = y_{t-p}, S_t = s_t) \\ &\quad = a_0^{(s_t)} + a_1^{(s_t)} Y_{t-1} + ... + a_p^{(s_t)} Y_{t-p} \end{aligned} \tag{3.8}$$

$$var(Y_t|Y_{t-1} = y_{t-1}, ..., Y_{t-p} = y_{t-p}, S_t = s_t) = (\sigma^{(s_t)})^{2\prime\prime} \tag{3.9}$$

METIS uses an expectation maximisation algorithm (EM) to fit the MS-AR model for the prescribed values p and M. This algorithm is based on the work of [129] and extended by [130]. The EM is applied in three steps. Firstly, randomly chosen values are used to identify an interesting maximum. The EM is applied across each of the initial values in the time series and a maximum likelihood reveals the most suitable parameters of μ and σ. Ailliot et al. [81] embed a 'forward-backward' computation from the Baum-Welch Algorithm, which is used to identify the unknown parameters within a hidden process. The EM is continuously applied, retaining the parameters from each recursion, until the algorithm converges at 10^{-7} or reaches the maximum number of 600 iterations. This was altered from the default 100 iterations in an attempt to ensure convergence is reached or at least comes very close to convergence in each recursion. The final estimate is then identified using a quasi-Newton algorithm, which identifies the most likely sequence of hidden states or weather types. The EM function provides the estimated parameters of the MS-AR model and the log likelihood of the model. The EM function computes smoothing probabilities which relate to the conditional distribution of the hidden state across the number of observations $(y_1, ..., y_N)$ for the month in question.

$$P[S_t = s|Y_1 = y_1, ..., Y_N = y_N] \tag{3.10}$$

where $s_t \in \{1, ..., M\}$

A Viterbi algorithm is used in the METIS toolbox to provide a visual representation of the path of the hidden states and the plot indicates which autoregressive weather regime is most likely, given the observation time as shown in Figure 3.22. This plot was produced for the model with six lags and three hidden states for the second December observation at the UK North East location. In this plot, the allocation of the first weather type or regime is denoted by the solid line, regime two by the dashed line and regime three with the dotted line. An accompanying table listing the features of the each hidden states is also included in Figure 3.22. In regime two, the wind speed is the greatest on average, whereas in regime one the wind speed is the lowest on average and appears to change much more slowly, as confirmed by the values for mean (μ) and standard deviation (σ) listed in the table in Figure 3.22. Regime three appears to serve as an intermediate state and shares the same variability as regime two; this makes up the predominant allocation of states in this example. This indicates that the model is capable of defining weather types and that the allocation of a separate autoregressive model to each of these states should result in well informed predictions arising from simulation of the weather series.

The MS-AR model can then produce a defined number of monthly sets through simulation. The simulation function simulates the AR process with Markovian switching, which are dictated by the hidden Markov chain. This computation uses the path of the hidden Markov variable, identified as part of the Viterbi algorithm and the parameters of the autoregressive models. The matrix of the initial observations is used to define the output dimension of the simulated instances.

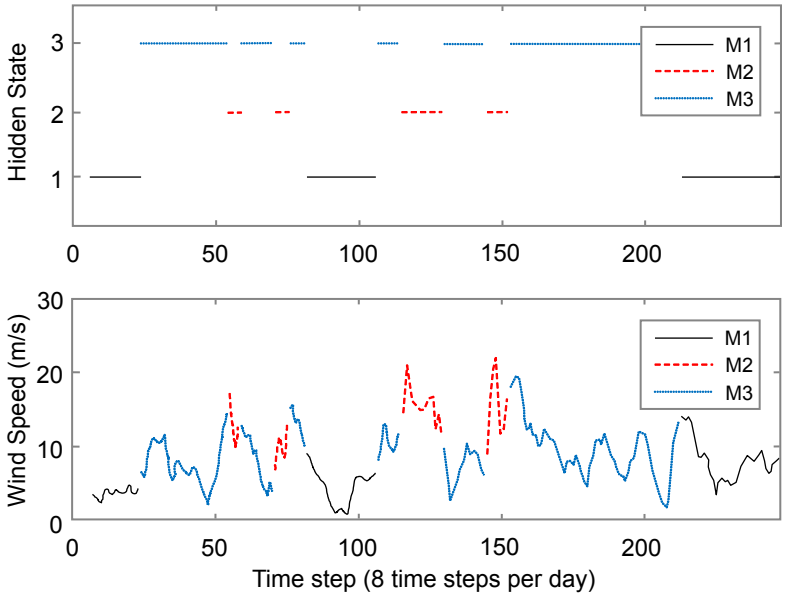

Hidden State (M)	μ	σ
1	5.9	3.0
2	14.3	3.6
3	8.9	3.6

Figure 3.22: Resulting Viterbi algorithm from homogeneous MS-AR Gaussian model; Wind speed at three hour Time-steps; 34 years of observations; December; UK North East, $p = 6, M = 3$

3.3.4 Model Selection

In order to identify the best model for U and H_s for every month at each location, the model parameters p and M can be adjusted to suit the weather conditions within an observed time series. Monbet and Ailliot [70] have found that the Bayesian Information Criterion (BIC) is suitable for selecting the best combination of AR model order p and the number of hidden states M. The BIC is defined as follows:

$$BIC = -2logL + klogN \tag{3.11}$$

L indicates the likelihood of the data, k is the number of parameters and N is the number of observations required, all of which can be obtained after the EM algorithm has converged for each model type for all months of data. It should be noted that in order to complete the BIC assessment, the various combinations of AR order and hidden states must be predefined, meaning an iterative approach when testing a range of model types is necessary before arriving at the most suitable model for each month.

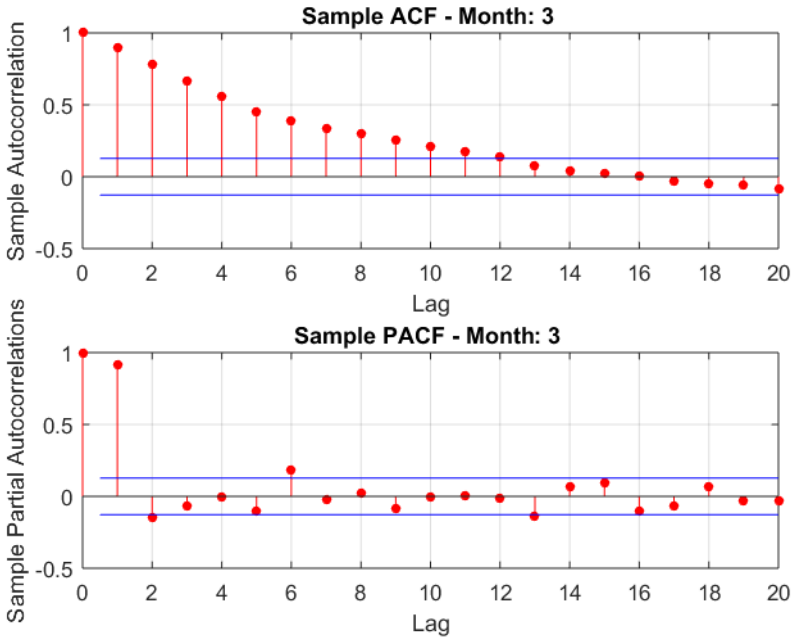

Figure 3.23: Sample autocorrelation (ACF) and partial autocorrelation (PACF) correlograms; U (m/s); UK North East; March

To understand the number of previous values or lags that are statistically significant for the AR part of the MS-AR model, the monthly data of all three locations in Table 3.6 were assessed in terms of the autocorrelation (ACF) and partial autocorrelation (PACF) functions. The PACF can be used to define the

partial correlation of a time series against its own lagged values. The purpose of this approach was to try and identify a ceiling for the AR model order and therefore constrain the maximum number of model types to be considered in the BIC assessment process. The ACF included in Figure 3.23 shows a fast geometrical decline, which is representative of stationary processes and shows that an AR model is suitable to describe the data. Moreover, the PACF shows that up to as many as six lags are statistically significant for the AR model prediction. It should be noted that the example shown in Figure 3.23 is taken from the UK North East data set and that the month of March was one of few months to demonstrate a dependence of up to six lags, which for three hourly samples corresponds up to 18 hours in the past.

Once a ceiling value for the AR model order is identified, the process of checking the MS-AR model types can be completed. This involves running the EM algorithm in the METIS toolbox to obtain the parameters L, N and k from model combinations $p\{1-6\}$, $M\{1,...,6\}$. In all, 36 model types were assessed for both U and H_s across each month at all three sites. The BIC score was produced for each model combination across all months and the model with the lowest BIC score was selected to produce the synthetic weather series.

It is costly in terms of time to run the EM algorithm for all of the model types each time a new observed weather series is to be assessed. Therefore a review of the model types selected across the three sites was completed and the results are shown in Figures 3.24 and 3.25. It shows that for the wind speed U the selection of the AR model order p is consistent for all sites at six lags, whilst the number of hidden states M jumps between two and five states. The AR model selection for the wave height H_s fluctuates between two to four lags and the number of hidden states between five and six. Generally it is shown that the wind speed tends to a larger number of AR lags and a lower number of hidden states whilst the opposite

is observed in the wave height. However, the model types shown in Figures 3.24 and 3.25 show a consistent range across the three sites and therefore reduce the number of model types that should be considered for each month to eight and six models for U and H_s respectively. By accounting for three different sites, each with different average characteristics, this demonstrates that constraining the model search to these windows should ensure it's adaptability for use in a variety of different offshore locations.

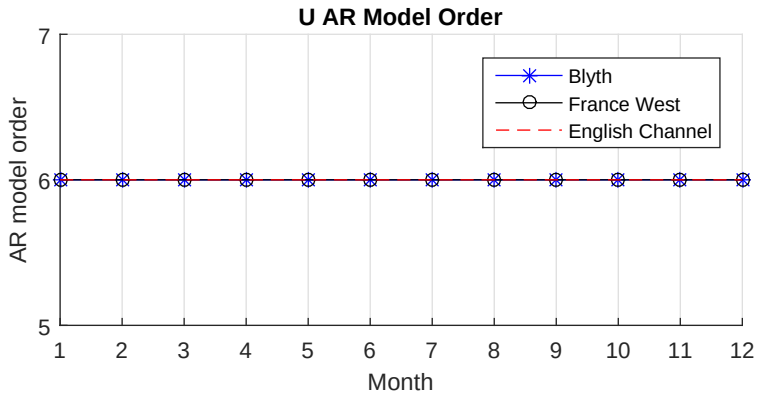

(a)

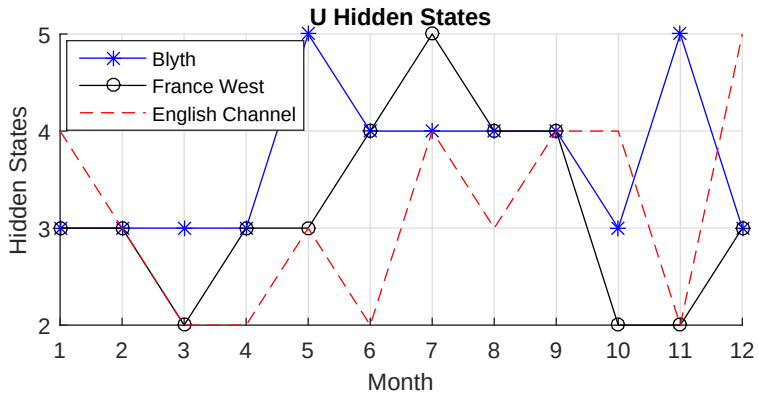

(b)

Figure 3.24: Wind Speed MSAR Model Selection - (a) AR model order p (b) hidden states M

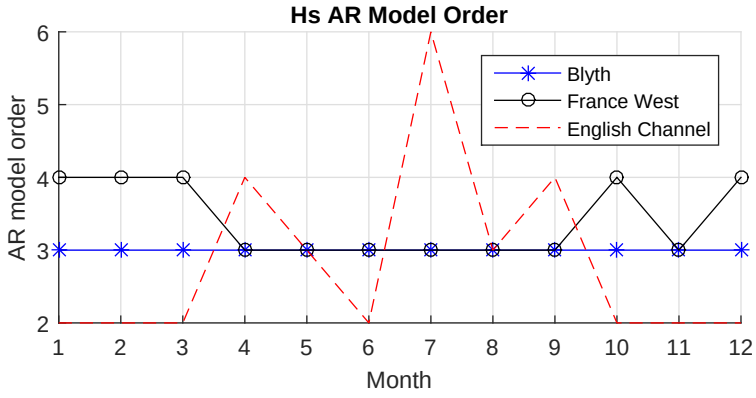

(a)

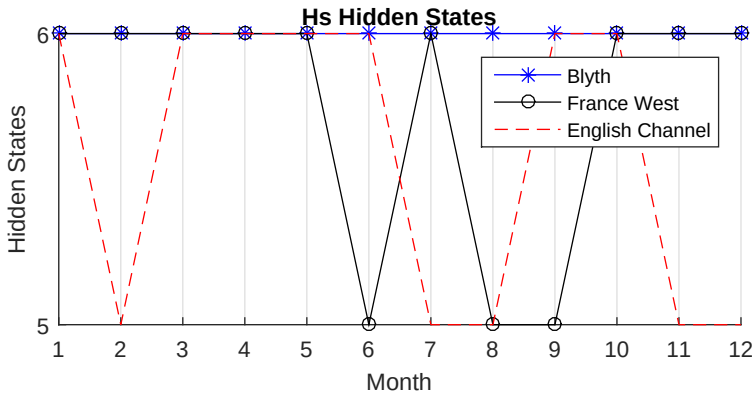

(b)

Figure 3.25: Wave Height (H_s) MSAR Model Selection - (a) AR model order p (b) hidden states M

3.3.5 Simulation and Time Series Composition

Once the most suitable model for each month and meteorological parameter is identified, the simulation process can be summarised as follows.

- The EM algorithm is run once again for each month based on the value for p and M identified from the BIC scoring process. The EM algorithm first relies on randomly selected initial state probabilities, transition matrix and parameters for each AR model, one for each hidden state $S_t \in \{1, ..., M\}$.

The EM algorithm is then run to determine an estimate for the parameters of the MS-AR models, identifying the likelihood of the model and most probable sequence of hidden states.

- For each simulation (normally 1000) the estimated parameters from the EM algorithm are then used to simulate one instance of the Markov chain, which allocates the hidden states to each time step and thus the allocation of each autoregressive model across the time series.

- This distribution of hidden states is then carried into the AR simulation. The AR simulation takes a random year of observations for the given month, which provides a reference for the first set of previous values corresponding with the model order p. Then for each step, the evolution of the weather series is handled by taking the conditional probabilities for the AR(p) lags within the hidden state allocation, which are then multiplied against the p lag values calculated in the previous time step. This produces a new value for the next time step which is altered accordingly with the associated parameters μ and σ for the AR model that operates in the hidden state.

- This process continues following the path of the hidden states until a new time series is produced. The process is repeated for each month for as many simulations as specified by the user, resulting in variable time series realisations, stemming from a combination of independent state allocations, random selection of observed data and the AR computation.

After the simulations are completed, multiple realisations of each month for U and H_s are produced. It should be noted that the MS-AR model is capable of producing negative values. These occurrences are very rare and a screening process to replace any negative values with zeros, was completed first to ensure realistic predictions can be drawn from the generated time series. Following the steps in Figure 3.21, the monthly realisations of U and H_s were produced

independently at three hour intervals. Therefore a method to pair each U and H_s time series was necessary to ensure realistic data sets were produced.

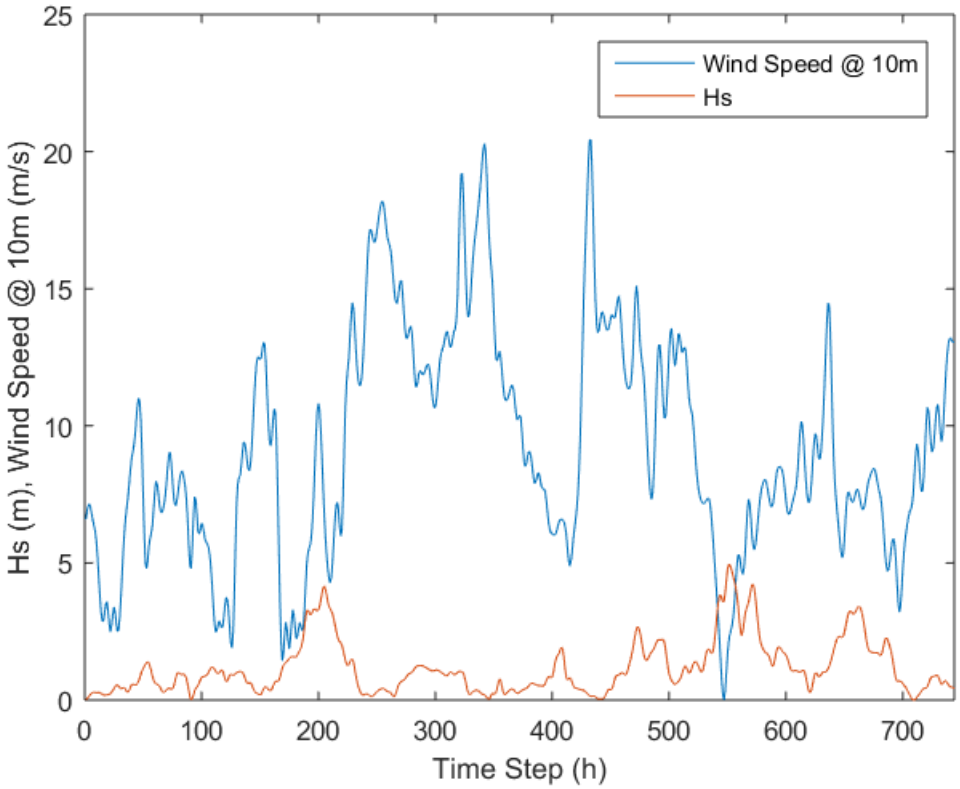

Figure 3.26: English Channel - January - Realisation 500 Pearson r:-0.078

To account for the correlation between wind and wave excitation, a pragmatic approach was initially used by calculating the mean of each monthly time series of U and H_s and then ranking these in ascending order. This ordering was then used to pair the U and H_s time series, before linear interpolation was applied to scale the realisations to hourly time steps. Finally, monthly sets were combined into annual data series, retaining the same ranking from the pairing method. As demonstrated by some of the primary plots in Section 6.3.1, it was found that significant deviations were observed for the winter months, particularly for the English Channel location. It was originally suspected that the complex relationship between the wind, waves and current within an enclosed passage

might have introduced a sensitivity to the methodology. However, a further review found that in many cases the wave time series contrasted against the wind pattern as exemplified in Figure 3.26, which when used in a logistical simulation package, may lead to significantly conservative estimates for the progression of marine operations.

To assess the severity of this mismatch between the simulated wind speed and wave height time series, the correlation between both parameters was investigated. The Pearson r correlation coefficients between the wind speed at 10m and Hs for each location are included in Table 3.6. The coefficients indicate that each data set has a different wind-wave relationship, with the English Channel location having the greatest correlation of 0.9. Therefore a review of the wind and wave correlations was completed for simulated English Channel data and resulted in a Pearson r of around 0.06, as exemplified for the month of January in Figure 3.27.

It was not intended that the data would be a perfect meteorological replication of the relationship between the wind and the waves; however, such a low coefficient did question the overall robustness of the weather model when compared to those of the observed data sets. To improve this relationship, a second pairing approach, which used Pearson correlation coefficients to pair the wind and wave time series, was investigated. A thorough description of Pearson's correlation coefficient can be found in [131]. The expression to define Pearson's correlation coefficient is listed in Equation 3.12 [132]. Firstly, this approach normalised all three hour wind speed and significant wave height realisations into monthly matrices. Then each wind speed and wave height realisation was systematically assessed using the Pearson R coefficient, thus identifying the wave height series that best matched each wind speed realisation.

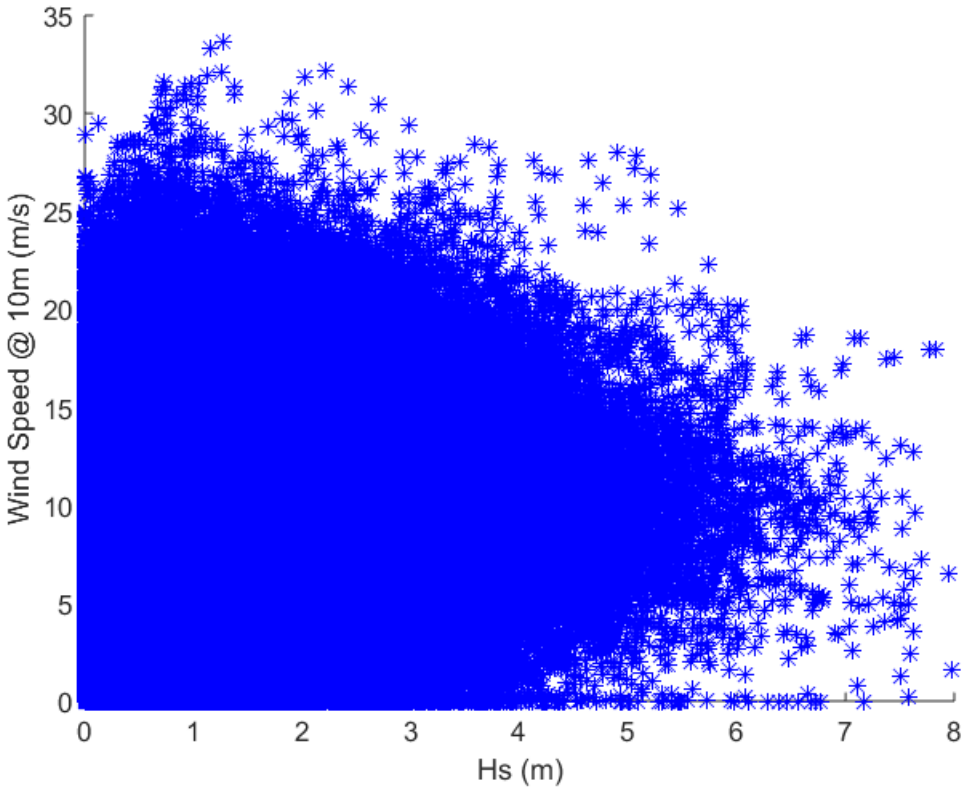

Figure 3.27: English Channel - January - All Realisations Pearson r:0.06

$$\rho(A,B) = \frac{1}{N-1}\sum_{i=1}^{N}\left(\overline{\frac{A_i-\mu_A}{\sigma_A}}\right)\left(\frac{B_i-\mu_B}{\sigma_B}\right) \tag{3.12}$$

where:

A = Monthly realisations of wind speed

B = Monthly realisations of significant wave height

N = Number of observations in each monthly realisation

$\mu_A,\ \sigma_A$ = mean and standard deviation of A

$\mu_B,\ \sigma_B$ = mean and standard deviation of B

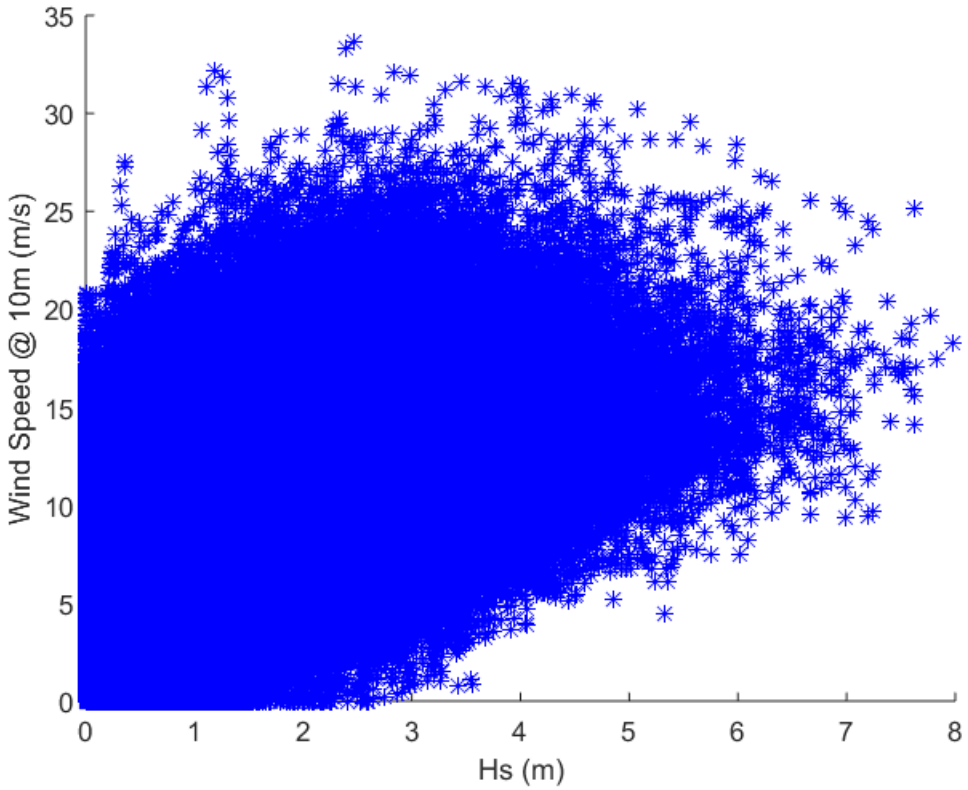

Figure 3.28: English Channel - January - All Realisations Pearson r:0.47

It was found that a number of duplicate wave height series would be selected using this method, thus removing some unique realisations from the final composition. However, this approach was found to significantly improve the outputs for the site and months in question. Once paired, the time series were again expanded to hourly time steps using linear interpolation. A review of the correlation and time series plots in Figures 3.28 and 3.29 for newly paired wind speed and wave height outcomes revealed that the Pearson r was improved to approximately 0.5 and that the wave height time series followed a similar pattern to the wind series.

These outcomes demonstrated a significant improvement using the correlation pairing approach and it was anticipated that this alteration would offer a more robust modelling methodology overall. It should be noted that the final Pearson

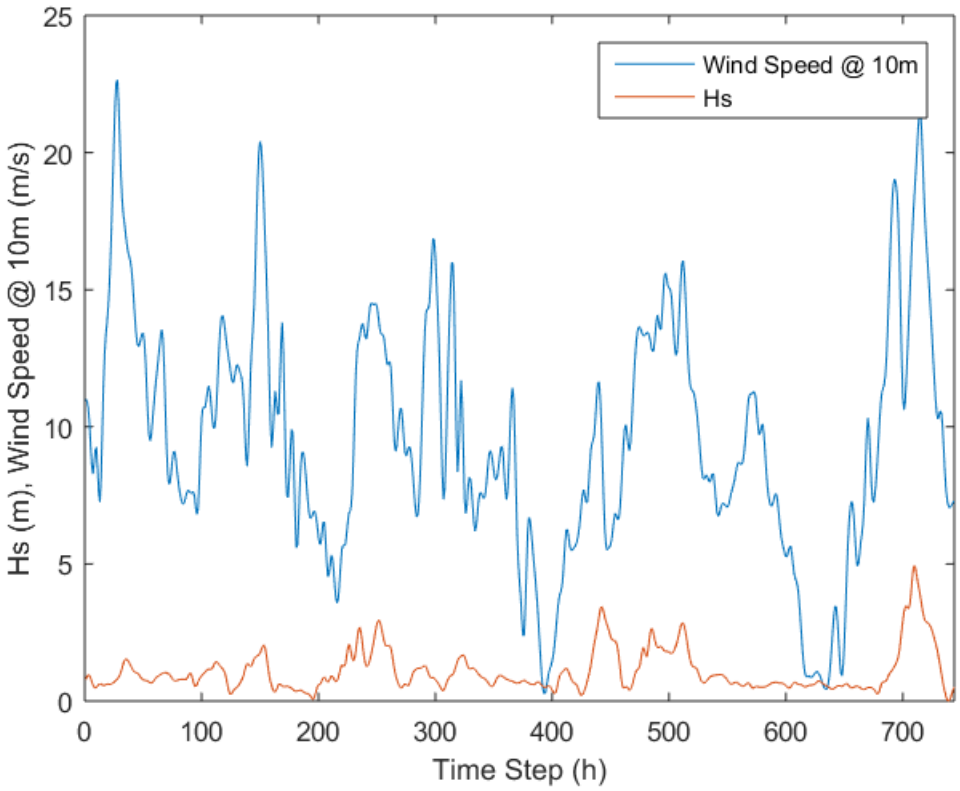

Figure 3.29: English Channel - January - Realisation 500 Pearson r:0.5

r for the simulated time series was lower than the observed series for the English Channel by approx 0.4; Figure 3.30 provides a perspective on the concentration of the simulated data against the scatter of the English Channel observations. The scatter of the observed data is represented by the white transparent plots, overlaid on the concentration map of the simulated data. It shows that the majority of the most densely concentrated simulated data falls within the spread of the observed scatter, indicating that the modelling approach and surrounding methodology is capable of producing a bivariate time series similar to observed data sets with high Pearson r coefficients. To ensure the simulated bivariate time series would exhibit reasonable characteristics suitable to assess marine operations. A number of assessments are completed in Chapter 6.

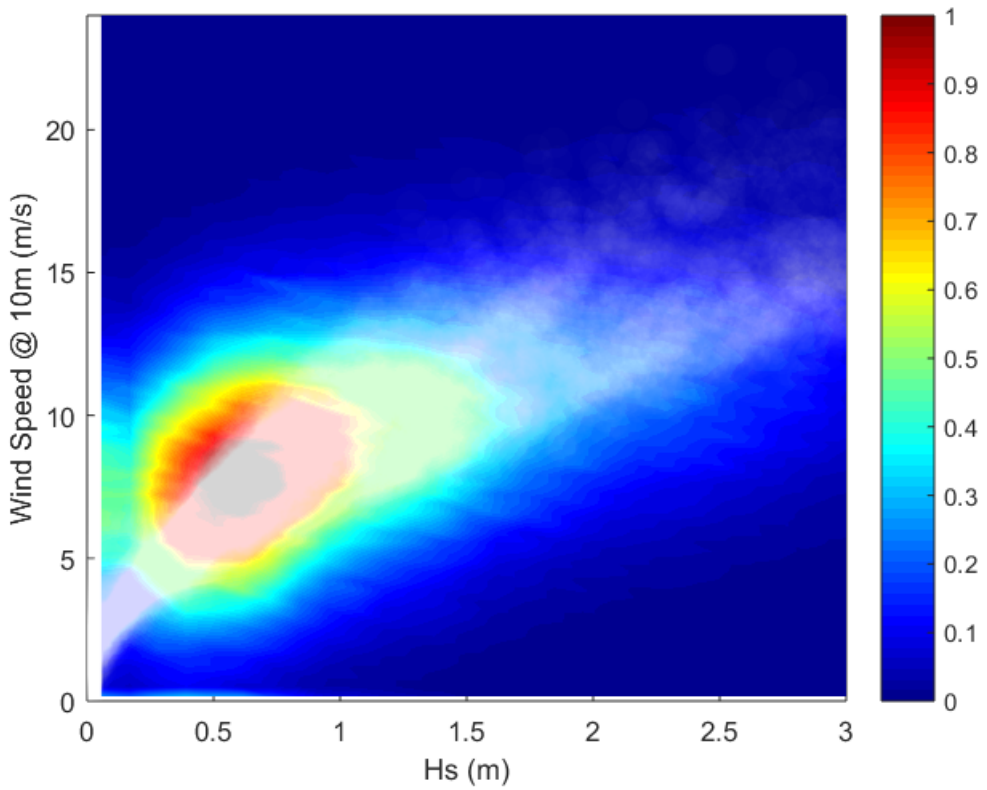

Figure 3.30: Concentration of simulated wind speed and H_s vs. scatter of observed data (white transparent plots) - English Channel

3.4 Summary

Three core methodologies have been presented to demonstrate the computational processes that will be applied to quantify the metocean risk associated with offshore wind installation operations. EDF R&D's existing in house software tool 'ECUME' has been comprehensively explained with focus on the Markov chain meteorological model to generate multiple stochastic metocean time series and the characteristics of the logistical model calculations applied in a Monte Carlo approach. The meteorological model highlights the potential of Markov processes to classify and simulate different meteorological states that exist within

three main parameters of wind speed, significant wave height and current speed. These descriptions are complemented by structured inputs that were selected to assess the capabilities and evolution of installation vessels characterised by UK offshore wind rounds one, two and three. This included the selection of metocean hindcasts, vessel spreads and operational limits for eight primary installation phases.

The formulation of two commercial metocean risk analyses are presented for EDF's Blyth Offshore Demonstrator (BOD) and Fecamp offshore wind farms using James Fisher Marine Service's Mermaid software. A structured method as highlighted in Figure 3.14 was presented to assess the metocean risk for the main installation phases of each project. The transparency of the modelling steps in Mermaid is contrasted against the ECUME I, whilst it is explained that a secondary Matlab data process was needed to extract the durations for concurrent phases in the Mermaid BOD model.

Building on the capabilities of these two methods, a stochastic MS-AR model is presented to test it's suitability for EDF's next generation simulation tool. The application of the autoregressive process is highlighted in conjunction to the overarching Markov chain, which was demonstrated to support the allocation of different weather states in each metocean realisation. The MS-AR model is built into a full metocean modelling methodology presented in 3.21, which includes a model selection process and two pairing methods to generate realistic correlation between wind speed and significant wave heights. It was identified that a Pearson R correlation method can reconstruct correlations for many sites, yet it may struggle to replicate time series for sites with Pearson r correlations above 0.8. Results from these methodologies are presented in the following chapters.

Chapter 4

Results - Comparative Vessel Assessment with ECUME I

4.1 Results Assessing Vessel Technology

To assess the impact of vessel technology on construction durations for offshore wind farms, the scenarios in Section 3.1.2.2 were applied using the simulation tool described in Section 3.1.1. For both wind rounds, 11 cases were constructed as follows: One mean case of all parameters; eight cases where each parameter was run with a maximum and minimum value in turn; and two extreme cases combining a maximum and minimum situation for the number of turbines and distance to shore. The main characteristics of the vessels under analysis are the transit and survival limits, which are composed of a maximum wave height and wind speed as listed in Table A.1. The transit speeds of each vessel for loaded and unloaded states are also specified. An overview of the vessel spreads used for each round is included in Table 3.4.

Each simulation is run for a 1000 iterations to obtain sufficiently accurate results. For each of the individual 11 cases, the software produces a calendar output for all installation phases, recorded under user specified exceedance quantiles. The predicted duration for each installation phase is presented with a start and an end date, meaning the results are rounded to the nearest day. The P90 duration quantile was selected for analysis in this study, as it provides greater certainty that the predicted values will not be exceeded, when conducting these operations offshore. The predicted P90 duration for each phase is divided by the number of turbines specified in each case to reveal the average installation rate (IR) in days per turbine (days/WTG). The IR represents the average number of days required to complete the installation task at each turbine in the model, including the impact of weather delay. To demonstrate how these results can be used in practice, an average result for weather downtime (WDT) is calculated by deducting the base duration from the predicted P90 duration for the phases in each case. The base duration in each phase is calculated using the net time to complete the installation tasks without the impact of weather delay, and multiplying this by the number of turbines in each case. The resulting WDT duration is once again divided by the number of turbines for each case, to reveal a WDT value for the individual installation phases in days/WTG.

Within each case, eight IR and WDT values are collected, corresponding to the number of installation phases. For each round, a total of 11 cases were collected and an average IR and WDT for the eight installation phases was computed from this compilation, as shown in Figures 4.1 and 4.2. As discussed in Section 3.1, the deviation from these averages is regarded as a means to estimate the installation risk in the potential outcomes.

Box plots showing the variation in the results are presented in Figures 4.3a to 4.3d and a comparison of the recorded variation in each phase in both rounds is

included in Figure 7.3. The greatest variability in the results was observed for the foundation, transition piece and wind turbine installation phases, as represented by the larger bars in Figure 7.3. This indicates that the greatest risk is estimated to occur within these phases, although the Round 2 figures demonstrate lower deviation despite higher durations.

4.2 Results Overview

The IR for each of the eight phases was used to compare the differences between the vessel spreads of each round. Figure 4.1 presents a summary of the installation rates in days per wind turbine (days/WTG).

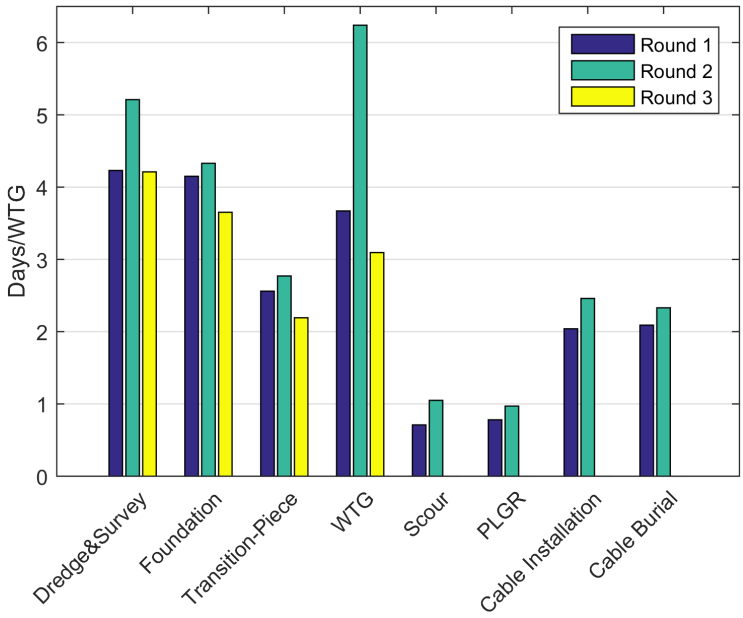

Figure 4.1: Average installation rate in days/WTG (or WTG location)

The results in Figure 4.1 show that Round 1 is estimated to have the second smallest IRs, with the largest individual phase recorded for the dredging and survey, foundation and WTG installation, predicted to be around 4.2, 4.1 and

3.6 days/WTG respectively. The results for Round 2 show the greatest IRs and the largest are again recorded for the same phases at 5.4, 4.4 and 6.3 days/WTG respectively. It can be generalised that Round 1 vessels appear to outperform Round 2 vessels in terms of installation rate, by approximately 25% on average across the eight installation phases. The biggest difference between Rounds One and Two is seen with the Dredge and Survey phase at around 1 day/WTG and the WTG installation phase at approximately 2.5 days/WTG. It is clear that data has not been obtained for all phases in Round 3, which was due to simulation performance but the completed phases can still be used for comparison. The higher IRs observed in Round 2 are not reflected in the completed phases for Round 3, which are closer and in many cases less than the results recorded for Round 1.

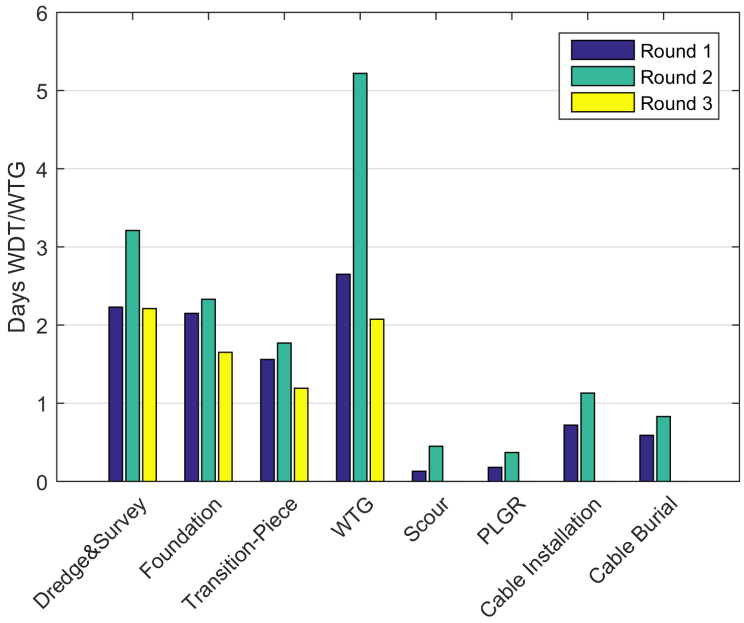

Figure 4.2: Average Weather Downtime in days/WTG (or WTG Location)

As a direct consequence, the results presented in Figure 4.1, knowing the base duration for each of the installation phases allows for the amount of WDT to be identified. The weather delay expected on average for each phase between the

two rounds, is presented in Figure 4.2 and confirms that the greatest delays are observed in the Round 2 phases. This process presents a method for predicting the average WDT for each installation phase. If this approach was used to analyse a case specific simulation, built to match the characteristics of a prospective development, it would provide a basis to scale the results by the number of turbines and reveal an approximate overall WDT for each installation phase.

4.3 Results by Round

The results for the individual rounds were further analysed to determine the distribution of phase durations predicted by the software. The box plots of the IRs and WDTs in each round have been aligned in Figures 4.3a to 4.3f. In terms of WDT, Figures 4.3b to 4.3f demonstrate the same range of distribution as the IRs, but at lower values. A plot of the quantification of the inter-quartile ranges for the IRs and WDTs from each phase across the two rounds, is included in Figure 7.1 and is used to demonstrate the spread in the results, which can be used to signify the installation risk for the combined vessel-phase configurations. This is calculated by simply subtracting the bounds of the first quartile from the third quartile, for each of the installation phases in Rounds One and Two.

Figure 4.3a demonstrates a considerable range for the installation phases in Round 1, particularly in the wind turbine (WTG), transition piece and foundation installation steps, as demonstrated by the broad space taken by the interquartile range (IQR). The variability of these IRs spans from approximately 2.4 - 5.5 days/WTG with an IQR of about 3 days/WTG for the foundations, 1.4 - 3.9 days/WTG with an IQR of 2.3 days/WTG for the transition pieces and 1.9 - 5.3 days/WTG with an IQR of 3.4 days/WTG for the turbines. All of the phases demonstrate a skew towards the upper values of the data. The dredging and

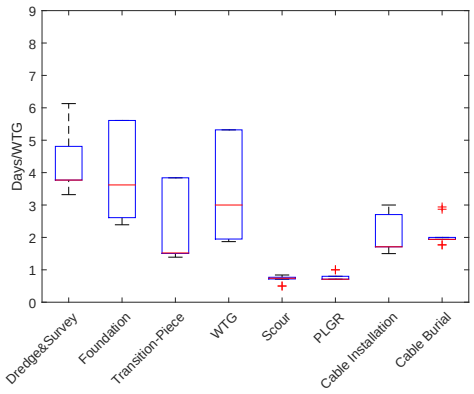

(a) Round 1 - IR distribution

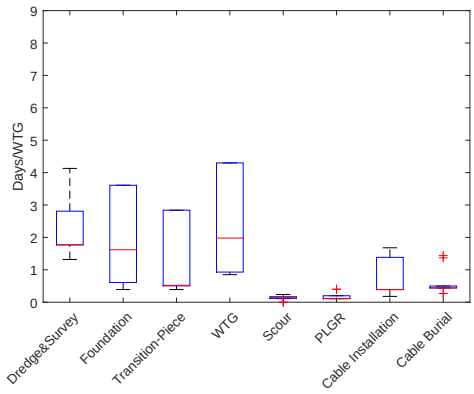

(b) Round 1 - WDT distribution

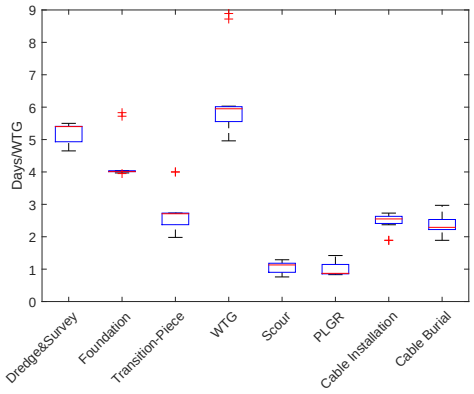

(c) Round 2 - IR distribution

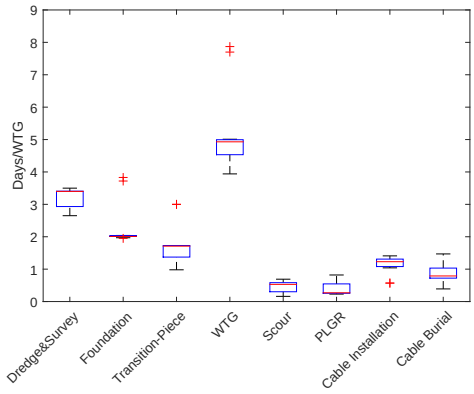

(d) Round 2 - WDT distribution

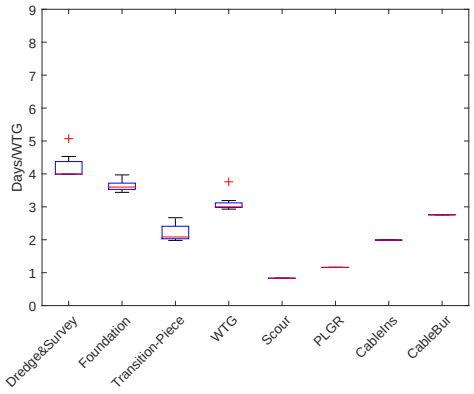

(e) Round 3 - IR distribution

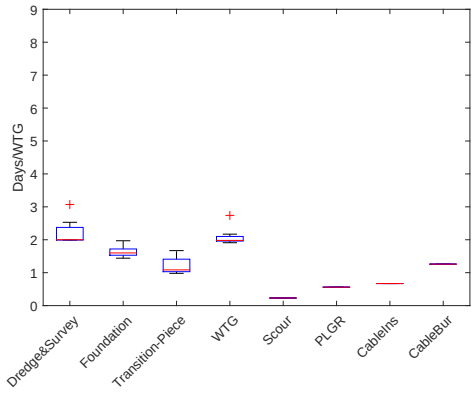

(f) Round 3 - WDT distribution

Figure 4.3: Installation Rates (IR) and Weather Downtime (WDT) by round

survey, cable installation and cable burial phases exhibit lower variance in the results and a nominal range was predicted for the scour and PLGR stages, with the majority of these phases taking one day or less per wind turbine.

Figure 4.3b shows similar variance between the Round 1 IR and WDT predictions. Based on the results in Figure 4.3a, it can be expected that the greatest ranges would be seen at the foundation, transition piece and wind turbine installation phases at 0.4 - 3.6 days/WTG with an IQR of 3 days/WTG , 0.4 - 2.8 days/WTG with an IQR of 2.3 days/WTG and 0.8 - 4.3 days/WTG with an IQR of 3.2 days/WTG respectively. Again, the medians for these phases are skewed towards the upper data in the plots. The distribution of all phases in Figure 4.3b have a near identical profile as seen the IRs. The scour and PGLR phases are predicted to have the lowest IRs and subsequent WDT in Round 1 without much variation, while the three key phases of the foundation, transition piece and wind turbine installation present the highest values in terms of delay.

Figure 4.3c shows generally smaller ranges for the results when compared to Round 1. The broadest IQR distributions relate to the dredging and survey, transition piece and wind turbine phases at 0.5, 0.4 and 0.45 days/WTG respectively. The foundation and transition piece installations have an overall range of approximately 2 days/WTG and the largest recorded for the WTG installation at 4 days/WTG. The same distribution profiles are again replicated in the WDT plots shown in Figure 4.3d and once more the scour Protection and PLGR phases demonstrate the lower weather downtime. The dredging and survey, foundation and WTG installation phases are shown to have the largest values in terms of WDT. Generally, it was found that the installation rates and WDT predicted for the phases in Round 2 are higher in comparison to Round 1. However the results seem more consistent as the distributions are quite narrow and this smaller variation indicates a reduction in installation risk.

The IR results for Round 3 are included in Figure 4.3e. It should be noted that only one of the scenarios reached completion when simulating this round but data was still obtained for the dredging and survey, foundation, transition piece and WTG installation phases, which can be used for comparison. The overall distributions of the results for these four phases are quite narrow with dredging and survey and transition piece installation exhibiting the broadest IQRs. The broadest overall ranges are seen with the transition piece and Turbine Installation phases at 0.7 and 0.8 days/WTG approximately. In Figure 4.3f the spread of the results for WDT in Round 3 are shown. The greatest range in WDT predictions was in the dredging and survey at 1.07 days/WTG and wind turbine installation phases at 0.8 days/WTG. Across the IR and weather downtime plots, the results are mainly skewed towards the lower end of values and by in large were predicted to have lower IRs and subsequent weather downtimes in comparison to Round 2.

4.4 Summary

The assessment of three different vessel spreads characterised by the UK's three offshore wind construction rounds is presented in this chapter. The analysis has shown the modelling approach was capable of identifying the metocean risk associated with primary installation vessels in each round. It was identified that Round 2 vessels were estimated to have the greatest average weather downtime overall, whilst a review of the results distribution have shown the greatest variability in Round 1 estimates. It is unfortunate that a clear limitation of the ECUME I tool was identified by the simulation of the Round 3 scenarios, which relates to a memory restriction inherent within the software. Nonetheless, the means of reducing the estimates using a per wind turbine metric has shown relevance to compare outputs of scenarios that vary drastically in size between the three rounds. In the next chapter a commercial metocean risk analyses are

completed using Mermaid software, which is of interest as it provides improved modelling transparency and is well aligned to the offshore standards presented in Chapter 2, section 2.3.1.

Chapter 5

Commercial Metocean Risk Assessments

The results for the commercial metocean risk assessments completed for the Blyth Offshore Demonstrator (BOD) and Fecamp offshore wind farms are presented in this chapter. The results for both projects follow the detail and methodological steps described in Section 3.2.2, utilising the Mermaid simulation tool. A different modelling approach was applied to each project, where a combined model that encapsulates all project installation phases was built for BOD and separate models were built for each phase of the Fecamp project. The purpose of the BOD weather risk assessment was to directly support contractual and contingency planning in the project, whilst the Fecamp study was completed to assess the feasibility of a segmented modelling methodology and the suitability of Mermaid in the assessment of downtime for a large scale offshore wind development.

5.1 Blyth Offshore Demonstrator - Installation Metocean Risk Analysis

This section presents the results obtained from metocean risk analyses completed for the Blyth Offshore Demonstrator following the detail and methodology presented in Chapter 3 Section 3.2.3.

Following discussion with the project team at the BOD, a variety of percentile values were produced for the primary installation phases. This approach applied a separate calculation across the main operations within each installation phase to produce P50, P70 and P90 duration and downtime estimates, using equations 3.4 to 3.6. This approach differs from the categorisation produced in Mermaid; which uses the final completion date for all installation operations throughout the simulations to summarise the results under percentile values. This can mask the presence of significant delays during individual and enclosed installation phases. The results are presented in days and represent potential durations and downtimes during the operations to install the necessary assets and associated infrastructure for all five turbine locations. The results are described in terms of percentage increase in respect of the base 'P0' duration, to highlight phases with the greatest level of associated risk. Percentage increase tables that correspond to the installation durations presented in each scenario are included in Appendix G.3 and compliment the description of the results.

5.1.1 Scenario 1 - No Learning

The results for the first modelled scenario are included in Table 5.1. This scenario represented the base set of operational durations without the impact of learning

rates on the GBF and WTG Installation phases. The breakdown of operations has been slightly extended from the original list presented in Section 3.2.3, where the GBF Installation step was split into three phases: Towing the GBFs out of the dry dock, towing the GBFs down the River Tyne and the overall GBF Installation, which is composed of a towing, anchoring, water and sand ballasting operations. The base duration to complete the installation operations without the impact of weather is included in the 'P0' column, with the largest associated with the mechanical completion, WTG, GBF and commissioning tasks at 38.65, 37.58, 25.24 and 22.08 days respectively.

Table 5.1: Percentile Results: BOD - No Learning

	Installation Duration (days)				**Weather Downtime (days)**		
	P0	**P50**	**P70**	**P90**	**P50**	**P70**	**P90**
Dredging & Survey	14.83	15.82	17.57	23.15	0.99	2.74	8.32
Filter Layer	15.26	20.7	23.82	30.43	5.44	8.56	15.17
Towing GBFs out of dry dock	0.42	19.40	28.44	54.90	18.98	28.02	54.48
Towing GBFs down River Tyne	2.65	3.7	3.88	5.57	1.05	1.23	2.92
GBF Installation	25.24	30.32	32.04	36.22	5.08	6.80	10.98
Scour Protection	5.04	6.24	6.3	7.85	1.20	1.26	2.81
PLGR	5.83	5.83	6.7	8.63	0.00	0.87	2.80
Export Cable	8.96	10.04	12	15.26	1.08	3.04	6.30
Array Cable	7.4	7.4	8.02	9.2	0.00	0.62	1.80
Hang-off, Stripping & Routing	10.5	10.5	11.34	12.75	0.00	0.84	2.25
Cable Burial	10.58	10.58	10.72	11.3	0.00	0.14	0.72
WTG Installation	37.58	42.44	44.38	51.83	4.86	6.80	14.25
Mechanical Completion	38.65	50.48	53.3	60.1	11.83	14.65	21.45
Final Routing	8.75	10.41	11	13.66	1.66	2.25	4.91
Commissioning	22.08	27.91	30.26	36.17	5.83	8.18	14.09

The largest recorded installation durations and subsequent downtimes were recorded for Towing GBFs out of dry dock consistently across all percentiles and were predicted to be approximately 46 and 130 times bigger than the base duration for the P50 and P90 outcomes respectively. These large durations are

caused by specific tidal elevation constraints that were applied to this task in the model. This was subsequently used to simulate the required under-keel clearance for the GBFs when passing over the sill of the flooded dry dock. The next largest percentage increase in predicted installation duration was recorded for the Filter Layer and Towing GBFs down River Tyne tasks, demonstrating approximately 35% and 100% increase for P50 and P90 respectively. The Export Cable, Mechanical Completion and Commissioning tasks were also predicted to have significant increases, with percentage increases ranging between 50% and 70% for P90 estimates. Some variability is recorded for the Dredging and Survey, GBF Installation and Scour Protection phases in terms of percentage increase across the percentiles, whilst the Array Cable, Hang-off stripping and routing and Cable Burial were predicted to have the lowest increase for all percentiles.

A P90 weathered Gantt chart was extracted from Mermaid for the entire BOD installation campaign and is presented in Appendix C. The P90 Gantt chart was selected to exemplify a worst case scenario and associated completion date for all installation operations. It was noted for this worst case, that a completion date of 31/10/2017 could be anticipated for the project. It is reiterated that this completion date is taken from a P90 weathered Gantt chart and does not necessarily represent the worst case for all operational phases in the project but the overall project duration.

5.1.2 Scenario 2 - GBF & WTG Learning

The results from the second modelled scenario are presented in Table 5.2 and include learning rates for the GBF and WTG Installation phases, presented in Figure 3.19.

Table 5.2: Percentile Results: BOD - GBF & WTG Learning

	Installation Duration (days)				Weather Downtime (days)		
	P0	**P50**	**P70**	**P90**	**P50**	**P70**	**P90**
Dredging & Survey	14.83	15.82	17.57	23.15	0.99	2.74	8.32
Filter Layer	15.26	20.7	23.82	30.43	5.44	8.56	15.17
Towing GBFs out of dry dock	0.42	19.40	28.44	54.90	18.98	28.02	54.48
Towing GBFs down River Tyne	2.65	3.7	3.88	5.57	1.05	1.23	2.92
GBF Installation	28.24	35	36.86	39.92	6.76	8.62	11.68
Scour Protection	5.04	6.24	6.3	7.85	1.20	1.26	2.81
PLGR	5.83	5.83	6.7	8.63	0.00	0.87	2.80
Export Cable	8.96	10.04	12	15.26	1.08	3.04	6.30
Array Cable	7.4	7.4	8.02	9.2	0.00	0.62	1.80
Hang-off, Stripping & Routing	10.5	10.5	11.34	12.75	0.00	0.84	2.25
Cable Burial	10.58	10.58	10.72	11.3	0.00	0.14	0.72
WTG Installation	38.84	43.25	46.15	53.91	4.41	7.31	15.07
Mechanical Completion	38.65	50.48	53.3	60.1	11.83	14.65	21.45
Final Routing	8.75	10.41	11	13.66	1.66	2.25	4.91
Commissioning	22.08	27.91	30.26	36.17	5.83	8.18	14.09

The learning rates are shown to increase the 'P0' GBF and WTG Installation durations by 3 days and 1.3 days respectively. It is shown in the results that the increase in these durations has a near negligible impact in the overall durations and weather downtimes with the P90 for the GBF Installation, demonstrating a slightly lower percentage increase by approximately 2%, which corresponds to approximately 0.7 days. Similarly, there was little impact to the percentile values for the WTG Installation, with a slight increase in P50 and P90 estimates by approximately 1%, at approximately 0.5 days and 1 day respectively. The rest of the other and subsequent installation phases were predominantly unaffected by these slight deviations in the GBF and WTG Installation phases; this is further exemplified by the P90 weathered Gantt chart in Appendix D that identified the same completion date as Scenario 1.

5.1.3 Scenario 3 - GBF & WTG Learning - 1 Month Delay

Table 5.3: Percentile Results: BOD - GBF & WTG Learning - 1 Month Delay

	Installation Duration (days)				Weather Downtime (days)		
	P0	**P50**	**P70**	**P90**	**P50**	**P70**	**P90**
Dredging & Survey	14.83	14.83	15.73	20.38	0	0.9	5.55
Filter Layer	15.26	16.14	17.31	19.39	0.88	2.05	4.13
Towing GBFs out of dry dock	0.42	43.88	53.72	72.14	43.46	53.30	71.72
Towing GBFs down river tyne	2.65	3.88	3.88	4.49	1.23	1.23	1.84
GBF Installation	28.24	32.39	34.05	36.43	4.15	5.81	8.19
Scour Protection	5.04	6.24	6.54	7.4	1.20	1.50	2.36
PLGR	5.83	5.83	6.42	7.66	0.00	0.59	1.83
Export Cable	8.96	10.58	11.74	16.19	1.62	2.78	7.23
Array Cable	7.4	7.65	8.07	9.38	0.25	0.67	1.98
Hang-off, Stripping & Routing	10.5	11.23	12.34	17.93	0.73	1.84	7.43
Cable Burial	10.58	10.71	11.76	12.62	0.13	1.18	2.04
WTG Installation	38.84	48.74	50.04	60.43	9.90	11.20	21.59
Mechanical Completion	38.65	60.28	64.72	71.93	21.63	26.07	33.28
Final Routing	8.75	12.56	15.63	21	3.81	6.88	12.25
Commissioning	22.08	33.34	37.48	53.54	11.26	15.40	31.46

Scenario 3 was modelled to investigate the impact of learning rates for the GBF and WTG Installation with a one month delay to the start of the entire installation campaign. The original start date for the first phase (Dredging and Survey) was the middle of March 2017, which was moved to the middle of April. The results for this scenario are presented in Table 5.3. The largest recorded percentage increase was once again associated with the 'Towing the GBFs out of dry dock'. The results show that for this particular phase, the predicted durations are consistently over 100 times greater than the base duration for all percentiles. When compared to the downtimes for the no learning and learning cases, the one month delay case exhibits an increase in weather downtime of 23, 25 and 17 days for the P50, P70 and P90 values respectively. The phases with the next greatest

percentage increase were the Commissioning and Final Routing phases, which both demonstrate approximately 70% and 140% increases in recorded duration for the P50 and P90 percentiles. This is another clear difference in comparison with Scenario 1 and 2, where the Filter Layer and Towing the GBFs down the river demonstrated the next greatest percentage increase in delayed operation. The Towing the GBFs down the River task was still amongst the largest percentage increase recorded overall, sharing similar trends with the Mechanical Completion and Export Cable phases.

A P90 Gantt was also produced for the one month delay case and is included Appendix E. This scenario has a completion date that is approximately two months later in comparison to Scenarios 1 and 2. It can be deduced from the predicted durations and the outcome of the weathered Gantt chart that the one month delay will lead to significantly greater downtime overall. This difference can be largely attributed to the later phases such as WTG Installation, Mechanical Completion and Commissioning spanning over the winter months. It is also clear that a change in tidal availability for towing the GBFs out of the dry dock is experienced, due to the increase in downtime. The completion date for the project is impacted considerably with one month of delay, which in a P90 case is 26/12/2017 and approximately two months later than the prediction for Scenario 1. However the gaps in the simulated schedule mean that these delays do not directly impact the completion date for the project.

5.1.4 Scenario 4 - 1 x WTG Only (assumed GBF has been towed out of dry dock and is ready at Port of Tyne)

This scenario was investigated to identify the latest possible start date to install the necessary infrastructure, ensuring one wind turbine was operational and

generating electricity before 31/03/2018, which was the deadline to qualify to the UK's Renewable Obligation (ROC) financial incentive. Through discussion with the planning team at the BOD project, the base 'P0' durations were altered to reflect the change in the operations for the installation of one turbine. It should be noted that this analysis assumed that the GBF to be installed during this campaign had already been towed out of the dry dock and down the River Tyne awaiting installation. It is also assumed that the gaps or buffer that existed in the original five GBF schedule did not exist and the phases were completed sequentially. In this scenario, the phases found to have the greatest percentage increase in duration were the Export Cable and WTG Installation phases. It is noted that the P90 for the WTG Installation is approximately eight times greater than the P0 duration, whilst the Export Cable spans between a 2.5 - 3.5 times greater duration across the three percentiles. Scour Protection durations were predicted to increase considerably, up to as much as five times greater for the P90 percentile. The Filter Layer, Hang off & stripping were amongst the next greatest percentage increase in duration across the percentiles, predicted to reach up to three times greater at P90. The GBF Installation and commissioning tasks show notable increases, ranging between 0.65 - 0.9 and 1.2 - 1.8 times greater for P50 and P90 respectively. The weathered Gantt chart was a key reference in this study to identify the latest possible start date for the operations.

Table 5.4: Percentile Results: Scenario 4 - 1 x WTG Only

	Installation Duration (days)				Weather Downtime (days)		
	P0	**P50**	**P70**	**P90**	**P50**	**P70**	**P90**
Dredging & Survey	5.10	5.10	5.55	8.61	0	0.44	3.51
Filter Layer	5.79	9.13	12.57	22.6	3.34	6.78	16.81
GBF Installation	5.09	7.09	8.86	11.13	2	3.77	6.04
Scour Protection	4.19	8.95	13.90	28.39	4.76	9.71	24.20
PLGR	3.44	4.22	5.26	6.2	0.78	1.82	2.76
Export Cable	10.25	37.21	41.05	48.03	26.96	30.8	37.78
Array Cable	18.22	19.23	20.24	21.39	1.01	2.02	3.17
Hang-off, Stripping & Routing	1.75	2.38	2.78	7.78	0.63	1.03	6.03
Cable Burial	5.39	6.22	7.23	8.72	0.83	1.84	3.33
WTG Installation	4.47	12.36	25.91	40.55	7.89	21.44	36.08
Mechanical Completion	7.73	12.9	14.51	19.6	5.17	6.78	11.87
Final Routing	1.75	1.75	2.66	4.86	0	0.91	3.11
Commissioning	4.42	5.88	7.34	12.59	1.46	2.92	8.17

The P90 weathered Gantt chart was selected to review an extreme outcome for this scenario and in order to identify the latest start date, a number of iterative simulations were completed, altering the start date in the model each time until the target date of 31/03/2018 was predicted for a P90 case. In Appendix F it is shown that 07/09/2017 was the latest possible P90 start date. It should be noted that this Gantt chart represents a P90 case for the entire range of marine operations, whilst the duration downtime figures included in Table 5.4 represent percentile outcomes for each phase individually, which can differ from the example in Figure F.1. It shows that a large amount of downtime is predicted for the P90 case in Figure F.1, which appears to be impacted by poorer conditions experienced across the winter months of November, December and January.

5.2 Fecamp - Installation Metocean Risk Analysis

The results from the Mermaid simulations for the Fecamp weather risk analysis are presented in this section. The first set of results is taken from independently simulated models. The results tables list the recorded durations in days and resulting weather downtimes (WDT) under exceedance quantiles P50, P60, P70 and P90. A P0 duration is included in each table, which represents the net duration for the operations without the impact of weather delay. The WDT values are identified by deducting the unweathered installation duration produced in Mermaid, from the predicted duration for each quantile. A secondary review of the planned start dates in combination with the summarised installation durations was also completed. This is presented in the form of 'mock' weathered Gantt charts for the same quantiles as before and aims to demonstrate any cross-over between phases that may lead to resourcing challenges or delays.

5.2.1 Fecamp - Predicted Durations and Weather Downtime

The results for each installation phase under the P50 and P90 quantiles are taken directly from the summary tables produced by Mermaid. The recorded duration and weather downtime (WDT) values are based on the percentile (Pxx) durations in days, which is a summary statistic produced from the 21 simulations completed for each installation phase. The P60 and P70 outcomes are derived from the dates included on weathered Gantt charts created in Mermaid. The Gantt chart referenced for each Pxx value is based on the closest lying simulation to the Pxx duration, meaning the completion dates are sourced from a slightly different

statistic in comparison to the summarised duration and WDT values. The results are described in terms of percentage increase to highlight the phases with the greatest associated risk in each percentile.

5.2.1.1 Percentile Results: Installation Campaign 1

Table 5.5: Fecamp - Installation Campaign 1

	Installation Duration (days)					Weather Downtime (days)			
	P0	**P50**	**P60**	**P70**	**P90**	**P50**	**P60**	**P70**	**P90**
GBS Bedding	35.9	40.2	41	42	46.9	4.3	5.1	6.1	11
GBS Installation	123.7	143.1	144	148	152.6	19.4	20.3	24.3	28.9
GBS Scour & Ballast	117.4	137.2	141	143	148.2	19.8	23.6	25.6	30.8
IAG Laying	33.8	39.1	39.2	42	43.4	5.3	5.4	8.2	9.6
IAG Burial	50.2	58.4	59	60	66.9	8.2	8.8	9.8	16.7
IAG Termination	67.4	77.5	78	79	90.1	10.1	10.6	11.6	22.7

The percentile results for the first installation campaign are included in Table 5.5. Overall it shows that the largest weather downtimes are recorded for the GBF Installation and Scour and Ballast phases across all percentiles ranging from approximately 20 days to 30 days between P50 and P90 estimates. The inter-array grid/cabling (IAG) Termination and burial phases show the next greatest number of days downtime at around 23 and 16.7 days for P90 respectively. In terms of percentage increase, the IAG Termination and burial phases show approximately a 30% extension in duration at P90. For P50, the IAG Laying is predicted to have the largest percentage increase at 24%, whilst the greatest increase in the P50 and P60 percentiles was predicted for the GBF Scour and Ballast at 17% and 20% respectfully.

5.2.1.2 Percentile Results: Installation Campaign 2

Table 5.6: Fecamp - Installation Campaign 2

	Installation Duration (days)					Weather Downtime (days)			
	P0	**P50**	**P60**	**P70**	**P90**	**P50**	**P60**	**P70**	**P90**
GBS Bedding	21.9	28.1	28	29	35	6.2	6.1	7.1	13.1
GBS Installation	79.9	100.1	104	105	113.6	20.2	24.1	25.1	33.7
GBS Scour & Ballast	72.8	94.6	97	99	102.5	21.8	24.2	26.2	29.7
IAG Laying	58.7	69.7	70	72	76.9	11	11.3	13.3	18.2
IAG Burial	88.8	103.8	108	110	117.9	15	19.2	21.2	29.1
IAG Termination	119.4	134.8	136	137	147.3	15.4	16.6	17.6	27.9
WTG Installation	199.1	248.2	254	256	282.1	49.1	54.9	56.9	83

Percentile results for the second installation campaign are listed in Table 5.5. It is shows that the largest downtimes are associated with the WTG Installation phase, at 55 days and 83 days downtime for the P50 and P90 percentiles respectively. These large downtimes are directly related to the scale of this phase as it enclosed all 83 WTG Installations, while the other phases in this campaign had 32 GBF and 51 IAG tasks. The next largest overall downtimes are related to the GBF Installation and Scour and Ballast phases, ranging from between 20 and 30 days downtime, and are very similar to the results from the first campaign for these phases despite the lower number of overall installation tasks. The greatest percentage increase in net duration was recorded for the GBF Scour and Ballast across the P50, P60 and P70 percentiles at 30%, 33% and 36% increase respectively, with similar values observed for the GBS Bedding and installation phases. The greatest increase in P90 estimate was observed for the GBF bedding at 60%, with the next greatest P90 percentage increase recorded across the GBF Installation, Scour and Ballast and WTG Installation at approximately 40%.

5.2.1.3 Fecamp - Mock Gantt Charts - Campaigns One and Two

To investigate the impact of cross-overs or delays that could occur between the installation phases, Gantt charts were produced using the planned installation dates and predicted durations identified for each installation phase for the P50 to P90 quantiles. As each phase in Campaigns 1 and 2 was built using a separate Mermaid study, the impact of knock-on delays could not be exemplified in the same way as the BOD analysis, which incorporated all project phases in the one model. Whilst it is unlikely that the investigated Pxx outcome will occur for all phases in the project, in reality, the Gantt charts provide a perspective of how the operations might progress and highlights potential scheduling or resourcing issues that could occur. An unweathered Gantt chart is included to demonstrate the ideal progression of the operations without any downtime. An attempt has been made to highlight any perceived issues with the progress of installation phases, which are presented using red bars in each figure and are supported by a short discussion.

ID	Task Name	Duration	Start	Finish
1	GBS Bedding (C1)	35.9 days	Sun 15/03/20	Mon 20/04/20
2	GBS Installation (C1)	123.7 days	Wed 01/04/20	Mon 03/08/20
3	GBS Scour & Ballast (C1)	117.4 days	Sun 05/04/20	Fri 31/07/20
4	IAG Laying (C1)	33.8 days	Wed 01/07/20	Tue 04/08/20
5	IAG Burial (C1)	50.3 days	Sat 01/08/20	Sun 20/09/20
6	IAG Termination (C1)	67.38 days	Sat 15/08/20	Wed 21/10/20
7	GBS Bedding (C2)	21.9 days	Mon 15/02/21	Tue 09/03/21
8	GBS Installation (C2)	79.9 days	Mon 01/03/21	Thu 20/05/21
9	GBS Scour & Ballast (C2)	72.8 days	Sat 06/03/21	Tue 18/05/21
10	WTG Installation	199.1 days	Thu 15/04/21	Sun 31/10/21
11	IAG Laying (C2)	58.7 days	Tue 15/06/21	Fri 13/08/21
12	IAG Burial (C2)	88.8 days	Sat 10/07/21	Thu 07/10/21
13	IAG Termination (C2)	119.4 days	Sun 25/07/21	Sun 21/11/21

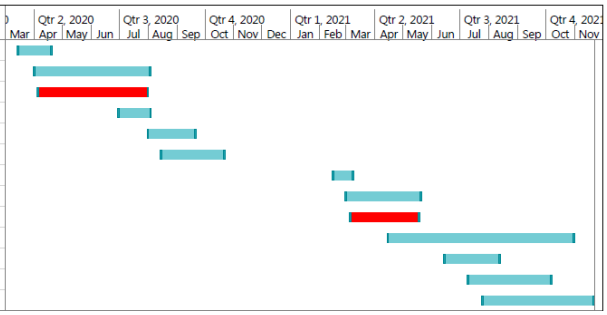

Figure 5.1: Fecamp Unweathered Gantt Chart - Campaigns One and Two

The P0 Unweathered Gantt chart is shown in 5.1. This chart demonstrates the progression of operations without the impact of weather delay. It is noted that the Scour and Ballast operations appear to finish before the installation of the GBS Installation phase in both campaigns. This reveals a potential issue, as in

reality the Scour and Ballast phase cannot possibly complete before the GBS foundations have been installed. Further investigation and/or modelling of the interdependencies between these installation phases may produce a more realistic outcome. It is understood that alternative start dates have been considered for the Fecamp project and adjustments in the scheduling of the GBS Scour and Ballast phases could prevent potential delays in this phase whilst waiting for the GBS Installations to complete. As this interaction has been identified in the unweathered Gantt chart, it is probable that this same issue will occur in the Gantt charts for the other quantiles. It is clear that the WTG Installation phase runs in parallel to GBS and IAG operations in the second campaign. The interaction between these phases is unlikely to be an issue, as the GBS and IAG operations in the first campaign installation should be completed by the time the WTG Installation begins. The WTG Installation will begin at the 30 locations in Campaign 1, limiting interaction with other works being completed as part of Campaign 2. It is noted that the IAG Termination tasks in Campaign 2 run in parallel to the WTG Installations. It is possible some tasks could coincide at the same turbine location and will require careful coordination to prevent access problems for both vessels and personnel.

ID	Task Name	Duration	Start	Finish
1	GBS Bedding (C1)	**40.2 days**	Sun 15/03/20	Fri 24/04/20
2	GBS Installation (C1)	**143.1 days**	Wed 01/04/20	Sat 22/08/20
3	GBS Scour & Ballast (C1)	**137.2 days**	Sun 05/04/20	Thu 20/08/20
4	IAG Laying (C1)	**39.1 days**	Wed 01/07/20	Sun 09/08/20
5	IAG Burial (C1)	**58.4 days**	Sat 01/08/20	Mon 28/09/20
6	IAG Termination (C1)	**77.5 days**	Sat 15/08/20	Sat 31/10/20
7	GBS Bedding (C2)	**28.1 days**	Mon 15/02/21	Mon 15/03/21
8	GBS Installation (C2)	**100.1 days**	Mon 01/03/21	Wed 09/06/21
9	GBS Scour & Ballast (C2)	**94.6 days**	Sat 06/03/21	Tue 08/06/21
10	WTG Installation	**248.2 days**	Thu 15/04/21	Sun 19/12/21
11	IAG Laying (C2)	**69.7 days**	Tue 15/06/21	Tue 24/08/21
12	IAG Burial (C2)	**103.8 days**	Sat 10/07/21	Fri 22/10/21
13	IAG Termination (C2)	**134.8 days**	Sun 25/07/21	Tue 07/12/21

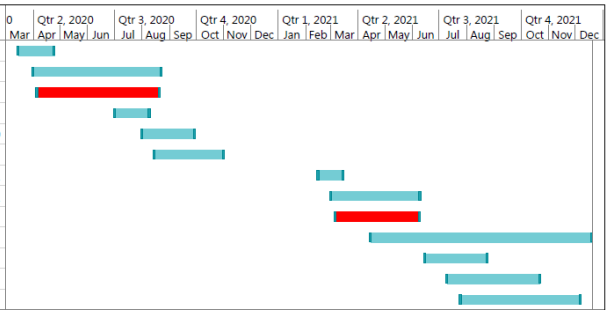

Figure 5.2: Fecamp P50 Gantt Chart - Campaigns One and Two

Figure 5.2 presents a weathered Gantt chart for the P50 summarised durations. The issue with the Scour and Ballast phase completing prior to the GBS

Installation phases is observed again, although the gap between the completion dates of the two phases has reduced. The completion of the WTG Installation phase is now shown to extend beyond the IAG Termination indicating care may be required when coordinating the tasks between these phases. No other clear issue is observed with the P50 durations.

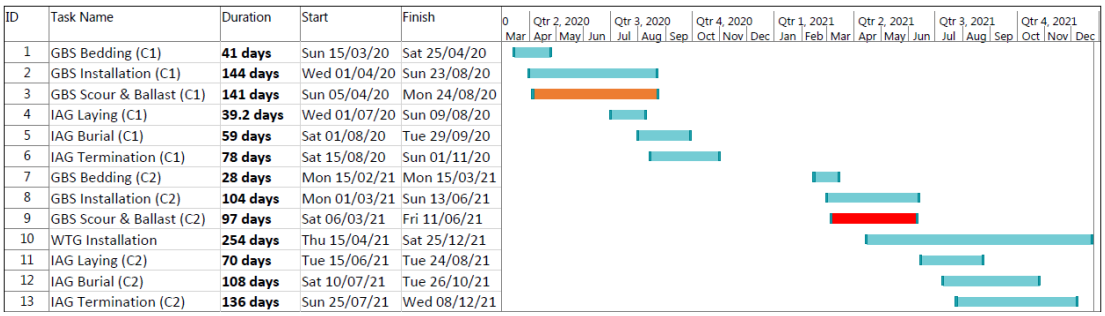

ID	Task Name	Duration	Start	Finish
1	GBS Bedding (C1)	**41 days**	Sun 15/03/20	Sat 25/04/20
2	GBS Installation (C1)	**144 days**	Wed 01/04/20	Sun 23/08/20
3	GBS Scour & Ballast (C1)	**141 days**	Sun 05/04/20	Mon 24/08/20
4	IAG Laying (C1)	**39.2 days**	Wed 01/07/20	Sun 09/08/20
5	IAG Burial (C1)	**59 days**	Sat 01/08/20	Tue 29/09/20
6	IAG Termination (C1)	**78 days**	Sat 15/08/20	Sun 01/11/20
7	GBS Bedding (C2)	**28 days**	Mon 15/02/21	Mon 15/03/21
8	GBS Installation (C2)	**104 days**	Mon 01/03/21	Sun 13/06/21
9	GBS Scour & Ballast (C2)	**97 days**	Sat 06/03/21	Fri 11/06/21
10	WTG Installation	**254 days**	Thu 15/04/21	Sat 25/12/21
11	IAG Laying (C2)	**70 days**	Tue 15/06/21	Tue 24/08/21
12	IAG Burial (C2)	**108 days**	Sat 10/07/21	Tue 26/10/21
13	IAG Termination (C2)	**136 days**	Sun 25/07/21	Wed 08/12/21

Figure 5.3: Fecamp P60 Gantt Chart - Campaigns One and Two

The P60 Gantt chart in Figure 5.3 shows that the Scour and Ballast phase now completes after the GBS Installation phase. This is highlighted in amber as the Scour and Ballast phase correctly completes after the GBS Installation phase but the gap of one day between these dates may still cause waiting delays for the FFPV vessel that would be used to complete these operations. The Scour and Ballast phase is predicted to complete two days before the GBS Installation in Campaign 2. It is clear that the repetitive scheduling employed within the Mermaid models action the Scour and Ballast operations faster than they would be able to occur in reality, as they would be dependent on the progression of the GBS Installations. A dedicated Mermaid model could be built to implement the interdependency of each Scour and Ballast tasks on the completion of the preceding GBS Installation. This would demonstrate the delay time incurred by the FFPV vessel as it waits to begin the installation task. The impact of this waiting time would be dependent on the contract agreed with the vessel owner, sub-contractors and operatives completing these tasks.

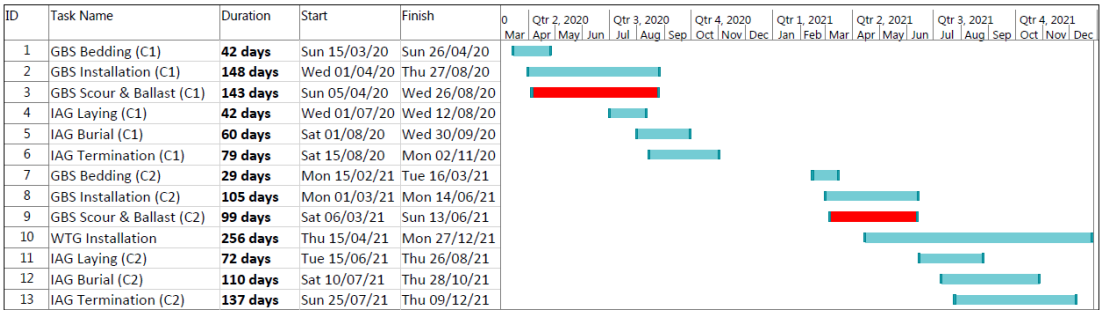

ID	Task Name	Duration	Start	Finish
1	GBS Bedding (C1)	**42 days**	Sun 15/03/20	Sun 26/04/20
2	GBS Installation (C1)	**148 days**	Wed 01/04/20	Thu 27/08/20
3	GBS Scour & Ballast (C1)	**143 days**	Sun 05/04/20	Wed 26/08/20
4	IAG Laying (C1)	**42 days**	Wed 01/07/20	Wed 12/08/20
5	IAG Burial (C1)	**60 days**	Sat 01/08/20	Wed 30/09/20
6	IAG Termination (C1)	**79 days**	Sat 15/08/20	Mon 02/11/20
7	GBS Bedding (C2)	**29 days**	Mon 15/02/21	Tue 16/03/21
8	GBS Installation (C2)	**105 days**	Mon 01/03/21	Mon 14/06/21
9	GBS Scour & Ballast (C2)	**99 days**	Sat 06/03/21	Sun 13/06/21
10	WTG Installation	**256 days**	Thu 15/04/21	Mon 27/12/21
11	IAG Laying (C2)	**72 days**	Tue 15/06/21	Thu 26/08/21
12	IAG Burial (C2)	**110 days**	Sat 10/07/21	Thu 28/10/21
13	IAG Termination (C2)	**137 days**	Sun 25/07/21	Thu 09/12/21

Figure 5.4: Fecamp P70 Gantt Chart - Campaigns One and Two

The P70 Gantt chart in Figure 5.4 shows approximate increases of one to four days across the installation phases in comparison to the P60 predications. The same issue with the Scour and Ballast phases is evident, which complete one day before the GBS Installation. A later start date for the GBS Scour and Ballast phases could be investigated without modelling interdependencies, however this model would rely on the assumption that the water ballasted GBFs can be left in position for extended periods. This assumption would require a supportive civil/geotechnical analysis to provide assurance on the maximum endurance of a water ballasted GBS foundation.

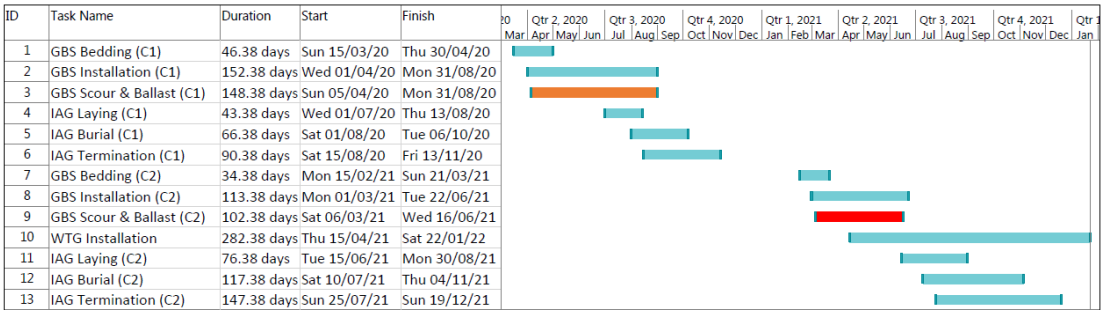

ID	Task Name	Duration	Start	Finish
1	GBS Bedding (C1)	46.38 days	Sun 15/03/20	Thu 30/04/20
2	GBS Installation (C1)	152.38 days	Wed 01/04/20	Mon 31/08/20
3	GBS Scour & Ballast (C1)	148.38 days	Sun 05/04/20	Mon 31/08/20
4	IAG Laying (C1)	43.38 days	Wed 01/07/20	Thu 13/08/20
5	IAG Burial (C1)	66.38 days	Sat 01/08/20	Tue 06/10/20
6	IAG Termination (C1)	90.38 days	Sat 15/08/20	Fri 13/11/20
7	GBS Bedding (C2)	34.38 days	Mon 15/02/21	Sun 21/03/21
8	GBS Installation (C2)	113.38 days	Mon 01/03/21	Tue 22/06/21
9	GBS Scour & Ballast (C2)	102.38 days	Sat 06/03/21	Wed 16/06/21
10	WTG Installation	282.38 days	Thu 15/04/21	Sat 22/01/22
11	IAG Laying (C2)	76.38 days	Tue 15/06/21	Mon 30/08/21
12	IAG Burial (C2)	117.38 days	Sat 10/07/21	Thu 04/11/21
13	IAG Termination (C2)	147.38 days	Sun 25/07/21	Sun 19/12/21

Figure 5.5: Fecamp P90 Gantt Chart - Campaigns One and Two

Finally, a P90 weathered Gantt chart is provided in Figure 5.5. It is observed that the Scour and Ballast phase completes on the same date as the GBS Installation phase in Campaign 1. However, in the second campaign the Scour and Ballast

phase is predicted to complete approximately six days sooner than the GBS phase. The susceptibility of the GBS Installation tasks and installation vessels is made apparent in the Gantt charts, particularly in those of the upper quantiles. With the exception of the WTG Installation phase, it is shown in Tables 5.5 and 5.6 that the GBS Installation phase is amongst the highest recorded WDT values in Campaigns One and Two. The Scour and Ballast operation record similar downtimes, which suggests that any vessel optimisations, hydrodynamic assessments and model testing would be best focused on these installation phases. Any improvement in the vessel capabilities and endurance found could improve the efficiency of these installation steps in conjunction with a strategised installation schedule. The WTG Installation phase is found to complete in mid-late January 2022. As a significant stretch of the WTG Installation phase is completed over December and January, the likelihood of poor weather is increased, resulting in a significant extension in the predicted installation duration.

5.3 Summary

Two commercial metocean risk analyses have been investigated using Mermaid software in this chapter. The BOD assessment was broken into four different scenarios following the direction of the project team at EDF Renewables. It was specified that results should be provided under three percentiles and explicitly listed in a per phase basis. As a number of the phases were executed concurrently in the the Mermaid model, the Matlab processing presented in Chapter 3, Section3.2.4.2 was needed to extract and classify the durations of each phase. These outputs were presented in individual tables and the addition of the Matlab process has added further reporting capabilities in conjunction with Mermaid modelling. The allocation of the three percentiles comprehensively described the risk profile of the individual scenarios, phases and project overall. The addition of

the Mermaid weathered Gantt charts also provided a useful reference, presenting a narrative of how each scenario could transpire in reality.

The Fecamp modelling results were presented in a similar way but differed as each operational phase was simulated in individual Mermaid models for four different percentiles, whilst the weather Gantt charts generated by Mermaid were needed to extract the duration results for P60 and P70. As individual models were used for each phase this led to easier reporting overall as no secondary Matlab processing was needed, yet it is evident that this method cannot accurately capture the knock-on effect of delays between interdependent installation phases. For both projects percentage increase tables were generated to highlight the operational phases with the greatest installation risk. These tables included in Appendix G, generally highlighted that the greatest risks were associated with the GBF installations in each project, which can be used by project teams to inform the allocation of contingencies for the execution of these operations. These two analyses have demonstrated the potential of Mermaid software to support commercial metocean risk assessments and the learning gained from the ECUME I analyses in Chapter 4 and the evident flexibility of Mermaid, can inspire the development of new simulation tools for EDF Energy.

Chapter 6

Results from Stochastic Metocean Model

This chapter begins with numerical and visual outputs from the presented methodology in Chapter 3, Section 3.3. The results as produced by the MS-AR model with Gaussian innovations are presented to demonstrate the accuracy and consistency of the wind speed and H_s simulations independently. The characteristics of the bivariate simulated data for each site are then assessed in terms of a typical marine operation, firstly with the pairing method using mean values and then pairing with Pearson r correlation coefficients, which is described in Section 3.3.5.

6.1 Simulation Results

Table 6.1 compares the mean metocean values across all three sites. The mean values for the observed and simulated data have not been included and instead the percentage difference is listed to convey the variation between the observed and simulated data. A full table which includes the mean values for wind speed and H_s for each month and location is included in Appendix H.

Table 6.1: Percentage difference, average percentage difference and absolute average percentage difference for wind speed U and wave height H_s - observed vs. simulated

	UK North East		**France West**		**English Channel**	
	U (m/s)	Hs (m)	U (m/s)	Hs (m)	U (m/s)	Hs (m)
	% Difference	% Difference	% Difference	% Difference	% Difference	% Difference
μ	0.50	0.95	0.38	2.27	-0.21	0.67
January	0.20	0.23	-0.42	2.53	-0.44	2.93
February	0.76	0.73	1.26	4.24	-0.27	1.49
March	-0.58	1.26	0.22	1.48	-0.23	-0.24
April	-0.71	0.63	0.02	3.15	-0.64	0.34
May	-0.38	0.34	-1.08	1.34	-0.63	-1.96
June	0.25	1.14	1.62	0.66	0.54	-1.65
July	0.74	1.72	0.83	1.13	-1.06	-2.27
August	0.90	0.59	0.12	-0.42	-0.29	-1.40
September	-0.02	1.51	-0.28	3.12	-0.01	-0.74
October	0.99	0.38	0.78	4.00	-0.12	2.33
November	1.86	2.03	0.49	0.71	0.60	2.28
December	1.43	1.07	0.84	2.36	-0.19	1.84
$\lvert\mu\rvert$	0.74	0.97	0.66	2.12	0.42	1.62

It can be seen that the MS-AR model, tuned to each site and month, is capable of following the seasonal changes in the observed series, with the majority of errors below three percent. Generally the models were found to have larger average values for U and H_s, with the exception of the wind speed for the English Channel location. The largest average difference for wind speed and wave height was recorded for UK North East at 0.5% and for France West at 2.27% respectively.

The largest singular differences are recorded for H_s at France West, which has an absolute average percentage variation of 2.12% across all months, while the average percentage difference for wave height is greater than wind speed across the three sites. For the majority of the sites, the largest variations are observed for the winter months, particularly for H_s at France West and the English Channel. Despite these observations, the differences between the model and observed series are small and are all below 5%, indicating that the produced data sets can be progressed for further analyses.

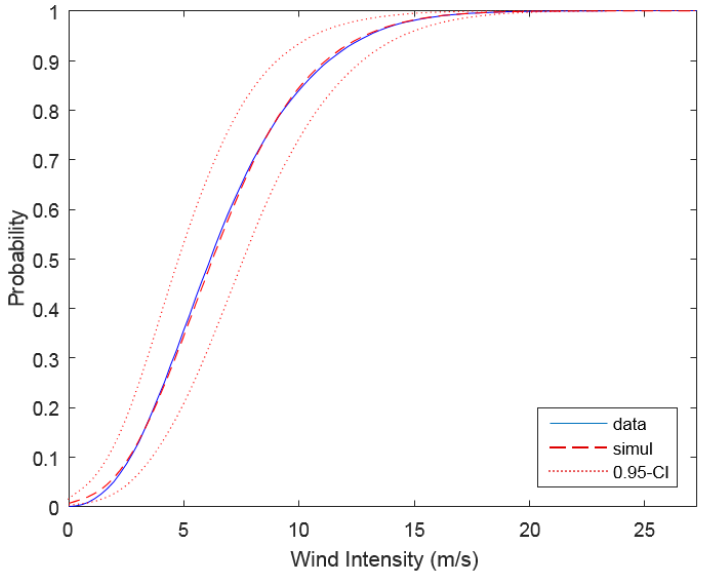

Figure 6.1: CDFs of annual wind speed - Observed vs. simulated - UK North East

Comparisons for the UK North East site are used in the following figures to summarise the typical outcomes of the analysis. In Figures 6.1 and 6.2 the CDFs are shown for the wind speed and wave height respectively. Each figure represents the distribution of U and H_s across 34 years of observed data and 1000 years of simulated data. The solid line represents the observed data, the dashed line for the simulated data with 90% confidence interval indicated by the dotted line.

It is evident from Figures 6.1 and 6.2 that the CDF of the simulated data follows

the observed years of annual data. Looking at the lower wind speeds and wave heights in both figures shows that there is a tendency for the model to over-predict the occurrence of U and H_s below 3m/s and 0.4m respectively. The Kolmogorov-Smirnov Distance was used to identify the maximum absolute difference between the observed and simulated CDFs. This test produces the maximum vertical distance between the two CDFs, which were recorded as 0.018 and 0.014 for U and H_s respectively. This indicates that both simulations are statistically representative of the observed data.

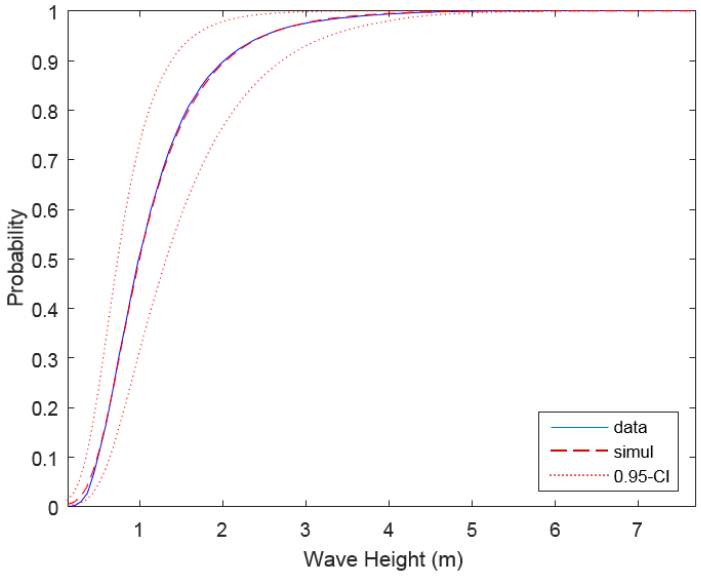

Figure 6.2: CDFs of annual wave height - Observed vs. simulated - UK North East

An additional visual inspection uses a quantile-quantile plot (QQ plot) of the annual observed and simulated time series. This tests if the simulated outcomes are related to the same distribution as the observed data. The QQ plots for for U and H_s variables are shown in Figures 6.3 and 6.4. Both plots show a predominantly linear outcome, which indicates that the simulated data is from the same distribution as the observed. In Figure 6.3 a right skew tail is shown, indicating that some extreme wind speeds may have been produced in the simulation, compared to the observed data set. However, the concentration of the

points is quite low, especially for the most extreme points. Figure 6.4, shows a much slighter skew than was observed with the wind speed. A review of the two other sites demonstrated similar behaviour at the tails as shown in both figures. It should be noted that Figure 6.3 demonstrates the largest skew observed across the three sites and two weather parameters.

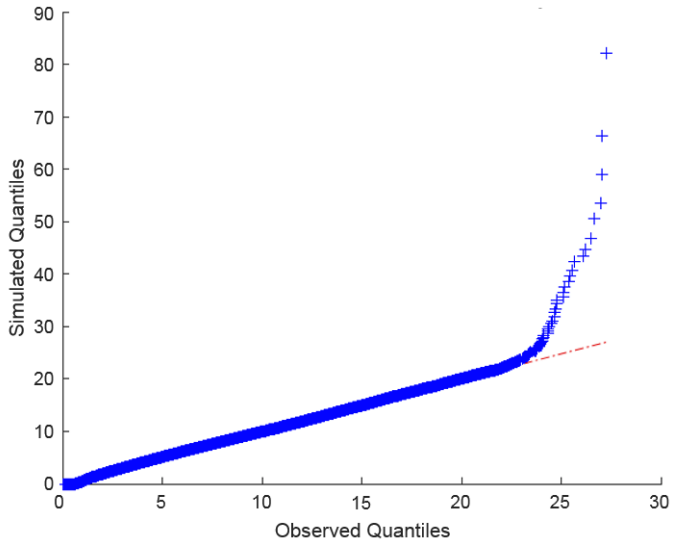

Figure 6.3: QQ plot: observed and simulated wind speed - UK North East

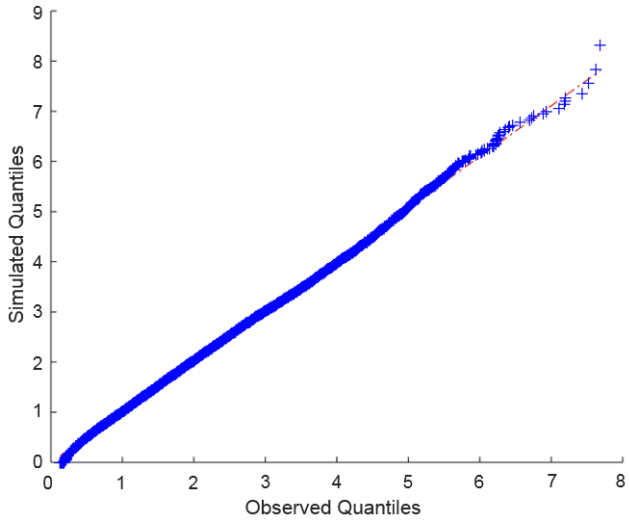

Figure 6.4: QQ plot: observed and simulated wave height - UK North East

6.2 Weather Window Assessment

This section presents the results for a weather window assessment across all three sites investigated. By considering a typically constrained offshore task against the simulated data series, the suitability of the employed methodology and generated time series can be reviewed.

Table 6.2: Weather Window requirements

Parameter	Limit
Wind Speed U	$\leq$ 13.6 m/s
Wave Height H_s	$\leq$ 1.5 m
Duration*	$\geq$ 30 hours

*applied in workability assessment only

For this assessment, specified weather limits and duration for a personnel transfer operation were applied against the three data sets and are summarised in Table 6.2. This type of task is regularly completed during offshore wind installation, particularly when personnel are transferred to transition pieces for turbine installation, as shown in Figure 6.5. Similar tasks are also completed regularly in other marine sectors and therefore present a relevant case study against which to test the model. A weather window can be defined simply as weather conditions that are less than or equal to the environmental limits of a task for a period of time. In some instances, a fixed period less than or equal to the environmental limits is specified for the weather window criteria. These predefined window lengths are often applied in offshore planning to account for uncertainties in weather forecasting, ensuring that suitable contingencies are included to allow for safe completion of the marine operations.

Figure 6.5: Typical Crew Transfer Task - Turbine Transfers Ltd.

The assessment is next considered in the context of the two different pairing methods for the wind speed and wave height time series discussed in Chapter 3, Section 3.3.5: i) ranking and subsequently pairing the monthly wind speed and wave height realisations in terms of mean value and ii) pairing the monthly realisations of wind speed and wave height by the highest Pearson r correlation coefficient. Primarily, an assessment for weather window persistence and average window length is presented, which considers only the wave height and wind speed parameters. This is applied to assess the general characteristics of the simulated and observed data without considering a constraint for a minimum weather window duration. The implication of a predefined weather window is also considered and the results are presented for each month in terms of the average percentage workability of each observed and simulated month.

The average workability percentage represents the average portion of time in each month that is below or equal to the wind speed and wave height limits for the

transfer task, above or equal to the 30 hour constraint. This calculation considers all years of data in the observed and simulated data sets to summarise and directly compare the calculated workability. Equation 6.1 below is used to calculate the average workability for each month of the observed and simulated data.

$$\overline{W}_{\%_i} = \frac{\sum_{j=1}^{n} \left(\frac{h_{(i,j)}}{h_{T_i}} * 100 \right)}{n} \tag{6.1}$$

where:

$\overline{W}_{\%_i}$ = Average workability percentage for month i
h_{T_i} = Total number of hours in month i
$h_{i,j}$ = Combined duration of weather windows $\geq$ 30 hours for month i in realisation j
n = number of monthly meteorological realisations for month i
$i = \{1, ..., 12\}$

6.3 Weather Window Persistence and Lengths - i) Paired-by-means

In Figure 6.6, the weather window persistence and average window length is shown for each location. The weather window persistence is presented as normalised frequencies of 10 hour bins and, for all three sites and clustering towards the lower bin values between 10 and 40 hours, is demonstrated for all three sites. The comparison of the observed and simulated data shows reasonable consistency with the largest differences identified for the France West and English Channel locations.

Figure 6.6: Weather window persistence histogram and average window length $\leq$ 13.6 m/s & $\leq$ 1.5 m

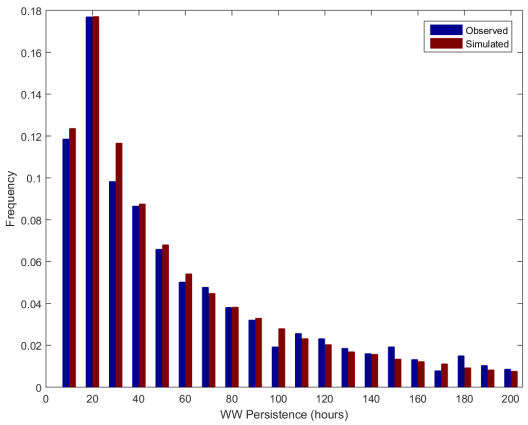

(a) Weather window persistence - 10 hour bins - UK North East

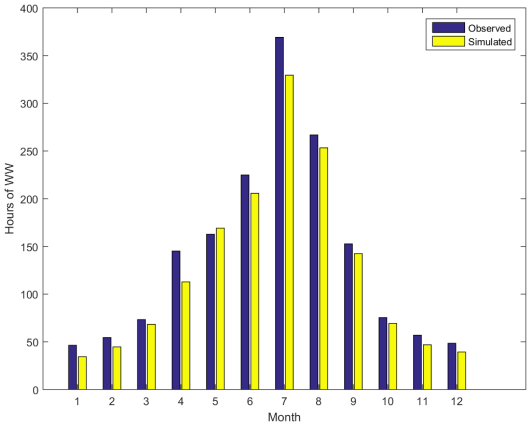

(b) Average weather window duration - UK North East

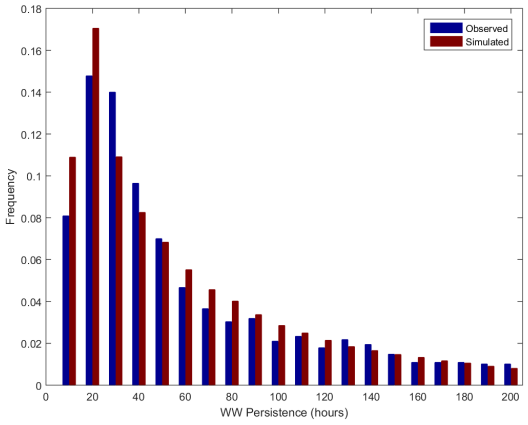

(c) Weather window persistence - 10 hour bins - France West

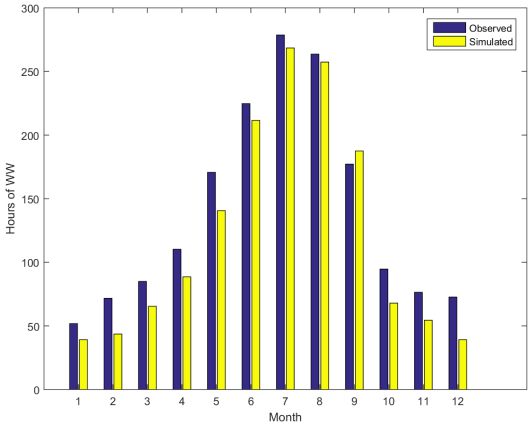

(d) Average weather window duration - France West

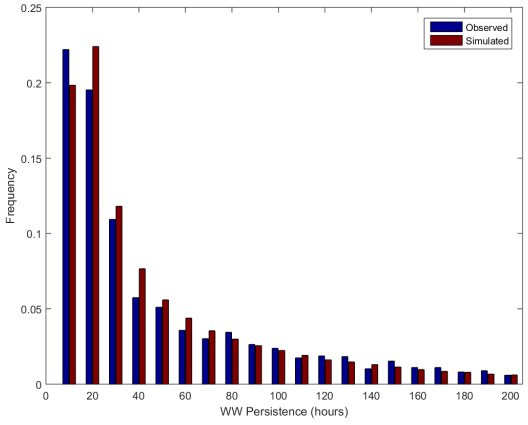

(e) Weather window persistence - 10 hour bins - English Channel

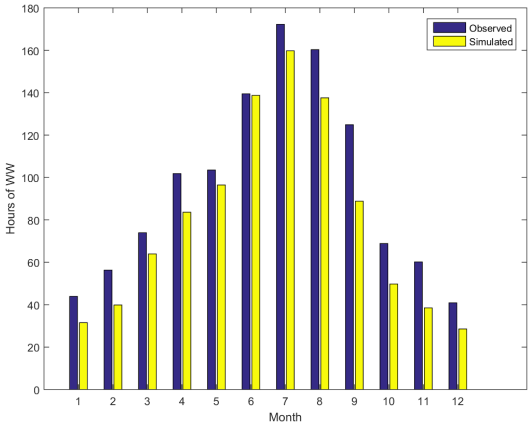

(f) Average weather window duration - English Channel

It is apparent that the simulations have a tendency to over predict the frequency of weather windows between the 20 and 100 hour bins, particularly for France West and the English Channel, whilst UK North East shows the closest comparison to the observed bins overall. The general outcome of persistence histograms shows little difference between the observed and simulated data, which indicates that the simulatedtime series captures the characteristics at each site.

The average weather window length for each month and location are shown in Figures 6.12b, 6.12d and 6.12f. The largest difference is seen for the English channel, which demonstrates that the simulated data generally produces smaller weather windows for each month of approximately 10 to 30 hours. A similar outcome is shown for UK North East, but with smaller average differences. France West exhibits similar characteristics, but is the only location where a slight over-prediction is made for September by approximately five hours. The outcomes for all three sites suggest that some differences can be expected when simulating the progression of marine operations against the simulated data and is reviewed in the following section.

6.3.1 Average Monthly Workability

This section considers the assessment of all limitations included in Table 6.2 and is completed to extend the weather window assessment for a predefined duration of more than or equal to 30 hours. This duration constraint is introduced to assess the simulatedtime series against a realistic condition that may be applied to an operation by marine warranty surveyors or planning personnel. This assessment considers the average percentage workability of the personnel transfer operation, which includes the average amount of time available to complete the operation for each month and location, above or equal to the 30 hour threshold as defined

by Equation 6.1. In Figures 6.7 to 6.9 scatter plots are shown for the workability across the three sites and error bars are included for a 90% confidence interval from the observed and simulated data sets. Accompanying tables are included with each scatter plot that specify the overall monthly workability percentages and differences between the observed and simulated data for each month.

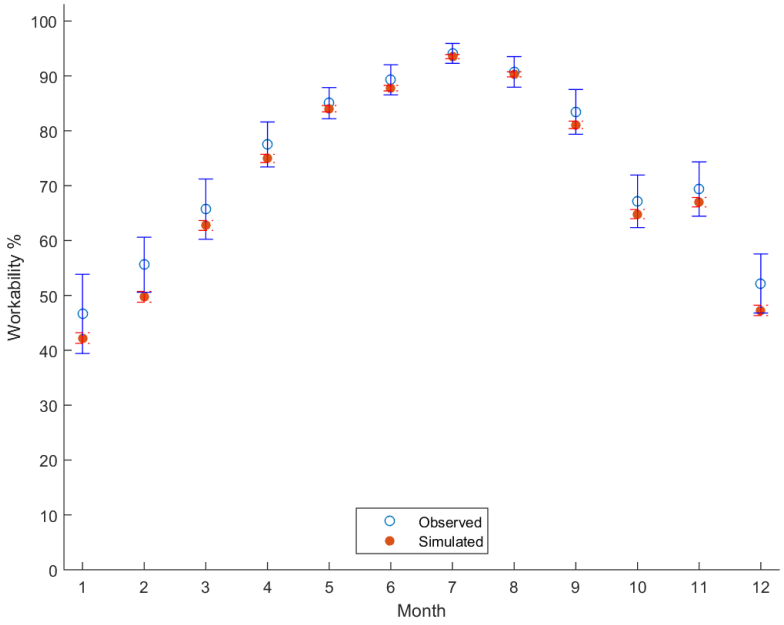

	Mean Workability % Observed	Standard Deviation Observed	Mean Workability % Simulated	Standard Deviation Simulated	% Difference Observed Vs. Simulated
January	46.63	21.46	42.23	16.48	-9.43
February	55.58	14.92	49.75	16.58	-10.50
March	65.73	16.33	62.74	15.26	-4.54
April	77.51	12.20	74.97	12.82	-3.28
May	85.04	8.46	84.03	9.80	-1.19
June	89.29	8.16	87.77	8.45	-1.70
July	94.11	5.41	93.51	6.57	-0.63
August	90.73	8.30	90.29	7.79	-0.49
September	83.45	12.12	81.09	11.31	-2.83
October	67.15	14.24	64.83	14.10	-3.45
November	69.38	14.72	66.99	14.57	-3.45
December	52.17	16.00	47.27	15.92	-9.40
Average	73.06	12.69	70.45	12.47	-4.24

Figure 6.7: Mean percentage workability for time $\geq$ 30 h at $\leq$ 13.6 m/s & $\leq$ 1.5 m - **UK North East**

The site with the closest percentage workability was UK North East with the largest variations observed for January, February and December. Overall the simulated data was found to have 4.24% less workability on average when compared to the observed data set.

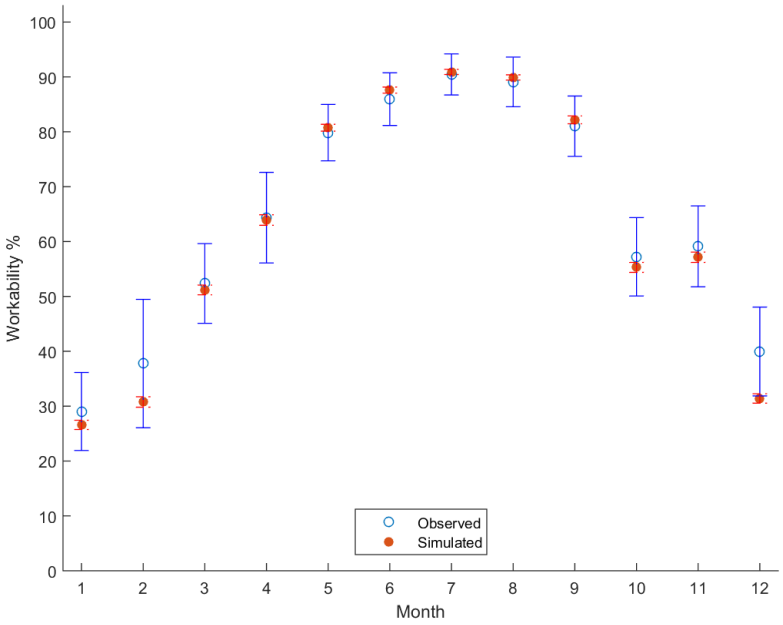

	Mean Workability % Observed	Standard Deviation Observed	Mean Workability % Simulated	Standard Deviation Simulated	% Difference Observed Vs Simulated
January	29.03	16.61	26.59	14.26	-8.41
February	37.76	27.37	30.76	16.13	-18.54
March	52.36	16.98	51.18	14.94	-2.26
April	64.35	19.31	63.92	16.19	-0.68
May	79.85	12.01	80.74	10.51	1.12
June	85.95	11.22	87.59	9.44	1.91
July	90.46	8.75	90.91	7.98	0.50
August	89.09	10.58	89.90	8.08	0.91
September	81.03	12.84	82.18	12.16	1.42
October	57.22	16.68	55.29	15.35	-3.36
November	59.13	17.24	57.14	15.86	-3.36
December	39.96	18.92	31.40	14.46	-21.42
Average	63.85	15.71	62.30	12.95	-4.35

Figure 6.8: Mean percentage workability for time $\geq$ 30 h at $\leq$ 13.6 m/s & $\leq$ 1.5 m - **French West**

The next closest average workability was identified for the French West site at 4.35% less workability on average with the simulated data showing larger variations in the winter months, with the largest recorded differences of 21.42% and 18.54%, indicating less workability for December and February respectively.

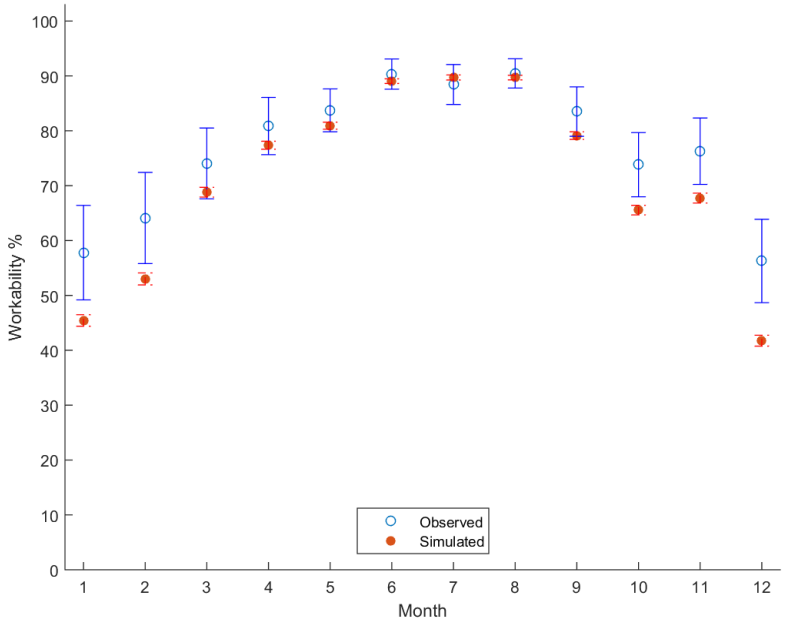

	Mean Workability % Observed	Standard Deviation Observed	Mean Workability % Simulated	Standard Deviation Simulated	% Difference Observed Vs. Simulated
January	57.80	20.14	45.44	17.79	-21.39
February	64.11	19.43	53.00	18.49	-17.32
March	74.05	15.08	68.81	15.11	-7.09
April	80.87	12.21	77.37	12.34	-4.33
May	83.73	9.14	80.93	10.93	-3.35
June	90.34	6.44	89.04	7.12	-1.43
July	88.44	8.51	89.72	7.81	1.44
August	90.46	6.23	89.70	7.12	-0.84
September	83.50	10.53	79.13	11.74	-5.24
October	73.82	13.68	65.55	14.81	-11.21
November	76.28	14.14	67.73	15.30	-11.21
December	56.27	17.77	41.75	16.85	-25.81
Average	76.64	12.77	70.68	12.95	-8.98

Figure 6.9: Mean percentage workability for time $\geq$ 30 h at $\leq$ 13.6 m/s & $\leq$ 1.5 m - **English Channel**

These single values demonstrate that the simulated data has significantly lower workability, which is approximately double that of UK North East for the same months. It is also shown that the simulated data produces slightly more workability on average from May to June. The English Channel site reveals considerable deviations and the workability of the simulated outcomes was found to exhibit 8.98% less workability on average. Particularly large deviations are observed for the winter months, most notably December, January and February at approximately 25.81%, 21.39% and 17.32% respectively. It is also observed that the simulated data results in a slight increase in workability for July at 1.44%.

Table 6.3: Average Number of Weather Windows $U \leq 13.6$ m/s, $H_s \leq 1.5$ m for ≥ 30 hours

	UK North East		France West		English Channel	
	μ Obs WW	μ Sim WW	μ Obs WW	μ Sim WW	μ Obs WW	μ Sim WW
January	4	5	3	3	4	4
February	4	4	2	3	4	4
March	5	5	3	4	4	5
April	4	4	3	4	4	5
May	4	4	3	4	4	5
June	3	3	3	3	4	4
July	2	1	3	1	4	7
August	3	3	3	3	4	4
September	4	4	3	3	4	5
October	5	5	3	4	5	6
November	5	5	3	4	5	5
December	4	5	3	3	5	5

To produce a further perspective on these results, the average number of weather windows in each month was analysed for the three sites. On average, the simulated data exhibits more windows for the first six to seven months. It should be noted that this does not necessarily mean more workability in the simulated data and is more likely due to the fragmentation of weather windows, which are believed to be less prominent in the observed data. Nevertheless, this outcome shows

that despite the larger deviations in the winter months, there would likely be a similar amount of time to complete the required marine operations in each month. However, if the English Channel time series were contained within a dedicated planning and simulation tool, it is likely the simulated data set would exhibit an increase in waiting times, or more frequent interruptions, than the observed data set.

Overall, Figures 6.7 to 6.9 show that the simulated data has reduced workability in the winter months and in some instances an increase in the summer months for two of the three sites. The reduction in workability in the winter months is much greater than the over-predictions in each case; the absolute average percentage difference for UK North East, France West and the English Channel were found to be 4.24%, 5.33% and 9.22% respectively. The 90% error bars show that the mean outcomes for the simulated data are within the range of the observed data sets across all months for UK North East and Teesside. Figure 6.9 shows that the mean outcome lies well outside the 90% confidence interval for January, February, October, November and December at the English Channel site. This outcome indicates that there may be considerable differences between the observed and simulated data sets using the pairing by means approach, which required further analysis.

6.3.1.1 Distributions of Weather Windows and Workability

To review the results for each site in more detail, box plots, cumulative distributions and percentile plots were produced to characterise the distributions of the weather windows below 13.6 m/s wind speed, 1.5 m H_S and equal to or above the 30 hour minimum threshold. The box plots are presented in Appendix I and additional percentiles of P10, P70, P90 and P99 have been plotted to provide further insight in the results. Figures, I.1a, I.1c and I.1d show the distribution of

all weather windows greater than the 30 hour threshold, whilst Figures I.1b, I.1d and I.1f show the distribution of the average percentage workability between the observed and simulated data. Figures 6.10 and 6.11 provide summary of these box plots and support the following review.

In Figures I.1a, I.1c and I.1e, it is clear that the interquartile range (IQR) of the simulated outcomes is smaller and generally more constrained across the three locations. The largest IQRs were recorded for the observed data, particularly for the summer months. The comparison between the observed and simulated distributions show that the simulated data tends to lower weather window durations in comparison to the observed outcomes. The largest difference in IQR is generally around the months of May to July, closely followed by some Autumn or winter months across the three sites. The largest differences in the IQRs are identified at the P75 boundary for July at the UK North East and for June at the English Channel locations, both of which exhibit differences of approximately 50-80 hours. The median is generally quite similar between the simulated and observed outcomes, although if more extreme percentiles such as the P90 or P99 are compared, these can exhibit considerably different outcomes, where difference between the two P90 values for June at the English Channel site are greater than 100 hours. A large number of outliers are associated with the simulated examples and these are limited for the observed months. For the majority of months across the three sites, the P99 in the simulated cases is significantly lower than the observed results, demonstrating the sensitivity to this statistic when using a limited data set. In Figure 6.10, summarising plots for the distribution of all monthly weather window durations for the personnel transfer task are included for all three sites. The outcomes show that the simulated data tends to smaller weather windows overall and use of the two sided Kolmogorov-Smirnov (K-S) test revealed the maximum difference between the observed and simulated window distributions was recorded for the English Channel at 0.09.

The average percentage workability boxplots are presented in Figures I.1b, I.1d and I.1f and again the same constrained distribution was observed for the simulated data. The largest difference in IQRs was recorded for the winter months with the observed data generally exhibiting the largest ranges overall. The median for the simulated outcomes tend to be below the recorded values, altering the skew of the overall distribution towards lower workability percentages. This behaviour is clearly shown in Figure I.1f for the winter months for the English Channel site. The median for the simulated October, November and December workabilities is outside the IQR of the observed data set and is indicative of considerable differences between the simulated and observed outcomes. The P90 and P10 values exhibit similar differences to the median, demonstrating consistently lower workability estimates in the simulated data for this site. This is exemplified further in Figure 6.11 where the distribution of the average monthly workabilities are compared. Both the UK North East and France West locations show generally similar distributions but some significant deviation is observed for the English Channel with a K-S distance of 0.14.

Figure 6.10: CDFs and percentiles of monthly weather windows: ≥30 hours, ≤ 13.6 m/s & ≤ 1.5 m - **Paired-by-means**

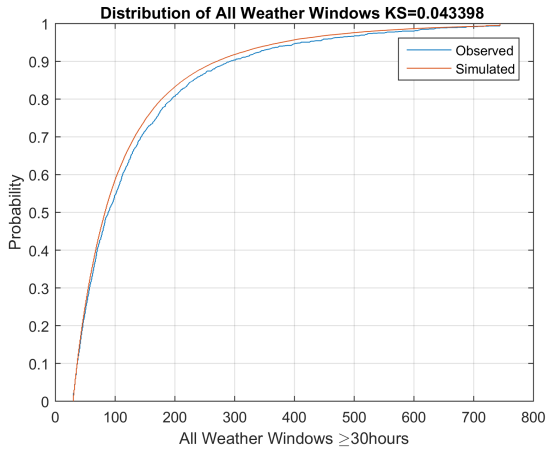

(a) UK North East: CDFs of monthly weather windows ≥ 30 hours

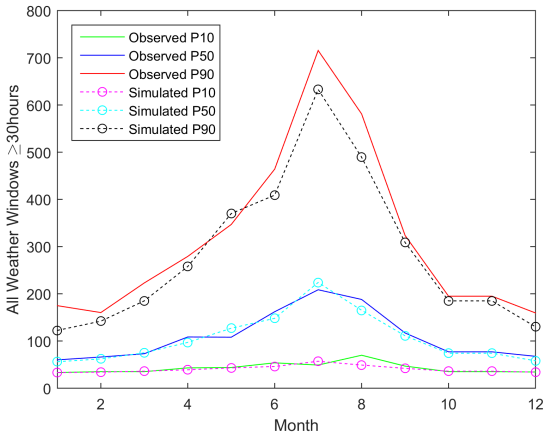

(b) UK North East: Percentile plots of monthly weather windows ≥ 30 hours

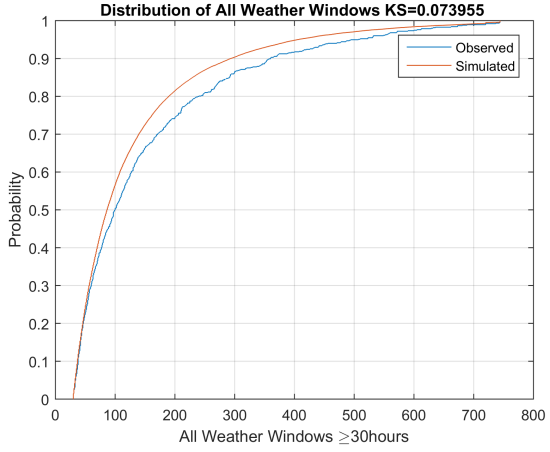

(c) France West: CDFs of monthly weather windows ≥ 30 hours

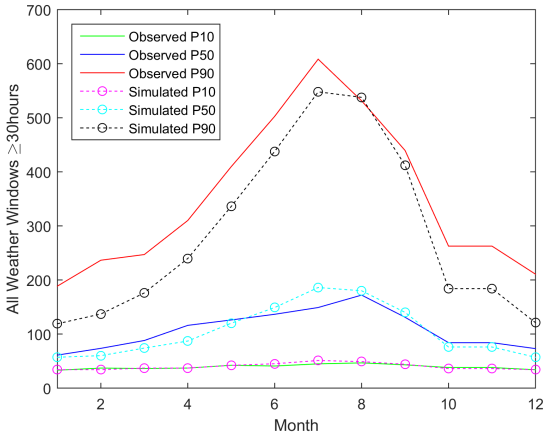

(d) France West: Percentile plots of monthly weather windows ≥ 30 hours

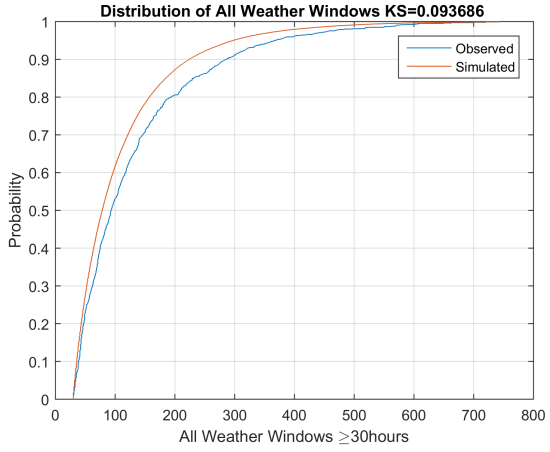

(e) English Channel: CDFs of monthly weather windows ≥ 30 hours

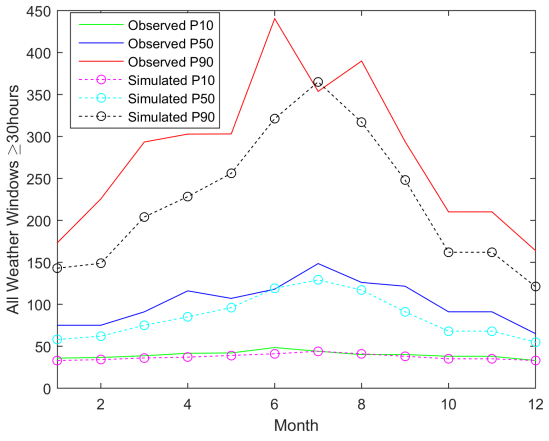

(f) English Channel: Percentile plots of monthly weather windows ≥ 30 hours

Figure 6.11: CDFs and percentiles of monthly percentage workability: ≥30 hours, ≤ 13.6 m/s & ≤ 1.5 m - **Paired-by-means**

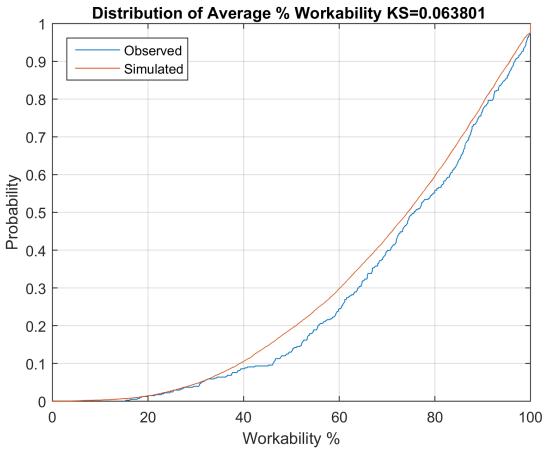

(a) UK North East: CDFs of monthly percentage workability

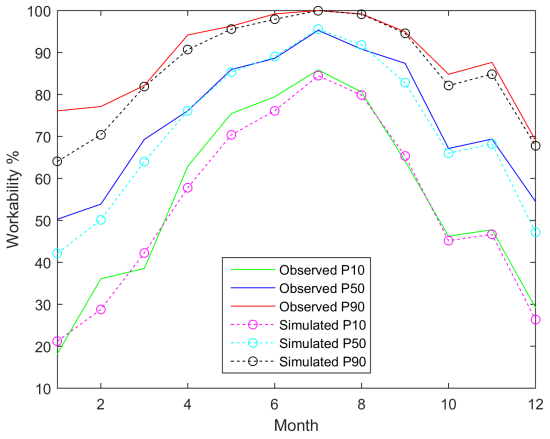

(b) UK North East: Percentile plots of monthly percentage workability

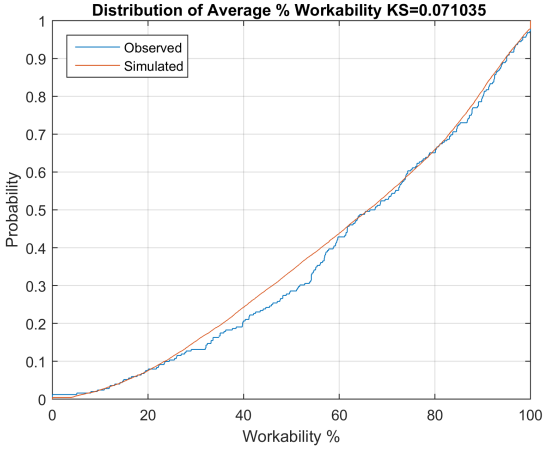

(c) France West: CDFs of monthly percentage workability

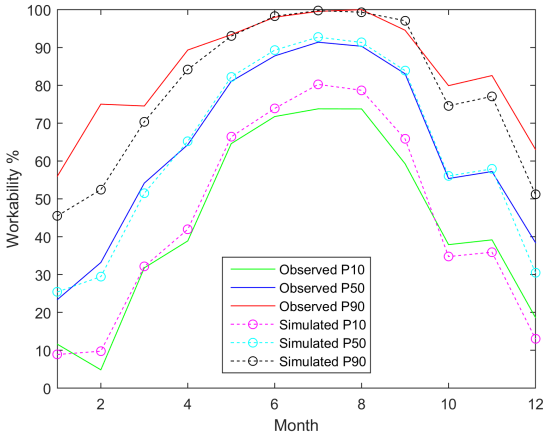

(d) France West: Percentile plots of monthly percentage workability

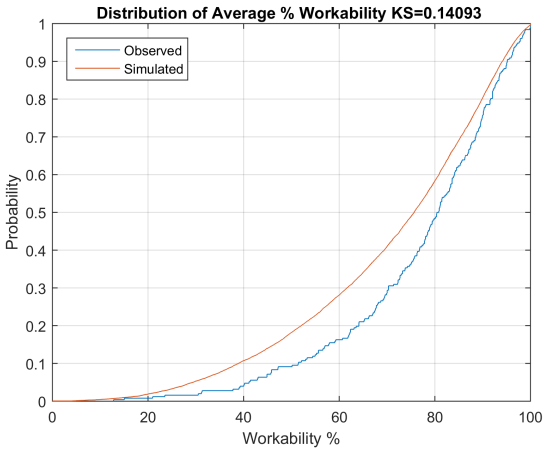

(e) English Channel: CDFs of monthly percentage workability

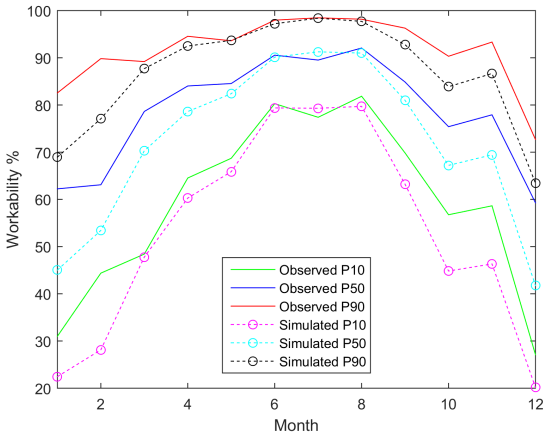

(f) English Channel: Percentile plots of monthly percentage workability

6.4 Weather Window Persistence and Lengths - ii) Correlated Pairing

In section 3.3.5 an alternative method to pair the monthly simulated wind speed and significant wave height realisations using Pearson r coefficients is presented. From an initial assessment of the English Channel site it was shown that the pairing by means approach resulted in a very low Pearson r coefficient 0.06 in comparison to the observed data set at 0.9. Figures 3.27 and 3.28 indicate that the Person r pairing approach produced a better coefficient of 0.47 for the simulated data. The significance of this improved coefficient is considered in terms of weather window persistence and workability, following the approach used in the previous section.

In Figure 6.12, the weather window persistence and average window length for each location are shown. The results for the ten hour weather window persistence show little difference form those produced using the paired-by-means approach. However, the window persistence for the English Channel shows a slight improvement between the observed and simulated outcomes. The bar charts for the average window length show that for the winter months across all three sites, the difference between the observed and simulated data is reduced compared to paired-by-means approach. In direct contrast a slight increase in difference is shown for the summer months across all three sites. The change in these average weather window outcomes share similar magnitudes ranging between 10 and 20 hours.

Figure 6.12: Weather window persistence histogram and average window length $\leq$ 13.6 m/s & $\leq$ 1.5 m

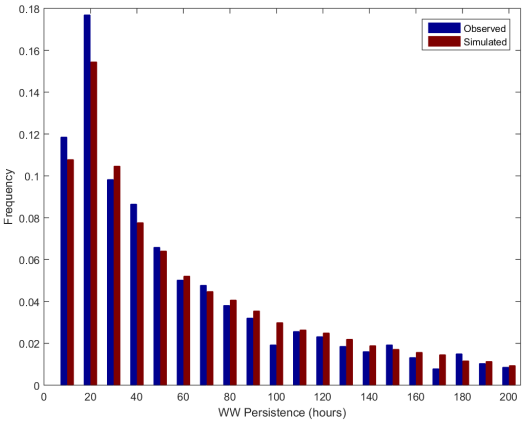

(a) Weather window persistence - 10 hour bins - UK North East

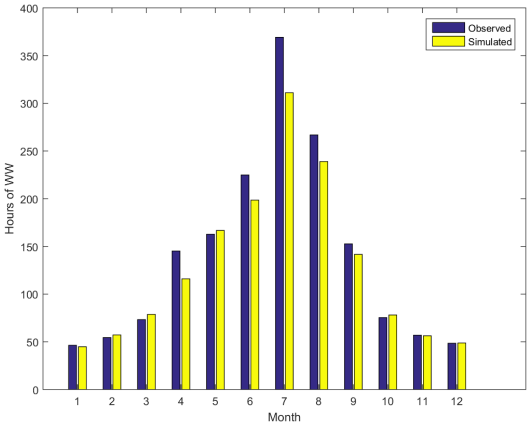

(b) Average weather window duration - UK North East

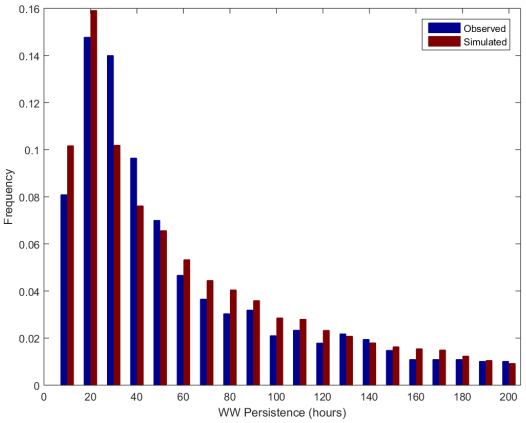

(c) Weather window persistence - 10 hour bins - France West

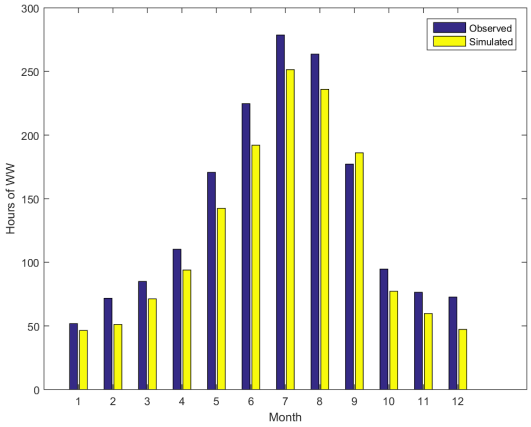

(d) Average weather window duration - France West

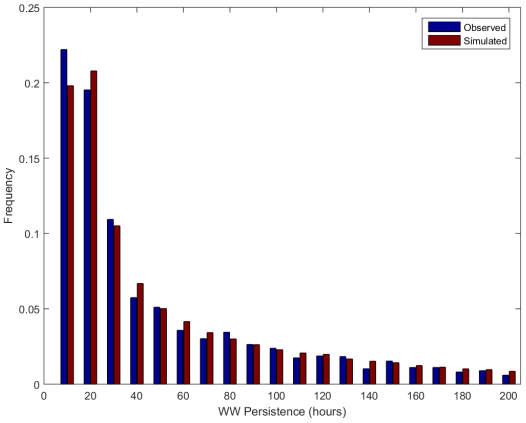

(e) Weather window persistence - 10 hour bins - English Channel

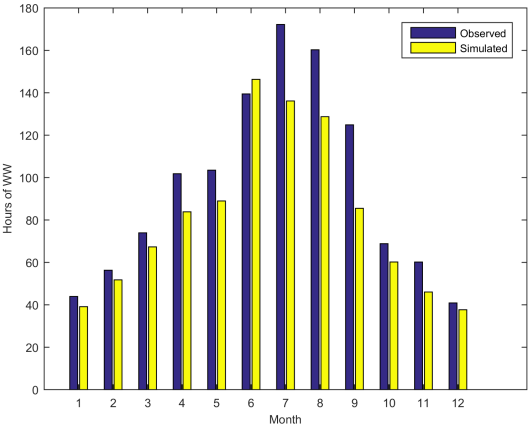

(f) Average weather window duration - English Channel

6.4.1 Average Monthly Workability

This section considers the same limits included in Table 6.2 to summarise and compare the weather window and workability characteristics of the correlated simulated data against the paired-by-means approach presented in Section 6.3.1.

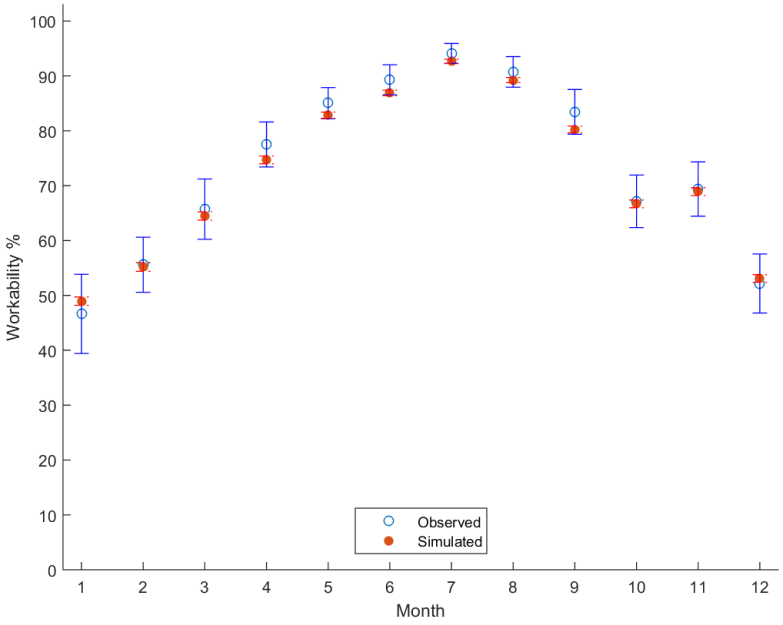

	Mean Workability % Observed	Standard Deviation Observed	Mean Workability % Simulated	Standard Deviation Simulated	% Difference Observed Vs. Simulated
January	46.63	21.46	48.96	12.82	4.99
February	55.58	14.92	55.18	13.24	-0.72
March	65.73	16.33	64.47	12.91	-1.91
April	77.51	12.20	74.69	12.13	-3.63
May	85.04	8.46	82.84	9.57	-2.59
June	89.29	8.16	86.91	8.40	-2.67
July	94.11	5.41	92.64	6.68	-1.55
August	90.73	8.30	89.25	7.96	-1.64
September	83.45	12.12	80.25	10.61	-3.83
October	67.15	14.24	66.68	11.85	-0.69
November	69.38	14.72	68.90	12.25	-0.69
December	52.17	16.00	53.08	11.99	1.75
Average	73.06	12.69	71.99	10.87	-1.10

Figure 6.13: Mean percentage workability for time $\geq$ 30 h at $\leq$ 13.6 m/s & $\leq$ 1.5 m - **UK North East**

In Figures 6.13 to 6.15 scatter plots present the average percentage workability across the three sites and include error bars for a 90% confidence interval of the mean from the observed and simulated data sets.

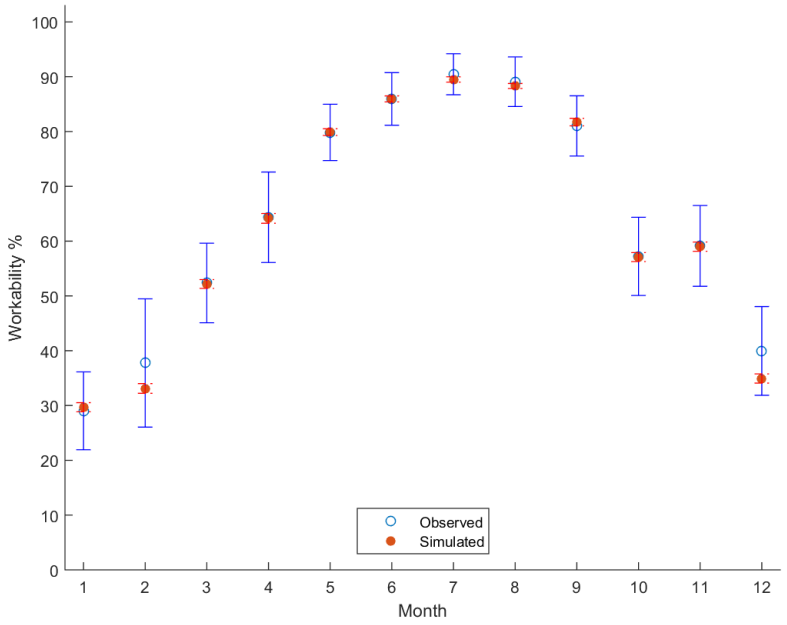

	Mean Workability % Observed	Standard Deviation Observed	Mean Workability % Simulated	Standard Deviation Simulated	% Difference Observed Vs Simulated
January	29.03	16.61	29.69	13.98	2.25
February	37.76	27.37	33.12	14.98	-12.31
March	52.36	16.98	52.18	13.48	-0.35
April	64.35	19.31	64.15	15.07	-0.31
May	79.85	12.01	79.90	10.30	0.07
June	85.95	11.22	85.96	9.25	0.00
July	90.46	8.75	89.51	8.17	-1.05
August	89.09	10.58	88.31	7.63	-0.87
September	81.03	12.84	81.73	11.67	0.86
October	57.22	16.68	57.08	13.75	-0.24
November	59.13	17.24	58.99	14.21	-0.24
December	39.96	18.92	34.93	14.17	-12.59
Average	63.85	15.71	62.96	12.22	-2.06

Figure 6.14: Mean percentage workability for time $\geq$ 30 h at $\leq$ 13.6 m/s & $\leq$ 1.5 m - **French West**

The site with the closest percentage workability was again the UK North East and the largest variations were observed for January, April and September. It is

evident that the average percentage workability is closer to the observed outcomes for the winter months when compared to the paired-by-means results. For January, an increase of approximately 15% more workability was calculated, shifting from a difference of -9.43% to approximately 5% above the observed results. It is also apparent that the workability in the summer months is approximately 1% lower than the paired-by-means predictions. Overall the simulated data shows just over 1% less workability on average when compared to the observed data set, which is an increase in average workability of approximately 3% against the paired-by-means approach. The average workability plots demonstrate that simulated data is again within the 90% confidence error bars and shows increased similarity between the two data sets.

France West was the next closest overall workability with significant increases in the overall percentage workability identified for the winter months. The results for January and December indicate a significant increase in workability of 10% and 8% respectively, in comparison to the paired-by-means method. A slight reduction in workability for the summer months is observed but is approximately limited to between 1% or 2%. The overall outcome shows that the simulated data has a lower average workability percentage across all months by 2%, which is an increase of 2% compared to the paired-by-means results.

The site with the least closest average percentage workability was the English Channel location with the simulated data showing 4% less workability on average overall across the 12 months. If this is compared to the paired-by-means outcome, this is an increase of 4% workability. Notably large increases in workability were calculated for January, February and December compared to the first pairing method, increasing by approximately 15%, 12% and 17% respectively. A reduction in workability is observed for April and August by 1% and 3%. A comparison of the average workability plots in 6.9 and 6.15 show that the plots for the simulated

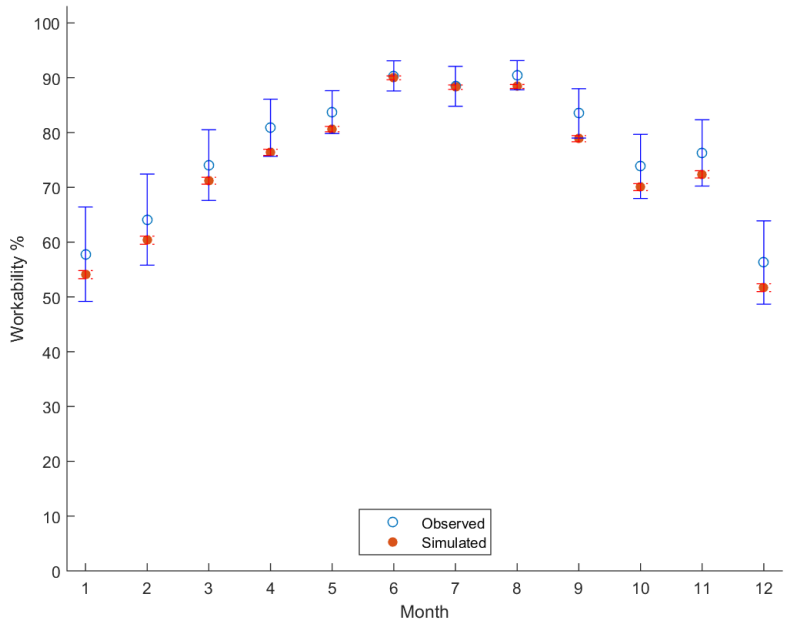

	Mean Workability % Observed	Standard Deviation Observed	Mean Workability % Simulated	Standard Deviation Simulated	% Difference Observed Vs. Simulated
January	57.80	20.14	54.07	12.51	-6.45
February	64.11	19.43	60.35	12.56	-5.86
March	74.05	15.08	71.20	10.58	-3.85
April	80.87	12.21	76.39	9.52	-5.54
May	83.73	9.14	80.63	8.18	-3.71
June	90.34	6.44	89.98	5.90	-0.40
July	88.44	8.51	88.29	6.81	-0.17
August	90.46	6.23	88.41	6.07	-2.27
September	83.50	10.53	78.88	9.47	-5.53
October	73.82	13.68	70.04	10.78	-5.13
November	76.28	14.14	72.37	11.14	-5.13
December	56.27	17.77	51.68	11.93	-8.15
Average	76.64	12.77	73.52	9.62	-4.35

Figure 6.15: Mean percentage workability for time $\geq$ 30 h at $\leq$ 13.6 m/s & $\leq$ 1.5 m - **English Channel**

data in correlated pairing approach fall well within the 90% confidence error bars, indicating a considerable increase in similarity between the two data sets.

The average number of weather windows in each month was reviewed once more for the three sites. There is little change in the number of weather windows between the two pairing approaches, with the paired by correlation demonstrating

a slight increase in similarity. The simulated data tends to have a larger number of weather windows in comparison to the observed data. This indicates that weather windows are more fragemented in the simulated data and suggest shorter weather windows could be expected overall when using the generated time series.

Table 6.4: Average Number of Weather Windows $U \leq 13.6$ m/s, $H_s \leq 1.5$ m for ≥ 30 hours

	UK North East		France West		English Channel	
	μ Obs WW	μ Sim WW	μ Obs WW	μ Sim WW	μ Obs WW	μ Sim WW
January	4	4	3	3	4	5
February	4	4	2	3	4	4
March	5	4	3	4	4	5
April	4	4	3	4	4	5
May	4	3	3	4	4	4
June	3	3	3	3	4	4
July	2	1	3	1	4	6
August	3	3	3	3	4	4
September	4	4	3	3	4	4
October	5	5	3	4	5	5
November	5	5	3	4	5	5
December	4	5	3	3	5	5

The workability outcomes from the correlated pairing technique have shown an increase in the similarity between the workability outcomes for all three sites. Despite this increase, the simulated data tends to lower workability percentages overall. However, the difference in average workability percentage using correlated pairing method is approximately halved when compared to the paired-by-means approach. The simulated data is still shown to generally have lower workability percentages and the absolute percentage difference for UK North East, France West and English Channel were 2.2%, 2.6% and 4.35% respectively. The absolute values indicate improved similarity all round using the correlated pairing approach, as summarised by the scatter plots.

6.4.1.1 Distributions of Weather Windows and Workability

The distributions of weather windows above the 30 hour threshold and the average workability of the correlation pairing data was reviewed against the observed data. The outcomes were also considered against the results for the paired-by-means approach to identify the difference in characteristics produced by both pairing methods. Summarising plots are included in Figures 6.16 and 6.17 to support the interpretation of these results.

The distributions of all weather windows greater than the 30 hour threshold are shown in Appendix J. The distributions of the simulated weather windows again appear more constrained than the observed outcomes, although they show closer resemblance than the paired-by-means approach. The largest IQRs are shown for the observed data over the summer months in the three locations.

The largest differences in IQRs were observed for the months of May, June and July across the three sites, with the biggest difference of approximately 80 hours at the UK North East in July. It is noted that the magnitude of difference for the winter months is reduced for the three locations with very similar distributions. The medians are very similar to those using the paired-by-means approach and a closer similarity for the P90 outcomes is generally demonstrated for all locations. For the P99 percentile, significant differences are shown. The summarising CDF plots for all monthly weather windows included in Figure 6.16 and establish that the simulated weather windows generally tend to lower weather windows yet it is apparent the distributions follow the observed distributions more closely. The K-S test was used to identify the maximum difference in CDFs for the three locations and were found to be 0.04, 0.06 and 0.04 for the UK North East, France West and English Channel respectively.

The K-S distance is reduced for all three sites using the paired-by-means approach, with the largest reduction of 0.05 observed for the English Channel site.

Boxplots for average percentage workability are included in J.1b, J.1d and J.1f and constrained distributions are observed for the simulated data. The size of the IQRs using the correlated pairing method is generally smaller in comparison to the paired-by-means approach. The IQRs with the largest difference are shown for the winter months, with the greatest at approximately 30% for February at the French West location. The medians of the simulated outcomes are slightly lower than the observed examples, although these are generally more consistent than the paired-by-means results, particularly for the English Channel. The P90 and P10 outcomes show generally little movement with the exception of the English Channel, where the P90 is less similar to the paired-by-means approach, while the P10 value clearly exhibits closer similarity. Overall it shows that the IQRs for simulated workability generally lie within the IQRs of the simulated data with exceptions being the UK North East and English Channel.

The CDFs for all monthly workability percentages are shown in Figures 6.17a, 6.17c, 6.17e and it can be seen that the average workability percentages show greater similarity to the observed simulations than the pairing by means approach. The K-S distances for the UK North East, France West and English Channel were recorded as 0.08, 0.06 and 0.12, which are lower than the paired-by-means results with the exception of the UK North, which increased by approximately 0.01. The CDFs indicate that more conservative workability estimates are associated with the greater percentiles as the CDF of the simulated data deviates from observed curve in these regions, particularly for the English Channel. Despite this observation, the simulated curves tend to intersect that of the observed data and the curve for the English Channel shows better consistency overall for the correlated outcomes.

Figure 6.16: CDFs and Percentiles of monthly weather windows: ≥30 hours, ≤ 13.6 m/s & ≤ 1.5 m - **Correlated Pairing**

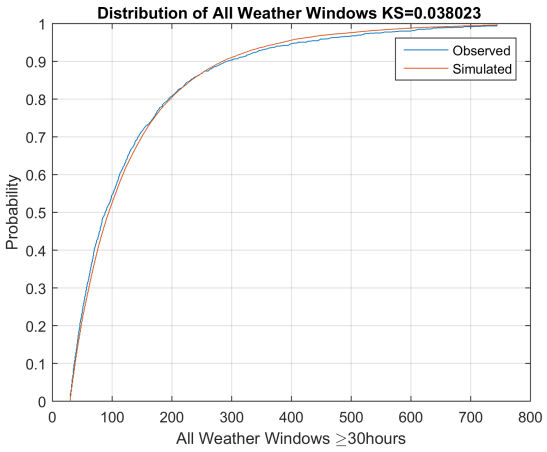

(a) UK North East: CDFs of monthly weather windows ≥ 30 hours

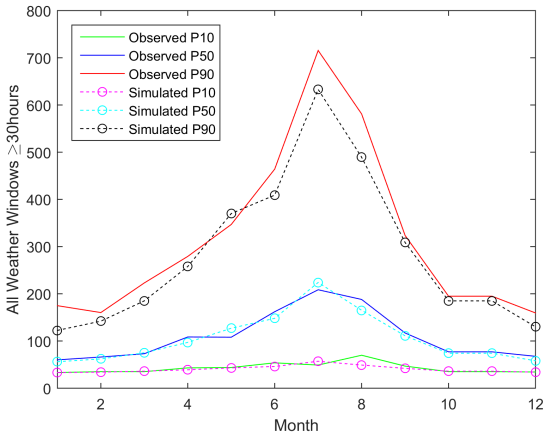

(b) UK North East: Percentile plots of monthly weather windows ≥ 30 hours

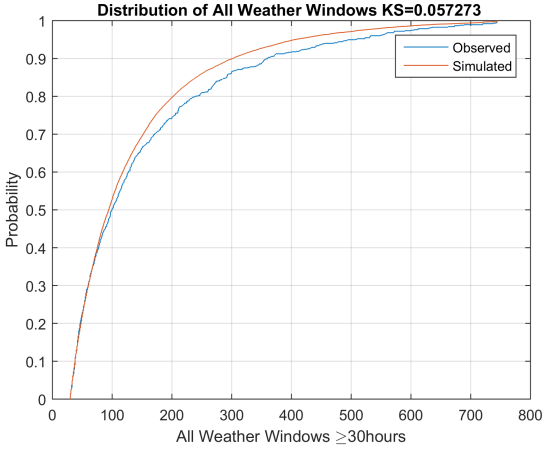

(c) France West: CDFs of monthly weather windows ≥ 30 hours

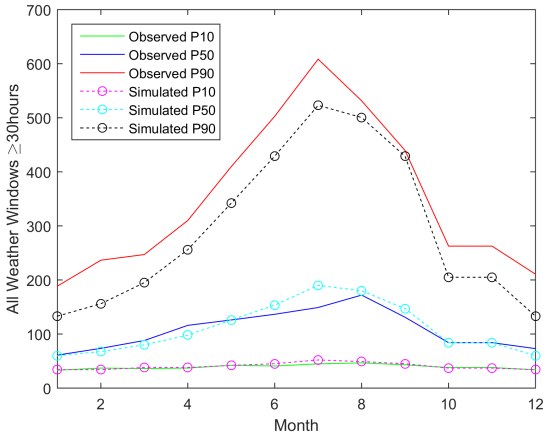

(d) France West: Percentile plots of monthly weather windows ≥ 30 hours

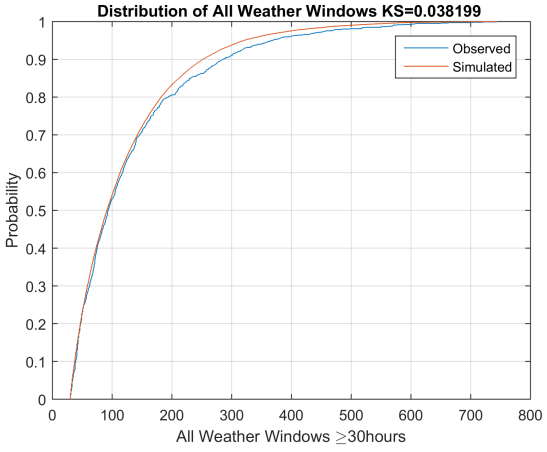

(e) English Channel: CDFs of monthly weather windows ≥ 30 hours

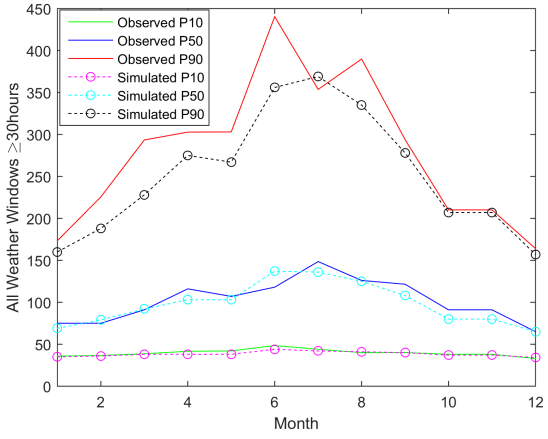

(f) English Channel: Percentile plots of monthly weather windows ≥ 30 hours

Figure 6.17: CDFs and Percentiles of monthly percentage workability: ≥30 hours, ≤ 13.6 m/s & ≤ 1.5 m - **Correlated Pairing**

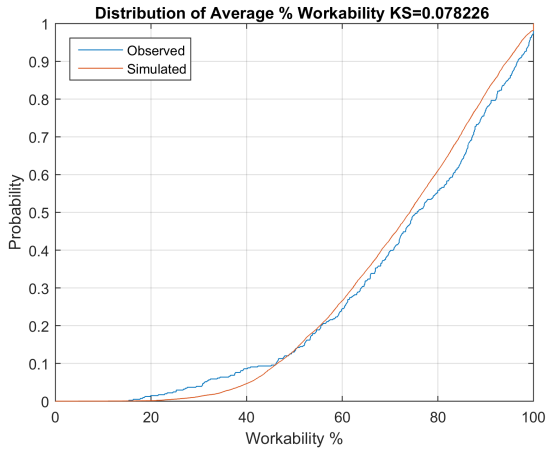

(a) UK North East: CDFs of monthly percentage workability

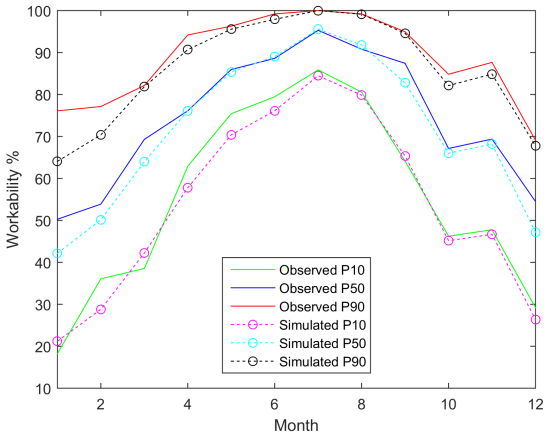

(b) UK North East: Percentile plots of monthly percentage workability

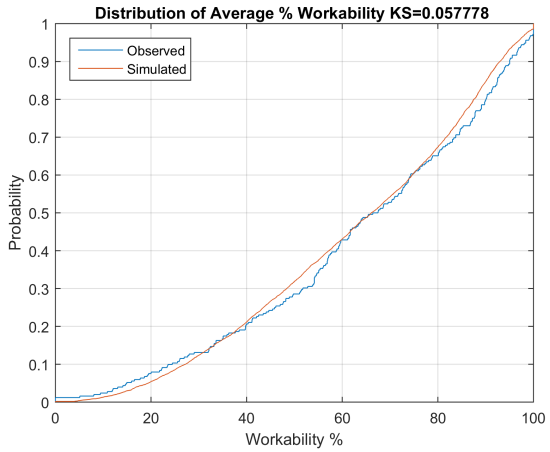

(c) France West: CDFs of monthly percentage workability

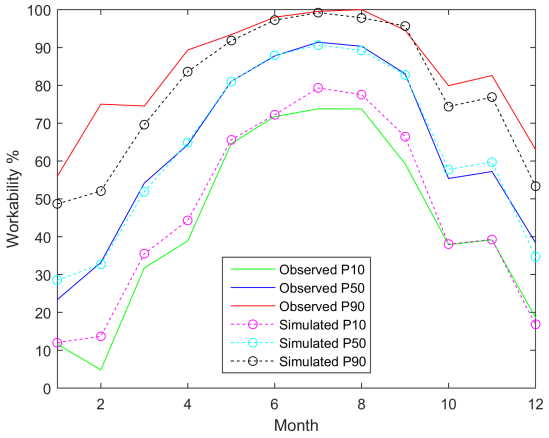

(d) France West: Percentile plots of monthly percentage workability

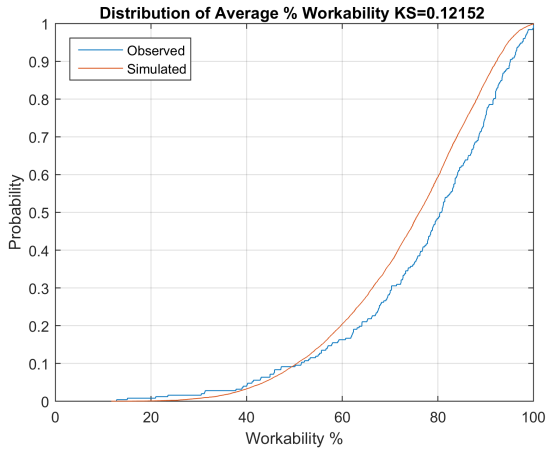

(e) English Channel: CDFs of monthly percentage workability

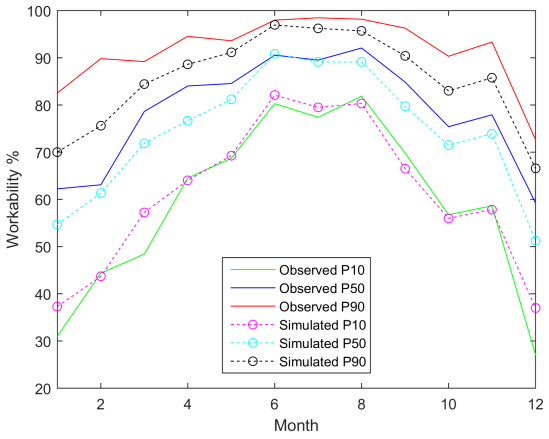

(f) English Channel: Percentile plots of monthly percentage workability

6.5 Example of MS-AR Metocean Model applied within EDF R&D's new Metocean Risk Simulation Software Prototype

This section presents the application of the bivariate time series produced by the model against the set of operations assembled using a logistical simulation engine, which was produced by a separate team in EDF R&D France. The stochastic weather modelling method was originally developed for inclusion in a prototype version of EDF R&D's next generation marine operations simulation package. Two primary installation phases were selected from the BOD project to benchmark the predictions produced by the logistical engine: 'Dredging & Survey' and 'Filter Layer'.

This short assessment was completed to review how the predictions produced by the logistical engine and time series compiled using the weather model compared to the durations produced by the Mermaid Software. Additionally, the logistical steps were simulated across the observed time series to compare the predictions against the simulated weather data. As Mermaid has the functionality to consider multiple different metocean data series, the original BOD model was re-run using only one met point reference in the simulation to provide a fair comparison against the functional prototype, which could only apply one time series in the simulations. The UK North East data set was applied directly in Mermaid and the observed simulation within the logistical prototype. The stochastic time series produced by the paired-by-means approach was used for the simulated results. The pairing approach was used as this was the only available pairing method that had been developed at the time of this early prototype testing.

6.5.1 Marine Operations and Vessel Parameters

The logistical steps using the BOD Mermaid assessment were replicated in prototype simulation package. For this analysis, the marine operations, vessel parameters and associated limits for wind speed at 10m, significant wave height H_s m are summarised in Tables 6.5 to 6.7. For both installation phases, the operations are repeated five times, one for each asset location and are highlighted in yellow Tables 6.5 to 6.7. Slight deviations were apparent in the base P0 duration calculated by the Mermaid and prototype models. For the Dredging phase, the prototype assembles a total duration of 15.06 days, whilst the Mermaid unweathered duration presented in Section 5.1 (Table 5.1) was 14.83 days. The base duration for the Filter Layer task was 15.09 days, whilst in Mermaid this was 15.26 days. The difference between the two base durations is believed to originate from either the 15 minute time step or slight differences in the transit durations compiled within Mermaid. Nonetheless, it was decided that these differences were fairly small and could still provide a reasonable benchmark as presented in the following section.

Table 6.5: Dredge & FPPV Vessel Limits [133]

Vessel	**Transit Wind Speed (m/s)**	**Transit Wave Height (m)**	**Station Keeping Wind Speed (m/s)**	**Station Keeping Wave Height (m)**	**Transit Speed (m/s)**
Dredger	15.00	2.50	15.00	3.00	7.97
FFPV	15.00	2.50	22.00	3.00	7.20

Table 6.6: Dredging Operations [133]

Operation	Duration (h)	Wind Speed Limit (m/s)	Wave Height Limit (m)
Dredger mobilization	17.4	-	-
Dredger transit to site	18.91	15	2.5
Pre-dredge survey	13.2	-	2.5
Dredging #1	15.6	-	2.5
Dredging #2	15.6	-	2.5
Post-dredge survey	13.2	-	2.5
Dredger in-field transit	0.24	15	2.5
Dredger transit from site	18.78	15	2.5
Dredger demobilization	17.4	-	-

Table 6.7: Filter Layer Operations [133]

Operation	Duration (h)	Wind Speed Limit (m/s)	Wave Height Limit (m)
FFPV mobilization	19.2	-	-
FFPV transit to site	29.4	15	2.5
Filter & foundation #1	13.2	20.6	2.5
Filter & foundation #2	13.2	20.6	2.5
Filter & foundation #3	13.2	20.6	2.5
Filter & foundation #4	13.2	20.6	2.5
FFPV in-field transit	0.24	15	2.5
FFPV transit from site	29.4	15	2.5
FFPV demobilization	19.2	-	-

6.5.2 Results Comparison

In this section CDFs are presented for the outcomes of both installation phases produced by Mermaid and the prototype simulation package. As a part of the original BOD analysis, ten percentile calculations were produced for each installation phase and rather than plotting these as CDFs, the individual percentile values are directly overlaid in each figure.

In Figure 6.18 the results for the Dredging phase are presented. Overall it appears that the predicted outcomes for the three cases are very similar. The average values for each outcome are included in the legend of Figure 6.18 and it is evident that the observed and simulated data share very similar values. The Mermaid average, taken from the percentile predictions was approximately 0.5 days higher and cannot be taken as a definitive value owing to the limited selection of percentiles used to derive this figure. The simulated data set demonstrates a much smoother distribution in comparison to the observed CDF and the maximum K-S distance between the two distributions was measured at 0.15, which appears to be between the P60 to P70 region. The percentile predictions from Mermaid from P30 to P70 show similar values to the simulated data while the Mermaid and observed outcomes show the biggest deviations for the lower and upper percentile values.

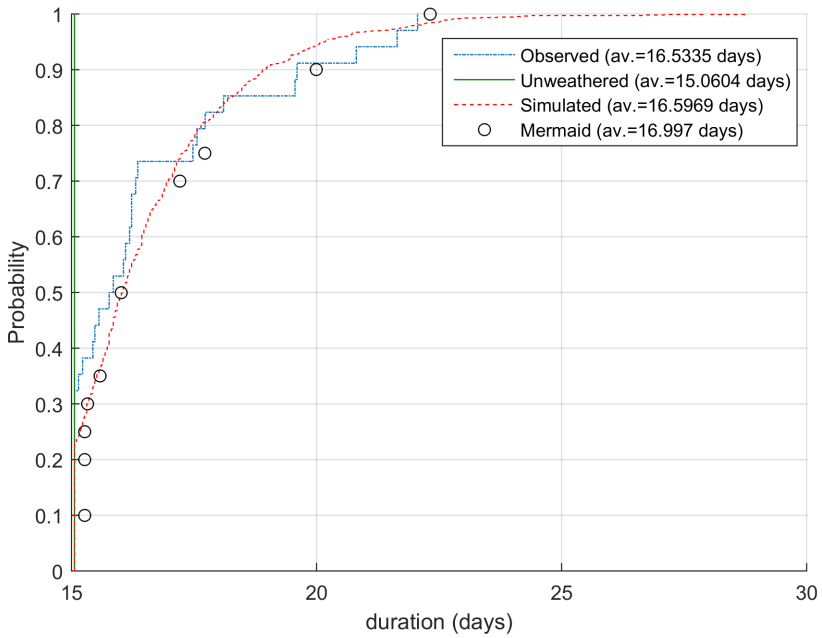

Figure 6.18: Dredging: CDF of Simulated, observed and overlaid percentiles from Mermaid simulation

The results for the Filter layer phase are presented in 6.19. Again, a similar overall trend in the CDFs and Mermaid percentiles is observed. The average durations are closest between the observed and Mermaid outcomes, whilst the simulated data is approximately 0.4 days lower than the Mermaid average. In this case, the CDF of the simulated predictions appears to intersect the observed time series at approximately P65 and the largest K-S distance was recorded as 0.13, occurring approximately between the P70 and P85.

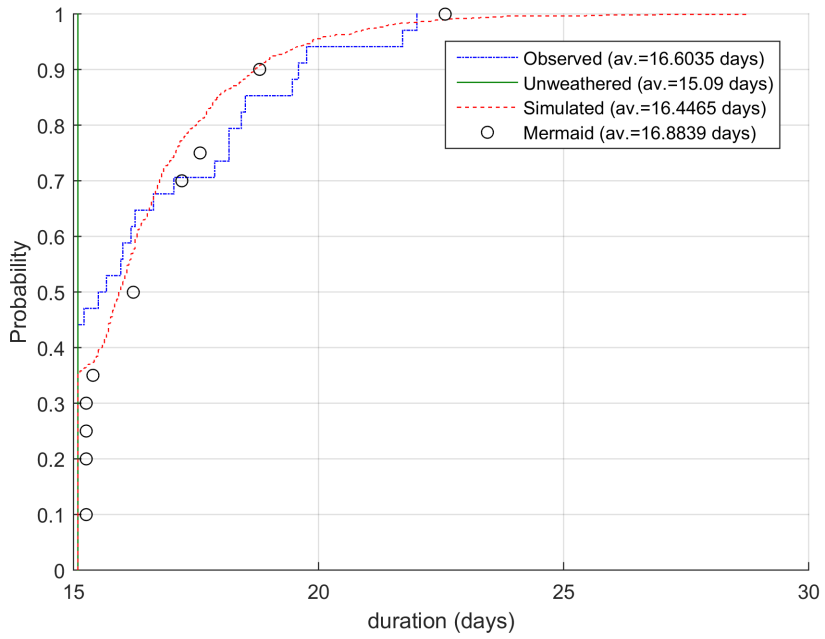

Figure 6.19: Filter layer: CDF of Simulated, observed and overlaid percentiles from Mermaid simulation

The distribution of the Mermaid results appear again more consistent with the simulated data overall, with the largest deviations at P70 to P75. Differences between the Mermaid and observed prototype results are clearly shown, despite sharing the same meteorological data in the simulations. This indicates that the simulations and embedded calculations differ slightly between the prototype and Mermaid. Generally this benchmarking exercise demonstrates that the

simulated time series and the functional prototype generate similar predictions in comparison to a commercially available simulation package and offers some verification on the functionality of the prototype with an embedded stochastic weather model.

6.6 Summary

The MS-AR model included within the METIS matlab toolbox has been applied and incorporated into a structured metocean modelling methodology and the results of various analyses are presented in this section. Primarily, it has been demonstrated that the MS-AR model is capable of simulating independent wind speed and wave height time series. To assess the application of the simulated data a weather window assessment was completed, characterised by a crew transfer task. The two paring methods presented in Chapter 3, Section 3.3.5 were investigated against the constraints of this operation and it was demonstrated that the paired-by-means method could produce characteristics that are similar to the observed time series for two sites, whilst the Pearson r correlation was shown improve the estimates for sites with high correlations between the wind speed and significant wave height. These observations are summarised by the supporting weather window, percentage workability distributions and percentile plots, which collectively corroborate that the greatest deviations are observed for larger percentiles such as P90. Generally, confidence can be taken from the adoption and expansion of the MS-AR model within the metocean modelling methodology to generate realistic stochastic metocean time series, yet the estimates at larger percentiles for sites with close wind speed and wave height correlations, can lead to pessimistic outcomes when used for metocean risk assessments. Time series generated by the modelling methodology was applied

within a prototype simulation tool and it was found data using the paired-by-means approach produced similar estimates in comparison to Mermaid results. This has further bolstered the validity of the metocean modelling methodology and the implications of these results are discussed in the next chapter.

Chapter 7

Discussion

7.1 Comparative Vessel Assessment with ECUME I

The Installation Rates and WDT values included in Figures 4.1 and 4.2, detail the average result for the various scenarios within each installation phase, across the three rounds. The results used to draw these averages were compiled separately to facilitate analysis on each round. The most notable average results from each round are covered in the following sections with consideration given to the source of these outcomes, including the contribution of each installation phase towards the averages obtained. Figure 7.1 represents the interquartile range of each round and phase from the box plots in Figure 4.3. These ranges are used to quantify the risk associated with the vessels in each round and supports the following discussion.

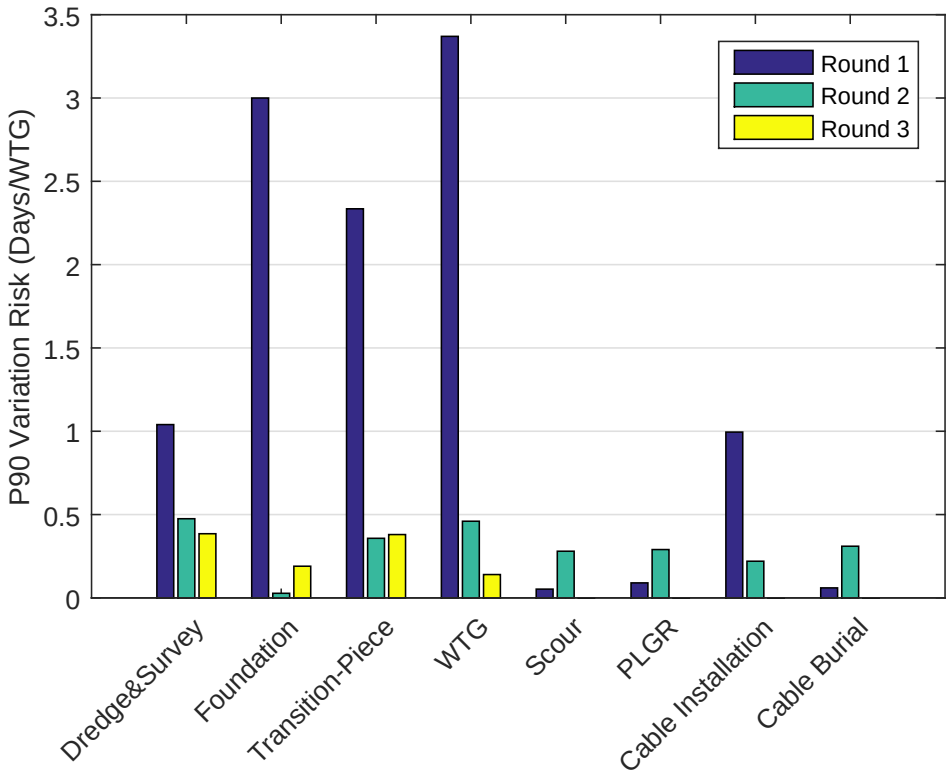

Figure 7.1: Phase IQR Quantification: Rounds 1, 2 & 3

7.1.1 Round 1

In Round 1, the average totals of construction days spent per wind turbine, which includes all phases across all scenarios, are the lowest for both rounds at 20.23 days/WTG. This is complemented by a WDT figure of 10.21 days/WTG on average and both exhibit a standard deviation of 3.2 days/WTG. Despite the adoption of less dedicated and specialised vessels, it appears that Round 1 sites benefit from their near shore locations. The provision of more sheltered conditions during construction reduces the impact of poor weather on the vessels and resulting delays. However, in Round 1 the averaged results suggest that over 50% of the charter time for the vessels would likely be attributed to downtime. The average combined construction duration was found to be 403 days, which

required a total of 640 individual boat days relating to the overlap of phases described in Section 3.1.2.4. These outcomes arrived at an approximate weather downtime value of 328 days per project on average.

A review of the individual phases revealed that the Wind Turbine Installation phase makes the largest contribution to downtime, recorded at 26%. The case which caused the largest impact in terms of IR and WDT was the mean case at 23.6 days/WTG for IR and 13.6 days/WTG for WDT. These were closely followed by very similar results for the distance to shore, inter-turbine distance cases at around 23-24 days/WTG IR and 13-14 days/WTG WDT. The lowest predicted duration was seen with the lower number of turbines scenario at 16 days/WTG and 6 days/WTG for IR and WDT respectively. It was expected that the maximum distance to shore and number of turbine cases would result in greatest recorded IRs and WDTs. However, as the number of turbines or distances in the model increase, so does the elapsed time for each phase and delays gradually shift the start date of successive phases. This suggests that seasonal conditions can happen at different moments, during different phases of an installation campaign, due to the size of the project to be completed. For example, the start date recorded for WTG installation in the case with the minimum number of turbines was 11/08/2017, whilst the start date for the maximum number of turbine cases was 12/05/2018. Despite this dramatic shift due to the size of the project, the start date for maximum number of turbine case is in May. It is likely that the weather conditions were more favourable in May than in August. This observation is further exemplified by the results for the start date cases, which have the same characteristics as the mean case but with a different date defined for the launch of the first phase. The results recorded for the upper start date case (starting: 01/04/2017) are the second lowest recorded at 16.8 days/WTG for IR and 6.8 days/WTG for WDT. It is also suggested that the weather downtime will increase if the vessel employed for each installation phase has to return to base to reload

various components, as is the case for the Foundation, Transition Piece and WTG vessels in this study.

Referring to the box plots in Figures 4.3a and 4.3b, it is evident that many of the phases are variable in terms of IR and WDT, with the largest spread of values observed for the Foundation, Transition Piece and Wind Turbine Installation. The large variation shown in Figure 7.1 shows a lack of consistency in the IR and WDT values for each scenario and indicates a significant amount of installation risk that could be expected for these phases throughout Round 1. This suggests that the vessels employed for these three phases at the time of Round 1 were susceptible to variations in their working climate, exemplified by the broad spread of values for the phases described above.

7.1.2 Round 2

Round 2 vessels are predicted to have the largest average IRs and WDT values between the two rounds. The average IR across all scenarios is 25.4 days/WTG and 15.4 days/WTG for the average WDT, with a standard deviation of 2.17 days for both. This deviation is lower than Round 1 and the installation risk is lower overall with the Round 2 vessels. The average WDT value represents an increase of 50% compared to Round 1. These initial outcomes convey the impact of more challenging offshore conditions typically experienced at these sites. The results indicate that on average over 60% of the entire vessel charter period would experience weather downtime, suggesting developers could have faced a significant bill for downtime for similar projects. The average and combined construction duration was predicted to be around 1384 days per project, requiring a large number of separate boat days, in excess of 2300 days in total. The average WDT value for all the scenarios in Round 2 was just over 1260 days per project.

Reference to the individual phases revealed that the WTG installation phase again made the largest contribution to overall WDT recorded at nearly 34% of all downtime on average, which is a considerable increase compared to Round 1. This implies that the typical turbine installation vessel employed during Round 2 was not ideally suited to the heightened weather conditions typical of more challenging waters further from shore. The scenario found to have the largest impact in IR and WDT was the lower number of wind turbines case with values of 29.67 days/WTG and 19.62 days/WTG respectively. The scenario with the least impact in the Round 2 predictions is the maximum start date (01/04/2017), with an IR of 23 days/WTG and WDT value of approximately 13 days. This outcome is surprising, as it may be expected that with fewer turbines, the installation rates might be greater or at least stay the same. It is suggested that the impact of successive scheduling can dramatically change the amount of downtime experienced, relating to the changing seasonal weather conditions. As there are fewer turbines in the minimum WTG case, this means phases such as the WTG installation would be achieved sooner and could be completed during more severe weather conditions, in comparison to larger projects that may not reach the most susceptible phases until a calmer weather season occurs. An example of this was the WTG installation start date for the case with the minimum number of turbines, which was recorded at 11/11/2017 and for the maximum start date case at 01/06/2018. It is again likely the weather was less severe in June than in November and therefore applying a consecutive installation schedule, may not be the optimum approach when planning offshore wind farm construction.

It is clear that on average, the majority of phases experienced an increase in WDT and again the WTG installation shows a 97% increase in average downtime in comparison to Round 1. Notably, the Scour Protection conveys a 250% increase, a 100% increase in PLGR, 58% for cable installation and approximately 40-45% increase for the Dredging and Cable Burial Phases. Two WDTs found to increase

slightly are the Foundation and Transition Piece installations each confirming on average an approximate increase of 8% and 13% respectively on average. It is suggested that Round 2 results demonstrate particular vessel availability restrictions as oversized and weather sensitive vessels were commonly chartered at this time. These vessels were used for phases such as foundation or transition piece installations and originated from other offshore industries, matched with inflated daily charter rates. It would be appropriate to apply a cost benefit analysis when considering the charter of these vessels in comparison to the resulting WDT costs that may be expected from more capable, but less available vessels. In some cases developers may have struggled to source a cheaper alternative with improved capabilities and to some extent, this demonstrates that optimum vessel designs were not available or had yet to be built during the construction of Round 2 sites. Thus the development of dedicated wind farm installation vessels was essential to the industry at this time.

The box plots in Figures 4.3c and 4.3d showed significantly less variation in comparison to Round 1. This suggests that despite an overall increase in WDT on average, the vessels employed for Round 2 performed more consistently and therefore a reduction in the installation risk is observed in Figure 7.1. This means more certainty could be drawn from WDT predictions, but the challenge in reducing the overall magnitude of these delays was still a concern. The Scour Protection and PLGR phases still exhibit fairly low IR and WDT values compared to Round 1, but the plots demonstrate more variability in the results, which suggests these vessels may perform less consistently when used in more challenging conditions.

7.1.3 Round 3

The results for the phases completed in the Round 3 simulations demonstrate that the IR and WDT values were predicted to be lower than Round 2 and similar to the Round 1 results. It is reiterated that the software did not complete a full simulation for all the scenarios in Table 3.3 and the only full set of results was obtained with the lower number of wind turbine scenario. Thus the results of this scenario can be used for an indicative analysis only. The outcome of this scenario indicates the average number of construction days spent at each turbine location was 21.96 days/WTG, WDT of 11.92 days/WTG demonstrating the WDT could account for roughly 50% of the total duration. Furthermore, this limited result implies an overall reduction of 26.5% in WDT could be expected due to the vessel technology used at Round 3 when compared to Round 2. When compared to Round 1, a slight increase in WDT of approximately 5% is observed.

Full results were obtained for the Dredging & Survey, Foundation, Transition Piece and WTG installation phases across the 11 scenarios. To obtain a picture of the phases with the greatest contribution in the predicted durations, the full results were combined with the outcomes of the fewer number of turbines scenario. This again revealed that the WTG installation may account for the majority of the WDT at just over 20%, although this is lowest contribution for the WTG phase across all three rounds. The results for the Round 3 WTG installation show a 40% and 62% reduction compared to Rounds 1 and 2 respectively. This demonstrates the advantage of hiring the most modern WTIVs as they are able to cope with more severe conditions either during operations or when station keeping, thereby reducing the duration and subsequent WDT of the turbine assembly offshore.

The Dredging & survey phase is the next largest contributor to WDT in Round 3 at 23%. Here the average WDT exhibits a 31% improvement when compared

to Round 2 and only a slight increase when compared to Round 1 at 5%. The Foundation Installation and Cable Burial phases were the next largest WDT contributors at 16% and 13% respectively. The WDT experienced for Foundation Installation was found to have an improvement of 43% and 31% in comparison to Rounds 1 and 2. Again as the foundation logistics were assumed to be handled by a modern WTIV, the delays are significantly reduced and when it is considered that expensive heavy lift vessels were employed widely in Round 2, the advantage of a long term charter is clear. Modern WTIVs can contribute to the Foundation, Transition Piece and Turbine installation phases and with costs at approximately 50% less than that of the of the heavy lift vessels, their value to a project is significant.

The figures for the transition piece are similar to the foundations and show a 44.5% and 36% improvement for Round 1 and Round 2. Both the PLGR and Cable Burial phases were predicted to have an increase in their durations round by round. Based on the PLGR average WDT for the Lower number of turbines scenario, the WDT increased by 270% compared to Round 1 and 63% against Round 2. In the Cable Burial phase, an increase of 112% and 38% is anticipated by the results. This suggests developers and ship designers alike, may consider alternative vessel designs or installation methods for these phases, although their limited stake in the overall WDT predictions may not result in significant savings.

Due to limited results for the Round 3 prediction, a full and reliable comparison on the impact of the 11 scenarios was not possible. Nevertheless, with data available for the first four phases across ten of the scenarios, a comparison on the combined average duration for these phases could be completed to give an indicative outcome.

The Upper and Lower Start Date cases predicted at approximately 8 days/WTG in downtime. This result differs considerably to the outcomes of Round 1 and 2

as the upper and lower start date scenarios resulted in the lowest recorded WDT figures. This demonstrates that while it may be beneficial to begin construction in winter or spring as the better weather is saved for more complex operations, when the project is much bigger (i.e. approximately 250 turbines), a revision of this approach is required. It might be better to consider a fragmented installation campaign such as installing the wind farm in two stages, essentially treating it as two separate projects or possibly double up on the number of vessels and personnel, to significantly reduce the overall time frame.

The box plots in Figures 4.3e and 4.3f are found to have slightly broader IQRs for the Foundation and Transition Piece phases in comparison to Round 2, meaning that more installation risk may experienced in these phases. The IR and WDT of the WTG installation phase exhibit narrower IQRs and a smaller range against the Round 2 outcomes, supporting the suggestion that modern WTIVs can offer a real advantage in terms of capability and observed durations. The data provided from the one complete scenario and indicates that a slight shift could occur in the IR and WDT predicted for the PLGR and Cable Burial phases. Table 3.4 shows that even when modern, specifically designed CLVs are employed an increase in the durations was predicted by the software. This indicates the difficulty in preparing the seabed and the cable burial processes as the stringent environmental limits of these operations can be prohibitive, negating the influence of improved vessel capabilities, suggesting further consideration of the overall installation method or technological innovation may improve the duration of these phases. However, as water depth and seabed conditions are not considered in this study, it is difficult to speculate how these operations may transpire for larger projects, farther from shore.

7.1.4 Model Validations & Comparisons

The IRs presented by Kaiser et. al [114] were used to complete a validation of the adopted method and analyses. Within this reference, Kaiser et. al list observed IRs (days/WTG) for foundations and wind turbines from eight UK Round 1 wind farms. These values are presented in a 'boat days' basis which represent the entire time spent per vessel for each foundation and turbine installation in days/WTG. This metric provides a suitable base for comparison and as these phases were predicted to have some of largest weather downtimes in Figure 4.2, it provides an interesting reference. Unfortunately, it is not believed that any other data set presents the remaining installation phases in this manner. P50 predictions were also computed during the simulations completed for this study and the P50 IRs were obtained using the same approach in Section 4.1. The average P90 and P50 predictions for the Foundation and WTG phases, are compared against the average IRs recorded across various Round 1 sites in Figure 7.2. In this figure, no data was available for the foundation installation at Robin Rigg or the WTG installation at Rhyl Flats in [114]. An initial review of the data demonstrates that for the average Round 1 predictions, both P90 and P50, are of similar order to the recorded values for the Round 1 site and indicates that the predictions produced by the software and the method to obtain the IRs, can produce realistic results.

The average predicted and recorded IRs for the Foundation and WTG Installation phases are compared in Figure 7.3. The error bars signify ± one standard deviation and represent the variation in the results. It is evident that the average P50 prediction is almost identical to the recorded IRs for the foundations at 3.8 days/WTG. The P90 results are on average greater than the P50 and recorded IRs at approximately 4.1 days/WTG, but are similar to the P50 values in the WTG installation phase at 3.7 days/WTG, compared to 3.4 days/WTG for the

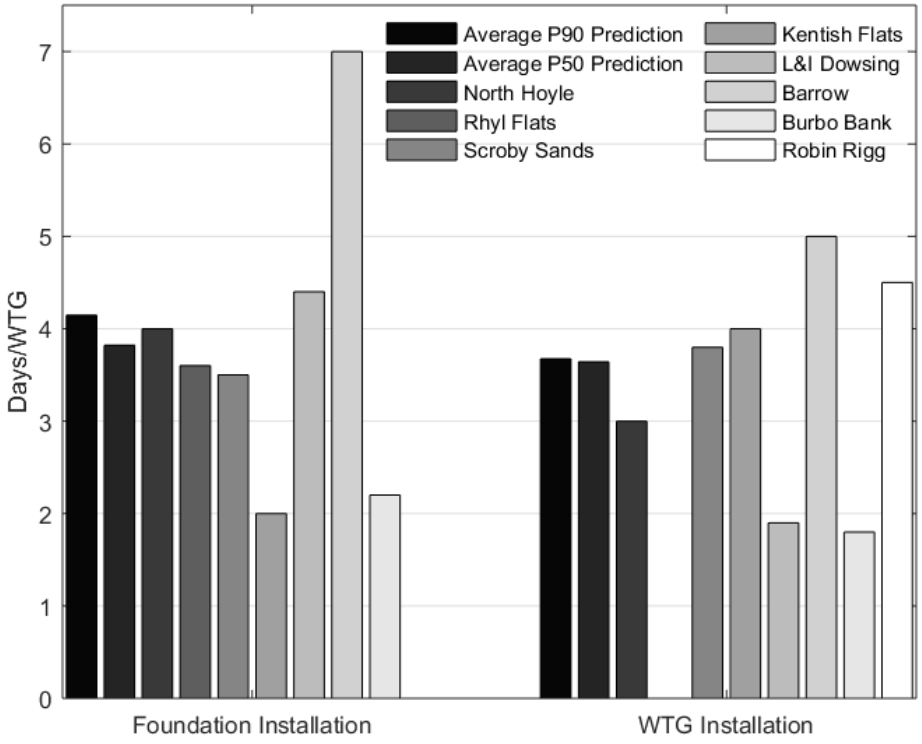

Figure 7.2: Average Prediction vs. Recorded Installation Rates - Round 1 [114]

recorded data. The error bars show a considerable spread for the data in both the P50 and P90 predictions and it can be deduced that as the recorded average lies within the error bar of the P50 and P90 values, the values show similarity to the recorded data, providing further confidence in the predicted results.

The error bars for the P values are much broader in the WTG data when compared to the recorded IRs while the P50 error bar has a smaller spread against the other two values for the foundation data. This indicates that the probabilistic results produced by the software can over and under predict the average IRs in specific cases. The average P50 values are closer to the recorded IRs and are only 6% greater in the WTG category. As the P90 outcomes were selected to represent the upper bounds of the software predictions, it was expected these values would be

greater than the recorded IRs, yet these show good agreement with the recorded data. The P90 predictions are approximately 10% greater than the recorded IRs on average and demonstrate this approach can be used to produce conservative estimates.

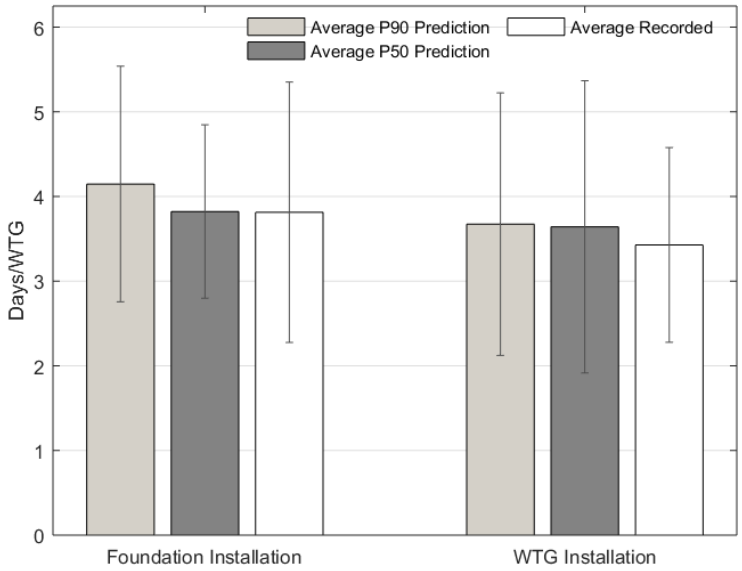

Figure 7.3: Average prediction vs average recorded installation rates - Round 1 [± 1 S.D.]

7.1.5 Value to Planning Personnel

The presented approach is of interest to planning personnel as a structured method to identify and benchmark offshore wind installation risks. Whilst the study and simulation do not relate to any specific project, it has provided a basis to schedule vessel missions based on the predominant characteristics of the three installation rounds.

Ensuring efficient, low cost installation strategies is essential if offshore wind is to make a meaningful, cost effective contribution to the UK's energy mix, aiming for

a levelised cost under £100/MWh [134]. Many of the delays identified have been tackled by the introduction of innovative vessel designs, to cope with more extreme weather conditions as well as increased deck space or lifting capabilities. Assessing the environmental capabilities of the vessels as well as their susceptibility to various project characteristics makes it possible to offer guidance on vessel charter, with the added potential benefit of reducing costs.

As the study has been categorised by the three UK offshore wind rounds it is intended that operatives will be able to assess which round of characteristics relate to their project and refer to the vessel performance predictions. This study provides a clear indication of the installation risks for the vessel spreads used in each round and the phases predicted to have the largest installation risk and highlight areas where precautionary or mitigation steps may be required when chartering vessels with similar capabilities. It demonstrates that the selection of the vessels identified in Round 1 would generally result in acceptable weather downtimes but there may be significant variation in the Foundation, Transition Piece and Turbine installation phases. The vessels specified for Round 2 exhibit considerably less variation but the generally large weather downtimes compared to Round 1. Management could take more certainty on their predicted WDT figures if they employ a similar vessel spread as listed in Table 3.4 however the adoption of more sophisticated vessels such as modern WTIVs could reduce the length of the installation schedule, as this phase was the largest WDT contributor in Round 2 at over 30%.

The impact of the most modern vessel fleet in Round 3 is demonstrated in both sets of results. It is suggested that a reasonable degree of confidence can be assumed for the first four phases as a near-full range of results was gathered, however the singular results for the last four phases should be reviewed with caution. The approximated overall view suggests that a reduction of over 25% in

WDT could be achieved if a similar vessel spread is employed as listed in Table 3.4 and suggests that the evolution of vessel technology has addressed the needs of offshore wind development as projects extend into deeper and more challenging waters.

To generalise, Round 1 vessel technology exhibits the lowest WDT, although a considerable amount of variation in the observed delays may occur when employed for more remote, unsheltered locations. The vessels employed for Round 2 offer more certainty as the results appear more consistent, but are predicted to experience larger WDTs. This demonstrates that despite the adoption of a more standardised approach for these projects, there was an opportunity to reduce the WDT figures with more sophisticated and capable vessels. In Round 3 the impact of the vessel improvements is demonstrated as the figures appear more consistent and show a reduction in WDT despite the more severe conditions associated with these sites.

7.2 Commercial Metocean Risk Analyses

The Mermaid simulation tool was employed in response to modelling restrictions embedded in EDF'S ECUME I simulation package. Mermaid provides a flexible logistical interface that can be used to specify intermediate operations and improved task interdependencies in comparison to ECUME I. As a number of intermediate tasks were specified in the BOD installation, Mermaid presented a practical option to accurately model the marine operations. Furthermore, it was of interest to model the transits of some of the primary installation vessels and as Mermaid can include multiple meteorological hindcasts, the historical weather data could be applied along the transit routes to accurately assess potential delays.

In the following sections, the modelling and results for each project are discussed, with reference to the limitations of each study.

7.2.1 Blyth Offshore Demonstrator - Metocean Risk Analysis

A review of installation schedules provided by each contractor for the main installation phases was required to update the modelling scenarios in MERMAID. The review of information found that a number of planning details were unclear, requiring the MERMAID models to be built around a number of assumptions. These assumptions were carefully listed within the presentations constructed to provide an overview of the model structure and results. Once results were obtained for the various installation scenarios, these presentations were reviewed with representatives from EDF ER, the coordinators of the BOD project. In each case feedback on the modelling assumptions was provided to improve the accuracy of the models. The suspendability of the operations was often discussed throughout the presentations to ensure the minimum length of the weather windows was accurately modelled in MERMAID. A number of iterations of the installation model and results were provided to EDF ER for the entire installation campaign with a final submission provided in December 2016. In addition to the percentile outcomes presented in Section 5.1, corresponding weathered Gantt charts were extracted from Mermaid which represented the impact of delay on the progression of operations under a chosen percentile. Each Gantt chart originated from one of the simulations that was closest to the Nth quantile in question and feedback from EDF EN project team indicated that this provided useful visual reference.

The primary steps in modelling of the BOD Project in MERMAID was fairly time consuming, owing to a number of factors. As EDF ER wanted to assess the

impact of weather on the transit of the main installation vessels, 24 individual meteorological points were introduced into the model. This step required careful importing of the data sets for each met point. In addition, at this time MERMAID did not include the functionality to model different vessel speeds for loaded and unloaded transits and this required duplication of some key installation vessels with corresponding speeds, also increasing complexity of the model. As the BOD project is made up of only five turbines, it was decided that the installation steps could be modelled explicitly in the flowchart diagram in MERMAID. This helped with the overall understanding of the task functionality in MERMAID and by introducing groups with different rates of suspension, this ensured that the final model was an accurate reconstruction of the constraints on the installation campaign.

Four different scenarios were modelled in Mermaid to assess the impact of learning, a delay of one month to the start date of the operations and a contingency installation procedure. It was found that the learning rates applied to the GBF and WTG installation phases resulted in negligible impact on these specific operations and on the completion date. Learning rates were applied to the first two GBF installations and it was assumed some learning would be maintained during the last WTG installation task. The impact of one month delay is clearly demonstrated in scenario three, where different weather downtimes were identified across the phases. There was a notable reduction in many of the earlier installation phases in scenario three, with the exception of towing the GBFs out of the dry dock. This is likely to relate to the more favourable conditions experienced by these phases throughout the simulation, although a notable increase in the later phases was observed, demonstrating the impact of the change in season. When combined, the results led to a completion date of two months later than the first and second scenario schedule; this clearly exemplifies the weather risk that could be experienced.

The towing out of the GBFs from the dry dock task was consistently predicted to produce the largest delay across the first three scenarios. A significant increase for this operation was predicted for the scenario with a one month delay,which increased the weather downtime by approximately 20 days across all percentiles. The consistency of this increase indicated that tidal dependency was the most likely cause for the delays predicted for these operations. The tugs employed to install the GBFs were under significant speed restrictions on the outward leg of the GBF installation, while it was specified by the method statements that the unloaded, return leg would be much quicker. To mimic this behaviour, a number of duplicate tugs with corresponding transit speeds were introduced into the model. Whilst it appears that this approach would facilitate the different transit durations based with reference to the compiled Gantt charts in Mermaid, the large weather downtimes associated with the GBF installation might have been exaggerated as a result of this modelling technique. A recent Mermaid update features mobile tasks that can be used to specify constraints for vessel transit operations. It is proposed that implementation of this modelling feature could potentially build a more accurate representation of vessel transits and may reduce the exceptionally large weather downtimes for the towing of the GBFs out of the dry dock. Nevertheless, representatives of the project were aware that the stringent tidal dependencies posed one of the greatest risks in terms of delays to the project and the results highlighted this issue, despite the suspected modelling inadequacies.

7.2.2 Fecamp Offshore Wind Farm - Metocean Risk Analysis

The successful delivery of the BOD weather risk assessment led to a second project, as operatives in EDF EN in France were keen to review the application performance of the Mermaid software for the upcoming Fecamp development.

The Fecamp project was significantly larger than the Blyth project at 83 turbines in total. From experience, when modelling the BOD project as one Mermaid file that embedded all operational phases, it was sometimes difficult to identify modelling issues that caused simulations to fail. Additionally, owing to the shear scale of the Fecamp project, including all phases in one Mermaid file could have led to particularly long simulation times. It was agreed with the EDF EN team in France that the individual phases would be assessed in separate Mermaid models to overcome these potential issues. This approach meant that the impact of knock-on delays would not be captured by the assessment and therefore mock weathered Gantt charts would be produced for each percentile to highlight any obvious resourcing issues.

The modelling of the installations was less explicit for the Fecamp installation models, with the repeat function utilised for the identical tasks to be completed at each turbine location. This led to significantly less complex modelling in comparison to the BOD project, where interdependencies between project phases could not be applied. Furthermore, an extensive review of planning documentation was not required as an abbreviated breakdown of tasks was provided by the project team and easily replicated in Mermaid; this sped up the modelling of the project phases.

The results were presented in tables highlighted the durations and downtimes

under different percentiles in Section 5.2.1. Two tables were provided, each representing the results from the two installation campaigns. Overall, the wind turbine installation phase was identified to produce the largest weather downtimes, which could be attributed to the scale of these operations since all turbines would be installed in one campaign. It was identified that the next largest downtimes were attributed to the GBS installation and the Scour and Ballast phases in both campaigns, indicating that these phases posed a significant risk to the progress of the project.

In an attempt to demonstrate any potential issues with project scheduling and resources, mock Gantt charts were constructed using the installation durations for each phase. The Gantt charts were produced using MS Project for each percentile using the results in Tables 5.5 and 5.6. From an initial review of the unweathered Gantt chart in Figure 5.1, which included no weather delay, it was apparent that the Scour and Ballast tasks would be completed before the GBF installation. This is unrealistic, as the Scour and Ballast task would be dependent on the progress of the GBF installation phase, which was a useful observation. It was anticipated that a similar effect would be demonstrated in the percentile Gantt charts and is confirmed in Figures 5.2 to 5.5. Additionally, the unweathered Gantt charts identified a potential issue with the WTG installation phase and the IAG termination. As the turbine installation was identified to complete before the second IAG termination, it was possible that both phases could coincide at the same turbine location, leading to inevitable delays. However, the weathered Gantt charts indicated that the IAG termination was predicted to complete before the WTG installation in all percentile examples, indicating that this interaction is unlikely in reality. However, care should be taken to monitor the progress of these operations during the full installation campaign. It is worth noting that the the same percentile value would not be experienced in reality and that the

mock Gantt charts should provide a sense check rather than a narrative of how the installations will progress in reality.

7.3 Discussion on the Stochastic Metocean Modelling Method

In Section 3.3 a methodology to produce annual time series of wind speed at 10m (U) and significant wave height (H_s) was presented, which included two approaches to pair univariate wind speed and wave height simulations. In Section 6.2 an assessment of a typical offshore operation was completed, comparing the resulting weather windows with the observed and simulated time series. A brief benchmark assessment was completed to compare the predictions produced for two phases from the BOD project. This assessment compared the predictions produced in Mermaid against those from a marine operations software simulation prototype, produced in collaboration with EDF R&D in France. In this assessment two time series were used in the prototype simulations: i) the observed time series (as used in the Mermaid simulations) and ii) the simulated paired-by-means time series. The findings from the development and testing of stochastic weather modelling methodology are presented in this section, with consideration of issues such as overall functionality as well as sensitivities and an assessment of its potential viability for inclusion in a fully functional simulation package.

7.3.1 Stochastic Metocean Modelling - Simulations

Following the outcome of preliminary discussion and after considering the specification of the marine operations simulation tool, there was a clear desire to

develop a dynamic metocean model capable of adapting to any location and able to select the most appropriate model type for each month or season. The MS-AR model developed by Monbet & Alliot [81] can be applied to monthly data using a dedicated model in each instance, to produce monthly outcomes with similar characteristics to observed time series. The MS-AR model addresses the inadequacy of using a single autoregressive model to describe the evolution of weather parameters; in each month it applies numerous autoregressive models that operate within defined weather regimes. To reduce the number of model types and subsequent number of simulations, it is proposed that a future assessment could segment the data into four seasonal sets, which would be analysed using the same methods presented in Chapter 6. This would determine if similar or improved results can be obtained using this approach and could theoretically reduce overall simulation durations.

Monbet and Ailliot [70] suggested that the Bayes Information Criterion (BIC) is a suitable method to select the best model order and number of hidden states to fit the data, while acknowledging that this approach is not theoretically justified for MS-AR models. Therefore, an investigation using this assessment approach was presented and it was found that an envelope of model types was consistent across the three offshore sites for U and H_s. The numerical outputs, CDF comparisons in Figures 6.1 and 6.2 and the Q-Q plots in 6.3 and 6.4 demonstrate that the identified models produce good outcomes for U and H_s and confirms the validity of this model selection process. It is likely however that there would be some variation in the model selections each time the BIC scoring process is re-run, owing to the probabilistic nature of the EM algorithm. It is important therefore that a model selection envelope be incorporated if this modelling methodology is included as part of a offshore planning simulation tool, allowing for this variation and offer adaptability to any offshore location. It should be noted that if a seasonal modelling approach is investigated, this may require an alteration to this model

envelope and therefore a broad assessment of model types should be completed prior to running full simulations.

The simulated outcomes for U and H_s were found to show similar characteristics to the observed data as exemplified by the various plots presented in Section 6.1. In Figures 6.1 and 6.2, the CDF of the simulated data follows the observed years of annual data. Looking at the lower wind speeds and wave heights in both figures indicates that the model has a tendency to over predict the occurrence of U and H_s below 3m/s and 0.4m respectively. This observation is consistent with similar observations completed by Ailliot and Monbet [70], who note that this behaviour will have limited impact for applications that are insensitive to lower magnitudes, such as the intended application in a marine operations simulation tool.

In Figure 6.3 a right skew tail is shown, indicating that some extreme wind speeds may have been produced by the simulation compared to the observed data set. However, the concentration of the points is quite low, especially for the most extreme points. Figure 6.4, shows a much slighter skew than was observed with the wind speed. This behaviour at the tails is expected to have little impact for marine planning applications as these extreme values are likely to span well beyond the operational constraints for these tasks.

7.3.2 Weather Window and Workability Assessments

To assess the validity of the overall stochastic weather modelling methodology, the final annual compositions of U and H_s were initially compared using weather window persistence histograms and average monthly weather window durations for a crew transfer task. The plots included in Section 6.2 were produced to summarise characteristics most relevant to the assessment of marine operations

and provide a perspective on how simulated logistical scenarios may progress when using the synthetic time series.

7.3.3 Paired-by-means

It was demonstrated that for the UK North East both the weather window persistence and average weather window lengths have good agreement. The differences increase steadily moving from France West to the English Channel location, the latter having the greatest difference overall. In Figures 6.12a to 6.12a, ten hour bins were used in the histograms to maximise the perspective of the weather window availability across the three sites. These demonstrate some sensitivity when comparing the data for the France West and English Channel locations. Figure 6.12c suggests that the synthetic data for this site may produce different outcomes when used to plan marine operations; a comparison of smaller bin sizes would be necessary to fully understand and validate any potential risk in using this data.

The workability plots presented in Figures 6.7 - 6.9 provide a further insight into the characteristics of the simulated data by introducing a 30 hour minimum threshold for the weather window limitations. The scatter plots have shown that the mean percentage workability of the simulated data falls within the 95% confidence interval for all months at each site, with the exception of five months for the English Channel. The average number of weather windows was also reviewed for the same thresholds across the three sites and revealed that the fragmentation of the windows was fairly consistent with the observed data for UK North East and France West. The English Channel generally shows a larger number of weather windows in the simulated data, which indicates that more frequent delays or interruptions may be predicted using the generated time series. This suggests that

the simulated outcomes for the English Channel may lead to incorrect predictions if used for offshore planning and simulation applications. The observed data for the English channel is shown to have the largest average wind speed for all three sites in Table 3.6 and may mean that the MS-AR model types considered have difficulty recreating data with larger excitations. However, when the values listed in Table 6.1 were reviewed, it was found that the largest absolute average percentage difference was recorded for the wave height simulations at the English Channel. Despite this outcome, the 1.62% difference is relatively small, which indicates that the cause of the differences exhibited in the weather window and workability plots may stem from elsewhere in the overall methodology.

The independently simulated U and H_s monthly realisations were ranked by average value and paired accordingly to produce the final time series composition. Whilst this approach has demonstrated its ability to produce realistic characteristics for two locations, it is possible that this pairing method is not suitable for sites with certain characteristics. The English channel is located between two land masses and this narrowing effect or limited fetch, may have an influence on the complexity of the relationship between the wind and the waves at this site. Therefore, it is suggested that the presented methodology is used with caution for sites within an enclosed basin or constrained offshore passage, until further assessments for similar locations demonstrate better and consistent outcomes.

Generally, the simulated data exhibits the largest deviations in the winter months for all three sites, which is exemplified by the results in Table 6.1 and the workability plots in Figures 6.7 - 6.9. However, it is shown that for Teesside and UK North East the average workability of the simulated data is within the 95% confidence error bars for each month. Moreover, the very small error bars for the simulated data in Figures 6.7 - 6.9, demonstrate that generating a large number of simulation realisations provides more certainty for the predicted outcomes when

compared to the observed data, which demonstrate considerable variability across the three sites. It is therefore proposed that the presented methodology and embedded modelling steps could be integrated into a risk planning tool to predict the progression of marine operations, whilst caution should be applied when used for sites with complex metocean conditions.

The monthly weather window and monthly CDF and percentile plots in 6.10 to 6.11 help summarise the box plots and overlaid percentiles presented in Figure I.1. The CDF plots for monthly weather windows in Figures I.1a to I.1e demonstrate the consistency between the observed and simulated data. The French West and English Channel sites show the greatest overall difference in the distribution of all weather windows from approximately 30% upwards, with the simulated data consistently more pessimistic across all three locations. These results combined with the K-S statistics indicate that the outcomes for two out of three sites have the potential to generate considerably different predictions for the occurrence of weather windows above the 30 hour threshold. The greatest deviations for the French West and English Channel sites appear to exist with the P90 estimates as shown in Figures I.1d to I.1f, which demonstrate different behaviour in the tail of the distributions for the larger weather windows in simulated cases and are generally more conservative. The P10 and P50 values are relatively close to the observed months for the UK North East and French West, indicating that similar weather window predictions would be produced between the observed and simulated data for these percentile predictions. Larger deviations are shown in I.1f for the P50 at the English Channel, which, when considered along with the P90 outcomes, point to a consistently different distribution overall.

The percentage workability summaries provided in Figures I.1a to I.1f provide further insight into the predictions that could be generated using the simulated data in comparison to observed data sets. The workability percentage is an

extension from the weather window review to exemplify how much time is available above the minimum threshold duration subject to the meteorological constraints. This provides an indication of the extent of delay that could be predicted for the personnel transfer operation between the two meteorological data sets.

Firstly, the CDFs show generally similar outcomes for the UK North East and France West locations, whilst for the English Channel there is a consistent difference in the distribution of percentage workability is emphasised by the K-S distance of 0.14. This outcome demonstrates that use of the simulated data for the UK North East and France West locations should provide predictions similar to the observed data, whilst smoother CDFs are indicative of a more consistent distribution in percentage workability. It is expected that the simulated data would provide better resolution for estimates in regions where the observed data appears to deviate, exhibiting clear step-like formations, which are believed to relate to the limited number of years available in the observed data. A similar smooth distribution is observed for the English Channel site, yet the difference between the observed and simulated predictions is clearly apparent for the majority of the probabilities, suggesting that the simulated data could lead to consistently erroneous predictions when applied to marine operations.

The percentile plot for the English Channel in Figure I.1f further emphasises the difference in the simulated data for the English Channel, where larger and consistent deviations are shown for the P10, P50 and P90 estimates, particularly for the first and last four months of the year. It is demonstrated in Figures 3.26 and 3.27 in Chapter 3 that the correlation for the paired-by-means approach was very low, which was believed to cause the large deviations in weather windows and workability exemplified for the English Channel site. The following

subsection reviews the same results using the correlated pairing method that was implemented to improve the predictions of the overall modelling methodology.

7.3.4 Correlated Pairing

As noted in Section 6.4, the summarising weather window persistence plots in Figure 6.12 demonstrated little difference for the 10 hour bins presented, although a closer approximation between the observed and simulated results is obtained for the English Channel. A similar effect is shown in the average weather window length plots for the majority of months across the three sites, once an increase in the difference for the summer months was introduced. Overall, these results were encouraging, particularly for the English Channel, which showed greater similarity to the observed data set when compared to the paired-by-means approach. Moreover, the average number of weather windows listed in Table 6.4 show a closer resemblance to the observed examples at this site.

The percentage workability plots and supportive tables reproduced in Figures 6.13 to 6.15 illustrate that the mean values are much closer for the majority of months when compared to the paired-by-means outcome, with the exception of the summer months at all three sites. It is of note that the average percentage difference is approximately halved and the standard deviations are slightly reduced in the correlated pairing results. From these outcomes it can be reasoned that the correlated pairing approach seems to produce predictions that are closer to the observed data set. The significant improvements shown for the winter months at English Channel location in Figure 6.15, the closening of the weather window persistence and average window lengths further supports this statement. The results for all three sites show that a decrease in workability can occur in summer months using the correlated pairing approach, which may introduce

unwanted effects, particularly for sites with a lower correlation demonstrated between the wind and the waves, such as the UK North East site.

It is stated in Section 7.3.3 that the differences in the paired-by-means results may be due to its inability to reproduce the sea state conditions in an enclosed basin or wind sea. The correlated pairing targeted this potential issue and the workability plots indicate that it had the greatest impact in the English Channel site. It is shown in Chapter 3 that the English Channel site has the closest correlation between the wind speed and wave height and as the results have shown a closer resemblance to the observed data set, this appears to improve the versatility and overall scope of the weather modelling methodology.

CDF and percentile plots for the weather windows above the 30 hour threshold were produced for each site in Figures 6.16 and show that the correlated pairing approach produced distributions that appeared much closer than the paired-by-means approach. This is supported by the reduction in the K-S distance in each case, with the greatest reduction recorded for the English Channel site from 0.09 to 0.03. The largest difference was recorded for the France West location at 0.05 and was closer to the observed results of 0.02 in comparison for the paired-by-means results. The percentile plots show that all three percentiles are closer to the observed case, yet the P90 estimates showed notable deviations in the French West and English Channel results. Any deviation in the P90 values are mainly on the pessimistic side, which can be considered more risk averse and preferable to optimistic predictions that could lead to unanticipated delays.

The summarising plots for the percentage workability are included in Figure 6.17 and the same closening effect is not observed for all distributions. It is noted from Figure 6.16a the simulated distribution seems to intersect the observed example for the UK North East, and an increase in the K-S distance from 0.6 to almost 0.8 is demonstrated between the paired-by-means and correlated

pairing methods respectively. There is no obvious difference in the percentile plots between both pairing methods in Figures 6.17b and 6.10b. For the French West location the CDF appears to be slightly closer to the observed distribution where a reduction of the K-S distance by approximately 0.2 was identified. The percentile plot in Figure 6.17d exemplified slight differences with some P10 estimates showing variable increases and decreases in comparison to the paired-by-means plot in Figure 6.10d. However, the P50 estimates appear more consistent with the observed outcomes, whilst the P90 estimates are only very slightly more similar to the observed predictions. The significant reduction in the K-S distance exemplified in the weather window plots for the English Channel site, was not carried through to the percentage workability outcomes in 6.17e, yet a reduction of 0.2 was still observed. It is clear that the overall distribution appears to agree more closely with the observed CDF, but that a consistent difference in the curve is apparent from 10% probability upwards.

While it is evident that the correlated pairing approach improves the similarities for the majority of the plots and statistics presented, the bivariate modelling methodology has some limitations. It is apparent that the correlated pairing approach may not be best suited to simulate the conditions at sites with a Pearson r coefficient between the wind and waves of around 0.5 or lower. As a part of the correlated pairing process, it was noted that some of the monthly wave height realisations are selected and paired more than once with the simulated wind speed realisations. This means that some of the wave height realisations are removed completely from the overall methodology and it is suspected that this may generate slightly more pessimistic predictions in some cases. In direct contrast, it seems that the correlated pairing has the greatest impact for sites with a very close relationship between the wind and waves, as demonstrated in the results for the English Channel. Despite a clear improvement in similarity to the observed data set, it seems that the methodology is incapable of reproducing a time series

with consistently similar weather window and workability characteristics for sites that have a Pearson r of approximately 0.9. In the following section, a review of some of the key statistics is presented, to provide insight and recommendations on the use of the methodology with either pairing technique.

7.3.5 Impact of Pairing Methods

To provide an overall perspective of the two pairing methods for wind speed and wave height applied in the weather modelling methodology, Table 7.1 was used to assemble the absolute percentage difference of the various statistics.

Table 7.1: Comparison of pairing techniques against observed

	UK North East		**France West**		**English Channel**	
	Mean	Correlated	Mean	Correlated	Mean	Correlated
Average % Difference P10 WW Duration	3.747	0.795	1.503	2.777	6.140	3.052
Average % Difference P50 WW Duration	3.619	6.374	5.504	0.385	17.088	3.742
Average % Difference P90 WW Duration	10.979	2.897	23.221	19.682	21.029	9.108
Average % Difference P10 Workability %	2.379	10.643	6.105	19.266	12.887	5.763
Average % Difference P50 Workability %	4.31	1.572	1.461	1.159	9.847	5.787
Average % Difference P90 Workability %	3.288	3.442	7.524	7.475	5.531	6.819
Average % Difference in Mean Workability %	4.240	1.100	4.350	2.060	8.980	4.350
Average % Difference in Mean WW Duration %	12.040	4.216	19.420	15.960	20.030	14.220
KS Stat CDF of WW Dur	0.043	0.038	0.074	0.057	0.094	0.038
KS Stat CDF of Workability %	0.064	0.078	0.071	0.058	0.141	0.122

The first six rows of the of Table 7.1 compare the average percentage differences for the percentile values across the workability and weather window durations between each pairing method. The average difference for each percentile across all months from each pairing approach is considered. For the UK North East, the lowest percentage difference tends to jump between each pairing method for

the weather window and percentage workability percentiles. It is apparent that for the window duration, the lowest difference tends to favour the correlated approach, whilst the opposite is observed for the percentage workability. The mean outcomes for the window duration, percentage workability and observed K-S distances were also compared. The results show that the correlated pairing approach produces lower percentage differences in both mean values and the K-S distance for the weather window duration with a slightly higher K-S distance for the mean workability.

The correlated pairing approach exhibits the smallest K-S distance and absolute percentage difference in all of the statistics for the France West and English Channel locations, with the exception of the P10 weather window duration and P90 workability respectively. It is evident that the difference between the two pairing techniques is generally greater for the English Channel site.

The results presented in Table 7.1 provide further confirmation that the correlated pairing approach should be applied at sites where a distinct relationship between the wind and the waves is applied. Furthermore, it is suggested that a threshold Pearson r coefficient could be identified for implementation of the correlated pairing technique. As only three sites have been investigated,each with a different Pearson r as listed in Table 3.6, the results suggest that correlated pairing should be applied for sites with correlations of 0.7 and above. It is possible that the correlated pairing approach may be suitable for sites with slightly lower correlations, but until additional data sets are reviewed, this value is advisory only.

It is clear that for very large correlations of 0.9, this pairing technique may not consistently produce similar weather windows and workability characteristics, resulting in slightly more pessimistic outcomes when compared to the observed data. and will have an impact on the estimates generated in a fully developed

simulation tool. The closer results between the P10 and P50 percentiles is demonstrated for the English Channel site in Figures 6.16f and 6.17f suggest greater confidence in the modelling methodology that embeds the correlated pairing technique. The assessments indicate that extreme predictions such as P90, should always be reviewed with care if the modelling methodology was implemented in a dedicated simulation package. However, the apparent pessimism at these percentiles can be seen as advantageous, describing an extension of the metocean risk in comparison to the observed data set, and thus more risk averse.

Furthermore, irrespective of the pairing technique used, the methodology demonstrates some difference in the prediction for sites with close wind and wave relationships. It is possible that the differences presented in the weather window and workability assessments may be less pronounced when applying a sequence of logistical tasks. Application of the generated time series using the paired-by-means approach in Section 6.5, showed similar predictions to a commercially available simulation package, although a full set of simulations for all project phases and for multiple sites, would be necessary to confirm this behaviour.

7.3.6 Model Sensitivity to Number of Years of Observed Data

It is desirable that any weather modelling methodology be capable of generating realistic predictions particularly when a limited number of observations are available. The methodology was assessed for its sensitivity to the number of years of observed wind speed and wave height data, used to inform the MS-AR process. The weather model was run for four different data sets as listed in Table 7.2 and were constructed by randomly selecting years from the original observed

data. The site selected to test the sensitivity was the English Channel and the simulations were completed using the correlated paring approach.

Table 7.2: Percentage difference of simulated data to number of years of observed data used to train the model

	1	**5**	**10**	**15**	**21**
Average % Difference P10 WW Duration	3.0	-3.0	-4.8	-5.6	-3.1
Average % Difference P50 WW Duration	-1.3	-6.8	-12.6	-13.2	-3.7
Average % Difference P90 WW Duration	-11.3	-13.6	-21.1	-18.8	-9.1
Average % Difference P10 Workability %	-5.2	-4.4	-13.1	-7.7	5.8
Average % Difference P50 Workability %	-12.4	-12.0	-16.9	-12.4	-5.8
Average % Difference P90 Workability %	-12.3	-11.8	-13.4	-10.4	-6.8
Average % Difference in Mean Workability %	-11.0	-10.6	-15.2	-11.0	-4.3
Average of all % Differences	-7.2	-8.9	-13.9	-11.3	-3.9

To summarise the performance of each data set, the average percentage difference of the percentiles are compared with reference to 21 years of observations. Generally it was found that the sensitivity of the model varies between the different data sets. The methodology shows reduced sensitivity for the smaller data sets of between one and five years overall, with the largest average percentage difference related to the ten years of data. Pragmatically, it could be assumed that the model would show smaller differences for the larger data sets, but this was not the outcome. It is deduced from these findings that the number of years of data used to inform the model is not the dominating factor and that it is more crucial to ensure that a suitable collection of the variable weather regimes be enclosed within any observed data set. To ensure a suitably broad range of weather regimes will inform the simulation process, it is recommended that the model is always applied using the maximum number of observed years available

for a particular location or that the annual and monthly components have been screened in advance.

7.3.7 Summarised Workability Distributions for other Marine Operations

The characteristics of the weather modelling methodology and embedded pairing techniques have been developed and evaluated for potential application during a personnel transfer operation. It is important that the overall methodology be considered for other operations to ensure reasonable estimates will be produced for varying metocean constraints.

Table 7.3 presents a number of tasks that have been investigated using both pairing techniques. Each task has an associated wind speed, significant wave height and weather window requirement as before. This extension attempts to summarise the performance of the weather modelling method for different operations.

Table 7.3: Marine operations, environmental limits and weather window requirements

Operation	Wind Speed (m/s)	Hs (m)	Weather Window (h)
Dredging	11	1.5	24
Foundation	12	2	24
Wind Turbine Installation	10	2	3
Cable Installation	15	1.5	16
Personnel Transfer	13.6	1.5	30

In Figures 7.4, 7.5 and 7.6 summarising distributions are presented for the UK

North East, France West and English Channel respectively. The figures on the left represent the paired-by-means outcomes with the correlated pairing examples are on the right. The percentage workability assessment was selected to assess the operations listed in Table 7.3 as this outcome presented the greatest sensitivities when compared to the observed data Sections 6.3 and 6.4. The percentage workability is presented in one percent bins in all figures and the P10, P50 and P90 values were also overlaid with black and red dashed lines for the observed and simulated percentiles respectively.

It is shown by the large difference between the P10 reference lines in Figures 7.4, 7.5 and 7.6 that the paired-by-means approach exhibits the largest differences towards the lower percentiles, whilst this approach is consistently close to the P90 workability percentages in comparison to the observed data set. The largest overall differences were observed for the English Channel location in Figure 7.6, as exemplified by the P10 outcomes. The P50 estimates show very similar results across the majority of operations with the largest overall difference for the English Channel Site.

The correlated pairing figures demonstrate a consistently constrained distribution for all tasks and sites in comparison to the paired-by-means technique. This is clearly demonstrated by the P10 and P90 markers in Figures 7.4, 7.5 and 7.6. It is noted that despite a significant reduction in the difference between the observed and simulated P10 value at the English Channel, this percentile tends to be more pessimistic than the observed workability. For the UK North East and France West sites, the P50 estimates were very close to the observed data set for both pairing techniques. However, despite the closer outcomes of this percentile for the correlated pairing approach, the simulated data for the English Channel consistently returns a lower workability at P50 for all operations.

It can be inferred that as this pessimism is demonstrated by the overlaid marker

lines for all tasks in the English Channel, the distributions are not constrained within the observed outcomes, thus indicating that the workability distributions are generally different in comparison to the observed data. This provides further confirmation that the modelling methodology struggles to fully replicate the characteristics of sites where there is a very close correlation between wind speeds and significant wave height. Therefore, caution is advised when using the weather modelling methodology to sites of this nature.

Overall, the distributions shown in Figures 7.4, 7.5 and 7.6 demonstrate that the simulated data provides a much smoother distribution in comparison to the observed data. The workability distributions for the observed data have a clear block-like appearance and occasionally no data at some percentages, whereas the simulated data seems to provide a substantially populated data set. Carol et al. [135] state that "gaps in the record are a serious obstacle to using historical sequences directly" and that "even if the records are continuous, probabilities estimated by naive methods may be seriously in error." Furthermore, De Masi et al. [72] suggest that modelled synthetic time series "should have not only the same statistical properties but also a different yet consistent temporal sequence of weather windows." As it is demonstrated that the simulated data for the UK North East and France West sites follow a similar, but more populated, distribution compared to the observed data, particularly for the correlated pairing approach, the outcomes presented align with these recommendations. Overall it is apparent that the modelling methodology is capable of producing realistic and better defined estimates than would otherwise be generated via means of linear interpolation and may be employed to overcome a lack of historical data. However, consistent statistical differences can be expected for sites that demonstrate very close wind speed and wave height correlations.

Figure 7.4: Workability Percentage Distributions - **UK North East**: Paired-by-means (L); Correlated Pairing (R). Black Lines: Observed Percentiles. Red Lines: Simulated Percentiles (P10, P50 and P90)

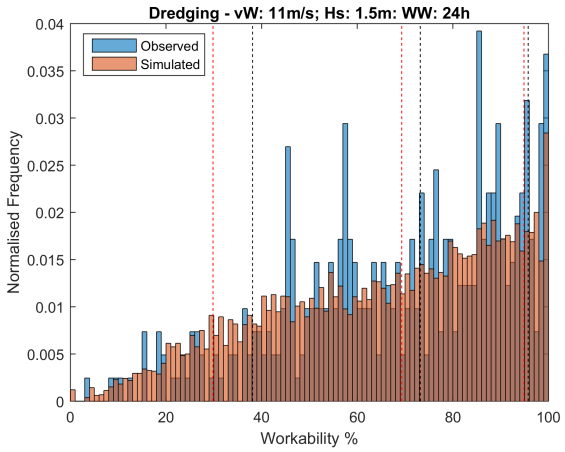

(a) UK North East: Distributions of monthly % workability - Dredging - Mean

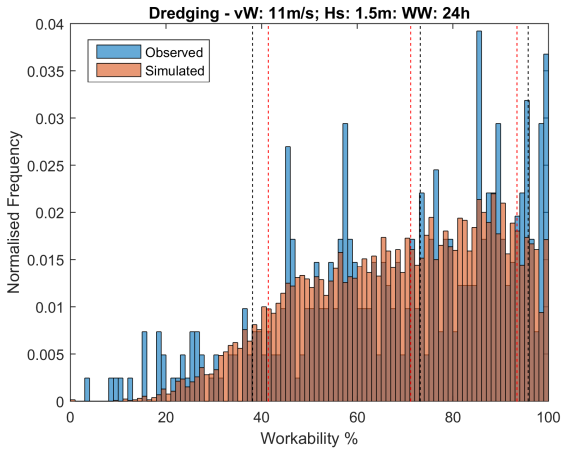

(b) UK North East: Distributions of monthly % workability - Dredging - Correlated

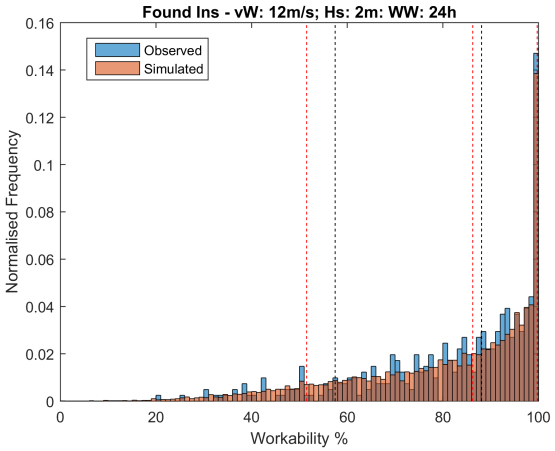

(c) UK North East: Distributions of monthly % workability - Foundation Inst. - Mean

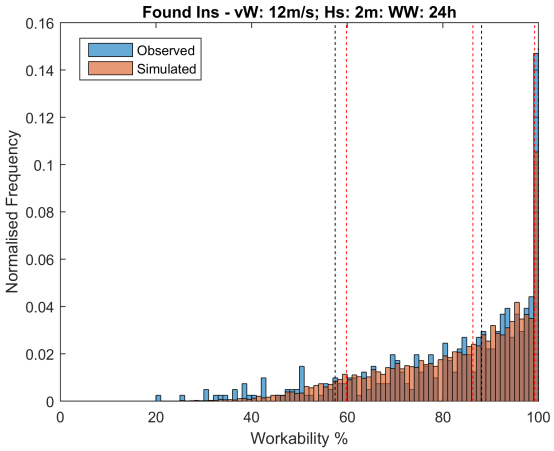

(d) UK North East: Distributions of monthly % workability - Foundation Inst. - Correlated

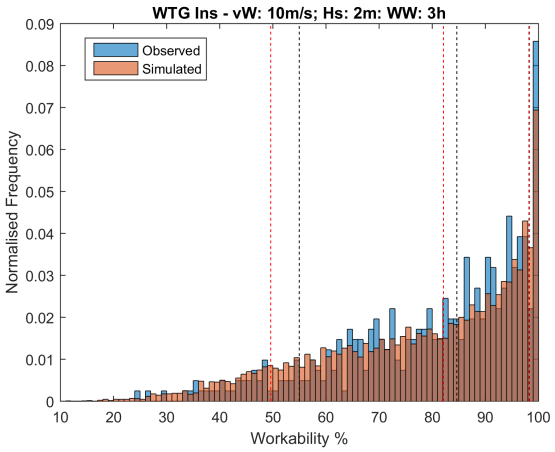

(e) UK North East: Distributions of monthly % workability - WTG Inst. - Mean

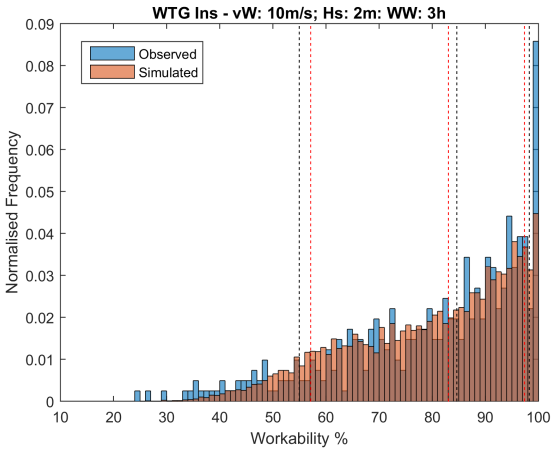

(f) UK North East: Distributions of monthly % workability - WTG Inst. - Mean

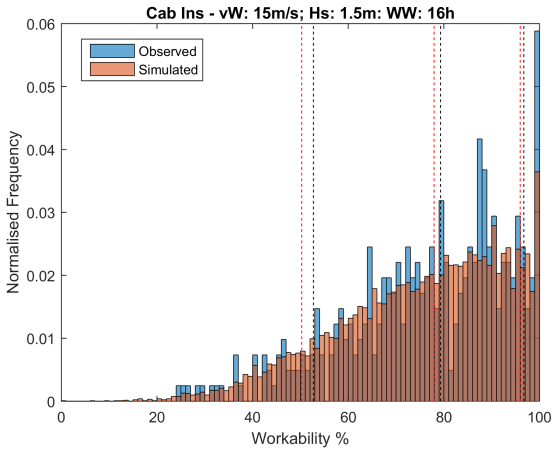

(g) UK North East: Distributions of monthly % workability - Cable Inst. - Mean

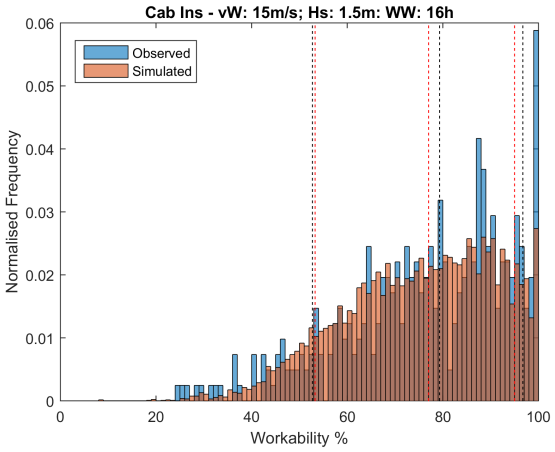

(h) UK North East: Distributions of monthly % workability - Cable Inst. - Correlated

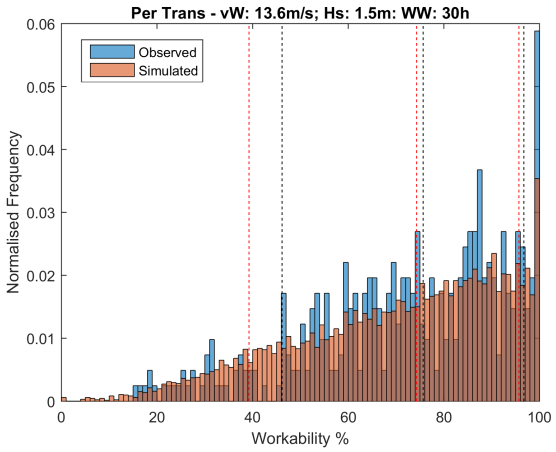

(i) UK North East: Distributions of monthly % workability - Personnel Trans. - Mean

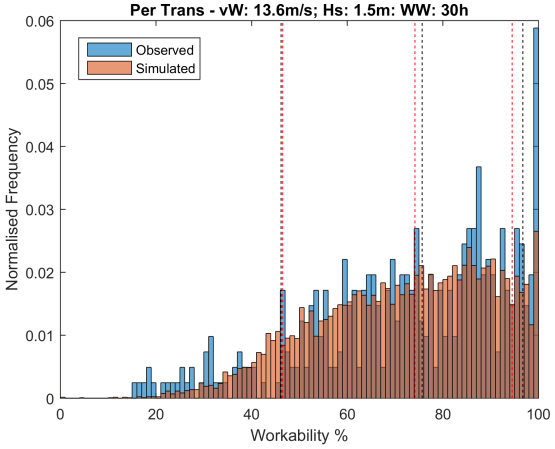

(j) UK North East: Distributions of monthly % workability - Personnel Trans. - Correlated

Figure 7.5: Workability Percentage Distributions - **France West**: Paired-by-means (L); Correlated Pairing (R). Black Lines: Observed Percentiles. Red Lines: Simulated Percentiles (P10, P50 and P90)

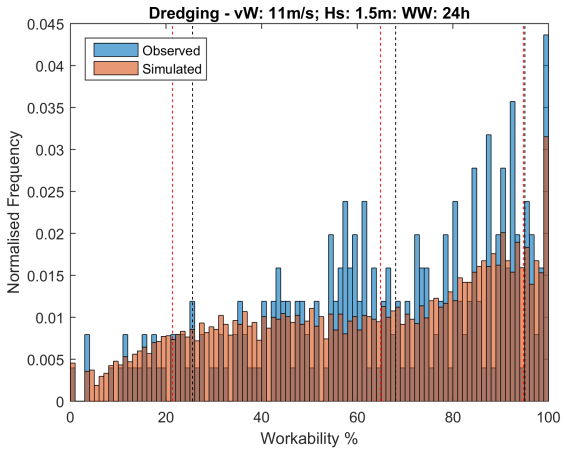

(a) France West: Distributions of monthly % workability - Dredging - Mean

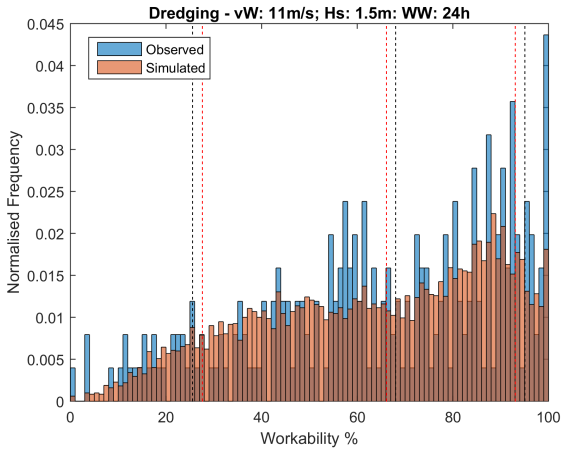

(b) France West: Distributions of monthly % workability - Dredging - Correlated

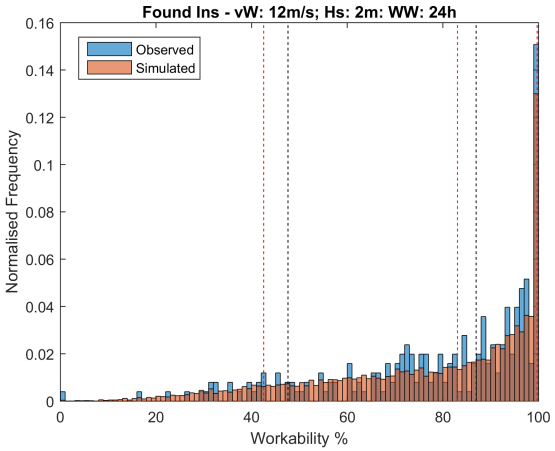

(c) France West: Distributions of monthly % workability - Foundation Inst. - Mean

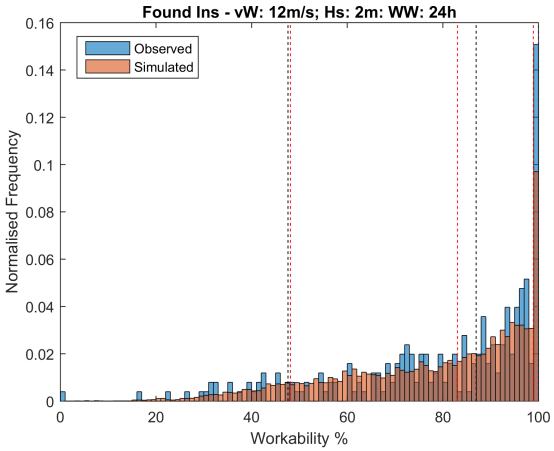

(d) France West: Distributions of monthly % workability - Foundation Inst. - Correlated

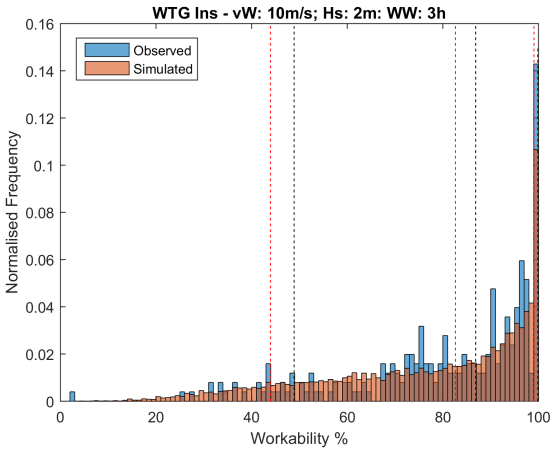

(e) France West: Distributions of monthly % workability - WTG Inst. - Mean

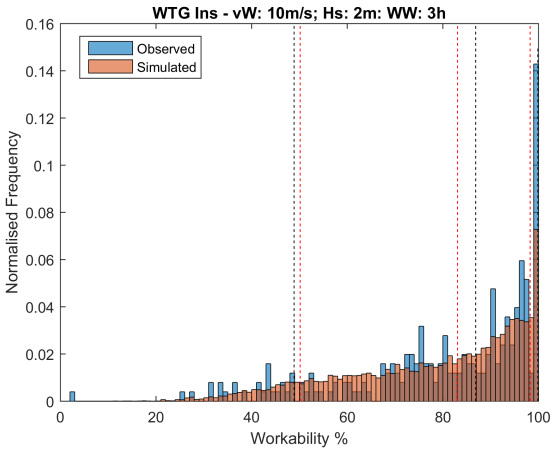

(f) France West: Distributions of monthly % workability - WTG Inst. - Mean

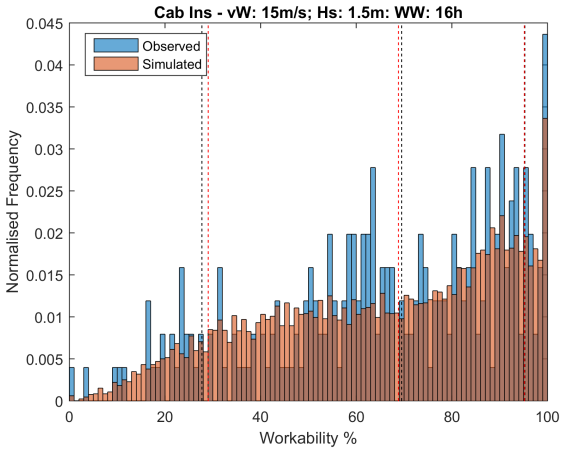

(g) France West: Distributions of monthly % workability - Cable Inst. - Mean

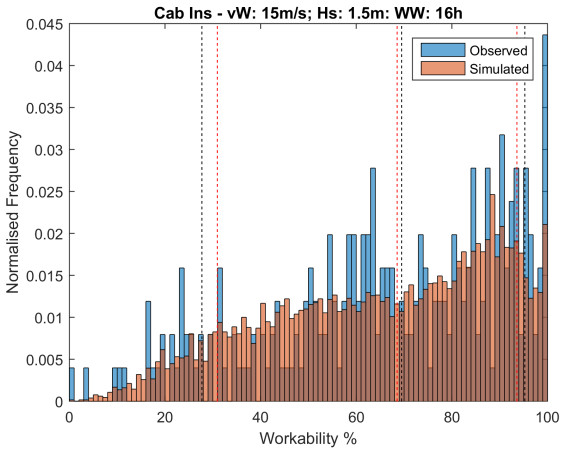

(h) France West: Distributions of monthly % workability - Cable Inst. - Correlated

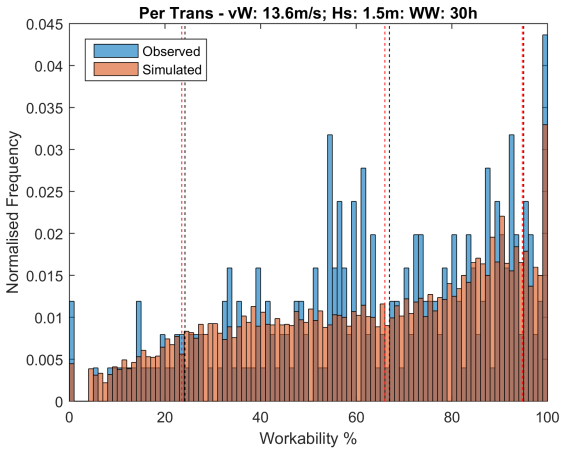

(i) France West: Distributions of monthly % workability - Personnel Trans. - Mean

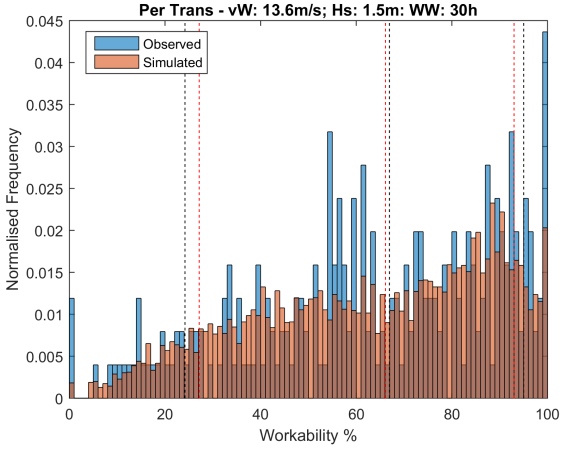

(j) France West: Distributions of monthly % workability - Personnel Trans. - Correlated

Figure 7.6: Workability Percentage Distributions - **English Channel**: Paired-by-means (L); Correlated Pairing (R). Black Lines: Observed Percentiles. Red Lines: Simulated Percentiles (P10, P50 and P90)

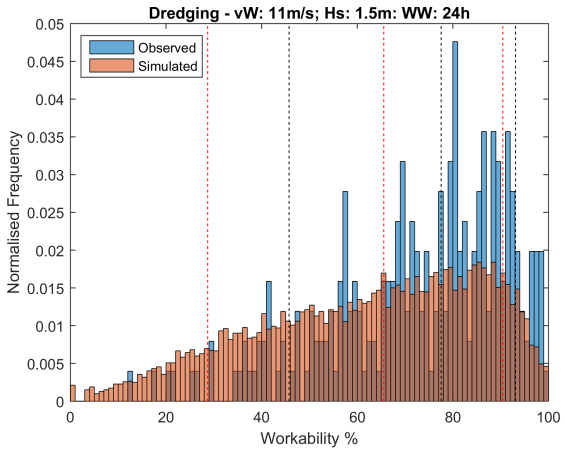

(a) English Ch.: Distributions of monthly % workability - Dredging - Mean

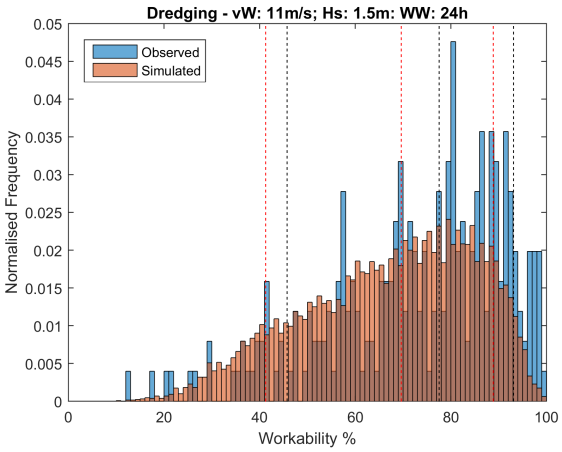

(b) English Ch.: Distributions of monthly % workability - Dredging - Correlated

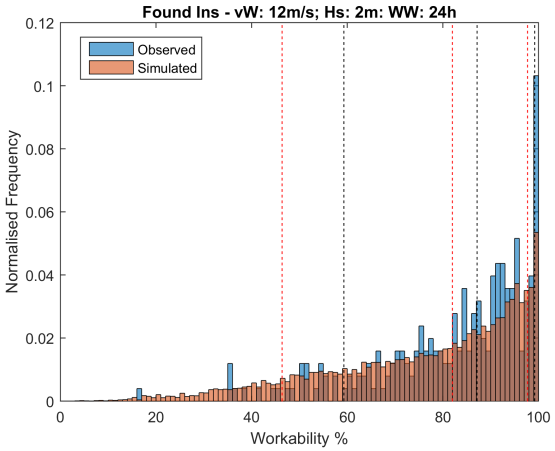

(c) English Ch.: Distributions of monthly % workability - Foundation Inst. - Mean

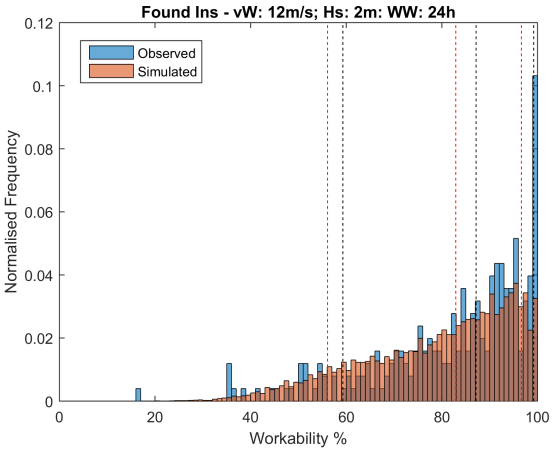

(d) English Ch.: Distributions of monthly % workability - Foundation Inst. - Correlated

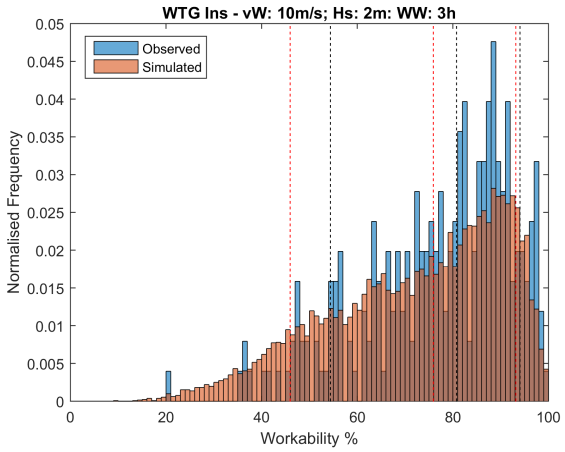

(e) English Ch.: Distributions of monthly % workability - WTG Inst. - Mean

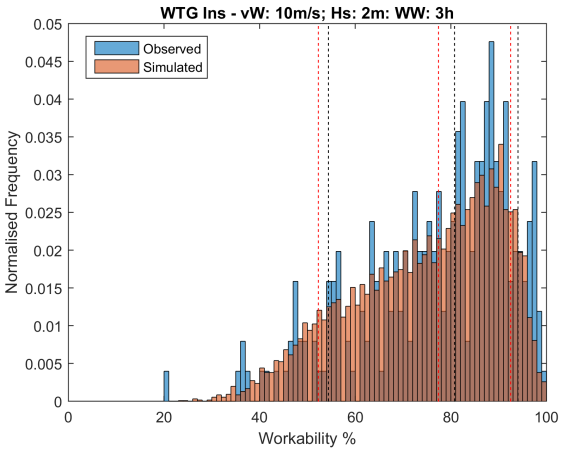

(f) English Ch.: Distributions of monthly % workability - WTG Inst. - Mean

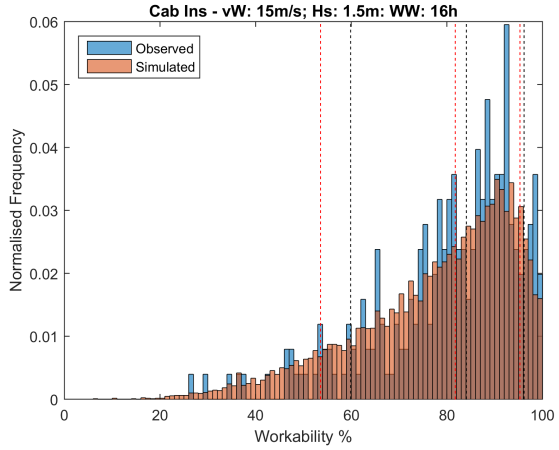

(g) English Ch.: Distributions of monthly % workability - Cable Inst. - Mean

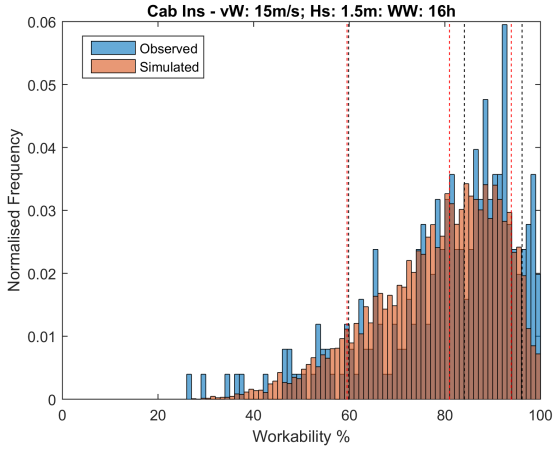

(h) English Ch.: Distributions of monthly % workability - Cable Inst. - Correlated

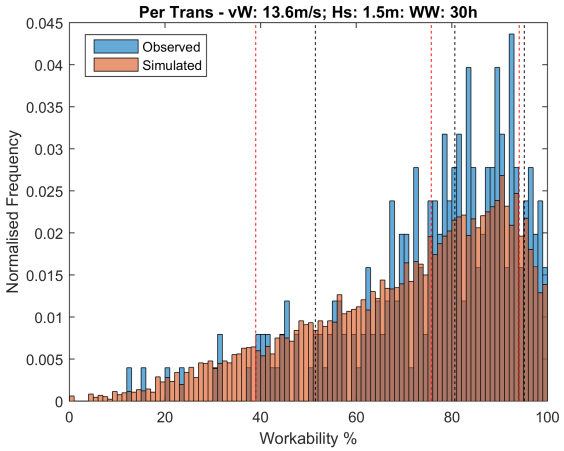

(i) English Ch.: Distributions of monthly % workability - Personnel Trans. - Mean

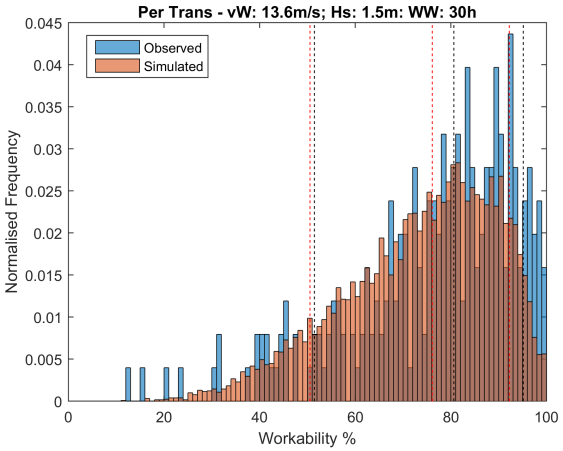

(j) English Ch.: Distributions of monthly % workability - Personnel Trans. - Correlated

7.4 Summary

The results from the three metocean risk assessments completed within Chapters 4, 5 and 6 have presented means to quantify metcocean risk profiles. The generalised methodology to assess and compare vessel metocean risk has exemplified the application of a per wind turbine metric to compare the results between each installation round. Furthermore, quantifying the variation of these results has been proposed to summarise the associated vessel risk, as highlighted in Figure 7.1. In Section 7.1.4, the results from Round 1 were compared to recorded field data for two installation phases from several Round 1 sites, which has validated the results and the methodology overall. Therefore, is it is suggested this approach could be adopted planning personnel to execute a preliminary, high level assessment for metocean risk analyses.

Mermaid modelling software was applied to two commercial metocean risk assessments. Mermaid has demonstrated clear modelling improvements compared to ECUME I, providing enhanced transparency and reporting features. The two modelling approaches have exemplified that one Mermaid model can be built to represent an entire wind farm installation, whilst independent models for each installation phase can be applied to reduce model and reporting complexity. The results from both approaches have been presented in consistent formats such as percentile durations and weathered Gannt charts. It is evident that secondary quantification may be needed to generate downtime predictions when concurrent phases are modelled within Mermaid, whilst independent models will not capture the impact of knock-on delays between interdependent phases. Percentage increase estimates have summarised the associated metocean risk of each phase and can be adopted by project teams to pinpoint operations that could lead to significant delays.

The application of the stochastic MS-AR model within a metocean time series simulation method, has shown that similar workability predictions can be generated in comparison to observed time series, whilst providing improved granularity to quantify residual metocean risks. It was identified that a pairing method should be included in the methodology to regenerate the correlation between wind speed and wave height and the results presented in Table 7.1 highlighted that the correlated paring technique is the preferred method. The addition of weather window and workability percentage distributions in Section 7.3.7 corroborate this, as the separation between P10 and P50 percentiles is reduced for several marine operations at all three sites. These distributions have also exemplified a common characteristic of the correlated pairing technique, as it generates pessimistic P90 estimates in comparison to the paired by means approach. It is noted that this pessimism may be beneficial as it prevents overly optimistic estimates and can be regarded as more risk averse. It is confirmed that the metocean time series methodology appears less consistent for sites with Pearson r correlations greater than 0.8 between U and H_s. No clear sensitivity has been identified for the number of years of metocean data referenced by the MS-AR model and it is recommended that users should ensure the referenced metocean data captures the full range of meteorological characteristics for the site under review.

Chapter 8

Conclusions, Industrial Impact, Limitations and Future Work

The methods presented have been applied and investigated to support decision making, vessel selection and downtime estimates for offshore wind installation. Computational methods to assess the impact of metocean conditions has been demonstrated, highlighting that synthetic and observed weather data can be used to estimate delays associated with marine operations, and thus the underlying risk. The conclusions, limitations, impact and recommendations for future work, drawn from the independent studies first presented in Chapter 3, are presented in the following sections.

8.1 Conclusions

8.1.1 Numerical Modelling and Vessel Assessments with ECUME I

This method applied an offshore wind farm installation simulation tool, ECUME I, to assess the performance of vessel technology employed across the three offshore wind development rounds in the UK. The study presents an analysis on the expected performance of the vessel types employed and describes a structured method to identify and benchmark offshore wind installation risks.

Generally the results indicate that the lowest IRs and WDTs are associated with Round 1, which is justified by the sheltered near-shore location of these sites, meaning the vessels were protected from severe weather conditions expected at Rounds 2 and 3 sites. This is confirmed by the results for Round 2 which exhibit the largest IRs and WDT values and is believed to demonstrate the limitations of the vessels employed for these installations. As incomplete data was obtained for Round 3 it is difficult to draw firm conclusions from this specific outcome but the results suggest that the evolution of vessel technology will bring down IRs and WDTs for sites of this size and location.

The box plots presented in Figures 4.3a-4.3f highlighted that Round 1 vessels experienced moderate levels of WDT. However, the results exhibited a large amount of variability in several phases, meaning less certainty can be drawn from the downtime estimates. For Round 2, the variability is reduced while the WDT increases overall, showing the vessels would perform more consistently although the delays experienced may be prohibitive towards the LCOE of each project. Finally, the Round 3 box plots show a similar level of consistency as seen in

Round 2 and WDTs of a similar order to Round 1. The quantification of IQRs in the results across the three rounds, has provided a view of the installation risk associated with the representative vessel spreads and highlights where precautionary strategies may be best applied to overcome costly delays. These outcomes confirm that the development of more efficient offshore installation vehicles is key to addressing delays during significant installation phases.

8.1.2 Commercial Metocean Risk Analyses

Two different modelling approaches have been presented using the Mermaid simulation package to assess the anticipated weather downtime for the Blyth Offshore Demonstrator (BOD) and Fecamp wind farms. This simulation package was employed because of the modelling flexibilities and reporting features offered by Mermaid in comparison to EDF's internal tool, ECUME I.

Weathered Gantt charts produced by Mermaid were extracted and delivered with overlaid completion dates and served as primary references for the completion of each installation scenario. It was found that the impact of learning on GBF and WTG installation had a negligible impact on the overall completion date, whilst a delay of one month led to a two month delay overall. A single WTG scenario was also presented and the weathered Gantt chart was vital to the assessment of a latest possible start date to ensure first power was realised before an incentive deadline.

The percentile estimates for each scenario were presented in Tables 5.1-5.4 and the percentage increase included in Appendix G.3, highlighted that the towing the GBFs out of the dry dock presented the greatest risk in all cases. Furthermore, a significant amount of risk was associated with the other installation tasks for

the GBFs, whilst the completion and commissioning tasks demonstrated some sensitivity with respect to the season in which they were executed the simulations. It is noted the individual predictions should not be accumulated to produce a corresponding schedules, as this would provide an inaccurate picture of how the phases would transpire in reality.

For the Fecamp assessment, individual models were built for each operational phase, which meant that knock-on delays from phase to phase were not considered in the results. As the the individual models did not resemble any concurrent operations, the statistics generated in Mermaid could be used directly to populate results in Tables 5.5 and 5.6. The percentage increase values included in Appendix G.3 demonstrated that the largest metocean risk was associated with the GBF Scour and Ballast tasks from P50 to P70, whilst the GBS Bedding and cable installation tasks were found to increase considerably at the P90 percentile.

As the Mermaid model could not fully assess the impact of knock-on delays, mock weathered Gantt charts were produced to identify any unintended phase interactions that may lead to planning and resourcing issues. This revealed that the scheduling of the Scour and Ballast phase should be reviewed, which was initially presented in the unweathered case. Similar issues were also identified in the weathered Gantt charts produced for each percentile, demonstrating that delays on the GBF installation phase would lead to delays in the Scour and ballast phase in reality. It was stated in Section 8.2.2 that it was unlikely the corresponding percentile estimates would be experienced across all individual phases for the entire installation campaign in reality and these Gantt charts can only be used to identify potential conflicts in the operations. It is proposed that a targeted set of phases could be built into one Mermaid model to appreciate the extent of knock-on delays between the most critical interactions identified.

Both assessments appear to be valid for the analysis of weather downtimes;

however, each approach has notable limitations. The BOD assessment was the most complete analysis, where an appreciation of the entire installation duration and individual project phases were presented. The Fecamp analysis was quicker to implement and review as separate models provided greater transparency for each individual installation phase, although an appreciation of knock-on delays was limited. The Mermaid simulation package provided improved modelling flexibility and it is intended that the experiences and methods presented will provide support for future weather risk assessments completed within EDF Group.

8.1.3 Stochastic Metocean Modelling Methodology

This study presented a metocean modelling methodology using a MS-AR model with Gaussian innovations to produce stochastic wind speed and wave height time series for inclusion in EDF's next generation marine risk planning and simulation tool.

The embedded MS-AR model, constructed by Monbet and Ailliot [81], was originally intended to produce wind speed outputs, although it was demonstrated that realistic wave height simulations can be produced with this approach. A pragmatic method was initially implemented to rank and pair the individual monthly wind speed and wave height simulations by taking the mean value of each realisation and this was introduced to prevent realisations with higher and lower energies from being paired together, to produce realistic final time series.

It was shown that the paired-by-means approach was capable of producing similar operability characteristics when compared to observed data. Summarising statistics produced to compare the simulated and observed data against the weather limits of a personnel transfer operation, show that the data for two out

of three sites provide similar predictions for the progression of this operation, indicating the suitably of the proposed modelling approach for metocean risk planning activities. An average percentage workability assessment completed across the three sites again demonstrates that the simulated data has consistently realistic characteristics for two locations. This method was also applied to the Blyth Offshore Demonstrator data set and used directly to simulate two of the primary installation phases in a prototype simulation package, developed by colleagues in EDF R&D France. This showed that the synthetic time series produced similar outcomes when compared to a commercial weather risk assessment tool that referenced the observed data set, although a more thorough examination of a larger installation campaign may be required to verify and eventually validate the performance of both the prototype and simulated weather data.

A second pairing approach that used Pearson r correlation coefficients was investigated to improve the flexibility of the modelling methodology at all sites. The summarising statistics confirmed that this approach improved the consistency of the modelled data for sites with larger observed Pearson r correlations and that the mean workability percentages consistently fell within the error bars of the observed data. A comparison of percentage difference of key statistics indicated that the correlated pairing may not improve the similarity of the data for all sites and that the paired-by-means approach had the most similar percentages for the UK North East Site overall. A further review of percentage workability distributions was completed for a range of different marine operations and it was confirmed that a closening of the distributions for the majority of tasks was introduced by the correlated pairing approach, for all sites. It was observed that the correlated paring method seemed to cause an increase in the differences for summer months and it was proposed that the weather modelling methodology

could be built using both pairing methods, generating more realistic estimates when compared to the observed data.

The higher resolution and more constrained distributions for the simulated outcomes demonstrate that the modelling process can provide a means to assess delays at intermediate percentile values, as the modelling methodology provides sufficient data to infer these predictions and thus better quantification of residual operational risks. The methodology demonstrates sensitivity, particularly for key percentiles at sites with wind sea characteristics, yet the overall largest difference was no greater than seven percent in comparison to the observed data set. It is concluded that the methodology presented will produce suitable wind speed and wave time series for the assessment of marine operations, although it should be used with caution for sites with strong correlations between wind speed and wave height.

8.2 Limitations

8.2.1 Comparative Vessel Assessment

This study aimed to model the scenarios, vessel spreads and offshore wind farm characteristics using ECUME I offshore wind installation software. As the analysis progressed, it became clear that a few amendments to the modelling approach may have produced a more comprehensive set of results and offered more insight into the progression of the marine operations across the various scenarios and rounds.

Firstly, it should be noted that all of the results presented are based on P90 predictions from the software. This implies that the predictions are somewhat

pessimistic in their outlook, offering 90% certainty that the values will not be exceeded. It may be the case that these results do not resemble what will occur in reality, although this metric does provide a good level of confidence that observed durations will be within bounds of recorded predictions. It can be argued that the metric of 'average number of days spent per WTG' (days/WTG) may not be the most suitable way of depicting the IR of cable sections or burial operations, however it was identified as the most applicable approach for use within the software tool. The cable lay and burial durations were obtained using reference to in-house planning documentation, and an average installation rate was obtained by dividing the total duration by the number of turbines for the particular project.

In each of the simulated cases, the same environmental limits are assumed for the installation tasks in both rounds. However, with improved vessel capabilities, it is possible that the limits for the installation tasks could be extended. More modern capable vessels may improve attributes such as stability and lifting capacity beyond the transit and station keeping limits considered in this study. Therefore, different environmental limits could be allocated to each round and method statements produced by installation contractors could be used to obtain variable inputs for these parameters, subject to the vessel and equipment employed for installation. Furthermore, the impact of water depth is not considered in this study. The task durations could have been altered to account for this, by again consulting method statements or by applying an assumed α-factor. In many cases, an α-factor may be imposed by a marine warranty surveyor (MWS) to account for uncertainty in the forecast and/or applied as a contingency in the execution of the marine operations [17]. The uncertainty relating to water depth could be quantified for various installation tasks and applied to obtain contingency durations. It is assumed that the operational limits in this study (Table 3.5), do not include an applied α-factor and the task durations are believed to be a fair representation of the values used in reality.

The main environmental limits considered for the vessels and operations in this analysis were predominantly focused on wave height and wind speed. Vessel transit speeds were also included to reflect the expected travel durations. The software is also able to account for the minimum wave period (s) and current speeds (m/s) but owing to the lack of available data for operations and vessels, those parameters were not used. It would be more informative and would allow greater accuracy if these parameters were considered; this would rely on input from vessel owners and experience professionals in the field.

Additionally, it is assumed throughout that all vessels are capable of remaining offshore for the entire installation campaign (i.e. for the entire set of WTGs to be installed), with the exception of those for the Foundation, Transition Piece and WTG phases, set at a maximum of three phases per voyage. This was selected as the number of inward and outward transits required for the remaining vessels and is significantly variable in reality. It is fair to suggest that if the remaining vessels were allocated with a maximum number of phases per voyage, a change in WDT would be observed for these installation phases. Within the software, vessels have specific waiting conditions, which when exceeded require the vessels to return to shore. It should noted that a weather window is not sought for a vessel's outward or inter-turbine voyages in the software. In some instances, a vessel may partially cover the distance of a voyage and may return port when the weather exceeds transit limits. This is a limitation of the software and a go/no-go decision mechanism similar to those used in reality, which are usually based 12 hour ahead forecasts, could be built into the software to prevent the likelihood of unsuccessful voyages and improve the authenticity of the results.

For the modelling of WTG installation in the software, it was assumed that the associated duration was based on the 'bunny-ear' installation configuration. It would be of interest to extend this study, considering impact variable WTG

installation strategies as presented in [114] and [119]. It is noted that the sequence of the installation phases considered is not standard to all offshore wind installation projects. The analysis completed is not wholly dependent on this sequence and if altered, the results for each phase could change, as these would begin different periods in the simulated weather scenarios. However, as various knock-on delays are incurred as a result of the consecutive scheduling approach, the phases are applied at various months and seasons throughout the simulation.

As with many meteorological data sets, a number of missing entries were discovered and as the tool is reliant on evenly spaced intervals when forecasting the weather, linear interpolation was applied to compensate for these missing entries. This inevitably introduces a degree of approximation within the weather forecasting that may have altered the results slightly and a complete set of entries would provide further confidence in the results.

It is unlikely in practice that a typical wind farm in Round 3, predicted to consist of 251 turbines on average, will be installed within one year if only one of each major installation vessel is employed for each phase, as was the case in this study. An alternative approach is to consider the use of multiple primary installation vessels for each phase, which could be replicated by halving the size of these projects or by mimicking concurrent installation phases within the software. Nonetheless, the outcomes obtained for Round 3 did provide a meaningful comparison.

The software implements suspension of the marine operations between specified sequences if the vessel is able to hold station offshore. However, in the interests of modelling time, only one sequence was specified within each installation phase, encompassing the entire duration of all the sub-tasks. If the phases had been modelled with multiple embedded sequences, this might have provided a higher resolution in the results and adjusted the WDT predictions. As each of the phases

across all the models only consisted of one sequence, it is fair to presume that the simulations were completed on a level basis and can be used for comparison in terms of overall vessel performance. It is not recommended that the predicted IRs or WDT values be used as a direct reference and should only serve as guide or sense check for similar analyses. The results used to formulate the IRs and WDT values are initially taken from the calendar outputs produced by the software. These outputs are presented in the form of dates and each completion date for the phases, is a result of the duration rounded to the nearest day. Although the results may tend to over or under predict the phase durations, but are believed to provide a good level of approximation for comparison.

8.2.2 Commercial Metocean Risk

A different method was used to generate the durations and weather downtimes in each of the Mermaid studies. In the BOD analyses, the percentile values were produced using a separate Matlab analysis using the external task logs produced by Mermaid. This method was employed as all operational phases were embedded within one Mermaid model. This meant that the automatic percentile categorisation produced in Mermaid was applied, based on the complete installation duration and may not fully describe the delays experienced for individual phases.

The project team at the BOD opted to assess the size of the risk for each installation phase and the percentile values were calculated to this specification following the steps in Section 3.2.3.1. Whilst this approach was useful in presenting the potential delays for each phase, it is important to note that the percentile predictions for each phases should not be gathered to produce a corresponding Pxx schedule, as this would not present an realistic progression

of the entire installation campaign. In reality, differing levels of delay would be experienced in each installation phase, resulting in a blend of percentiles to arrive at the final completion date. However, the weathered Gantt charts extracted from Mermaid were a convenient method to show the way the operations could progress in reality and provided an alternative perspective for the BOD project team.

It was intended that validation of the installation predictions would be completed by reviewing the actual durations recorded across the installation campaign. In reality, the installation campaign began approximately three months later than the start dates applied in all models. It would therefore be inaccurate to complete a comparison of the predicted and actual downtime as a significant change in the weather conditions would have been experienced in reality compared to the modelled scenarios.

The Fecamp weather risk analysis was more simplistic than the BOD example. Separate Mermaid models were constructed for each installation phase, allowed the percentile values automatically generated in Mermaid to be used directly, as no external review was required to reveal the full extent of the risk in each phase. The results for the P0, P50 and P90 outcomes were taken directly from the summary table produced in Mermaid, whilst the P60 and P70 durations were referenced from the weathered Gantt chart. The P50 and P90 estimates presented in the summary tables are produced by reviewing the outcome of all simulation runs and the weathered Gantt chart durations are based on one particular run that is closest to the selected summarising percentile. This means that two different statistical methods were combined in the results, This may not be appropriate, but a disclaimer that explained this difference was provided on delivery of the results to EDF EN.

It is advised that the percentile results are not assembled to produce a corresponding schedule. However, this technique was employed to produce mock weathered Gantt charts, which were constructed to identify potential scheduling issues. The unweathered Gantt chart proved to be particularly useful as this highlighted some issues between the GBF, Scour and Ballast phases and WTG Installation phases.

It is suggested that an alternative and iterative modelling technique could have been employed to obtain a perspective of knock-on delays, where the completion dates or progress for each percentile could be used to inform the start date in subsequent models. This would mean that four separate models would need to be run in subsequent phases, each starting at different dates corresponding to the percentiles in the preceding phase and would increase the time required for the simulations to be completed. It is also expected that the continuation of a percentile value from model to model would present an inaccurate picture of how the operations would progress in reality, as it would be assumed the same percentile would prevail over time.

This has demonstrated a clear limitation for the Fecamp weather risk analysis as realistic completion dates for the entire installation were not obtained. Thus there is a clear trade off between modelling complexity and the level of detail sought from Mermaid assessments. If modelling and review of project phases individual phases is sufficient, it is much simpler to produce separate Mermaid models. If an accurate account of the interdependencies and knock-on delay is required by project planners, all installation phases should be modelled within one Mermaid model where possible, although this will require a secondary analysis if percentile categorisation for embedded, concurrent installation phases is specified.

8.2.3 Stochastic Metocean Modelling Method and Analyses

The weather modelling method and the approaches used to review the performance have a few limitations that merit further consideration. Firstly, the final time series that is produced from the overall methodology is built from monthly simulations, which are interpolated from three to one hour intervals after being paired by either approach. In some cases, a noticeable transition or spike in the wind speeds and wave heights at monthly interfaces was observed, which may impact on the predictions produced for continuous operations. Furthermore, the weather window, workability and general characteristics of the simulated weather data were predominantly completed from a monthly perspective, which may not fully demonstrate how the generated time series would perform when applied against a continuous sequence of operations.

The time series produced for the Blyth project using the paired-by-means approach was applied in this manner in Section 6.5 and showed very similar outcomes to the observed data and Mermaid percentile results. However, as the Blyth project was fairly small with only five turbines, the impact of anomalies within the time series may not always be apparent. It is suggested that an alternative approach to the interpolation from three hour to hourly intervals could be employed to introduce smoother transitions or better consistency with the final time series. One strategy would be to use interpolation as a last step in the methodology, after the assembly of the final time series, as this could introduce smoother transitions, although it is possible that the correlation between the wind and the waves could be affected. Alternatively, interpolation could be completed before the pairing step, scaling up the monthly realisations to hourly intervals and then the pairing could be implemented. However, this modification would not

address the issue of the monthly interfaces and the correlated pairing technique would take much longer to assess the extended data sets.

The pairing approaches for the wind speed and wave height were implemented to account for the relationship between the wind and the waves. As this relationship changes from site to site each pairing method may demonstrate inadequacies. It is evident that the correlated pairing approach leads to similar characteristics for sites with a strong relationship between the wind speed and wave height, yet an increase in the differences for the summer months was observed when compared to the results from the paired-by-means approach. It is suggested that the correlated pairing method may not be the best predictor for the summer months, where the bivariate correlation is less important as calmer weather is experienced in these months, meaning weather interruptions are less pronounced. It appears that the paired-by-means method is able to generate more similar predictions for these months and it is suggested that a methodology could be built with a blend of both pairing methods to obtain improved similarity overall.

It was also observed that the correlated pairing method, does not allow for the retention of all wave height realisations and only those that had the greatest correlations relative to the wind speed simulations, were taken forward in the methodology. To overcome this, consideration could be given to simulating a larger number of monthly wave height realisations, thereby increasing the available 'pool' of wave heights available for selection, which may improve the correlation between parameters in the final time series. Furthermore, the correlated pairing has a bias to the wind speed, where the wave heights are screened for their similarity and it is not known how the model will perform if the opposite is applied. If the weather model were to be implemented in a simulation tool it is advised that an assessment of the Pearson R correlation coefficient between the wind speed and wave height data be automatically completed before running the

stimulations. Applying the most effective or relevant pairing method to all or individual months as necessary, could enhance the adaptability of the model.

Overall, the simulated data appears more pessimistic when compared to the observed time series. To some extent this may originate from the lack of correlation within the simulated data, as the correlated pairing method still generates conservative estimates, particularly at the P90 percentiles. Independent weather window analyses were completed for only one weather parameter (wind speed or wave height) and revealed some differences when compared to the observed data for weather window and workability predictions. For example K-S distances of 0.05 were identified for weather window and workability CDFs that considered only the wind speed and duration for the personnel transfer task. This suggests that the difference in the predictions is not solely related to an inadequately constructed time series, but reflects the nature of the MS-AR model. It is intended that a large number of meteorological simulations are to be generated to facilitate Monte Carlo analyses, which can be used to resolve residual risk. The majority of the iterations of the weather model have relied on comparisons made against the characteristics of the observed data and whilst this is a good benchmark or sense check, an identical output cannot be expected when generating approximately 50 times more years of data. The lower weather windows and workability estimated at the extreme percentiles may actually be beneficial, as they demonstrate a perspective on the 'worst case' that would not be described by the observed data set.

8.3 Industrial Impact

It is intended that the methods presented and analysed in this work will make a positive contribution to metocean risk assessments for offshore wind installations.

These approaches have supported both academic and commercial practices within EDF Energy, the sponsoring company of this project.

The weather downtime and subsequent vessel performance assessment completed using EDF's ECUME I software were compiled, submitted and published in the Ocean Engineering journal as part of an IDCORE special issue. The study presented a structured method to identify and benchmark offshore wind installation risks relating to vessel capabilities. This study and the published article, also compared predictions against recorded installation rates and provided a degree of validation of the tool, despite limited flexibilities in the embedded logistical engine.

The BOD commercial weather risk assessment was used directly by the project team to appreciate the potential downtimes that may be experienced throughout the installation phases. The downtime predictions were used to consider the financial or operational contingencies that may be required to ensure the project was delivered on time and in budget. The response from the team at the BOD project has been extremely positive and has led to further R&D assessments for marine activities throughout EDF Group.

The Fecamp weather risk analysis was completed to support the EDF EN planning team in France. As the models were built on a preliminary set of installation tasks, (yet to be fully defined for the project), this assessment was used mainly to review the application of the Mermaid simulation tool and the overall modelling methodology employed. It was demonstrated that a segmented approach may be useful in assessing the weather risk for individual project phases while it may be useful to consider combined models for concurrent operational phases.

The weather modelling methodology has been built as a result of close collaboration with colleagues in EDF R&D in France, who were responsible for building a

next generation marine operations simulation tool. The development of the overall methodology was regularly presented to this team and the embedded functionality scrutinised throughout the progression of the project. The impact of two different pairing methods for a bivariate wind speed and wave height simulation has been demonstrated to improve the flexibility of the method for sites with close correlations between both parameters. The weather modelling methodology has been delivered to this team in the form of a fully functional Matlab script and standalone executable file. It is intended that this model will be embedded in a prototype simulation package, which will aid the assessment of marine operations in a variety of industrial sectors within the EDF Group.

8.4 Future Work

8.4.1 Numerical Modelling and Vessel Assessments with ECUME I

The methodology and analysis completed to summarise vessel capabilities using the ECUME I software has a number of possible extensions.

In this study a number of assumptions and modelling constraints were applied. Building on the points raised in Section 8.2.1, the logistical durations and constraints for the operational tasks could be reconsidered to account for improved operability offered by the most modern installation vessels. Therefore a predefined set of durations and limits could be built for each round, which could provide an improved assessment of vessel performance. Furthermore a full description of the results at difference percentiles could be completed and provide greater insight on vessel performance and varying levels of confidence.

It is accepted that the adoption of upper (April) and lower (January) start dates may not offer the same benefits as seen in smaller projects as it is infeasible to complete the installation of a Round 3 site with only one main vessel for each installation phase. It is therefore suggested that future work could consider the optimum vessel size or adoption of multiples of similar installation vessels in the development of Round 3 sites that consist of ≥ 250 turbines. Additionally, it is foreseen expansion in the fragmentation of installation sequences to assess the impact of suspendability during the operations.

Modelling and investigation of the impact of learning rates observed by Kaiser and Snyder [114] could also be introduced. This can be modelled in the ECUME I software tool and presents an interesting expansion of this study. Lastly, a review on the associated costs for the WDT predictions against charter rates for the vessels would provide a helpful means of assessing potential trade-offs when employing particular vessels and sub-contractors.

8.4.2 Commercial Metocean Risk Analyses

The commercial weather risk assessments delivered for the BOD and Fecamp projects have yet to be validated. As the installation of the BOD project has now been completed, it is suggested that the predicted and actual delays be compared to confirm the validity of the modelling approach. It is noted that the actual installation operations began approximately two months later than the original Mermaid model for Scenario 1. This implies that the Mermaid models should be simulated again with updated start dates to provide a fair basis for comparison.

Future analysis of the Fecamp installation should focus on the development of combined Mermaid models for phases that were predicted to complete before

preceding tasks. This would give further insight on the impact of knock-on delays and would improve the planning of these key interactions.

8.4.3 Stochastic Metocean Modelling Methodology

A number of limitations of the stochastic weather modelling methodology were presented in Section 7.3 and a few generalised alterations to the modelling process are envisaged for future development.

The interpolation of the simulated monthly sets and the assembly of monthly realisations have the ability to introduce inconsistencies in wind speed and wave heights at monthly and annual interface in a fully constructed time series. This can introduce abrupt shifts or incoherent patterns in the meteorological predictions at these interfaces and in turn may impact the weather window characteristics and overall workability. To minimise the presence of these interfaces, it is proposed that before any interpolation is completed, the monthly simulations be firstly paired and then assembled into a continuous three hourly time series. It is expected that if interpolation is then applied to the entire three hour time series, this would lead to smoother transitions throughout and improve the overall comparison with observed data.

The approach of pairing the monthly wind speed and significant wave height realisations after the MS-AR simulations was introduced to improve the consistency of the final time series. It was found that this approach may fail to replicate similar characteristics for sites with strong correlations between the wind and the waves. It is proposed that the wind speed and wave heights simulations could be completed simultaneously within the overall methodology, ensuring that the year of data randomly selected for the MS-AR simulation is kept consistent for both

parameters, which may maintain any apparent correlations. The authors of the METIS toolbox, Monbet and Ailliot, offer a bi-variate MS-AR model that relies on wind direction to resolve the wave height realisations; further testing on this model type may improve the consistency of the time series. It is reiterated that this model was not suitable for many of the in-house data sets made available as they did not contain wind direction data.

It is suggested that the assessment presented in Section 6.5 could be extended to assess a full set of installation phases with a larger number of tasks, each with varying wind speed and wave height limitations. The original analysis only considered two phases across five turbine locations and therefore differences and inconsistencies in the simulated data may be less pronounced. Additionally, it is proposed that a time series generated by the correlated pairing technique is applied, which would provide further insight into the suitability of this modelling technique.

Lastly, the importance of other meteorological parameters must be acknowledged. From metocean modelling experience, discussions with operatives and offshore contractors, weather parameters such as peak wave period, tidal elevation and current can have a significant impact on vessels and marine operations, either as singular or multi-dimensional constraints. It is clear that the weather modelling methodology could be extended to simulate these other metocean conditions, which may investigate further adaptability of the MS-AR approach or include other computational techniques to obtain reliable operational predictions.

References

[1] Offshorewind.biz, "Offshore Wind to Remain UK's Cash Cow in 2016," 2016.

[2] Renewable UK, "UK leads Europe with £8.5bn boost from offshore wind - RenewableUK," 2016.

[3] G. Brindley, D. Fraile, and F. Selot, "Offshore Wind in Europe - Key trends and statistics 2018," 2018.

[4] S. Krohn, P.-E. Morthorst, S. Awerbuch, and The European Wind Energy Association, "The economics of wind energy," 2005.

[5] P. Higgins and A. Foley, "The evolution of offshore wind power in the united kingdom," *Renewable and Sustainable Energy Reviews*, vol. 37, pp. 599–612, 2014.

[6] Offshore-technology.com, "Healthy competition: demand grows for specialised offshore vessels - Offshore Technology," 2012.

[7] Offshore Renewables Special Interest Group, "Metocean Procedures Guide for Offshore Renewables," Tech. Rep. September, IMarEST, 2015.

[8] Health and Safety Executive, "HSE Information sheet Guidance on Risk Assessment for Offshore Installations," 2006.

[9] (DNV) Det Norske Veritas for HSE, "Marine Risk Assessment," 2002.

[10] The British Standards Institution, "BS EN ISO 17776:2016 - Petroleum and natural gas industries - Offshore production installations - Major Accident hazard management during the design of new installations," 2016.

[11] The British Standards Institution, "BS EN 61025:2007 - Fault tree analysis (FTA)," 2007.

[12] The British Standards Institution, "BS EN 61165:2006 - Application of Markov techniques," 2008.

[13] The British Standards Institution, "Petroleum and natural gas industries - Specific requirements for offshore structures. Part 6: Marine operations (ISO 19901-6:2009)," 2011.

[14] The British Standards Institution, "BS EN ISO 19901-1:2015 BSI. Petroleum and natural gas industries - Specific requirements for offshore structures. Part 1: Metocean design and operating considerations," 2015.

[15] Det Norske Veritas (DNV), "DNV-RP-H103: Modelling and Analysis of Marine Operations." 2011.

[16] The British Standards Institution, "Draft International Standard - ISO 29400 Ships and marine technology - Offshore wind energy - Port and marine operations," 2018.

[17] Det Norske Veritas (DNV), "DNV-OS-H101 Marine Operations , General," no. October, 2011.

[18] American Petroleum Institute, "Derivation of Metocean Design and Operating Conditions - ANSI/API Recommended Practice 2MET," 2014.

[19] E. Barlow, D. Tezcaner Öztürk, M. Revie, E. Boulougouris, A. H. Day, and K. Akartunali, "Exploring the impact of innovative developments to the installation process for an offshore wind farm," *Ocean Engineering*, vol. 109, pp. 623–634, 2015.

[20] J. Paterson, F. D'Amico, P. R. Thies, R. E. Kurt, and G. Harrison, "Offshore wind installation vessels - A comparative assessment for UK offshore rounds 1 and 2," *Ocean Engineering*, vol. 148, pp. 637–649, 2018.

[21] B. R. Sarker and T. I. Faiz, "Minimizing transportation and installation costs for turbines in offshore wind farms," *Renewable Energy*, vol. 101, pp. 667–679, 2017.

[22] B. Hagen, I. Simonsen, M. Hofmann, and M. Muskulus, "A multivariate Markov weather model for OandM simulation of Offshore wind parks," *Energy Procedia*, vol. 35, no. 1876, pp. 137–147, 2013.

[23] V. Monbet, P. Ailliot, and M. Prevosto, "Survey of stochastic models for wind and sea state time series," *Probabilistic Engineering Mechanics*, vol. 22, no. 2, pp. 113–126, 2007.

[24] A. Hering, K. Kazor, and W. Kleiber, "A Markov-Switching Vector Autoregressive Stochastic Wind Generator for Multiple Spatial and Temporal Scales," *Resources*, vol. 4, no. 1, pp. 70–92, 2015.

[25] L. Castro-Santos, A. Filgueira-Vizoso, I. Lamas-Galdo, and L. Carral-Couce, "Methodology to calculate the installation costs of offshore wind farms located in deep waters," *Journal of Cleaner Production*, vol. 170, pp. 1124–1135, 2018.

[26] K. E. Thomsen, *Offshore Wind - A Comprehensive Guide to Successful Offshore Wind Farm Installation*. 2012.

[27] R. Lacal-Arántegui, J. M. Yusta, and J. A. Domínguez-Navarro, "Offshore wind installation: Analysing the evidence behind improvements in installation time," *Renewable and Sustainable Energy Reviews*, vol. 92, no. July 2017, pp. 133–145, 2018.

[28] I. Tyapin, G. Hovland, and J. Jorde, "Comparison of Markov Theory and Monte Carlo Simulations for Analysis of Marine Operations Related to Installation of an Offshore Wind Turbine," *Proceedings of the 24th International Congress on Condition Monitoring (COMADEM), 30th May - 1st June*, pp. 1071–1081, 2011.

[29] T. Worzyk, *Submarine Power Cables: Design, Installation, Repair, Environmental Aspects*. 2009.

[30] L. P. Kerkhove and M. Vanhoucke, "Optimised scheduling for weather sensitive offshore construction projects," *Omega (United Kingdom)*, pp. 1–21, 2015.

[31] VdS, "International guideline on the risk management of offshore wind farms - Offshore Code of Practice," 2014.

[32] G. Marsh, "Vessel supply chain shapes up for offshore wind," *Renewable Energy Focus*, vol. 11, no. 3, pp. 18–23, 2010.

[33] Carbon Trust, "Cable Burial Risk Assessment Methodology," 2015.

[34] T. Boehme and D. J. Robson, "Offshore wind farm cabling: incidents and required learning," *Proceedings of the ICE - Forensic Engineering*, vol. 165, no. 4, pp. 185–197, 2012.

[35] M. Sharples, "Offshore Electrical Cable Burial for Wind Farms: State of the Art, Standards and Guidance & Acceptable Burial Depths, Separation Distances and Sand Wave Effect," 2011.

[36] International Cable Protection Commitee Ltd, "About Submarine Power Cables," 2011.

[37] F. Dinmohammadi and M. Shafiee, "A Fuzzy-FMEA Risk Assessment Approach for Offshore Wind Turbines," *International Journal of Prognostics and Health Management*, pp. 1–10, 2013.

[38] A. Koukal and M. H. Breitner, "A Decision Support Tool for the Risk Management of Offshore Wind Energy Projects," no. March, pp. 1683–1697, 2013.

[39] M. J. Kaiser and B. F. Snyder, "Modeling offshore wind installation costs on the U.S. Outer Continental Shelf," *Renewable Energy*, vol. 50, pp. 676–691, 2013.

[40] J. J. Nielsen and J. D. Sørensen, "On risk-based operation and maintenance of offshore wind turbine components," *Reliability Engineering and System Safety*, vol. 96, no. 1, pp. 218–229, 2010.

[41] M. a. Kougioumtzoglou and I. Lazakis, "Developing a Risk Analysis and Decision Making Strategy for an Offshore Wind Farm," no. 1, 2014.

[42] M. Borunda, O. Jaramillo, A. Reyes, and P. H. Ibargüengoytia, "Bayesian networks in renewable energy systems: A bibliographical survey," *Renewable and Sustainable Energy Reviews*, vol. 62, pp. 32–45, 2016.

[43] F. O'Carroll, "Weather Modelling for Offshore Operations," *Journal of the Royal Statistical Society. Series D (The Statistician)*, vol. 33, no. 1, pp. 161–169, 1984.

[44] A. J. A. Bowers and G. I. Mould, "Weather Risk in Offshore Projects," *The Journal of the Operational Research Society*, vol. 45, no. 4, pp. 409–418, 1994.

[45] O. T. Gudmestad, "Risk Assessment Tools for Use During Fabrication of Offshore Structures and in Marine," vol. 124, no. August 2002, pp. 153–161, 2002.

[46] J. E. Vinnem, F. Vollen, T. Aven, H. Hundseid, K.-A. Vassmyr, and K. Øien, "Risk Assessments for Offshore Installations in the Operational Phase," in *ESREL 2003*, 2003.

[47] PAFA Consulting Engineers for the Health and Safety Executive, "Weather-sensitive offshore operations and Metocean data," tech. rep., Health and Safety Executive, 2001.

[48] C. A. Irawan, D. Jones, and D. Ouelhadj, "Bi-objective optimisation model for installation scheduling in offshore wind farms," *Computers & Operations Research*, pp. 1–15, 2015.

[49] I. F. Vis and E. Ursavas, "Assessment approaches to logistics for offshore wind energy installation," *Sustainable Energy Technologies and Assessments*, vol. 14, pp. 80–91, 2016.

[50] B. Scholz-Reiter, J. Heger, M. Lütjen, and A. Schweizer, "A milp for installation scheduling of offshore wind farms," *International Journal of Mathematical Models and Methods in Applied Sciences*, vol. 5, no. 2, pp. 371–378, 2011.

[51] A. Ait-Alla, M. Quandt, and M. Lütjen, "Simulation-based aggregate Installation Planning of Offshore Wind Farms," *International Journal Of Energy*, vol. 7, no. 2, pp. 23–30, 2013.

[52] Y. T. Muhabie, J.-d. Caprace, C. Petcu, and P. Rigo, "Improving the Installation of Offshore Wind Farms by the use of Discrete Event Simulation," in *World Maritime Technology Conference (WMTC), At ,Providence, RI, USA*, pp. 1–10, 2015.

[53] D. Ahn, S. C. Shin, S. Y. Kim, H. Kharoufi, and H. C. Kim, "Comparative evaluation of different offshore wind turbine installation vessels for Korean west-south wind farm," *International Journal of Naval Architecture and Ocean Engineering*, vol. 9, no. 1, pp. 45–54, 2017.

[54] E. Barlow, D. Tezcaner Öztürk, M. Revie, K. AkartunalÄś, A. H. Day, and E. Boulougouris, "A mixed-method optimisation and simulation framework for supporting logistical decisions during offshore wind farm installations," *European Journal of Operational Research*, vol. 264, no. 3, pp. 894–906, 2018.

[55] M. Morandeau, R. T. Walker, R. Argall, and R. F. Nicholls-Lee, "Optimisation of marine energy installation operations," *International Journal of Marine Energy*, vol. 3-4, pp. 14–26, 2013.

[56] R. T. Walker, J. Van Nieuwkoop-Mccall, L. Johanning, and R. J. Parkinson, "Calculating weather windows: Application to transit, installation and the implications on deployment success," *Ocean Engineering*, vol. 68, pp. 88–101, 2013.

[57] H.-w. Chang, M.-j. Maa, and M.-c. Lin, "Comparitive analysis of wave weather windows in operation and maintenance of offshore wind farms at Hsinchu and Changhua, Taiwan," *Journal of Marine Science and Technology*, vol. 25, no. 5, pp. 563–570, 2017.

[58] M. O'Connor, D. Burke, T. Curtin, T. Lewis, and G. Dalton, "Weather windows analysis incorporating wave height, wave period, wind speed and tidal current with relevance to deployment and maintenance of," *Proceedings of the 4th ...*, pp. 1–9, 2012.

[59] Y. Kikuchi and T. Ishihara, "Assessment of weather downtime for the construction of offshore wind farm by using wind and wave simulations

Assessment of weather downtime for the construction of offshore wind farm by using wind and wave simulations," 2016.

[60] W. Skamarock, J. Klemp, J. Dudhi, D. Gill, D. Barker, M. Duda, X.-Y. Huang, W. Wang, and J. Powers, "A Description of the Advanced Research WRF Version 3," 2008.

[61] H. L. Tolman, "User manual and system documentation of WAVEWATCH-IIITM version 3.14," 2009.

[62] T. Jardine and F. Latham, "An analysis of wave height records for the NE Atlantic," *Quarterly Journal of the Royal . . .*, vol. 107, pp. 415–426, 1981.

[63] G. Box, G. Jenkins, and G. Reinsel, *Time series forecasting and control, 4th edition.* New York: John Wiley and Sons, 2008.

[64] T. L. Walton and L. E. Borgman, "Simulation of Nonstationary, Non-Gaussian Water Levels on the Great Lakes," 1990.

[65] P. J. Brockwell and R. A. Davis, *Time Series: Theory and Methods - Second Edition.* Springer Science & Business Media, LLC, 2006.

[66] G. E. P. Box and D. R. Cox, "An Analysis of Transformations," *Journal ofthe Royal Statistical Society. Series B (Methodological)*, vol. 26, no. 2, pp. 211–252, 1964.

[67] J.-p. Kreiss and E. Paparoditis, "Bootstrap methods for dependent data : A review," *Journal of the Korean Statistical Society*, vol. 40, no. 4, pp. 357–378, 2011.

[68] K. Young, "A multivariate chain model for simulating climatic parameters from daily data," *Jounrnal of Applied Meteorology*, vol. 33, pp. 661–671, 1994.

[69] O. Makarynskyy, A. A. Pires-silva, D. Makarynska, and C. Ventura-soares, "Artificial neural networks in wave predictions at the west coast of Portugal," vol. 31, pp. 415–424, 2005.

[70] P. Ailliot and V. Monbet, "Markov-switching autoregressive models for wind time series," *Environmental Modelling and Software*, vol. 30, pp. 92–101, 2012.

[71] R. S. J. Tol, "Autoregressive Conditional Heteroscedasticity in Daily Wind Speed Measurements," *Theoretical and Applied Climatology*, vol. 122, no. 53, pp. 113–122, 1997.

[72] G. De Masi, R. Bruschi, and M. Drago, "Synthetic metocean time series generation for offshore operability and design based on multivariate Markov

model," in *MTS/IEEE OCEANS 2015 - Genova: Discovering Sustainable Ocean Energy for a New World*, 2015.

[73] K. Brokish and J. Kirtley, "Pitfalls of modeling wind power using Markov chains," *2009 IEEE/PES Power Systems Conference and Exposition*, pp. 1–6, 2009.

[74] G. Leontaris, O. Morales-Nápoles, and A. Wolfert, "Probabilistic scheduling of offshore operations using copula based environmental time series - An application for cable installation management for offshore wind farms," *Ocean Engineering*, vol. 125, pp. 328–341, 2016.

[75] C. N. Stefanakos, G. A. Athanassoulis, and S. F. Barstow, "Time series modeling of significant wave height in multiple scales, combining various sources of data," *Journal of Geophysical Research: Oceans*, vol. 111, no. 10, pp. 1–12, 2006.

[76] G. A. Athanassoulis and C. N. Stefanakos, "A nonstationary stochastic model for long-term time series of significant wave height," *Journal of Geophysical Research: Oceans*, vol. 100(C8), pp. 16149–16162, 1995.

[77] Y. Guanche, R. Mínguez, and F. J. Méndez, "Climate-based monte carlo simulation of trivariate sea states," *Coastal Engineering*, vol. 80, pp. 107–121, 2013.

[78] G. Pérez-Landa, L. Sainz de Aja, and P. Orellana, "Seasonality of wave prediction skills for supporting marine operations in an offshore wind farm," in *OCEANS 2015 - Genova*, (Genoa, Italy), 2015.

[79] The SWAN team, "SWAN Cycle III version 41.20A."

[80] P. Pinson, L. E. A. Christensen, H. Madsen, P. E. Sørensen, M. H. Donovan, and L. E. Jensen, "Regime-switching modelling of the fluctuations of offshore wind generation," *Journal of Wind Engineering and Industrial Aerodynamics*, vol. 96, pp. 2327–2347, 2008.

[81] V. Monbet and P. Ailliot, "Metocean Time Series (METIS) Toolbox Documentation," 2005.

[82] Det Norske Veritas, "DNV-RP-H103 Modelling and Analysis of Marine Operations," no. April, 2010.

[83] L. R. Rabiner and B. H. Juang, "An introduction to hidden Markov models.," *IEEE ASSP MAGAZINE*, jan 1986.

[84] I. Dinwoodie, F. Quail, and M. D, "A Novel Time Domain Meteo-Ocean Modelling Approach," in *Proceedings of ASME Turbo Expo 2012*, (Copenhagen,), pp. 1–11, http://strathprints.strath.ac.uk, 2012.

[85] W. Lair, R. Sueur, and EDF R&D, "Offshore Wind Turbine Project - Specifications for the development of the ECUME tool - Installation," 2014.

[86] The Crown Estate, "Marine Data Exchange," 2015.

[87] Renewable UK, "Offshore Wind Projects Offshore Wind Project Timelines," 2015.

[88] 4C Offshore Ltd, "4C Offshore," 2016.

[89] Y. Dalgic, I. Lazakis, O. Turan, and S. Judah, "Investigation of optimum jack-up vessel chartering strategy for offshore wind farm O&M activities," *Ocean Engineering*, vol. 95, pp. 106–115, 2015.

[90] Douglas Westwood, "OWF and WTIV Study," 2013.

[91] I. B. Sperstad, M. Stålhane, I. Dinwoodie, O.-e. V. Endrerud, and E. Warner, "Testing the Robustness of Optimal Vessel Fleet Selection for Operation and Maintenance of Offshore Wind Farms," pp. 1–13.

[92] K. E. Thomsen, *Offshore Wind: A Comprehensive Guide to Successful Offshore Wind Farm Installation*. 2012.

[93] Van Oord ACZ, "Cable installation study for DOWEC," 2001.

[94] Van Der Kamp, "Multipurpose Injection Dredger Maasmond," 2015.

[95] Royal Boskalis Westminster N.V., "Argonaut - Trailing Suction Hopper Dredger," 1999.

[96] Van Oord, "Trailing Suction Hopper Dredger - Utrecht," 2015.

[97] MPI Offshore, "MPI Resolution Operating Capabilities," 2016.

[98] Seaway Heavy Lifting, "Stanislav Yudin."

[99] GustoMSC, "NG series of jack-up vessels," 2012.

[100] Van Oord, "Heavy lift installation vessel - Svanen," 2015.

[101] A2Sea, "Sea Jack: Technical Specifications," 2013.

[102] Peter Madsen Rederi A/S, "Aase Madsen," 2013.

[103] DEME Group, "D. P. Fall Pipe Vessel - Rollingstone."

[104] Van Oord, "Subsea Rock Installation Vessel - Bravenes."

[105] Damen Shipyards Group, "Damen multi-cat 3213," 2012.

[106] Peter Madsen Rederi A/S, "Peter Madsen," 2013.

[107] S. M. Services, "Anna B," 2014.

[108] Ugland Construction AS, "UR 101," 2006.

[109] Royal Boskalis Westminster N.V., "Specification sheet Cable lay vessel - Stemat Spirit," 2014.

[110] Van Oord, "Jan Steen - Multi purpose support vessel - Principal particulars," 2015.

[111] Fugro, "Fugro Saltire," 2016.

[112] Helix Canyon Offshore, "Grand Canyon - Purpose Built Offshore Construction/ROV/Survey Vessel," 2015.

[113] QPS BV, "Trailing Suction Hopper Dredger (TSHD) - Object Definitions," 2018.

[114] M. J. Kaiser and B. F. Snyder, *Offshore Wind Energy Cost Modeling*. 2012.

[115] Http://renews.biz, "Svanen grabs Baltic 2 plum - Offshore Wind | reNEWS - Renewable Energy News," 2013.

[116] Marinelink, "Rampion Offshore Wind Farm Work Underway Again," 2016.

[117] M. Gambino, "Getting Up Close and Personal With America's First Offshore Wind Farm," 2016.

[118] Fred Olsen Windcarrier, "Alstom Haliade Demonstrator - Fred. Olsen Windcarrier," 2013.

[119] B. Maples, G. Saur, M. Hand, R. van de Pietermen, and T. Obdam, "Installation, Operation and Maintenance Strategies to Reduce the Cost of Offshore Wind Energy," no. July, 2013.

[120] Heavyliftnews, "Jan de Nul's TIGER converted into a Dynamic Positioned Rock Dumping vessel with inclined Fallpipe," 2018.

[121] Offshore Wind Programme Board (OWPB) Grid Group, "Overview of the offshore transmission cable installation process in the UK," 2015.

[122] HVS Dredging Support BV, "Zwerver III - DP1," 2018.

[123] Energy Institute, "Construction vessel guideline for the offshore renewables industry," 2014.

[124] J. Bard and F. Thalemann, "Offshore Infrastructure : Ports and Vessels," 2011.

[125] Renews, "First Sandbank wires installed - Offshore Wind | reNEWS - Renewable Energy News," 2015.

[126] Mojo Maritime Limited and James Fisher Marine Services, "Mojo Mermaid," 2017.

[127] The MathWorks Inc., "Percentiles of a data set - MATLAB prctile - MathWorks United Kingdom," 2018.

[128] E. Vanem, *Ocean Engineering & Oceanography: Bayesian Hierarchical Space-Time Models with Application to Significant Wave Height*, vol. 2. Springer Science & Business Media, 2013.

[129] L. E. Baum, T. Petrie, G. Soules, and N. Weiss, "A maximization technique occuring in the statistical analysis of probabilistic functions of markov chains," *The Analysis of Mathematical Statisitics*, vol. 41, no. 1, pp. 164–171, 1970.

[130] A. P. Dempster, N. M. Laird, and D. B. Rubin, "Maximum Likelihood from Incomplete Data via the EM Algorithm," *Journal of the Royal Statistical Society Series B (Methodological)*, vol. 39, no. 1, pp. 1–38, 1977.

[131] P. Chen and A. D. Krauss, "The SAGE Encyclopedia of Social Science Research Methods - Pearson's Correlation Coefficient," 2004.

[132] The MathWorks Inc., "Correlation Coefficient," 2018.

[133] Blyth Offshore Demonstrator Ltd., "Construction Method Statement for Bed Preparation," 2016.

[134] The Crown Estate, "Offshore wind cost reduction-Pathways study," p. 88 pp, 2012.

[135] F. O'Carroll, "Weather Modelling for Offshore Operations," *Journal of the Royal Statistical Society*, vol. 2, no. May 2016, pp. 129–136, 1984.

Appendix A

Assumed vessel characteristics

Table A.1: Assumed vessel characteristics

				Transit Conditions		Waiting Conditions	
Vessel	**Round**	**Transit Speed Loaded (kn)**	**Transit Speed Unloaded (kn)**	**Max. Wind Speed (m/s)**	**Max. Wave Height (m)**	**Max. Wind Speed (m/s)**	**Max. Wave Height (m)**
Injection Dredger	1	10	11.2	12	1.2	15	1.8
WTIV	1	11	12.1	15.3	2.8	36.1	10
WTIV	1	11	12.1	15.3	2.8	36.1	10
Jack-up Barge	1	10	11.5	10	1.5	15	2
Rock Dump	1	6.5	8	10	1.5	15	1.8
Multicat	1	10.8	12	10	1.8	15	2
Barge	1	6	8	10	1	12	1.5
MPSV	1	7	7.7	12	2	15	2.5
TSHD	2	10	11.3	15	2	20	2.5
Heavy Lift Vessel	2	9	12	15	1.8	20	3
Floating Crane	2	2.8	7	15	2.5	20	3
WTIV	2	11	12.1	15.3	2.8	36.1	10
Fall Pipe Vessel	2	11	12	15	2	20	2.2
Offshore Vessel	2	6	8.5	10	1.2	15	1.7
CLV	2	7	9	15	1.5	20	2.8
MPSV	2	12.5	16	15	1.5	20	3

Appendix B

Inputs used in Mermaid modelling

B.1 Inputs Used in MERMAID modelling

1. Met Points

#	MET Point Name	Lat °N	Long °E	WS (m/s)	WS (m/s) @ Height (m)	Hs (m)	Tp (s)	Swell Height (m)	Tidal Elevation (m)	Current Speed (m/s)
1										

2. Task Limits and Weather Windows

Installation Phase/Work Package	Task	Suspendability	Total Duration (days)	Total Duration (hours)	Repeat Duration (h)	n Repeats	Repeats /Asset or WTG Location	Min WW (h)	vW (m/s)	vW (m/s) @ Height (m/s)	Hs (m)	Swell Height (m)	Tp (s)	Tidal Elevation (m) +CD	Current (m/s)	Daylight Required (Y/N)	Vessel
Installation Phase A	*Task 1*	*Suspendable between each Repeat*	*2.75*	*66*	*13.2*	*5*	*1*	*13.2*	*-*	*-*	*2.5*	*0.5*	*-*	*1.5*	*1*	*N*	*Survey Vessel*
	Task 2	*Suspendable between each Repeat*	*6.5*	*156*	*15.6*	*10*	*2*	*15.6*	*-*	*-*	*2.5*	*0.5*	*7*	*-*	*-*	*N*	*Dredger*
	Task 3	*Suspendable between each Repeat*	*2.75*	*66*	*13.2*	*5*	*1*	*13.2*	*-*	*-*	*2.5*	*0.5*	*14*	*-*	*2*	*N*	*Survey Vessel*
	Task 4	*Not suspendable*	*3*	*72*	*14.4*	*5*	*1*	*132*	*20.5*	*-*	*2.5*	*0.5*	*-*	*-*	*-*	*N*	*FFPV*
	Task 5		*2.5*	*60*	*12*	*5*	*1*		*20.5*		*2.5*	*0.5*	*-*	*-*	*-*	*N*	*FFPV*
	Task 6	*Suspendable between each **Asset***	*11*	*264*	*13.2*	*20*	*4*	*52.8*	*20.6*	*-*	*2.5*	*0.5*	*-*	*-*	*-*	*N*	*FFPV*

3. Vessel Limits & Parameters

Vessel Name	Transit Hs (m)	Transit Wind Speed (m/s)	On Station Hs (m)	On Station Wind Speed (m/s)	Transit Speed (m/s)
Dredger	*2.5*	*15*	*3*	*15*	*7.97*

4. Start Dates

#	Installation Phase/Operation(s)	Scheduled Start Date
1	*Installation Phase A*	*15/03/2017 05:00*

Appendix C

BOD weathered Gantt charts - Scenario 1 - No learning

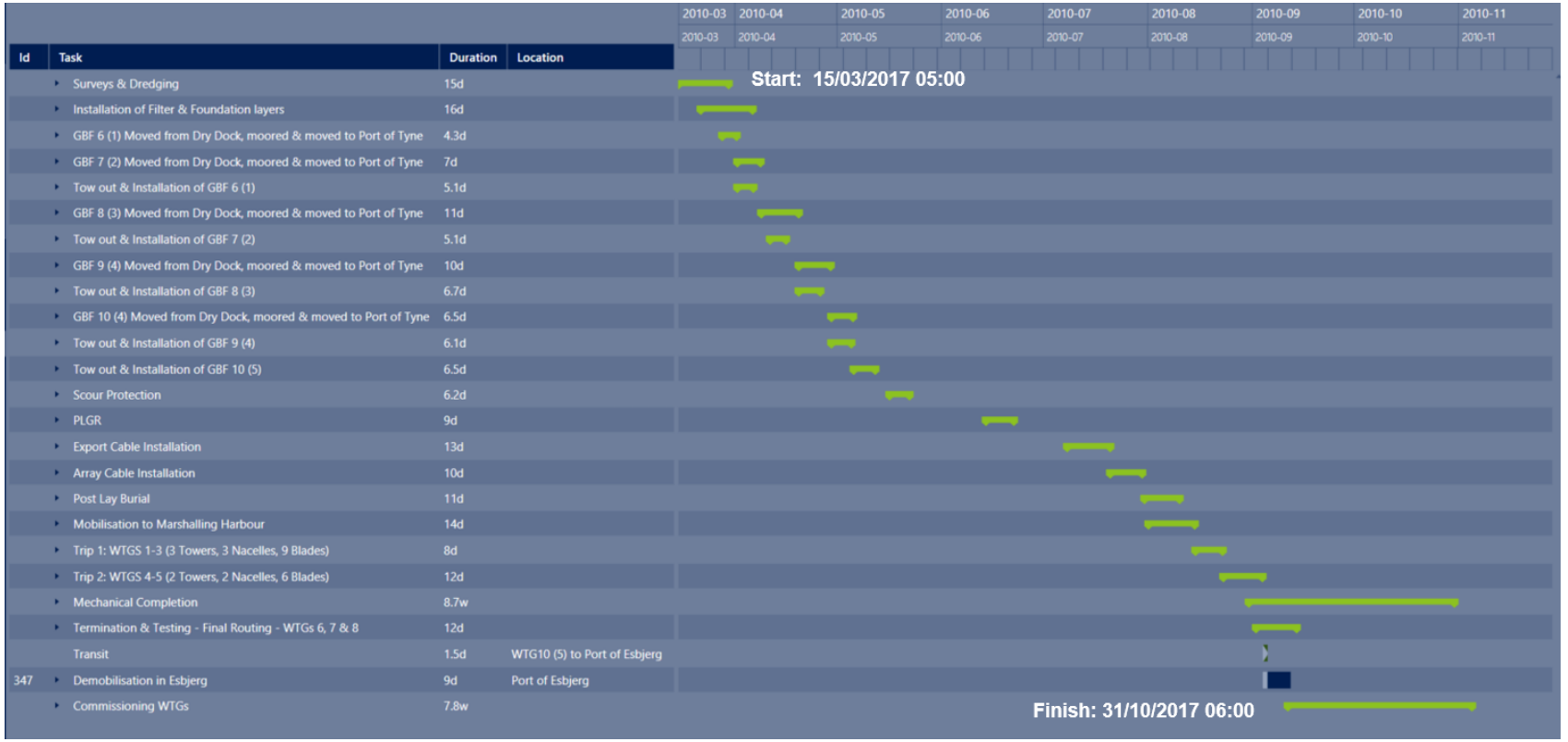

Figure C.1: BOD P90 Weathered Gantt Chart - No Learning

Appendix D

BOD P90 weathered Gantt chart - Scenario 2 - GBF & WTG learning

Figure D.1: BOD P90 Weathered Gantt Chart - GBF & WTG Learning

Appendix E

BOD P90 weathered Gantt chart - Scenario 3 - GBF & WTG learning - 1 Month delay

Figure E.1: BOD P90 Weathered Gantt Chart - GBF & WTG Learning - 1 Month Delay

Appendix F

BOD P90 weathered Gantt chart - Scenario 4 - 1 x WTG only

Figure F.1: BOD P90 Weathered Gantt Chart - 1 x WTG Only

Appendix G

Percentage increase in duration by percentile tables - BOD & Fecamp metocean risk analyses

G.1

BOD S1 – No Learn

	P50	P70	P90
Dredging & Survey	6.68%	18.48%	56.10%
Filter Layer	35.65%	56.09%	99.41%
Towing GBFs out of Dry Dock	4555.63%	6725.05%	13074.95%
Towing GBFs down River Tyne	39.62%	46.42%	110.19%
GBF Installation	20.13%	26.94%	43.50%
Scour Protection	23.81%	25.00%	55.75%
PLGR	0.00%	14.92%	48.03%
Export Cable	12.05%	33.93%	70.31%
Array Cable	0.00%	8.38%	24.32%
Hang off, Stripping & Routing	0.00%	8.00%	21.43%
Cable Burial	0.00%	1.32%	6.81%
WTG Installtion	12.93%	18.09%	37.92%
Mechanical Completion	30.61%	37.90%	55.50%
Final Routing	18.97%	25.71%	56.11%
Commissioning	26.40%	37.05%	63.81%

BOD S2 – GBF & WTG Learning

	P50	P70	P90
Dredging & Survey	6.68%	18.48%	56.10%
Filter Layer	35.65%	56.09%	99.41%
Towing GBFs out of Dry Dock	4555.63%	6725.05%	13074.95%
Towing GBFs down River Tyne	39.62%	46.42%	110.19%
GBF Installation	23.94%	30.52%	41.36%
Scour Protection	23.81%	25.00%	55.75%
PLGR	0.00%	14.92%	48.03%
Export Cable	12.05%	33.93%	70.31%
Array Cable	0.00%	8.38%	24.32%
Hang off, Stripping & Routing	0.00%	8.00%	21.43%
Cable Burial	0.00%	1.32%	6.81%
WTG Installtion	11.35%	18.82%	38.80%
Mechanical Completion	30.61%	37.90%	55.50%
Final Routing	18.97%	25.71%	56.11%
Commissioning	26.40%	37.05%	63.81%

G.2

BOD S3 – GBF & WTG Learning – 1 Month Delay

	P50	P70	P90
Dredging & Survey	0.00%	6.07%	37.42%
Filter Layer	5.77%	13.43%	27.06%
Towing GBFs out of Dry Dock	10430.36%	12791.77%	17212.22%
Towing GBFs down River Tyne	46.42%	46.42%	69.43%
GBF Installation	14.70%	20.57%	29.00%
Scour Protection	23.81%	29.76%	46.83%
PLGR	0.00%	10.12%	31.39%
Export Cable	18.08%	31.03%	80.69%
Array Cable	3.38%	9.05%	26.76%
Hang off, Stripping & Routing	6.95%	17.52%	70.76%
Cable Burial	1.23%	11.15%	19.28%
WTG Installtion	25.49%	28.84%	55.59%
Mechanical Completion	55.96%	67.45%	86.11%
Final Routing	43.54%	78.63%	140.00%
Commissioning	51.00%	69.75%	142.48%

BOD S4 – 1 x WTG

	P50	P70	P90
Dredging & Survey	0.00%	8.64%	68.69%
Filter Layer	57.69%	117.10%	290.33%
GBF Installation	39.29%	74.07%	118.66%
Scour Protection	113.73%	231.94%	577.97%
PLGR	22.67%	52.91%	80.23%
Export Cable	263.02%	300.49%	368.59%
Array Cable	5.54%	11.09%	17.40%
Hang off, Stripping & Routing	36.00%	58.86%	344.57%
Cable Burial	15.40%	34.14%	61.78%
WTG Installtion	176.51%	479.64%	807.16%
Mechanical Completion	66.88%	87.71%	153.56%
Final Routing	0.00%	52.00%	177.71%
Commissioning	33.03%	66.06%	184.84%

G.3

Fecamp – Installation Campaign 1

	P50	P60	P70	P90
GBS Bedding	11.98%	14.21%	16.99%	30.64%
GBS Installation	15.68%	16.41%	19.64%	23.36%
GBS Scour & Ballast	16.87%	20.10%	21.81%	26.24%
IAG Laying	15.68%	15.98%	24.26%	28.40%
IAG Burial	16.33%	17.53%	19.52%	33.27%
IAG Termination	14.99%	15.73%	17.21%	33.68%

Fecamp – Installation Campaign 2

	P50	P60	P70	P90
GBS Bedding	28.31%	27.85%	32.42%	59.82%
GBS Installation	25.28%	30.16%	31.41%	42.18%
GBS Scour & Ballast	29.95%	33.24%	35.99%	40.80%
IAG Laying	18.74%	19.25%	22.66%	31.01%
IAG Burial	16.89%	21.62%	23.87%	32.77%
IAG Termination	12.90%	13.90%	14.74%	23.37%
WTG Installation	24.66%	27.57%	28.58%	41.69%

Appendix H

Average values & percentage difference, average and absolute average error for wind speed U and wave height H_s - observed and simulated

Table H.1: Average magnitudes, percentage difference, average and absolute average for wind speed U and wave height H_s - observed and simulated

	Blyth						French West						English Channel					
	Observed U	Simulated U	U (m/s) % Difference	Observed Hs	Simulated Hs	Hs (m/s) % Difference	Observed U	Simulated U	U (m/s) % Difference	Observed Hs	Simulated Hs	Hs (m/s) % Difference	Observed U	Simulated U	U (m/s) % Difference	Observed Hs	Simulated Hs	Hs (m/s) % Difference
Average	6.62	6.66	0.50	1.15	1.16	0.95	5.68	5.70	0.38	1.39	1.42	2.27	7.48	7.47	-0.21	0.85	0.86	0.67
January	8.89	8.90	0.20	1.47	1.47	0.23	7.03	7.00	-0.42	2.10	2.16	2.53	9.34	9.30	-0.44	1.19	1.23	2.93
February	8.25	8.31	0.76	1.42	1.43	0.73	6.56	6.64	1.26	1.93	2.02	4.52	8.57	8.55	-0.27	1.09	1.10	1.49
March	7.22	7.18	-0.58	1.29	1.30	1.26	5.80	5.82	0.22	1.54	1.56	1.48	7.55	7.53	-0.23	0.89	0.89	-0.24
April	5.94	5.89	-0.71	1.14	1.15	0.63	5.56	5.56	0.02	1.30	1.34	3.15	6.73	6.68	-0.64	0.72	0.73	0.34
May	5.40	5.38	-0.38	0.98	0.98	0.34	5.08	5.03	-1.08	1.05	1.06	1.34	6.62	6.58	-0.63	0.70	0.69	-1.96
June	4.98	4.99	0.25	0.89	0.90	1.14	4.75	4.82	1.62	0.93	0.94	0.66	6.06	6.09	0.54	0.58	0.57	-1.65
July	4.84	4.87	0.74	0.76	0.77	1.72	4.70	4.74	0.83	0.88	0.89	1.13	6.09	6.02	-1.06	0.59	0.58	-2.27
August	5.22	5.27	0.90	0.82	0.82	0.59	4.56	4.57	0.12	0.87	0.87	-0.42	6.14	6.12	-0.29	0.59	0.58	-1.40
September	5.90	5.89	-0.02	1.00	1.02	1.51	4.77	4.76	-0.28	1.02	1.05	3.12	6.80	6.80	-0.01	0.73	0.72	-0.74
October	6.93	7.00	0.99	1.23	1.24	0.38	5.64	5.69	0.78	1.45	1.51	4.00	8.08	8.07	-0.12	0.91	0.93	2.33
November	7.70	7.84	1.86	1.38	1.41	2.03	6.54	6.57	0.49	1.65	1.66	0.71	8.55	8.60	0.60	1.03	1.05	2.28
December	8.25	8.36	1.43	1.42	1.43	1.07	7.15	7.21	0.84	1.89	1.93	2.36	9.25	9.23	-0.19	1.20	1.22	1.84
$\lvert\mu\rvert$			0.74			0.97			0.66			2.12			0.42			1.62

Appendix I

Distribution of monthly weather windows and percentage workability: $\geq$30 hours, $\leq$ 13.6 m/s & $\leq$ 1.5 m - Paired-by-means

Figure I.1: Distribution of monthly weather windows and percentage workability: ≥30 hours, ≤ 13.6 m/s & ≤ 1.5 m - **Paired-by-means**

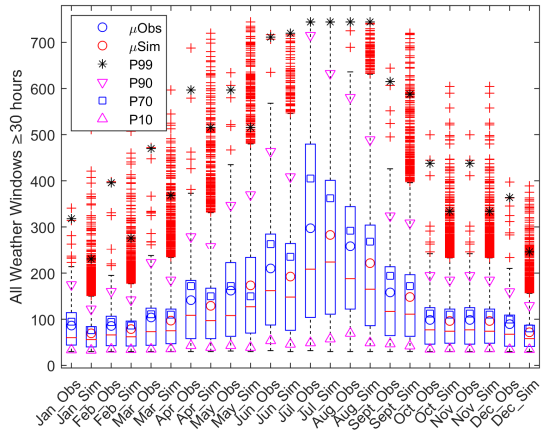

(a) UK North East: Boxplot of monthly weather windows ≥ 30 hours

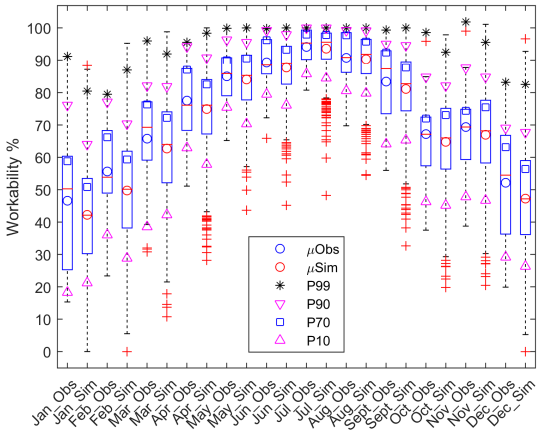

(b) UK North East: Boxplot of monthly percentage workability

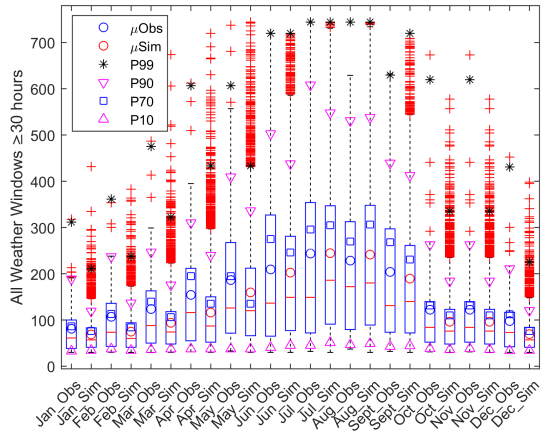

(c) France West: Boxplot of monthly weather windows ≥ 30 hours

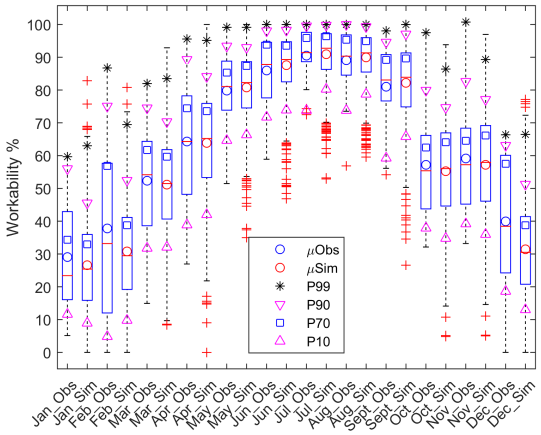

(d) France West: Boxplot of monthly percentage workability

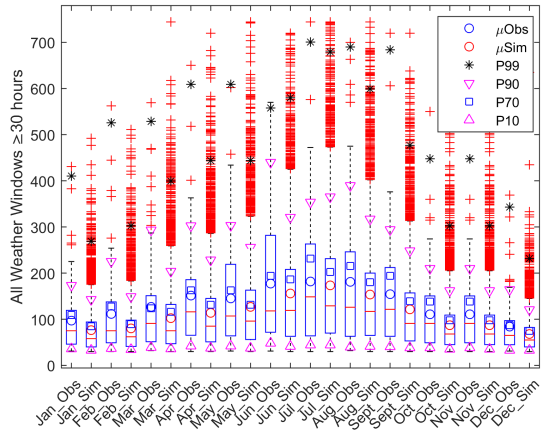

(e) English Channel: Boxplot of monthly weather windows ≥ 30 hours

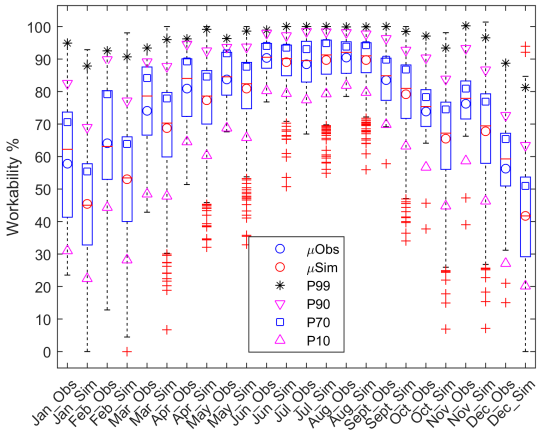

(f) English Channel: Boxplot of monthly percentage workability

Appendix J

Distribution of monthly weather windows and percentage workability: $\geq$30 hours, $\leq$ 13.6 m/s & $\leq$ 1.5 m - Correlated Pairing

Figure J.1: Distribution of monthly weather windows and percentage workability: ≥30 hours, ≤ 13.6 m/s & ≤ 1.5 m - **Correlated Pairing**

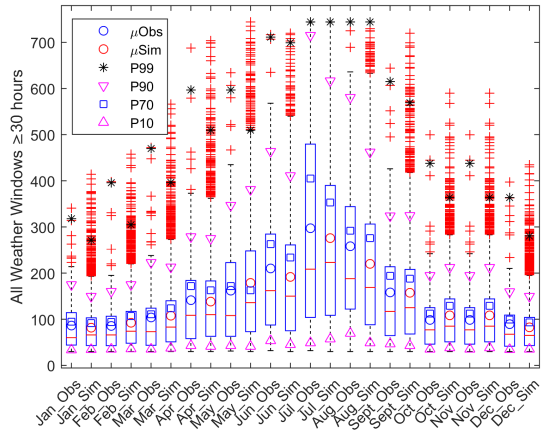

(a) UK North East: Boxplot of monthly weather windows ≥ 30 hours

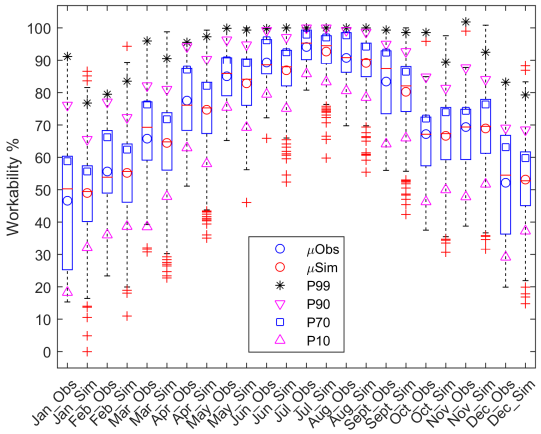

(b) UK North East: Boxplot of monthly percentage workability

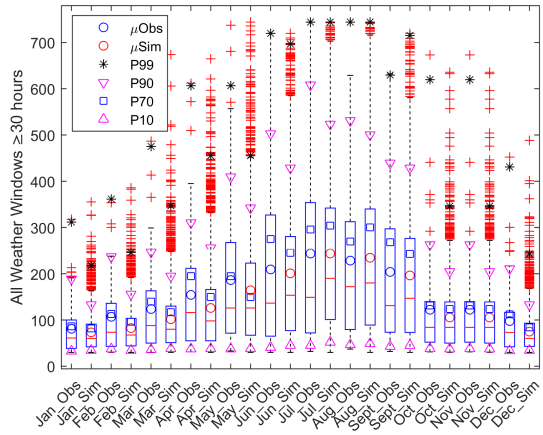

(c) France West: Boxplot of monthly weather windows ≥ 30 hours

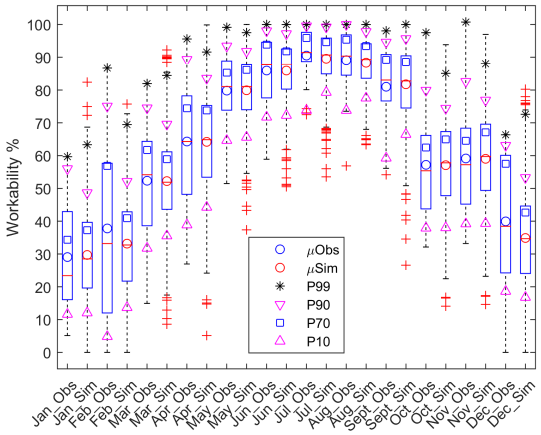

(d) France West: Boxplot of monthly percentage workability

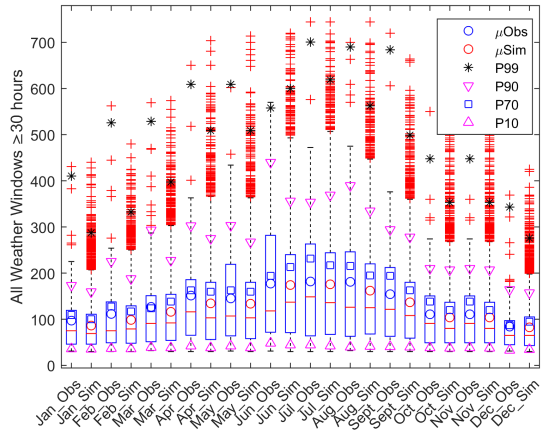

(e) English Channel: Boxplot of monthly weather windows ≥ 30 hours

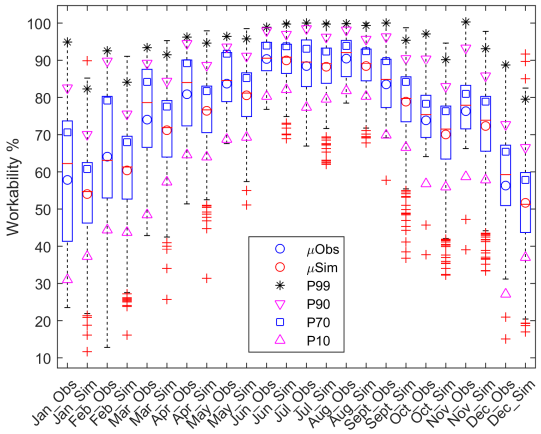

(f) English Channel: Boxplot of monthly percentage workability

Appendix K

Publications

This chapter contains a list of publications related to this thesis ordered by academic publication status.

K.1 Published

- J. Paterson, F. D'Amico, P. R. Thies, R. E. Kurt, and G.Harrison, "Offshore wind installation vessels - A comparative assessment for UK offshore rounds 1 and 2," Ocean Engineering, vol. 148, pp. 637-649, 2018 [Available at: https://bit.ly/2PAMZft]

K.2 Submitted

- J. Paterson, P. R. Thies, F. D'Amico, R. Sueur and J. Lonchampt, "Assessing marine operations with a Markov-switching autoregressive metocean model," European Journal of Operational Research, 2018

K.3 Conference Presentations

- J. Paterson, F. D'Amico, P. R. Thies, R. E. Kurt, and G.Harrison, "Offshore wind installation vessels - A comparative assessment for UK offshore rounds 1, 2 and 3," 1st EDF Energy Post Graduate Researchers Event, Cannington, 2016.

- J. Paterson, F. D'Amico, P. R. Thies, R. E. Kurt, and G.Harrison, "Offshore wind installation vessels - A comparative assessment for UK offshore rounds 1, 2 and 3," 2nd IDCORE Symposium, Edinburgh, 2017.

- J. Paterson, F. D'Amico, P. R. Thies, R. E. Kurt, and G.Harrison, "Offshore wind installation vessels - A comparative assessment for UK offshore rounds 1, 2 and 3," 8th Wind Power Monthly Vessels and Access Forum, Amsterdam, 2018.

- J. Paterson, P. R. Thies, F. D'Amico, R. Sueur and J. Lonchampt, "Assessing marine operations with a Markov-switching autoregressive metocean model," 3rd IDCORE Symposium, Edinburgh, 2018

K.4 Conference Posters

J. Paterson, F. D'Amico, P. R. Thies, R. E. Kurt, and G.Harrison, "Risk Management of Offshore Wind Project Development" 1st EDF Energy Post Graduate Researchers Event, Cannington, 2016.

J. Paterson, F. D'Amico, P. R. Thies, R. E. Kurt, and G.Harrison, "Offshore wind installation vessels - A comparative cost assessment for UK offshore rounds 1, 2 and 3" Offshore Wind Energy 2017, London [Available at: https://bit.ly/2o7JqRt]

K.5 Attached Publications

Ocean Engineering 148 (2018) 637–649

Contents lists available at ScienceDirect

Ocean Engineering

journal homepage: www.elsevier.com/locate/oceaneng

Offshore wind installation vessels – A comparative assessment for UK offshore rounds 1 and 2

J. Paterson [a,*], F. D'Amico [a], P.R. Thies [b], R.E. Kurt [c], G. Harrison [d]

[a] EDF Energy R&D UK Centre, Interchange, 85 Station Road, Croydon, London CR0 2AJ, UK
[b] College of Engineering, Mathematics and Physical Science, University of Exeter, Cornwall Campus, Penryn TR10 9EZ, UK
[c] Department of Naval Architecture, Ocean and Marine Engineering, University of Strathclyde, Glasgow G4 0LZ, UK
[d] Institute for Energy Systems, School of Engineering, The University of Edinburgh, Edinburgh EH9 3JL, UK

ARTICLE INFO

Keywords:
Offshore wind installation
Vessel technology
Stochastic weather
Weather downtime
Installation risk

ABSTRACT

Marine operations play a pivotal role throughout all phases of a wind farm's life cycle. In particular uncertainties associated with offshore installations can extend construction schedules and increase the capital expenditure (CAPEX) required for a given project. Installation costs typically account for approximately 30% of the overall project cost. This study considers the installation modelling for UK offshore Wind Rounds 1 and 2 using probabilistic simulation tool. The tool is used to output time-domain predictions for the completion of key installation phases. By varying key wind farm characteristics such as distance to shore and the number of turbines, an assessment of vessel performance was completed for each round by reviewing recorded durations predicted by the software. The results provide a quantification of installation vessel performance and the associated deviations present a measure of installation risk. It is identified that the Round 1 vessels experience less weather downtime but higher variability and the Round 2 vessels perform more consistently but experience larger delays. The paper provides a structured method to identify and benchmark offshore wind installation risks, to support developers and project planners.

1. Introduction

1.1. Background

Offshore wind farm (OWF) development has increased steadily throughout the UK over the last decade and is predicted to maintain this momentum until at least 2020 (Offshorewind.biz, 2016; Renewable UK, 2016). The UK has more offshore wind turbines than the whole of the rest of Europe. 1.5 GW is currently under construction with a further 5 GW of projects yet to begin development (The Crown Estate, 2015). As turbine sizes, distances from shore increase, weather becomes more severe and water depths span beyond 30 m, the logistical challenge becomes ever more prominent for prospective developers.

Marine operations play a pivotal role throughout all phases of a wind farm's life cycle, yet uncertainties associated with offshore installation can extend construction schedules and increase the capital expenditure (CAPEX) required for a given project. Installation costs can account for approximately 30% of the overall project cost and it is anticipated informed engineering decisions in this area present further cost saving potential (Krohn et al., 2005). The increasing remoteness and heightened weather conditions for the UK's future OWFs, increases the complexity of the marine operations and the importance of making the correct decisions prior to development and sourcing of the correct vessels to complete the tasks.

At the beginning of the OWF development in the UK in 2001, the vessels used for construction introduced bottlenecks and delays in construction. This was caused by a lack in availability of specialised vessels as these were predominantly used in the oil and gas sector, introducing competition for their services. In some cases the vessels were oversized or not ideally suited to the operations, which were often sourced at over-inflated charter rates. As OWF development increased, the industry began to manufacture purpose built offshore wind vessels that would offer more deck space, cope with more severe weather and reduce overall installation durations (Offshore-technology, 2012).

This paper considers the installation modelling for UK offshore Wind Rounds 1 and 2. The analysis is based on time-domain predictions for the completion of key installation operations under user specified exceedance probabilities, commonly used by investors to determine a project's

* Corresponding author.
E-mail address: jack.paterson@ed.ac.uk (J. Paterson).

https://doi.org/10.1016/j.oceaneng.2017.08.008
Received 27 December 2016; Received in revised form 26 July 2017; Accepted 5 August 2017
Available online 18 August 2017

viability and used by developers to assess their risk preferences. By varying key wind farm characteristics, an assessment on the performance of typical installation vessels adopted for each of the UK development rounds is investigated with the use of an OWF installation decision support software tool. A comparative analysis of the predicted durations between each of the two offshore wind rounds is completed. this analysis will help inform planning operatives when considering vessel selection in their next project and reveal if further innovation is needed to overcome delays when developing future OWFs.

The remainder of the paper is structured as follows: Section 2 presents a brief literature review of the most pertinent work in this field. In Section 3, we begin with a description of the wind farm installation software and an overview of the processes applied within the tool. We then describe in Section 3.3 the various sources of meteorological data used for each round and provide a justification for their selection. The key OWF characteristics to be varied throughout the simulations is included in Section 3.4. These are applied to resemble the range of OWF sizes and remoteness, typically experienced within each round. It is also intended that these highlight the characteristics that can significantly impact the progression of offshore installation operations and where further technological innovation can be explored. Section 3.5 describes the process used to identify the typical vessel spreads used in each offshore wind round and Section 3.6 describes the fundamental OWF installation operations and their associated environmental limits. Section 4 presents an overview of the results, which are supported with discussion in Section 5, covering the outcomes by round, value to planners and future work. Finally, a summary of our findings and relevant conclusions are presented in Section 6.

2. Literature review

The work on the modelling of logistical requirements and installation of OWFs has increased over the last five years in an attempt to reduce uncertainty associated with accessing and completing work at offshore locations. This type of modelling and analysis allows practitioners to review the installation of an OWF in advance, so that developers can prepare for certain outcomes in terms of cost or delay.

Many authors focus on the modelling of the construction operations and subsequent weather risk analyses. Irawan et al. (2015) look to address the scheduling issues surrounding offshore wind construction by means of an integer linear programming method to identify the optimal installation with lowest costs and shortest schedules, combining weather data and vessel availability. Their investigation in the use of meta-heuristic approaches such as Variable Neighbourhood Search (VNS) and Simulated Annealing (SA) was found to offer reasonable results with low computation time. Their approach is compared against a linear programming optimiser known as CPLEX, which is found to identify the optimum solution but takes longer to reveal the answer.

Others have considered the specific modelling of the logistics surrounding the installation steps, where Barlow et al. (2015) review what vessels and operations are most susceptible to weather constraints during the installation campaign. Their study aims to assess the impact of operational and vessel improvements over recent times, indicating that a non-linear relationship exists between vessel limits and the duration of the installation. It is also concluded that load out operations appear most susceptible in adverse weather conditions.

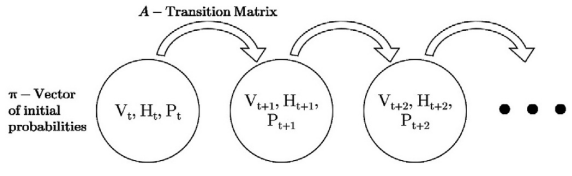

Fig. 3.1. Schematic representation of the Markov Chain: Wind Speed (V_t), Wave Height (H_t), Current Speed (P_t).

Logistics are again the topic in the paper presented by Vis and Ursavas (2016) where their modelling approach reveals that the key activities impacting performance are the vessel loads, distance to shore and the pre-assembly strategy adopted for the main wind turbine components. They recommend that a pre-assembly strategy should be employed that presents the optimum choice between the lowest number of lifts possible and the maximum number of turbines that can fit on a vessel. This reflects that the optimum will differ in each offshore wind project but careful consideration of these two parameters should help reveal the best solution for a given project.

Scholz-Reiter et al. (2011) point out that bad weather conditions are the main cause for delays in the logistics and installation of an offshore wind farm. They apply their mixed integer linear programming (MILP) model to identify the optimal installation schedule for different weather conditions and the loading operations. Their study considers the installation of 12 turbines across three synthetically produced weather scenarios, each representing either good, medium or bad weather and the tool is used to identify optimal installation schedules for the vessels. They acknowledge the stochastic nature of weather conditions and express an interest in developing their tool and assess the impact of weather uncertainty beyond these initial three categories.

Ait-Alla et al. (2013) developed a MILP model to minimise the installation costs by considering vessel utilisation and fixed costs that span the length of the installation period. Their approach considers the weather in a deterministic manner and reviews the outcome of two installation scenarios.

Muhabie et al. (2015) consider the use of discrete event simulation by considering weather restrictions, distances, vessel capabilities and assembly scenarios. They consider the use of real historical weather data and generated data sets adopting a probabilistic approach. The results demonstrate a good level of agreement between the two approaches when considering the average mean lead-time and reference future work to optimise the fleet sizes, capacities and overall installation strategies.

This paper evaluates the installation durations and subsequent vessel performance during the construction of an OWF. A probabilistic function to simulate the weather is enclosed within the adopted tool, which is capable of producing a range of results under user specified exceedance probability quantiles. The user defined exceedance quantiles provides an assessment of installation risk at different confidence levels. This presents a key benefit over the tools reviewed in this section as it offers the adaptability to planners and investors as required. The tool can simulate the full installation of an OWF, handled in phases and considers the environmental constraints of the operations and vessels across the predicted weather outcomes.

3. Methodology

This paper employs an offshore wind installation software simulation tool to determine the installation duration of an Offshore Wind Farm (OWF) in advance. Moreover, a focus on the predicted performance of vessel technology, synonymous of typical vessel spreads used throughout the first two UK offshore wind rounds, are analysed to identify the variation in installation durations and weather downtime.

3.1. Wind farm installation software

The software tool relies on Monte Carlo methods to simulate multiple independent scenarios of the defined installation strategy for an offshore wind farm. The tool considers risk as delays to the installation, imposed by adverse weather conditions. A HMM model (Rabiner and Juang, 1986) has been used to generate each meteorological scenario informed historical weather data, which begins with the evaluation of a transition matrix A for the Markov chain. This matrix represents the evolution of the weather parameters: wind speed (V_t), wave height (H_t) and speed of the sea current (P_t). In this study, the wind speed and wave height are the

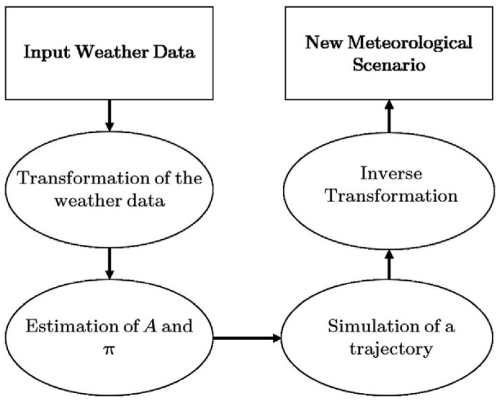

Fig. 3.2. Schematic of the principal method.

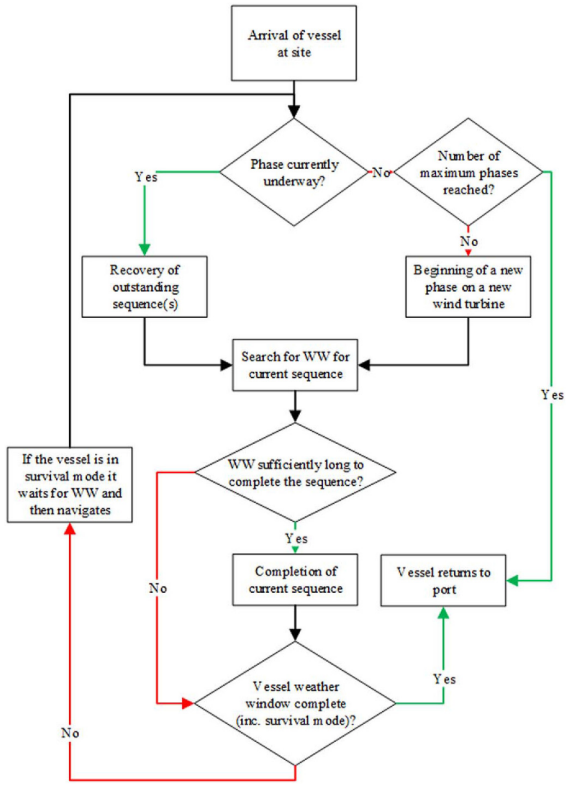

Fig. 3.3. Flowchart of logistical process.

only weather conditions evaluated. Meteorological parameters are intrinsically stochastic but also exhibit some continuity over time. Therefore, at any one time, if the sea is in a certain state, it is more likely that the next time (one hour, for example), the sea remains in a similar state. The main characteristic of a Markov chain is that the next state depends only on the state at the current point in time, which is described by Fig. 3.1. If the probability of moving from one state to another are known, then it is possible to generate meteorological parameters and thus to obtain a new weather scenario.

Each element of the transition matrix A, is the probability for the arrival of state j is knowing the initial state i. A is a matrix of size $n * n$ with n the number of states of the Markov chain. The vector π of the initial probability array of the hidden states is also determined for chain size n. It is possible to obtain empirical estimates of this matrix and vector by:

$$A = (a_{ij})_{1\le i,j\le n} \quad \textbf{and} \quad \pi = (\pi_i)_{1\le i\le n}$$

where:

$$a_{ij} = \frac{number\ of\ transitions\ i \to j}{number\ of\ transitions\ from\ i}$$

and

$$\pi_i = \frac{number\ of\ observations\ in\ the\ state\ i}{total\ number\ of\ observations}$$

For a given initial state, the number of arrivals of possible states is relatively low at a maximum of 30. Thus the matrix A, contains many zeros and forms what is called a matrix dig. For each initial state i, it is best to store only the non-zero values $\widetilde{A}(i)$ and associated indices $P(i)$, which is defined as:

$$P(i) = j | a_{ij} > 0 \quad \textbf{and} \quad \widetilde{A}(i) = (a_{ij})_{j\in P(i)}$$

Once the estimated transition matrix is established, the software will simulate a weather scenario over a period specified, which corresponds the maximum installation duration envisaged by the user. The software simulates the weather at the time $i+1$ knowing the state of the weather at the time i according to transition matrix. The method relies on a monthly transformation in the data in order to 'normalise' the environmental data to a stationary form, which is inspired by Dinwoodie et al. (2012). The transformed data is assumed to be embodiment of a Markov chain and the matrix A, and the vector π are estimated on these transformed data. After the simulation of the Markov chain is applied to reconstruct the monthly outcomes into one meteorological scenario. An overview of these steps is demonstrated by Fig. 3.2.

$X_{i.k} = (X_{i.k}^{(1)}, X_{i.k}^{(2)}, X_{i.k}^{(3)})$ is regarded as the vector of three meteorological parameters for the i-th observation, during month number $k, k \in \{1, 2\ldots, 12\}$. The monthly processing carried out in the method is as follows for each of the parameters $h\{1, 2, 3\}$

$$y_{i.k}^{(h)} = \frac{X_{i.k}^{(h)} - \mu_{i.k}^{(h)}}{\sigma_{i.k}^{(h)}}$$

Where $\mu_{i.k}^{(h)}$ and $\sigma_{i.k}^{(h)}$ are the mean and standard deviation of the parameter number h over the month number k. The meteorological parameters are supposed to take their values in a discrete space and have a finite number of states.

A given meteorological scenario is used directly within each Monte Carlo simulation to calculate a duration for each primary installation phase. Eight installation phases are considered within this study, which are as follows: Dredging&Survey, Foundation, Transition Piece, Turbine (WTG), Scour Protection, Pre-lay Grapnel Run (PLGR), Cable Installation and Cable Burial. These phases include sequences that comprise of subtasks, elementary to the operations. The tool allows phases to be suspended once a sequence has been completed and uses their base duration to determine if an adequate weather window is available, or if the vessel should hold station offshore. A weather window can be defined simply as weather conditions that are predicted to stay within the environmental limits of a sequence, for a specified duration.

Once the software has computed the predicted durations, these can be processed to reveal the average Installation Rates (IRs) and weather downtime (WDT) for each of the installation phases. The P90 exceedance quantile was selected as the referenced result category, providing 90%

Table 3.1
Round 1 OWF characteristics.

Parameter	Maximum	Mean	Minimum
No. of Turbines	60	31	2
Expected Start Date	01/04/2017	01/08/2017	01/12/2017
Inter-turbine distance (km)	0.82	0.67	0.46
Distance to shore (km)	11	6	2

Table 3.2
Round 2 OWF characteristics.

Parameter	Maximum	Mean	Minimum
No. of Turbines	175	93	18
Expected Start Date	01/04/2017	01/08/2017	01/12/2017
Inter-turbine distance (km)	1.08	0.84	0.63
Distance to shore (km)	40	19	7

confidence that the predicted durations will not be exceeded. The numerical results allow the calculation of Key Performance Indicators (KPIs). In this study we use the duration for each phase divided by the number of wind turbines associated to the given model to reveal an average IR in days per turbine (Days/WTG). Similarly, the base unweathered duration for each installation phase is deducted from the predicted duration to reveal the average weather downtime (WDT) that can be expected for each turbine location under the individual phases. These IRs and WDT values can then be generally compared between the rounds to assess the impact of vessel technology. Additionally, the variation about the mean IR and WDT predictions, can be used to estimate the installation risk that may be anticipated for each installation phase.

3.2. Model calculations

A high level description of the methodology applied within the tool for the execution of installation phases is as follows. Firstly, the ship to be used for an installation phase is mobilised. The vessel goes offshore as soon as it's shipping weather limits are satisfied. Next the logistics model, as outlined in Fig. 3.3 is used to apply the phases considering the make-up sequences within each phase. This process initially recognises phases that were not completed in the previous weather window and the process begins at the first of the remaining sequences, otherwise the tool identifies the maximum number of phases to be handled by the vessel and if it is within these bounds, the process begins with the next phase in hand. It is determined if a weather window exists, where the environmental limits of the next sequence are satisfied for the corresponding duration. If the conditions are not satisfied, the software continues to search for a suitable weather window and whilst none are available, the vessel holds station. This stands unless the weather conditions become worse than the waiting condition limits for the vessel, meaning the vessel returns to port and awaits the next opportunity to set sail to site.

The completion of each sequence marks the end of the weather window search and the tool assesses if the vessel can remain on site, either by the maximum number of phases or by the predicted weather conditions. Again, if poorer weather is predicted and the environmental limits allow, the vessel can hold station. If the vessel is in the middle of a current phase or there are phases to complete, the process starts over and searches for a window to complete the next sequence. This iterative process continues and is applied to all installation phases until they are complete for each wind turbine, after which the vessel for the given phase is demobilised and the next vessel begins the subsequent phase in the defined schedule. Finally, the process is complete when the maximum number of Monte Carlo simulations has been reached. The predicted durations for each installation phase are presented with a start and an end date. These dates are recorded under user specified exceedance quantiles such as P50, P70 and P90. It is these predicted durations that are used as the main source of results in this study, as presented in Section 4.

3.3. Meteorological data

Meteorological data was obtained from separate hindcasts used for the two offshore wind rounds. In each simulation, a single metocean time series is used to inform the HMM, which generates 1000 stochastic weather scenarios. These scenarios provide a basis to assess the progression of the installation phases by considering the environmental limits of the sub-tasks and vessels specified for each round. Data from Teesside and Greater Gabbard was selected, representing the conditions of Round 1 and Round 2 sites respectively. The wind speeds in each data set are referenced at 10 m. Teesside offshore wind farm is located off the north east coast of England and its near shore location is synonymous of a Round 1 project. The data set was developed by a private consultant, drawing on field and modelled data to construct a metocean time series. For Round 2, publicly available data for the Greater Gabbard offshore wind farm was sourced from The Crown Estate's Marine Data Exchange (The Crown Estate, 2015). Greater Gabbard is located off the English Suffolk coast and is close to the average distance of all Round 2 sites.

3.4. Wind farm characteristics

The key OWF characteristics for each project within the two offshore wind rounds have been reviewed based on the information included in Renewable UK (2015). This identified mean, maximum and minimum characteristic values across all of the OWFs in each round. The characteristics varied within the simulation tool and the values identified for each round, are listed in Tables 3.1, 3.2. For each OWF round, 11 cases were simulated, beginning with a mean case for all parameters and then varying one parameter at a time with either a maximum or minimum value. Two 'extreme' cases are included, comprising of maximum and minimum case for the number of turbines and distance to shore combined. To consider the impact of start date selection, three dates were selected to investigate the impact of seasonality across the two rounds. April was chosen to resemble construction beginning in the spring, August for summer and December for a winter start.

3.5. Vessel technology&spreads

An assessment of the vessels used across all of the OWFs within the consenting rounds in Renewable UK (2015), was completed to identify

Table 3.3
Vessel types and spread by round.

Phase	Round 1		Round 2	
	Vessel Type	Ref.	Vessel Type	Ref.
Dredging&Survey	Injection Dredger	Van Der Kamp (2015)	TSHD	Royal Boskalis Westminster (1999)
Foundation	WTIV	MPI Offshore (2016)	Heavy Lift Vessel	Seaway Heavy Lifting (2016)
Transition Piece	WTIV	MPI Offshore (2016)	Floating Crane	Van Oord (2015)
WTG	Jack-up Barge	A2Sea (2013)	WTIV	MPI Offshore (2016)
Scour Protection	Rock Dump	Peter Madsen Rederi (2013)	FPV	DEME Group (2014)
PLGR	Multicat	Damen Shipyards Group (2016)	Offshore Vessel	Peter Madsen Rederi (2013)
Cable Inst.	Barge	Ugland Construction AS (2006)	CLV	Royal Boskalis Westminster (2014)
Cable Burial	MPSV	Van Oord (2015)	MPSV	Fugro (2016)

Table 3.4
Task durations and operational limits.

Phase	Reference Duration (h/WTG)	Max. Wind Speed (m/s)	Max. Wave Height (m)
Dredging&Survey	48	11	1.5
Foundation	48	12	2
Transition Piece	24	12	2
WTG	24.5	8	2
Scour Protection	14.4	15	2.5
PLGR	14.4	20	2
Cable Inst.	31.7	15	1.5
Cable Burial	36	12	3

the typical vessel spread used at the time of installation. It is accepted that the categorisation by UK Offshore Wind rounds does not mean all construction activities were completed within an allocated time frame as some Round 2 sites were installed before Round 1 projects, however this classification was adopted to gauge the impact of step changes in vessel technology.

To identify the main vessel types used to install or planned for installation of each OWF, reference to the vessel listings for each respective wind farm on 4C Offshore were used to populate a vessel database for each round (4C Offshore Ltd, 2016). Using the parent installation phases as a guide, the vessel database for each round was then assessed to reveal the most common vessel type chartered for each phase, which produced a representative vessel spread for each round. It should be noted that the vessel spreads for each round, included in Table 3.3, are based on the transparency of information published on the 4C Offshore website. The provided references give more detail on the general vessel type, and a full list of vessel characteristics used in the study are appended in Table A.1. For each vessel type identified and listed in Table 3.3, the referenced vessel specifications were used to generate approximations for the loaded and unloaded transit speeds in conjunction to survival limits for wave height and wind speed. Where some environmental limits were not listed on the specification sheets, generic references or limits for similar vessels were used to approximate the relevant values (Dalgic et al., 2015; Douglas Westwood, 2013; Sperstad et al. 2016; Thomsen, 2012; Van Oord ACZ, 2001). Whilst this information is sufficiently detailed for modelling, analysts will have more specific information from the vessel operators to plan the marine operations. The commissioning phase of the wind farm, which predominantly adopts crew transfer vessels (CTVs) to transfer technical personnel to the turbines, has not been considered.

Eight offshore installation phases are considered for analysis and are summarised in Table 3.3, which specifies the installation phase and vessel used in the model set-up. It should be noted that all vessels are assumed to have the capacity to remain offshore to complete the work at all turbine locations, with the exception of the vessels used for the foundation, transition piece and WTG installation phases, which are limited to a maximum of three turbine locations per voyage. This limitation is discussed further in Section 5.4.

Each phase and vessel choice for the different rounds are described in the following passage. The dredging&survey phase prepares or clears the seabed before the main OWF construction activities begin and ensures the work has been completed to a sufficient standard. Dredging is not required for all projects but has been included to acknowledge some form of seabed preparation common to many sites. It is assumed that the dredging phase follows on from and is prescribed by, an extensive seabed survey. This is completed well in advance of the main construction activities to inform project teams of any unexploded ordnances, potential obstacles, seabed integrity, the applicable foundation type(s) for the site and the extent of dredging operations required. A dredge vessel can be fairly simple, consisting of a barge equipped with a backhoe excavator to more advanced dynamically positioned (DP) vessels that include trailing suction hopper technology (TSHD) (Kaiser and Snyder, 2012). Less sophisticated dredgers were used in earlier UK projects, but as installations have moved further from shore, developers have discarded traditional monopile foundations for gravity based or jacket structures. This requires improved accuracy and subsequent manoeuvrability of the dredge vessels, demanding the most advanced technology available to developers.

The second phase considered is the foundation installation phase. From review of the vessels used for foundation works in both rounds, it is evident that different types of vessels have been employed to deal with the variation or trends in foundation type used between rounds (Renewable UK, 2015). The majority of Round 1 sites adopted monopile foundations as these could be installed quite easily in the nearshore locations synonymous with the majority of these sites. This type of installation can be handled on board jack-up barges and dedicated wind turbine installation vessels (WTIVs) and this type of vessel was identified as the most common vessel in Round 1. Round 2 sites are generally greater in size and located further from shore, leading to more challenging conditions for installation. This shift presented further logistical challenges and often heavy lift vessels that could deliver and install foundations were employed to reduce materials handling at the offshore locations

The installation of the transition piece, which is the structural section that links the monopile and wind turbine, is the next installation phase. The transition piece provides a fendering area for crew transfer vessels to interface with the structure and a ladder for personnel to climb onto the platform before entering the turbine for either construction or maintenance tasks. It is common that the transition piece is prefabricated onto a jacket or tripod foundations, but it is assumed that monopile configurations are used for the installation campaigns considered throughout in this paper.

The wind turbine installation phase was found to adopt some form of dedicated WTIV across in both rounds. These vessel types incorporate four to six legs that rest on the seabed and elevate the main body of the WTIV above the water. This protects the vessel from wave heights between 1.5 – 3 Hs, depending on vessel design, and helps stabilise the lifting operations. These vessels are also used to transport between three to eight turbines at a time, depending on the available cargo capacity and the installation strategy adopted. As indicated in Section 3.5, the turbine installation vessel has an assumed capacity of three turbines per voyage. The whole lifting process remains sensitive to the conditions, particularly wind speed and when individual blades or assembled rotor sections are hoisted, the environmental limits are often lowered. A number of different WTG installation strategies have been used in various projects as presented in Kaiser and Snyder (2012). These range from individual sub-section lifts for the towers and single blades, through to fully assembled turbine lifts. It is assumed that the lifting strategy is identical in both rounds to limit the amount of modelling permutations considered.

The 'bunny-ear' configuration with a 2 stage tower lift was selected as the most applicable strategy as this presented a compromise between fully assembled and an individual component installation. In this installation strategy the maximum and minimum tower sections are connected on land, as with the rotor, which is pre-assembled, consisting of a nacelle and 2 blades attached. This results in a total of three lifts at the turbine location beginning with the tower, then rotor and finally the third blade (Maples et al., 2013). It should be noted that the reference duration in Table 3.4, represents the approximate time to install each turbine using in the bunny-ear configuration and this figure would fluctuate for each of the installation strategies presented in Kaiser and Snyder (2012). In Round 1, jack-up barges without their own means of propulsion were commonly used. These vessels often have modest elevation heights and are dependent on other vessels such as anchor handling tugs (AHTs) to transit and manoeuvre the barge to each wind turbine location. Self-propelled jack-ups started to be used in Round 1 but were more commonly chartered for Round 2 projects. This next stage in WTIV design presented improved manoeuvrability, elevation heights and deck space, offering improved cargo capacities and logistical options.

Scour protection is installed to prevent structural instability around

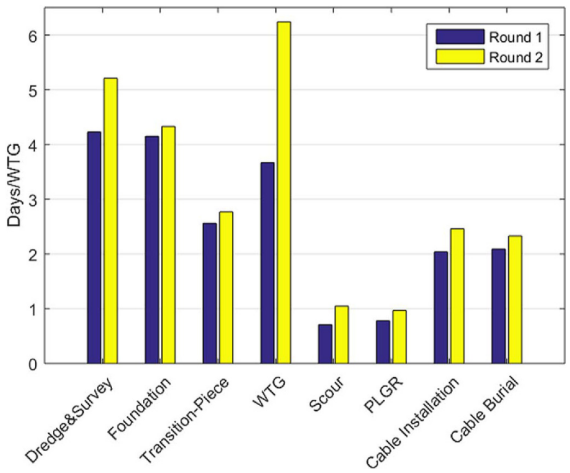

Fig. 4.1. Average Installation Rate in Days/WTG (or WTG Location) [± 1 S.D.].

the foundation of an offshore wind turbine, induced by tidal flow or wave action. The specific solution depends on the foundation selected, the long-term meteorological conditions and the seabed material. Rock-dumping is often used to place variable grades of stone around foundations or protection is placed over vulnerable cable lengths in the form of concrete mattresses. This phase can be completed with a hopper barge and towing tug or more commonly with a dedicated side stone dumping vessel or with more sophisticated fall pipe vessels (FPV). It is assumed in these analyses that the scour protection is installed around the base of the mono-pile foundations.

The pre-lay grapnel run (PLGR) is used to clear debris along the cable route before installation, ensuring that hazards do not interfere with cable laying and burial phases or during future maintenance operations (Offshore Wind Programme Board, 2015). A hook like anchor is pulled during this process and relies on the forward motion of the vessel to work the seabed, creating a narrow trench of approximately 1 m depth along the cable route. A multi-purpose workboat with a bollard pull of roughly 20 tons, is normally used for this activity.

Cable laying operations require a dedicated cable lay vessel (CLV) to lay the inter-array cables between the turbines and export cable to the onshore substation or from the offshore substation to the cable landfall point. Earlier projects often employed adapted barges that feed out cable from a pre-installed cable carousel due to the near shore, sheltered conditions (Energy Institute, 2014). These rely on other vessels to tow and install anchoring arrangements to keep the barge to the designated cable path as these vessels are not equipped with dynamic positioning (DP) systems. It is assumed that this type of installation was used for the Round 1 project and is modelled with a transit speed that resembles the speed of an AHT, of between 6 and 8 knots. In some instances an adapted supply vessel was used to take advantage of the DP capabilities but for the majority of the Round 2 projects, specifically designed CLVs were employed to cope with more extreme conditions and exposed cable routes. Many of these vessels can handle simultaneous laying, trenching and burial operations but often a secondary vessel is assumed to complete the trenching and burial phases (Bard and Thalemann, 2011).

The cable burial phase is assumed to enclose both the trenching process and final burial of the cable. The study also assumes that a post-lay burial operation is applied in both rounds utilising a secondary multi-purpose support vessel (MPSV) or large survey vessels. This 'lay and trench' technique deploys an ROV from the parent multi-purpose vessel to trench around and bury the cable in one operation. The main logistical steps of this phase are assumed to relate to the parent multi-purpose vessel and a burial duration was selected on a per wind turbine basis.

3.6. Operations, environmental limits&durations

To assess the vessel technology from Round 1 and 2, a set installation scenario is used, presented in Table 3.4. To resemble a typical installation programme, a number of the phases were set to run simultaneously. The Foundation phase was specified to begin once the Dredging and Survey phase had reached 60% completion, the Transition Piece installation began when 40% of the Foundation phase was completed, Turbine installation began after 20% of the foundations were installed, Scour Protection follows at 80% of completion, 100% for the PLGR phase, Cable Installation at 60% of the PLGR Phase and Cable Burial only begins after the Cable Installation had completed to 100%.

Each of the main installation phases were allocated with environmental limits, independent of the associated vessel restrictions and resemble the maximum conditions that can be experienced when completing these offshore operations, separate from vessel capabilities. The same task parameters are assumed in both rounds, which are to the author's best knowledge and experience, a fair representation of the expected values for these installation operations. It is reiterated that separate environmental limits exist for the different vessels in terms of transit and waiting modes. As soon as the weather conditions are below a vessel's transit limits, the vessel will set sail to the offshore site. The transit time is calculated simply by dividing the distance between the farm and the port by the vessel speed. If at any point, the weather conditions exceed the transiting limits during an outward or inter-turbine voyage, the vessel returns to port. When the transit duration has been completed, the vessel is on site and the software calls on the limits and durations applied to the installation phases. This determines if a sufficient weather window exists to start an installation sequence or if the vessel should wait for the next available weather window, if the waiting conditions of the vessel are satisfied.

Three main characteristics are used for each installation step within the models: 1. Reference Duration (average number of hours spent per WTG), 2. Maximum wind speed (m/s) and 3. Maximum wave height (m). Reference to available literature such as (Maples et al., 2013; Douglas Westwood, 2013) and in-house planning documentation was used to establish the base installation durations, wind speeds and wave heights for each phase listed in Table 3.4.

4. Results

To assess the impact of vessel technology on construction durations for offshore wind farms, the scenarios in Section 3.4 were applied using the simulation tool described in Section 3.1. For both wind rounds, 11 cases were constructed, initially taking one mean case of all parameters, eight cases where each parameter was run with an maximum and minimum value in turn, and two extreme cases combining a maximum and minimum situation for the number of turbines and distance to shore. The main characteristics of the vessels under analysis are the transit and survival limits, which are composed of a maximum wave height and wind speed as listed in Table A.1. The transit speeds of each vessel for loaded and unloaded states are also specified. An overview of the vessel spreads used for each round is included in Table 3.3.

Each simulation is run for a 1000 iterations to obtain sufficiently accurate results. The average simualtion time for a round one case was 1 day and 1.6 days for round two. For each of the individual 11 cases, the software produces a calendar output for all installation phases, recorded under user specified exceedance quantiles. The predicted duration for each installation phase is presented with a start and an end date, meaning the results are rounded to the nearest day. The P90 duration quantile was selected for analysis in this study, as it provides greater certainty that the predicted values will not be exceeded when conducting these type of operations offshore. The predicted P90 duration for each phase are divided by the number of turbines specified in each case, to reveal the average installation rate (IR) in days per turbine (Days/WTG). The IR represents the average number of days required to complete the

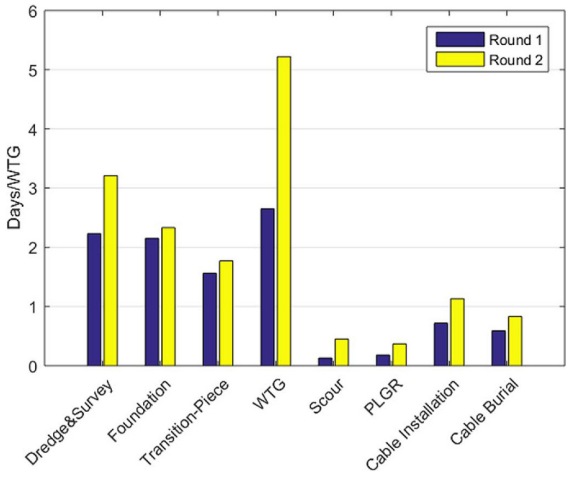

Fig. 4.2. Average Weather Downtime in Days/WTG (or WTG Location) [± 1 S.D.].

installation task at each turbine in the model, including the impact of weather delay. To demonstrate how these results can be used in practice, an average result for weather downtime (WDT) is calculated by deducting the base duration from the predicted P90 duration for the phases in each case. The base duration in each phase is calculated using the net time to complete the installation tasks without the impact of weather delay, and multiplying this by the number of turbines in each case. The resulting WDT duration is once again divided by the number of turbines for each case, to reveal a WDT value for the individual installation phases in Days/WTG.

Within each case eight IR and WDT values are collected, corresponding with the number installation phases. For each round, a total of 11 cases were collected and an average IR and WDT for the eight installation phases, was computed from this compilation, as shown in Figs. 4.1 and 4.2. As discussed in Section 3.1, the deviation from these averages is regarded as a means to estimate the installation risk in the potential outcomes.

Box plots that show the variation in the results are presented in Figs. 4.3a to d and a comparison of the recorded variation in each phase in both rounds, is included in Fig. 5.3. The greatest variability in the results were observed for the Foundation, Transition Piece and Wind Turbine installation phases, as represented by the larger bars in Fig. 5.3. This indicates that the greatest risk is estimated to occur within these phases, although the Round 2 figures demonstrate lower deviation despite higher durations.

4.1. Results overview

The IR for each of the eight phases was used to compare the differences between the vessel spreads of each round. Fig. 4.1 presents a summary of the installation rates in days per wind turbine (Days/WTG).

The results in Fig. 4.1 show that Round 1 is predicted to have the smallest IRs, with the largest recorded for the dredging and survey, foundation and WTG installation phases, predicted to be around 4.2, 4.1 and 3.6 Days/WTG respectively. The results for Round 2 show the greatest IRs and the largest are again recorded for the same phases at 5.4, 4.4 and 6.3 days/WTG respectively. It can be generalised that Round 1 appears to outperform Round 2 vessels in terms of installation rate, by approximately 25% on average across the eight installation phases. The biggest difference between Round 1 and 2 is seen with the Dredge&Survey phase at around 1 Day/WTG and the WTG installation phase at approximately 2.5 Days/WTG.

As a direct consequence of the results presented in Fig. 4.1, knowing the base duration for each of the installation phases allows for the amount of WDT to be identified. The weather delay expected on average for each phase between the two rounds, is presented in Fig. 4.2. This confirms that the greatest delays are observed in the Round 2 phases. This process presents a method for predicting the average WDT for each installation phase. If this approach was used to analyse a case specific simulation, built to match the characteristics of a prospective development, this would provide a basis to scale the results by the number of turbines and reveal an approximate overall WDT for each installation phase.

4.2. Results by round

The results for the individual rounds were further analysed to determine the distribution of phase durations predicted by the software. The box plots of the IRs and WDTs in each round have been aligned in Figs. 4.3a to d. In terms of WDT, Figs. 4.36c and d demonstrate the same range of distribution as the IRs, but at lower values. A plot of the quantification of the inter-quartile ranges for the IRs and WDTs from each phase across the two rounds, is included in Fig. 5.1.2 and is used to demonstrate the spread in the results, which can be used to signify the installation risk for the combined vessel-phase configurations. This is calculated by simply subtracting the bounds of the first quartile from the third quartile, for each of the installation phases in Rounds 1 and 2.

Fig. 4.3a demonstrates a considerable range for the installation phases in Round 1, particularly in the Wind Turbine (WTG), Transition piece and Foundation installation steps, as demonstrated by the broad space taken by the interquartile range (IQR). The variability of these IRs span from approximately 2.4 to 5.5 Days/WTG with an IQR of about 3 Days/WTG for the Foundations, 1.4 - 3.9 Days/WTG with an IQR of 2.3 Days/WTG for the Transition Pieces and 1.9 - 5.3/WTG days with an IQR of 3.4 Days/WTG for the turbines. All of the phases demonstrates a skew towards the upper values of the data. The Dredging&Survey, Cable Installation and Cable burial phases exhibit lower variance in the results and a nominal range was predicted for the Scour and PLGR stages, with the majority of these phases taking 1 day or less per wind turbine.

Fig. 4.3c shows similar variance between the Round 1 IR and weather downtime predictions (WDT). Based on the results in Fig. 4.3a, it can be expected that the greatest ranges would be seen at the Foundation, Transition piece and Wind Turbine installation phases at 0.4 - 3.6 Days/WTG with an IQR of 3 Days/WTG, 0.4 - 2.8 Days/WTG with an IQR of 2.3 Days/WTG and 0.8 - 4.3 Days/WTG with an IQR of 3.2 Days/WTG respectively. Again, the medians for these phases are skewed towards the upper data in the plots. The distribution of all phases in Fig. 4.3c have a near identical profile as seen the IRs. The Scour and PGLR phases are predicted to have the lowest WDTs and subsequent WDT in Round 1 without much variation, while the three key phases of the Foundation, Transition Piece and Wind Turbine installation present the highest values in terms of delay.

Fig. 4.3b shows generally smaller ranges for the results when compared to Round 1. The broadest IQR distributions relate to the Dredging&Survey, Transition Piece and Wind Turbine phases at 0.5, 0.4 and 0.45 days/WTG respectively. The Foundation and Transition Piece installations have an overall range of approximately 2 Days/WTG and the largest recorded for the WTG installation at 4 days/WTG. The same distribution profiles are again replicated in the WDT plots shown in Fig. 4.3d and once more the Scour Protection and PLGR phases demonstrate the lower weather downtime. The Dredging&Survey, Foundation and WTG installation phases are shown to have the largest values in terms of WDT. Generally, it was found that the installation rates and WDT predicted for the phases in Round 2 are higher in comparison to Round 1. However the results seem more consistent as the distributions are quite narrow and this smaller variation indicates a reduction in installation risk.

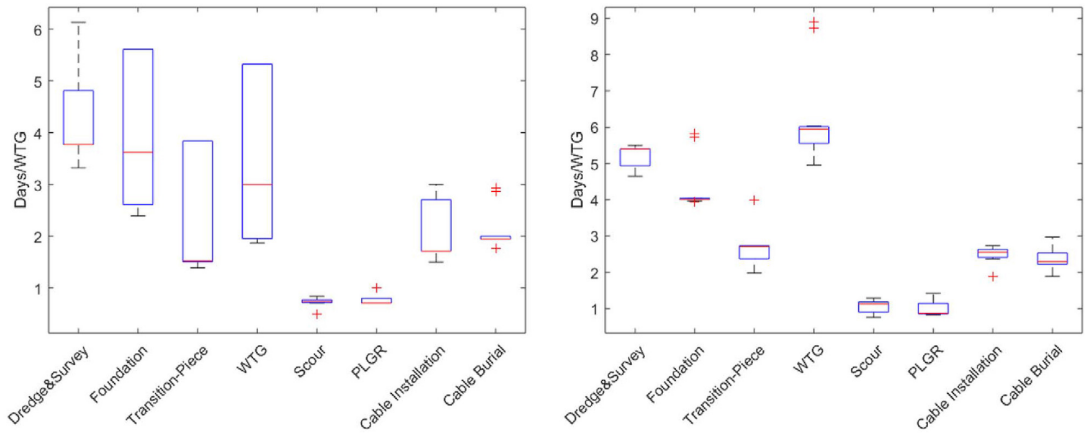

(a) Round 1 - Installation Rate (IR) Distribution

(b) Round 2 - Installation Rate (IR) Distribution

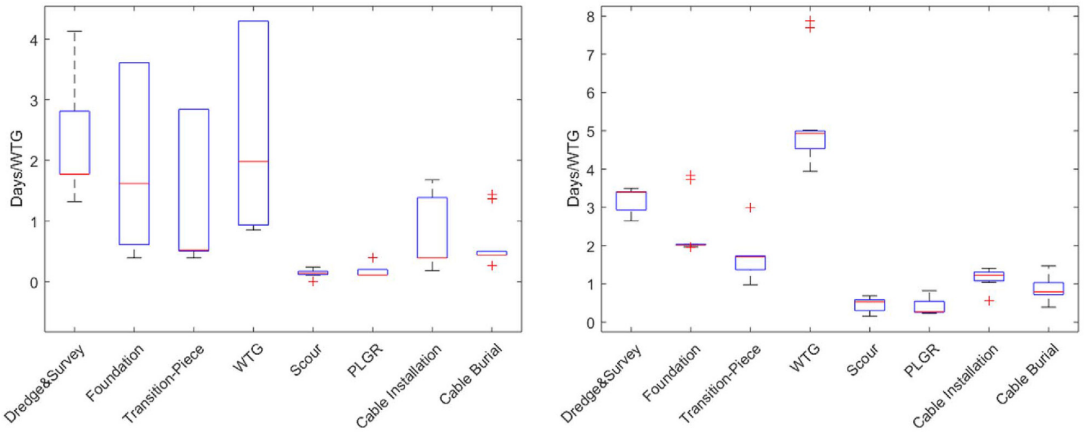

(c) Round 1 - Weather Downtime (WDT) Distribution

(d) Round 2 - Weather Downtime (WDT) Distribution

Fig. 4.3. (a) Round 1 - Installation Rate (IR) Distribution, (b) Round 2 - Installation Rate (IR) Distribution, (c) Round 1 - Weather Downtime (WDT) Distribution, (d) Round 2 - Weather Downtime (WDT) Distribution.

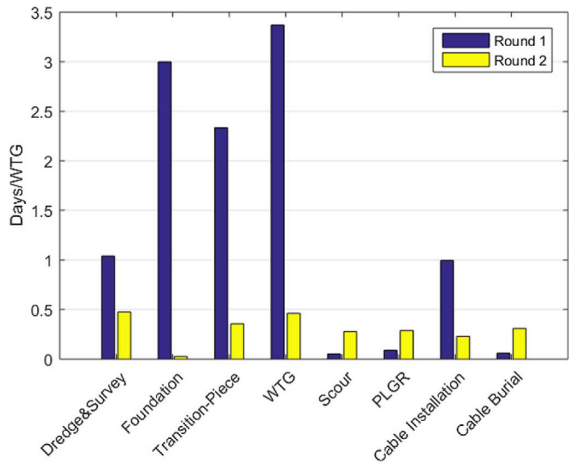

Fig. 5.1.2. Phase IQR Quantification: Rounds 1&2.

5. Discussion

The outcomes and reasoning surrounding the results is covered in this section. We begin with the Installation Rates and WDT values included in Figs. 4.1 and 4.2, which list the average result for the various scenarios within each installation phase, across the two rounds. The results used to draw these averages were compiled separately to allow analysis by rounds and review of the scenarios that resulted in the largest recorded durations.

5.1. Vessel performance by round

The most notable average results from each round is covered in the following sections and considers the source of these outcomes, including the contribution of each installation phase towards the averages obtained.

5.1.1. Round 1

In Round 1, the average total of construction days spent per wind turbine, which includes all phases across all scenarios, are the lowest for both rounds at 20.23 Days/WTG. This is complemented with a WDT figure of 10.21 Days/WTG on average and both exhibit a standard

deviation of 3.2 Days/WTG. Despite the adoption of less dedicated and specialised vessels on the market, it appears that Round 1 sites benefit from their near shore locations. This characteristic provides more sheltered conditions during construction reduces the impact of weather on the vessels and subsequent delays. However, in Round 1 projects the averaged results suggest that over 50% of the charter time for the vessels would likely be attributed to downtime. The average combined construction duration was found to be 403 days, which required a total of 640 individual boat days relating to the overlap of phases described in Section 3.6. These outcomes arrived at approximate weather downtime value of 328 days per project on average.

A review of the individual phases revealed that the Wind Turbine Installation phase makes the largest contribution to downtime recorded at 26%. The case which caused the largest impact in terms of IR and WDT was the mean case at 23.6 Days/WTG for IR and 13.6 Days/WTG for WDT. These were closely followed by very similar results for the distance to shore, inter-turbine distance cases at around 23–24 Days/WTG IR and 13–14 Days/WTG WDT. The lowest predicted duration was seen with the lower number of turbines scenario at 16 Days/WTG and 6 Days/WTG for IR and WDT respectively. It was expected that the maximum distance to shore and number of turbine cases would result in greatest recorded IRs and WDTs. However as the number of turbines or distances in the model increase, so does the elapsed time for each phase and delays gradually shift the start date of successive phases. This suggests that seasonal conditions can be incurred at different moments, during different phases of an installation campaign, stemming from the size of the project to be completed. For example the start date recorded for WTG installation in the case with the minimum number of turbines was 11/08/2017, whilst the start date for the maximum number of turbine cases was 12/05/2018. Despite this dramatic shift due to the size of project, the start date for maximum number of turbine case, is in May. It is likely that the weather conditions were more favourable in May than in August. This observation is further exemplified by the results for the start date cases, which have the same characteristics as the mean case but with a different date defined for the launch of the first phase. The results recorded for the upper start date case (starting: 01/04/2017) are the second lowest recorded at 16.8 days/WTG for IR and 6.8 days/WTG for WDT. It is also suggested that the weather downtime will increase if the vessel employed for each installation phase, has to return to base to reload various components, as is the case for the Foundation, Transition Piece and WTG vessels in this study.

Referring to the box plots in Figs. 4.3a and c, it is evident that many of the phases are quite variable in terms of IR and WDT with the largest spread of values observed for the Foundation, Transition Piece and Wind Turbine Installation. The large variation shown in Fig. 5.1.2 signifies a lack of consistency in the IR and WDT values for each scenario and indicate a significant amount of installation risk that could be expected for these phases throughout Round 1. This suggests that the vessels employed for these three phases at the time of Round 1, were susceptible to variations in their working climate, exemplified by the broad spread of values for the phases described above.

5.1.2. Round 2

Round 2 vessels are predicted to have the largest average IRs and WDT values between the two rounds. The average IR across all scenarios is 25.4 Days/WTG and 15.4 Days/WTG for the average WDT with a standard deviation of 2.17 days for both. This deviation is lower than Round 1 and it can be said that the installation risk is lower with the Round 2 vessels overall. The average WDT value represents an increase of 50% compared to Round 1. These initial outcomes convey the impact of more challenging offshore conditions typically experienced at these sites. The results indicate that on average over 60% of the entire vessel charter period would experience weather downtime, suggesting developers could have faced a significant bill for downtime for projects with similarities to this category. The average and combined construction duration was predicted to be around 1384 days per project, requiring a large number of separate boat days in excess of 2300 days combined. The average WDT value for all the scenarios in Round 2 was just over 1260 days per project.

Reference to the individual phases revealed that the WTG installation phase again made the largest contribution to overall WDT recorded at nearly 34% of all downtime on average, which is a considerable increase compared to Round 1. This implies that the typical turbine installation vessel employed during Round 2 was generally not ideally suited to the heightened weather conditions typical of more challenging waters further from shore. The scenario found to have the largest impact in IR and WDT was the lower number of wind turbines case with values of 29.67 Days/WTG and 19.62 Days/WTG respectively. The scenario with the least impact in the Round 2 predictions is the maximum start date (01/04/2017), with an IR of 23 Days/WTG and WDT value of approximately 13 days. This outcome is surprising as it may be expected that with less turbines, the installation rates may be better or at least stay the same. It is noted that for larger wind farms that the weather delays are averaged across a greater number of turbines, which may compensate the WDT predictions. It is again proposed, that the impact of successive scheduling can dramatically change the amount of downtime experienced, relating to the changing seasonal weather conditions. As there are less turbines in the minimum WTG case, this means phases such as the WTG installation, would be reached sooner and could be completed in more severe weather conditions, in comparison to larger projects that may not reach the most susceptible phases until a calmer weather season is incurred. To exemplify, the WTG installation start date for the case with the minimum number of turbines was recorded as 11/11/2017 and for the maximum start date case as 01/06/2018. It is again likely the weather was less severe in June than in November. It therefore suggested that a consecutive installation schedule as applied in this study, may not be the optimum approach when planning offshore wind farm construction.

It is apparent that the majority of phases experienced an increase in WDT on average and again the WTG installation phase has shown a 97% increase in average downtime in comparison to Round 1. Notably, the Scour Protection conveys a 250% increase, a 100% increase in PLGR, 58% for cable installation and approximately 40–45% increase for the Dredging and Cable Burial Phases. Two WDTs found to increase slightly are the Foundation and Transition Piece installation each confirming an approximate increase of 8% and 13% respectively on average. It is proposed that the vessels in Round 2 were not well suited to the conditions associated with these sites, which relates to the vessel types commonly chartered at this time. It is proposed that vessel availability restrictions are demonstrated in Round 2, as over-sized and weather sensitive heavy lift vessels were commonly employed. These vessels were used for phases such as foundation or transition piece installations and originated from other offshore industries, matched with inflated daily charter rates. It would be appropriate to apply a cost benefit analysis when considering the charter of these vessels in comparison to the resulting WDT costs that may be expected from more capable but less available vessels in the market. In some cases developers may have struggled to source a cheaper alternative with the improved capabilities and to some extent, this demonstrates that optimum vessel designs were not available or had yet to be built during the construction of Round 2 sites. Thus focus on the development of dedicated wind farm installation vessels was essential to the industry at this time.

The box plots in Figs. 4.3b and d show significantly less variation in comparison to Round 1. This suggests that despite an overall increase in WDT on average, the vessels employed for Round 2 performed more consistently and therefore a reduction in the installation risk is observed in Fig. 5.1.2. This means more certainty could be drawn from WDT predictions but the challenge in reducing the overall magnitude of these delays was still a concern. The Scour Protection and PLGR phases still exhibit fairly low IR and WDT values compared to Round 1 but the plots demonstrate more variability in the results, which suggests these vessels may perform less consistently when used in more challenging conditions.

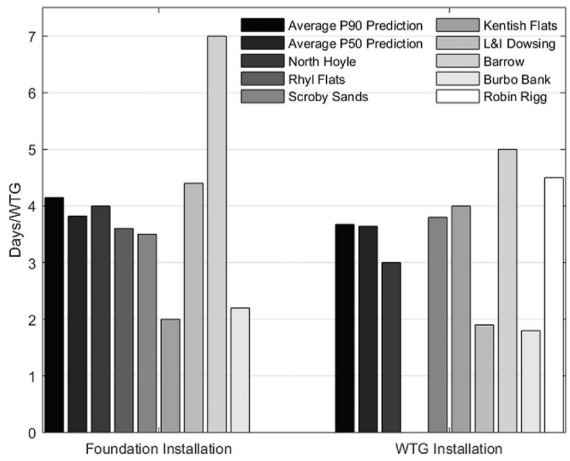

Fig. 5.2. Average Prediction vs. Recorded Installation Rates - Round 1 (Kaiser and Snyder, 2012).

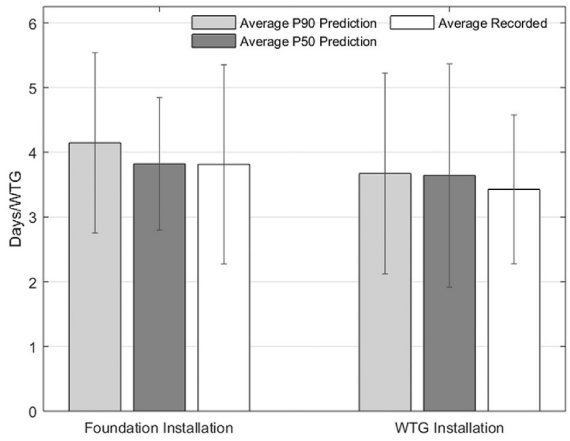

Fig. 5.3. Average Prediction vs Average Recorded Installation Rates - Round 1 [± 1 S.D.].

5.2. Value to planning personnel

The presented approach is of interest to planning personnel, as a structured method to identify and benchmark offshore wind installation risks. Whilst the study and simulation do not relate to any specific project, it has provided a basis to schedule vessel missions based on the bounds of the two installation rounds.

Ensuring efficient, low cost installation strategies is essential if offshore wind is to make a meaningful, cost effective contribution to the UK's energy mix, aiming for a levelised cost under £100/MWh (The Crown Estate, 2012). Many of the delays identified have been tackled by introducing innovative vessel designs, made to cope with more extreme weather conditions and increased deck space or lifting capabilities. This paper has assessed the environmental capabilities of the vessels and attempts identify their susceptibility to various project characteristics, to help reduce the costs of this industry and offer guidance on vessel charter.

As the study has been compartmentalised by UK offshore wind rounds 1 and 2, it is intended that operatives can benchmark these findings against the outcome of their own projects and compare vessel performance predictions. This study provides a clear indication of the installation risks for the vessel spreads used in each round and the phases predicted to have the largest installation risk, highlight areas where precautionary or mitigation steps may be required when chartering vessels with similar capabilities.

A method to approximate the WDT for each installation phase is discussed in Section 4.1. It is demonstrated that the selection of the vessels identified in Round 1 for a site of this category, would generally result in lower weather downtimes but there may be significant variation in the Foundation, Transition Piece and Turbine installation phases. The vessels specified for Round 2 exhibit considerably less variation but larger weather downtimes compared to Round 1. This result proposes that more modern vessels should perform more consistently. Management could take more certainty on their predicted WDT figures, if they opt for and can access the most sophisticated vessels available. It is also found that periodic scheduling of installation phases should be considered when conducting an offshore wind development. The consecutive nature of the phases employed within this study has revealed that the larger, less accessible projects may not experience the greatest downtime as a result of shifted schedules from delays incurred during earlier phases.

We have demonstrated the effect of successive scheduling of installation phases in these type of models, as delays incurred earlier in the project can shift the start date of phases waiting to begin. It is therefore suggested that individual models are primarily constructed for each installation phase, with a preferable or predicted start date. The effects of different start dates could be assessed by the individual models and would aid planners in the construction of a master installation schedule, compromising between the impact of delays and preferred installation periods.

To generalise these perspectives, Round 1 vessel technology exhibits the lowest WDT although a considerable amount of variation in the observed delays may occur if employed for more remote, unsheltered locations. The vessels employed for Round 2 offer more certainty as the results appear more consistent but are predicted to experience larger WDTs. This demonstrated that despite the adoption of a more standardised approach for these projects, there was an opportunity to reduce the WDT figures with more sophisticated and capable vessels.

5.3. Data validation

The IRs presented in Kaiser and Snyder (2012) were used to complete a validation of the adopted method and analyses. Within this reference, the Kaiser et. al list observed IRs (Days/WTG) for foundations and wind turbines from eight UK Round 1 wind farms. These values are presented in a 'boat days' basis which represent the entire time spent per vessel for each foundation and turbine installation in days/WTG. This metric provides a suitable base for comparison and, as these phases were predicted to have some of largest weather downtimes in Fig. 4.2, it should provide an interesting reference. Unfortunately, the authors are unaware of any other available data set that presents the remaining installation phases in this manner. P50 predictions were also computed during the simulations completed for this study and the P50 IRs were obtained using the same approach in Section 4. The average P90 and P50 prediction for the Foundation and WTG phases, are compared against the average IRs recorded across various Round 1 sites in Fig. 5.2. An initial review of the data demonstrates that the Average Round 1 predictions, both P90 and P50, are of similar order to the recorded values for the Round 1 site. This gives an indication that the predictions produced by the software and the method to obtain the IRs, can produce realistic results.

The average predicted and recorded IRs for the Foundation and Turbine installation phases are compared in Fig. 5.3. The error bars signify± one standard deviation and represent the variation in the results. It is evident in the average P50 prediction is nearly identical to the recorded IRs for the foundations at 3.8 days/WTG. The P90 results are on average greater than the P50 and recorded IRs at approximately 4.1 days/WTG, but are similar to the P50 values in the WTG installation

phase at 3.7 days/WTG, compared to 3.4 days/WTG for the recorded data. The error bars show a considerable spread for the data in both the P50 and P90 predictions. It can therefore be deduced that as the recorded average lies within the error bar of the P50 and P90 values, the values show similarity to the recorded data, providing further confidence in the predicted results.

The error bars for the Pxx values are much broader in the WTG data when compared to the recorded IRs and the P50 error bar has a smaller spread against the other two values for the foundation data. This indicates that these probabilistic results produced by the software, can over and under predict the average IRs in specific cases. The average P50 values are closer to the recorded IRs and are only 6% greater in the WTG category. As the P90 outcomes were selected to represent the upper bounds of the software predictions, it was expected these values would be greater than the recorded IRs, yet these show good agreement with the recorded data. The P90 predictions are approximately 10% greater than the recorded IRs on average and demonstrate this approach can be used to produce conservative estimates.

5.4. Limitations and future work

This paper aimed to model the scenarios, vessel spreads and offshore wind farm characteristics using an offshore wind installation software. As the analysis progressed it was clear a few amendments to the modelling approach may have produced a more comprehensive set of results and offered more insight in the progression of the marine operations throughout the various scenarios and rounds.

Firstly, it should be noted that all of the results presented are taken from P90 predictions from the software. This implies that the predictions are somewhat pessimistic in their outlook offering 90% certainty that the values will not be exceeded. It may be the case that these results do not resemble what will occur in reality, although this metric does provide a good level of confidence that observed durations will be within bounds of recorded predictions. It can be argued that the metric of 'average number of days spent per WTG' (hrs/WTG) may not be the most suitable way of depicting the IR of cable sections or burial operations but was identified to be the most applicable approach for use within the software tool. The cable lay and burial durations were obtained using reference to in-house planning documentation, and an average installation rate was obtained by dividing the total duration by the number of turbines for the particular project.

In each of the simulated cases, the same environmental limits are assumed for the installation tasks in both rounds. However with improved vessel capabilities, it is possible that the limits for the installation tasks could be extended. More modern, capable vessels may improve attributes such as stability and lifting capacity, beyond the transit and station keeping limits considered in this study. As such, different environmental limits could be allocated to each round and method statements produced by installation contractors could be used to obtain variable inputs for these parameters, subject to the vessel and equipment employed for installation. Furthermore, the impact of water depth is not considered in this study. The task durations could have been altered to account for this, by again consulting method statements or by applying an assumed α-factor. In many cases, an α-factor may be imposed by a marine warranty surveyor (MWS) to account for uncertainty in the forecast and/or applied as a contingency in the execution of the marine operations (Det Norske Veritas, 2011). The uncertainty relating to water depth could be quantified for various installation tasks and applied to obtain contingency durations It is assumed that the operational limits in this study (Table 3.4), are unconditional to an applied α-factor and the authors believe that the task durations are to the best of their knowledge, a fair representation of the values used in reality.

The main environmental limits that were considered for the vessels and operations in this analysis were predominantly focused on wave height and wind speed. Vessel transit speeds were also included to reflect the expected travel durations. The software can also account for the minimum wave period (s) and current speeds (m/s) however due to the lack of available data for operations and vessels, the parameters were not used. It would be more informative and would allow greater accuracy if these parameters were considered, which would rely on input from vessel owners and experience professionals in the field.

Additionally, it is assumed throughout that all vessels are capable of remaining offshore for the entire installation campaign (i.e. for the entire set of WTGs to be installed), with the exception of those for the Foundation, Transition Piece and WTG phases, set at a maximum of three phases per voyage. This was selected as the number of inward and outward transits required for the remaining vessels is considerably variable in reality. It is fair to suggest, if the remaining vessels were allocated with a maximum number of phases per voyage, a change in WDT be observed for these installation phases. The vessels have specified waiting conditions in the software and when these are exceeded, the vessel returns to shore. This means that these vessels did not remain offshore during bad weather and it is suggested that portion of the WDT calculated for these phases, will account for the time to transit to and from port. It should be noted that a weather window is not sought for a vessel's outward or inter-turbine voyages in the software. In some instances a vessel may partially cover the distance of a voyage and is required to return to port when the weather exceeds transit limits. This is a limitation of the software, as a forecasting mechanism similar to weather forecasts issued in reality, could be built into the software to prevent the likelihood of unsuccessful voyages and improve the authenticity of the results.

For the modelling of WTG installation in the software, it was assumed that the associated duration was based on the 'bunny-ear' installation configuration. It is of the author's interests to extent this study, considering impact variable WTG installation strategies as presented in Kaiser and Snyder (2012) and Maples et al. (2013). It is noted that the sequence of the installation phases considered, is not standard to all offshore wind installation projects. The analysis completed is not wholly dependent on this sequence but if this was altered, the results for each phase could change, as these would begin at different periods in the simulated weather scenarios. However, as various knock-on delays are incurred as a result of the consecutive scheduling approach, the phases are applied at various months and seasons throughout the simulation.

As with many meteorological data sets, a number of missing entries were discovered and as the tool is reliant on evenly spaced intervals when forecasting the weather, linear interpolation was applied to compensate for these missing entries. This inevitably introduces a degree of approximation within the weather forecasting that may have altered the results slightly and a complete set of entries would provide further confidence with the results.

The software implements suspension to the marine operations between specified sequences if the vessel is able to hold station offshore. However in the interests of modelling time, only one sequence was specified within each installation phase that encompassed the entire duration of all the sub-tasks. If the phases had been modelled with multiple embedded sequences this may have provided a higher resolution in the results and adjusted the WDT predictions. As each of the phases across all the models only consisted of one sequence, it is fair to presume the simulations were completed on a level basis and can be used for comparison in terms of overall vessel performance. It is not advised that the predicted IRs or WDT values are used as a direct reference and should only serve as reference or sense check for similar analyses. The results used to formulate the IRs and WDT values are initially taken from the calendar outputs produced by the software. These outputs are presented in the form of dates and each completion date for the phases, is a result of the duration rounded to the nearest day. This indicates that the results are likely to over or under predict the phase durations but are believed to provide a good level of approximation for comparison.

Modelling and investigation on the impact of learning rates observed by Kaiser and Snyder (2012), is of interest to the authors. This can be modelled in the software tool and presents an intriguing expansion for this study. A review on the associated costs for the WDT predictions

against charter rates of the vessels, would provide a helpful means to assess potential trade offs when employing particular vessels and sub-contractors.

6. Conclusion

This paper presents the application of an offshore wind farm installation simulation tool to assess the performance of vessel technology employed across offshore wind development Rounds 1 and 2 in the UK. The study provides a retrospective analysis on the expected performance of the vessel types employed and describes a structured method to identify and benchmark offshore wind installation risks

We have presented the fundamental architecture and functionality of the software tool, stipulating the application of Monte Carlo simulation in conjunction with embedded forecasting and logistical models that play out the operations across a set of stochastic weather scenarios. A description of the HMM used to generate weather scenarios is provided. We have explained the use of P90 exceedance probabilities in our results and the post-analysis used to determine installation rates (IRs) and weather downtime (WDT) values in days per wind turbine (Days/WTG) or turbine location.

Two meteorological data sets were used and sourced form recorded and modelled data, each were selected to resemble the conditions of a Round 1 and 2 site in turn. The variable wind farm characteristics considered within both rounds are presented in Tables 3.1, 3.2. In total 11 different scenarios were simulated for each round to gauge vessel performance. We completed a review of the available information to ascertain the most commonly used vessel for each installation phase within the rounds. A comprehensive description on the application of these vessels and the assumed installation strategies, is also presented before arriving at our selected vessel spreads in Table 3.3, which we believe to resemble the most commonly chartered vessel types in both rounds.

The operational limits and durations of the installation phases are presented in Section 3.6, which dictate the wave heights and wind speeds that must be satisfied for the work to be completed at site. We have proposed alteration of the task values in future analyses, to account for the logistical capabilities of the vessel types investigated. The influence of vessel performance is based on transit and survival limits, which dictate the transit progression, duration, station keeping and navigation to the next turbine location.

The results indicate that the lowest IRs and WDTs are associated with Round 1, which can be justified by the sheltered near-shore location of these sites, meaning the vessels were protected from severe weather conditions expected at Rounds 2 sites. This is affirmed with the results for Round 2 which exhibits the largest IRs and WDT values and is believed to demonstrate the limitations of the vessels employed for these installations.

The box plots presented in Figs. 4.3a– d have highlighted that Round 1 vessels experienced lower levels of WDT with potential for variability, exhibiting uncertainty in the predicted downtimes. For Round 2 the variability is reduced but the WDT increases overall, showing the vessels would perform more consistently but the delays experienced may be prohibitive towards the cost of each project. The quantification of IQRs in the results for the two rounds, has provided a view of the installation risk associated with the representative vessel spreads and highlights where precautionary strategies may be best applied to overcome costly delays. The limitations of the software, model construction and overall methodology, has been discussed in Section 5.4. We have found the IR results for the foundation and WTG installation phases in Round 1, compare well with the IRs recorded at a range of Round 1 projects.

It is noted that when consecutive installation sequence is adopted, start dates can be delayed and the knock-on effect can induce significant downtimes in successive phases. It is therefore suggested that future work could consider methodical analysis and scheduling to devise a robust master plan for an entire installation project, accounting for seasonal weather conditions. Additionally, we foresee expansion in the fragmentation of installation sequences to assess the impact of suspendability during the operations. Lastly, the authors are interested in the cost trade-offs between the predicted WDTs and vessel charter costs, to support planning and contracting processes.

Acknowledgements

1. This work is funded in part by the Energy Technologies Institute (ETI); Research Councils UK (RCUK); Energy programme for the Industrial Doctorate Centre for Offshore Renewable Energy (IDCORE) [grant number EP/J500847/1].
2. The Crown Estate - The Marine Data Exchange: http://www.marinedataexchange.co.uk/

Appendix A. Annexe

See Table A.1.

Table A.1
Assumed vessel characteristics.

Vessel	Round	Transit Speed Loaded (kn)	Transit Speed Unloaded (kn)	Transit Conditions		Waiting Conditions	
				Max. Wind Speed (m/s)	Max. Wave Height (m)	Max. Wind Speed (m/s)	Max. Wave Height (m)
Injection Dredger	1	10	11.2	12	1.2	15	1.8
WTIV	1	11	12.1	15.3	2.8	36.1	10
WTIV	1	11	12.1	15.3	2.8	36.1	10
Jack-up Barge	1	10	11.5	10	1.5	15	2
Rock Dump	1	6.5	8	10	1.5	15	1.8
Multicat	1	10.8	12	10	1.8	15	2
Barge	1	6	8	10	1	12	1.5
MPSV	1	7	7.7	12	2	15	2.5
TSHD	2	10	11.3	15	2	20	2.5
Heavy Lift Vessel	2	9	12	15	1.8	20	3
Floating Crane	2	2.8	7	15	2.5	20	3
WTIV	2	11	12.1	15.3	2.8	36.1	10
Fall Pipe Vessel	2	11	12	15	2	20	2.2
Offshore Vessel	2	6	8.5	10	1.2	15	1.7
CLV	2	7	9	15	1.5	20	2.8
MPSV	2	12.5	16	15	1.5	20	3

References

4C Offshore Ltd, 4C Offshore, 2016. [Online]. Available: ⟨http://www.4coffshore.com⟩.

A2Sea, Sea Jack: Technical Specifications, 2013. [Online]. Available: ⟨http://www.a2sea.com/wp-content/uploads/2013/04/Techsheet_SEA_JACK.pdf⟩.

Ait-Alla, A., Quandt, M., Lütjen, M., 2013. Simulation-based aggregate installation planning of offshore wind farms. Int. J. Energy 7 (2), 23–30.

Bard, J., Thalemann, F. Offshore Infrastructure : Ports and Vessels, 2011. [Online]. Available: ⟨http://www.orecca.eu/c/document_library/get_file?Uuid=6b6500ba-3cc9-4ab0-8bd7-1d8fdd8a697a&groupId=10129⟩.

Barlow, E., Tezcaner Öztürk, D., Revie, M., Boulougouris, E., Day, A.H., Akartunali, K., 2015. Exploring the impact of innovative developments to the installation process for an offshore wind farm. Ocean Eng. 109, 623–634.

Dalgic, Y., Lazakis, I., Turan, O., Judah, S., 2015. Investigation of optimum jack-up vessel chartering strategy for offshore wind farm O&M activities. Ocean Eng. 95, 106–115.

Damen Shipyards Group, Damen multi-cat 3213, 2016. [Online]. Available: ⟨http://products.damen.com/en/ranges/multi-cat/multi-cat-3213⟩.

DEME Group, D. P. Fall Pipe Vessel - Rollingstone, 2014. [Online]. Available: ⟨http://www.deme-group.com/technology/dp2-rollingstone⟩.

Det Norske Veritas (DNV), DNV-OS-H101 Marine Operations, General, no. October 2011. [Online]. Available: ⟨https://rules.dnvgl.com/docs/pdf/DNV/codes/docs/2011-10/Os-H101.pdf⟩.

Dinwoodie, I., Quail, F., M.D, 2012. A Novel Time Domain Meteo-Ocean Modelling Approach, in Proceedings of ASME Turbo Expo 2012. Copenhagen: ⟨http://strathprints.strath.ac.uk⟩, 2012, pp. 1–11. [Online]. Available: ⟨http://strathprints.strath.ac.uk/41214/1/Quail_F_Iain_Dinwoodie_et_al_Pure_Analysis_of_offshore_wind_turbine_operation_and_maintenance_using_a_novel_time_domain_meteo_ocean_modelling_approach_Jun_2012.pdf⟩.

Douglas Westwood, OWF and WTIV Study (In-house Report), 2013.

Energy Institute, Construction vessel guideline for the offshore renewables industry, 2014. [Online]. Available: ⟨https://www.thecrownestate.co.uk/news-and-media/news/2014/construction-vessel-guideline-for-the-offshore-renewables-industry-published/⟩.

Fugro, Fugro Saltire, 2016. [Online]. Available: ⟨https://www.fugro.com/Widgets/MediaResourcesList/MediaResourceDownloadHandler.ashx%3Fguid%3D829e6ef1-f3db-6785-9f9d-ff240019aa6e+&cd=2&hl=en&ct=clnk&gl=uk⟩.

Irawan, C.A., Jones, D., Ouelhadj, D., 2015. Bi-objective optimisation model for installation scheduling in offshore wind farms. Comput. Oper. Res. 1–15.

Kaiser, M.J., Snyder, B.F., 2012. Offshore Wind Energy Cost Modeling, [Online]. Available: ⟨http://link.springer.com/10.1007/978-1-4471-2488-7⟩.

Krohn, S., Morthorst, P.-E., Awerbuch S., 2005. and The European Wind Energy Association, The economics of wind energy, p. 158, [Online]. Available: ⟨http://www.inderscience.com/link.php?Id=6769⟩.

Maples, B., Saur, G., Hand, M., van de Pietermen, R., Obdam, T., July 2013. Installation, Operation and Maintenance Strategies to Reduce the Cost of Offshore Wind Energy, no. [Online]. Available: ⟨http://www.nrel.gov/docs/fy13osti/57403.pdf⟩.

MPI Offshore, MPI Resolution Operating Capabilities, 2016. [Online]. Available: ⟨https://www.vroon.nl/Files/VesselParticulars/MPIRESOLUTION20150506115757.pdf⟩.

Muhabie, Y.T., Caprace, J.-d., Petcu, C., Rigo, P., 2015. Improving the Installation of Offshore Wind Farms by the use of Discrete Event Simulation, in World Maritime Technology Conference (WMTC), At ,Providence, RI, USA, pp. 1–10.

Offshore Wind Programme Board (OWPB) Grid Group, Overview of the offshore transmission cable installation process in the UK, 2015. [Online]. Available:⟨https://ore.catapult.org.uk/wp-content/uploads/2016/05/Overview-of-the-offshore-transmission-cable-installation-process-in-the-UK.pdf⟩.

Offshore-technology.com, Healthy competition: demand grows for specialised offshore vessels - Offshore Technology, 2012. [Online]. Available: ⟨http://www.offshore-technology.com/features/featureoperation-maintenance-offshore-wind-oil-gas-hydrocarbons-installed-capacity-wind-farm-specialised-resources-ship-boat-vessel-installation/⟩.

Offshorewind.biz, Offshore Wind to Remain UK's Cash Cow in 2016, 2016. [Online]. Available: ⟨http://www.offshorewind.biz/2015/12/23/offshore-wind-to-remain-uks-cash-cow-in-2016/⟩.

Peter Madsen Rederi A/S, Aase Madsen, 2013. [Online]. Available: ⟨http://peter-madsen.com/PM-ukrev2013.pdf⟩.

Rabiner, L.R., Juang, B.H., January 1986. An introduction to hidden Markov models. IEEE ASSP MAGAZINE, no. January, [Online]. Available: ⟨http://ieeexplore.ieee.org/abstract/document/1165342/authors⟩.

Renewable UK, Offshore Wind Projects Offshore Wind Project Timelines, 2015. [Online]. Available: ⟨http://www.kentwindenergy.co.uk/ckfinder/userfiles/files/RenewableUK_offshore_wind_timeline_2015.pdf⟩.

Renewable UK, UK leads Europe with £8.5bn boost from offshore wind - RenewableUK, 2016. [Online]. Available: ⟨http://www.renewableuk.com/news/300594/UK-leads-Europe-with-8.5bn-boost-from-offshore-wind.htm⟩.

Royal Boskalis Westminster N.V., Argonaut - Trailing Suction Hopper Dredger, 1999. [Online]. Available: ⟨https://boskalis.com/download-center.html⟩.

Royal Boskalis Westminster N.V., Specification sheet Cable lay vessel - Stemat Spirit, 2014. [Online]. Available: ⟨http://www.vbms.com/en/equipment/vessels⟩.

Scholz-Reiter, B., Heger, J., Lütjen, M., Schweizer, A., 2011. A milp for installation scheduling of offshore wind farms. Int. J. Math. Models Methods Appl. Sci. 5 (2), 371–378.

Seaway Heavy Lifting, Stanislav Yudin, 2016. [Online]. Available: ⟨https://www.seawayheavylifting.com.cy/vessels/stanislav-yudin#⟩.

Sperstad, I.B., Stålhane, M., Dinwoodie, I., Endrerud, O.-e.V., Warner, E., Testing the Robustness of Optimal Vessel Fleet Selection for Operation and Maintenance of Offshore Wind Farms, 2016. pp. 1–13.

The Crown Estate, Marine Data Exchange, 2015. [Online]. Available: ⟨http://www.marinedataexchange.co.uk/⟩.

The Crown Estate, Offshore Wind - Operational Report 2015, London, 2015. [Online]. Available: ⟨https://www.thecrownestate.co.uk/media/5462/ei-offshore-wind-operational-report-2015.pdf⟩.

The Crown Estate, Offshore wind cost reduction-Pathways study, pp. 88, 2012. [Online]. Available:⟨http://www.thecrownestate.co.uk/media/5462/ei-offshore-wind-operational-report-2015.pdf⟩.

Thomsen, K.E., 2012. Offshore Wind: A Comprehensive Guide to Successful Offshore Wind Farm Installation.

Ugland Construction AS, UR 101, 2006. [Online]. Available: ⟨http://www.jjuc.no/files/UR101-rev.-18.04.06-.pdf⟩.

Van Der Kamp, Multipurpose Injection Dredger Maasmond, 2015. [Online]. Available: ⟨https://www.dredgepoint.org/dredging-database/sites/default/files/attachment-equipment/maasmond_0.pdf⟩.

Van Oord ACZ, Cable installation study for DOWEC, 2001. [Online]. Available: ⟨https://www.ecn.nl/fileadmin/ecn/units/wind/docs/dowec/10033_000.pdf⟩.

Van Oord, Heavy lift installation vessel - Svanen, 2015. [Online]. Available: ⟨https://www.vanoord.com/activities/offshore-wind-equipment⟩.

Van Oord, Jan Steen - Multi purpose support vessel - Principal particulars, 2015. [Online]. Available: ⟨https://www.vanoord.com/sites/default/files/leaflet_jan_steen_2015_lr.pdf⟩.

Vis, I.F., Ursavas, E., 2016. Assessment approaches to logistics for offshore wind energy installation. Sustain. Energy Technol. Assess. 14, 80–91.